

Attainable Moment Sets - Approaches to Understanding Trim Capability in  
Conceptual Design

by

Joshua Holden Heinz

A Thesis Presented in Partial Fulfillment  
of the Requirements for the Degree  
Master of Science

Approved August 2023 by the  
Graduate Supervisory Committee:

Timothy Takahashi, Chair  
Werner Dahm  
M. Christopher Cotting

ARIZONA STATE UNIVERSITY

December 2023

## ABSTRACT

This thesis addresses the issue of assessing longitudinal and lateral-directional trim capability during the conceptual design process. Modern high-performance aircraft are likely to feature complex flight control systems where the control system may independently command every control surface to develop necessary moments. However, to prove stability and controllability on such an aircraft requires a near-final set of control laws. This requirement is onerous at the conceptual design level, where engineering methods need to facilitate rapid, multidisciplinary design optimization trades. This work considers the differences in Attainable Moment Sets across a wide variety of airframes using a simplified “pre-mix” approach to controls as well as a model where the control systems have independent command authority over each control surface. This work indicates that the “independent-single-panel” model offers modest improvements in attainable moments over a “pre-mix” strategy. This suggests that a “pre-mix” approach used to assess basic combined trim problems will not lead to an overly conservative final design.

## DEDICATION

To my loving family, whose unwavering support and encouragement have been the driving force behind my academic journey. Your belief in me has been my guiding light, and I dedicate this Master's thesis to each of you with gratitude and love. Your presence in my life has made this achievement all the more meaningful and rewarding.

## ACKNOWLEDGMENTS

The preparation of this work was supported through several funding mechanisms. Professor Takahashi and Mr. Heinz were supported by the Air Force Summer Faculty Fellowship program at the U.S. Air Force Institute of Technology under the direction of Dr. Ramana Grandhi, administered by SysPlus, Inc. during the summer of 2022. Professor Takahashi and Mr. Heinz were also supported by the Postgraduate Research Participation Program at the U.S. Air Force Institute of Technology, administered by the Oak Ridge Institute for Science and Education through an interagency agreement between the U.S. Department of Energy and AFIT.

# TABLE OF CONTENTS

	Page
LIST OF TABLES .....	vi
LIST OF FIGURES .....	vii
CHAPTER	
INTRODUCTION .....	1
WHAT IS AN ATTAINABLE MOMENT SET?.....	6
ESTIMATING AERODYNAMIC STABILITY & CONTROL DATA.....	9
Pre-Mix Model.....	15
Independent Single Panel Model .....	21
RESULTS .....	25
Bell X-2.....	26
North American X-15.....	37
Airbus A320.....	47
Air Force GHV .....	57
DISCUSSION AND FUTURE DEVELOPMENT .....	65
REFERENCES .....	67
APPENDIX	
A VORLAX INPUT FILES.....	70
B Bell X-2 PRE-MIX MODEL AERODYNAMIC DATA .....	83
C Bell X-2 INDEPENDENT SINGLE PANEL MODEL AERODYNAMIC DATA .....	89
D “Son-of-X15” PRE-MIX MODEL AERODYNAMIC DATA.....	100

APPENDIX

Page

E	“Son-of-X15” INDEPENDENT SINGLE PANEL MODEL AERODYNAMIC DATA.....	106
F	Airbus A320 PRE-MIX MODEL AERODYNAMIC DATA .....	117
G	Airbus A320 INDEPENDENT SINGLE PANEL MODEL AERODYNAMIC DATA.....	123
H	Air Force GHV AERODYNAMIC DATA.....	134

LIST OF TABLES

Table		Page
1.	Attainable Moment Set, Volume Comparison for Bell X-2 .....	36
2.	Attainable Moment Set, Volume Comparison for North American X-15 .....	46
3.	Attainable Moment Set, Volume Comparison for Airbus A320 .....	58

## LIST OF FIGURES

Figure	Page
1. Explanation of Lockheed HTV-2 test flight #1 crash due to Control Coupling ....	3
2. Pressure Plot, A320 VORLAX Model with Elevators Deflected and with flaps extended.....	10
3. Reverse-Engineered A320 – CL vs Alpha .....	12
4. Reverse-Engineered A320 – Longitudinal Stability - CL vs Cm .....	13
5. Reverse-Engineered A320 – Directional Stability - $C_n\beta$ vs Alpha .....	14
6. Reverse-Engineered A320 – Dihedral Effect - $C_l\beta$ vs Alpha.....	15
7. Example Control Surface Deflections for a “Pre-Mix Model” .....	16
8. Reverse-Engineered A320 – “Collective Elevator” control power – $C_{m\delta_e}$ vs Alpha .....	18
9. Reverse-Engineered A320 – “Anti-Symmetric Aileron” control power – $C_{l\delta_a}$ vs Alpha.....	19
10. Reverse-Engineered A320 – Adverse Yaw from “Anti-Symmetric Aileron” control power – $C_{n\delta_a}$ vs Alpha .....	20
11. Reverse-Engineered A320 – “Rudder” control power $C_{n\delta_r}$ vs Alpha .....	21
12. Example Control Surface Deflections for an “Independent-Single-Panel Model” .....	22
13. Line Art of Bell X-2 .....	27
14. Bell X-2 Attainable Moment Set during Landing at Mach = 0.2, Alpha = 12°, $\beta =$ 0° .....	29



Figure	Page
15. Bell X-2 Attainable Moment Set During Crosswind Landing at Mach = 0.2, Alpha = 12°, $\beta$ = 10° .....	30
16. Bell X-2 Attainable Moment Set During Subsonic Gliding Flight at Mach = 0.8, Alpha = 6°, $\beta$ = 1° .....	31
17. Bell X-2 Attainable Moment Set During Subsonic Gliding Flight at Mach = 0.8, Alpha = 6°, $\beta$ = 1° with Zero-deflection Planes with volumes of zero deflection .....	32
18. Bell X-2 Attainable Moment Set During Supersonic Flight Mach = 3.0, Alpha = 4°, $\beta$ = 1° .....	33
19. Bell X-2 Attainable Moment Set During Supersonic Flight Mach = 3.0, Alpha = 12°, $\beta$ = 1° .....	34
20. “Son-of-X15” VORLAX Model.....	37
21. “Son-of-X-15” Attainable Moment Set during Landing at Mach = 0.3, Alpha = 12°, $\beta$ = 0° .....	40
22. “Son-of-X-15” Attainable Moment Set During Crosswind Landing at Mach = 0.3, Alpha = 12°, $\beta$ = 10° .....	41
23. “Son-of-X-15” Attainable Moment Set During Supersonic Level Flight at Mach = 3.0, Alpha = 6°, $\beta$ = 0° .....	42
24. “Son-of-X-15” Attainable Moment Set During Supersonic Level Flight at Mach = 3.0, Alpha = 6°, $\beta$ = 1° .....	43
25. “Son-of-X-15” Attainable Moment Set During Supersonic Re-Entry Mach = 3.0, Alpha = 16°, $\beta$ = 0° .....	44

Figure	Page
26. “Son-of-X-15” Attainable Moment Set During Supersonic Re-Entry Mach = 3.0, Alpha = 16°, $\beta$ = 1° .....	45
27. “Son-of-X-15” Attainable Moment Set During Supersonic Re-Entry Mach = 3.0, Alpha = 16°, $\beta$ = 1°. Pre-Mix and Independent Single Panel.....	46
28. Reverse Engineered A320 VORLAX Model.....	47
29. A320 flaps full Attainable Moment Set during Takeoff Climb at Mach = 0.2, Alpha = 6°, $\beta$ = 0° .....	49
30. A320 flaps full Attainable Moment Set during Takeoff Climb at Mach = 0.2, Alpha = 6°, $\beta$ = 7.5° .....	50
31. A320 flaps full Attainable Moment Set during Takeoff Climb at Mach = 0.2, Alpha = 6°, $\beta$ = 10° .....	51
32. A320 flaps full Attainable Moment Set During Crosswind Takeoff at Mach = 0.2, Alpha = 12°, $\beta$ = 0° .....	52
33. A320 flaps full Attainable Moment Set during Landing at Mach = 0.2, Alpha = 12°, $\beta$ = 7.5° .....	53
34. A320 landing flaps Attainable Moment Set During Crosswind Landing at Mach = 0.2, Alpha = 12°, $\beta$ = 10° .....	54
35. A320 flaps up Attainable Moment Set During Subsonic Flight at Mach = 0.6, Alpha = 6°, $\beta$ = 0° .....	55
36. A320 flaps up Attainable Moment Set During Subsonic Flight at Mach = 0.8, Alpha = 4°, $\beta$ = 0° .....	56
37. GHV VORLAX Model.....	60

Figure	Page
38. GHV Attainable Moment Set, Mach = 3, Alpha= 4°, a) $\beta = 0^\circ$ , b) $\beta = 1^\circ$ .....	61
39. GHV Attainable Moment Set, Mach = 5, Alpha= 2°, a) $\beta = 0^\circ$ , b) $\beta = 1^\circ$ .....	62
40. GHV Attainable Moment Set, Mach = 7, Alpha = 0°, a) $\beta = 0^\circ$ , b) $\beta = 1^\circ$ .....	63
B1. CL vs Alpha .....	84
B2. CL vs CM.....	84
B3. $C_{Y\beta}$ vs Alpha .....	85
B4. $C_{n\beta}$ vs Alpha .....	85
B5. $C_{l\beta}$ vs Alpha .....	86
B6. $C_{m_{\delta_e}}$ vs Alpha.....	86
B7. $C_{n_{\delta_a}}$ vs Alpha.....	87
B8. $C_{l_{\delta_a}}$ vs Alpha .....	87
B9. $C_{n_{\delta_r}}$ vs Alpha .....	88
B10. $C_{l_{\delta_r}}$ vs Alpha.....	88
C1. CL vs Alpha .....	90
C2. CL vs CM.....	90
C3. $C_{Y\beta}$ vs Alpha .....	91
C4. $C_{n\beta}$ vs Alpha .....	91
C5. $C_{l\beta}$ vs Alpha .....	92
C6. $C_{m_{\delta_e}}$ vs Alpha, Positive Deflection.....	92
C7. $C_{m_{\delta_e}}$ vs Alpha, Negative Deflection .....	93
C8. $C_{l_{\delta_e}}$ vs Alpha, Positive Deflection .....	93

Figure	Page
C9. $C_{l_{\delta_e}}$ vs Alpha, Negative Deflection.....	94
C10. $C_{n_{\delta_e}}$ vs Alpha, Positive Deflection .....	94
C11. $C_{n_{\delta_e}}$ vs Alpha, Negative Deflection.....	95
C12. $C_{m_{\delta_a}}$ vs Alpha, Positive Deflection .....	95
C13. $C_{m_{\delta_a}}$ vs Alpha, Negative Deflection.....	96
C14. $C_{l_{\delta_a}}$ vs Alpha, Positive Deflection.....	96
C15. $C_{l_{\delta_a}}$ vs Alpha, Negative Deflection .....	97
C16. $C_{n_{\delta_a}}$ vs Alpha, Positive Deflection .....	97
C17. $C_{n_{\delta_a}}$ vs Alpha, Negative Deflection .....	98
C18. $C_{m_{\delta_r}}$ vs Alpha.....	98
C19. $C_{l_{\delta_r}}$ vs Alpha.....	99
C20. $C_{n_{\delta_r}}$ vs Alpha.....	99
D1. CL vs Alpha.....	101
D2. CL vs CM .....	101
D3. $C_Y\beta$ vs Alpha .....	102
D4. $C_n\beta$ vs Alpha .....	102
D5. $C_l\beta$ vs Alpha.....	103
D6. $C_{m_{\delta_e}}$ vs Alpha.....	103
D7. $C_{n_{\delta_a}}$ vs Alpha .....	104
D8. $C_{l_{\delta_a}}$ vs Alpha .....	104

Figure	Page
D9. $C_{n_{\delta_r}}$ vs Alpha.....	105
D10. $C_{l_{\delta_r}}$ vs Alpha .....	105
E1. CL vs Alpha .....	107
E2. CL vs CM.....	107
E3. $C_{Y\beta}$ vs Alpha.....	108
E4. $C_{n\beta}$ vs Alpha.....	108
E5. $C_{l\beta}$ vs Alpha.....	109
E6. $C_{m_{\delta_e}}$ vs Alpha, Positive Deflection.....	109
E7. $C_{m_{\delta_e}}$ vs Alpha, Negative Deflection .....	110
E8. $C_{l_{\delta_e}}$ vs Alpha, Positive Deflection .....	110
E9. $C_{l_{\delta_e}}$ vs Alpha, Negative Deflection.....	111
E10. $C_{n_{\delta_e}}$ vs Alpha, Positive Deflection.....	111
E11. $C_{n_{\delta_e}}$ vs Alpha, Negative Deflection .....	112
E12. $C_{m_{\delta_a}}$ vs Alpha, Positive Deflection .....	112
E13. $C_{m_{\delta_a}}$ vs Alpha, Negative Deflection.....	113
E14. $C_{l_{\delta_a}}$ vs Alpha, Positive Deflection .....	113
E15. $C_{l_{\delta_a}}$ vs Alpha, Negative Deflection.....	114
E16. $C_{n_{\delta_a}}$ vs Alpha, Positive Deflection .....	114
E17. $C_{n_{\delta_a}}$ vs Alpha, Negative Deflection.....	115
E18. $C_{m_{\delta_r}}$ vs Alpha .....	115

Figure	Page
E19. $C_{l_{\delta_r}}$ vs Alpha.....	116
E20. $C_{n_{\delta_r}}$ vs Alpha.....	116
F1. CL vs Alpha .....	118
F2. CL vs CM .....	118
F3. $CY\beta$ vs Alpha.....	119
F4. $Cn\beta$ vs Alpha.....	119
F5. $Cl\beta$ vs Alpha.....	120
F6. $C_{m_{\delta_e}}$ vs Alpha .....	120
F7. $C_{n_{\delta_a}}$ vs Alpha .....	121
F8. $C_{l_{\delta_a}}$ vs Alpha.....	121
F9. $C_{n_{\delta_r}}$ vs Alpha .....	122
F10. $C_{l_{\delta_r}}$ vs Alpha.....	122
G1. CL vs Alpha.....	124
G2. CL vs CM .....	124
G3. $CY\beta$ vs Alpha .....	125
G4. $Cn\beta$ vs Alpha .....	125
G5. $Cl\beta$ vs Alpha.....	126
G6. $C_{m_{\delta_e}}$ vs Alpha, Positive Deflection .....	126
G7. $C_{m_{\delta_e}}$ vs Alpha, Negative Deflection.....	127
G8. $C_{l_{\delta_e}}$ vs Alpha, Positive Deflection .....	127
G9. $C_{l_{\delta_e}}$ vs Alpha, Negative Deflection .....	128

Figure	Page
G10. $C_{n_{\delta_e}}$ vs Alpha, Positive Deflection .....	128
G11. $C_{n_{\delta_e}}$ vs Alpha, Negative Deflection .....	129
G12. $C_{m_{\delta_a}}$ vs Alpha, Positive Deflection .....	129
G13. $C_{m_{\delta_a}}$ vs Alpha, Negative Deflection .....	130
G14. $C_{l_{\delta_a}}$ vs Alpha, Positive Deflection.....	130
G15. $C_{l_{\delta_a}}$ vs Alpha, Negative Deflection .....	131
G16. $C_{n_{\delta_a}}$ vs Alpha, Positive Deflection.....	131
G17. $C_{n_{\delta_a}}$ vs Alpha, Negative Deflection .....	132
G18. $C_{m_{\delta_r}}$ vs Alpha.....	132
G19. $C_{l_{\delta_r}}$ vs Alpha .....	133
G20. $C_{n_{\delta_r}}$ vs Alpha .....	133
H1. CL vs Alpha.....	135
H2. CL vs CM .....	135
H3. $CY\beta$ vs Alpha .....	136
H4. $Cn\beta$ vs Alpha .....	136
H5. $Cl\beta$ vs Alpha.....	137
H6. $C_{m_{\delta_e}}$ vs Alpha, Positive Deflection .....	137
H7. $C_{m_{\delta_e}}$ vs Alpha, Negative Deflection.....	138
H8. $C_{l_{\delta_e}}$ vs Alpha, Positive Deflection .....	138
H9. $C_{l_{\delta_e}}$ vs Alpha, Negative Deflection .....	139

Figure	Page
H10. $C_{n_{\delta_e}}$ vs Alpha, Positive Deflection .....	139
H11. $C_{n_{\delta_e}}$ vs Alpha, Negative Deflection .....	140
H12. $C_{m_{\delta_r}}$ vs Alpha, Positive Deflection .....	140
H13. $C_{m_{\delta_r}}$ vs Alpha, Negative Deflection.....	141
H14. $C_{l_{\delta_r}}$ vs Alpha, Positive Deflection .....	141
H15. $C_{l_{\delta_r}}$ vs Alpha, Negative Deflection .....	142
H16. $C_{n_{\delta_r}}$ vs Alpha, Positive Deflection .....	142
H17. $C_{n_{\delta_r}}$ vs Alpha, Negative Deflection .....	143



## CHAPTER 1

### INTRODUCTION

Future clean-sheet high-performance aircraft must push the boundaries of performance through marked improvements in speed, altitude and/or agility. In order for engineers to design such a vehicle, they must carefully evaluate many different attributes of the proposed system, for even on a subsonic aircraft “everything affects everything” when it comes to design, performance and costing. Many US government agencies, notably NASA and the Department of Defense have embraced the concept of “Model Based Systems Engineering” (MBSE) as an essential part of any new development plan.[1][2]

NASA defines MBSE as a “formalized application of modeling to support system requirements, design, analysis, verification and validation activities beginning in the conceptual design phase and continuing throughout development and later life cycle phases.”[1] Since MBSE is based on a “paradigm shift from document-centric engineering to model-based engineering,” engineers need to develop lean and flexible design evaluation tools to evaluate the flight performance of complex future flying machines. These tools can help “provide information that reduces the uncertainty about system performance, effectiveness, and suitability.” [1] Understanding the design features that make a flying machine a stable, controllable, and maneuverable platform is an important task for the aerodynamicist.

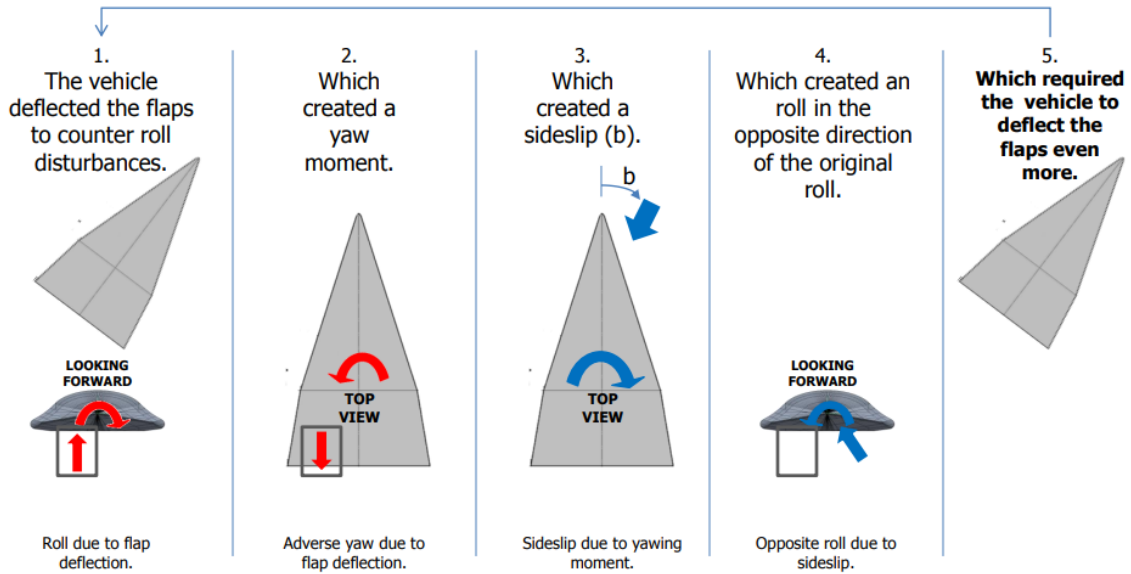
Since the United States Air Force has expressed considerable interest in developing clean-sheet high-speed platforms for atmospheric flight, these needs are particularly important since such a development can cost billions of dollars.[1][2][3]

Based on considerable experience with the Bell X-1, X-2, North American X-15 and Space Shuttle Orbiter; as well as the XB-70, the SR-71 and the various lifting body programs from the late 1960s, it is abundantly clear that high-speed maneuvering flight poses exceptional challenges to the designer.[4][5][6][7][8][9][10][11][12]

Under the best of circumstances, an aircraft configurator can shape the vehicle to be inherently stable in all three axes: pitch, roll and yaw. However, static stability alone is insufficient for successful maneuvering flight at these speeds. First, the proposed airframes must not exhibit “Control Coupling.” Control Coupling occurs when static yaw and roll stability interacts unfavorably with the moments from control surfaces in a manner that proves destabilizing; in other words, the adverse yaw of the roll control effectors over-power the static directional stability of an airframe.[5][13][14] When this occurs, pilots (or autopilots) can no longer trim their aircraft in yaw and roll. Aircraft response to control inputs might initially behave predictably, but then apparently ‘reverse;’ see Figure 1. Similarly, as flight speeds increase the balance between aircraft kinetic energy and aerodynamic damping forces change for the worse; the faster you fly, the more lightly damped even stable oscillatory modes become.[4][15]



## Roll-yaw coupling



**6.) Eventually, the adverse roll moment from the sideslip and disturbances overwhelmed the roll moment available from the differential flap deflections.**

Distribution Statement "A" (Approved for Public Release, Distribution Unlimited). DISTAR Case 16757.

FIGURE 1 - Explanation of Lockheed HTV-2 test flight #1 crash due to Control Coupling [14]

Beyond the identification of basic quasi-static analysis screening methods as discussed in Reference [4], the MBSE toolkit will need a collection of time-domain tools to assess the control power requirements of an airframe to command for example, a pitch without yaw or roll, a roll without pitch or yaw, or a yaw without a pitch or roll; the detailed time-domain simulation is beyond the scope of this thesis. At the same time, since flight at high speeds renders aerodynamic damping inherently ineffective, active control systems must develop synthetic damping to suppress the natural tendency of a statically stable airframe to oscillate in pitch (the longitudinal Short-Period) or roll/yaw (the Dutch Roll). Finally, since many designers wish to contemplate a weight savings by

reducing the size of stabilizing surfaces so that the basic airframe lacks inherent static stability in pitch, yaw and sometimes even roll, the MBSE toolkit needs time-domain tools to assess the control power requirements to achieve positive “synthetic static stability” on a multi-axis unstable airframe.

This thesis describes a methodology to help us understand the needs of that future MBSE framework for control power assessment. I will use the concept of the “Attainable Moment Set” to document if a simplified “pre-mix” approach to controls – i.e., where discrete control effectors - identified “up-front” to provide pitch, roll and yaw commands - can be used in the control power assessment tool.

Recall that most proposed aircraft are likely to feature complex flight control systems where every control surface on a vehicle can be independently commanded to develop necessary moments. Under such a paradigm, aerodynamics would develop a detailed “independent-single-panel” aerodynamic database that would be used to support the development of a much more complex set of flight control laws. This approach is tedious; it usually requires enough handwork to disrupt the pacing of rapid, MDO trades. A common work around would be for the MDO code to only consider the most superficial attributes of aircraft flight control, for example keeping static margin within bounds while neglecting all attributes of control surface sizing. Such an MDO process would hope “on a wing and a prayer” that the fin size was appropriate for successful detailed design.

If the simplified “pre-mix” approach to controls provides a reasonable quality assessment of total control power, it can then be incorporated as the basis for a “closed-

loop” MBSE control-power assessment tool that will smoothly integrate into an MDO process.

In this work, I will consider the difference in Attainable Moment Sets between a “pre-mix” and full “independent single panel” strategy for diverse configurations: a narrow body airliner reminiscent of the Airbus A320, the Bell X-2 Mach 3+ rocket plane, the North American X-15 hypersonic rocket plane, and a conceptual generic hypersonic vehicle.

## CHAPTER 2

### WHAT IS AN ATTAINABLE MOMENT SET?

Control allocation has been a necessary problem to solve for as long as control surfaces have been deployed on aircraft. As aircraft became more complex with more difficult mission sets, it has become evident that methods for allocating the control surface deflections in an effective and timely manner is an integral part of aircraft design. Bordignon, through work on his doctoral dissertation [16] and following work with Durham & Beck [17], addresses the concept of an Attainable Moment Set (AMS) as a method to understand the control surface deflections needed to attain a desired moment. His work focuses on methods for inverting a **B matrix** comprised of control effectiveness terms to provide the capability to readily yield the control deflections required for a given desired moment. In other recent works Zhang, et al. utilize similar concepts to derive an Attainable Moment Set and compare the results to a required moment set to validate the capabilities of a vehicle for its intended mission profile.[18] This thesis utilizes the useful visualization of moment capabilities presented by these past works in order to demonstrate the total Attainable Moment Set of a configuration as a means to assess the control power and trim capability of said vehicle.

To construct an AMS envelope, one must generate the basic aerodynamics as well as a control effectiveness matrix (CEM) for the desired flight conditions, upon which the range for which the control surfaces can be deflected is applied. In a CEM, each row indicates a moment about a principal axis: Pitch, Roll, and Yaw. The method for generating an attainable moment set only concerns the control effectiveness values about these axes; lift, drag and side force are not necessary for this procedure.

Each column entry of the control effectiveness matrix is a measure of how much a deflection in that control surface affects the moment generated in the principal axes. The method for calculating these is shown in Equations 1-3, where terms related to the dynamic derivatives have been neglected.

$$CPM = \left[ C_m + C_{m_{\delta_r}} \delta_r + C_{m_{\delta_a}} \delta_a + C_{m_{\delta_e}} \delta_e \right] \quad (1)$$

$$CRM = \left[ C_{l_\beta} \beta + C_{l_{\delta_r}} \delta_r + C_{l_{\delta_a}} \delta_a + C_{l_{\delta_e}} \delta_e \right] \quad (2)$$

$$CYM = \left[ C_{n_\beta} \beta + C_{n_{\delta_r}} \delta_r + C_{n_{\delta_a}} \delta_a + C_{n_{\delta_e}} \delta_e \right] \quad (3)$$

In the convention above,  $C_m$ ,  $C_l$ , and  $C_n$ , are the moment coefficients in pitch, roll, and yaw, respectively. Each subscript considers the change in that moment coefficient due to that value. For example,  $C_{m_{\delta_r}}$  can be read as the change in pitching moment coefficient due to rudder incidence. Functionally this would describe the dimensionless change in the nose up incidence due to a change in the rudder deflection, which would be expected to be marginal in typical conditions. In a classically configured transport-category aircraft, such as an A320, we would expect the elevator to be the primary pitch effector, which would translate to the  $C_{m_{\delta_e}}$  being the largest value for that model,  $C_{m_{\delta_r}}$  and  $C_{m_{\delta_a}}$  should be marginal – still nonzero - in this scenario. In less conventional configurations, it is possible that the control surfaces are no longer a pitch effector or roll effector alone, but rather have a significant impact on multiple moments in our primary axes. It is due to this possibility that the equations are formulated in a way to account for each control surface's effect on each of the axes in question. For more complicated configurations Equations 1-3 can be easily expanded to include the change in moment due to control surface deflection in any combination.

The AMS can be quite useful for a quick computation of the trim capability of an aircraft at a given flight condition. To trim, an aircraft must achieve a net zero moment in all three principal axes, which is quickly recognized as the origin of a 3-D space. Thus, if the origin is within the bounds of an AMS, then that vehicle can trim at that flight condition. In addition to an “at a glance” determination of trim, an AMS provides a visual in which it is easy to determine the relative degree of control power available in the principal axes, where a typical configuration will have much more pitching moment capability followed by rolling moment and then yawing moment. While the visualizations provided in this thesis may not directly provide an assessment of control surface saturation, it can also be inferred by the volumes which moment is lacking should trim not be achieved which could lead to an intelligently chosen next iteration of a design to achieve more favorable results.



## CHAPTER 3

### ESTIMATING AERODYNAMIC STABILITY & CONTROL DATA

VORLAX [19][20] is a legacy panel method code that gives valid aerodynamic data in both the subsonic and supersonic regimes. From an input file to create the geometry of the vehicle, VORLAX generates a grid on the surface and yields accurate pressure distributions, from which lift coefficients and induced drag are solved for. An example of the pressure information from VORLAX plotted onto a model is shown in Figure 2. VORLAX allows for many types of models to be constructed, from flat-plate models with no control surface paneling to full fusiform bodies and control surfaces both modeled and deflected at specific angles. In this study, flat-plate models were created for the Bell X-2, North American X-15, an Airbus A320, and the GHV.

The base cases of these models can be found in APPENDIX A, and the aerodynamic data generated from them is shown in APPENDIX B-H. The reader should note that the primary use of this data comes in the form of the moment effectiveness terms but other basic data is shown to demonstrate the completeness of the models. The importance of the other data provided, for example  $CL$  vs  $\alpha$  and  $CL$  vs  $C_m$ , is not discounted, however they are not necessary for the generation of attainable moment sets as described in this thesis. With a code such as VORLAX providing all of the data that is shown in this thesis, it is clear that my method of generating and evaluating an attainable moment set should be easy to integrate in any design process that already uses a similar code.

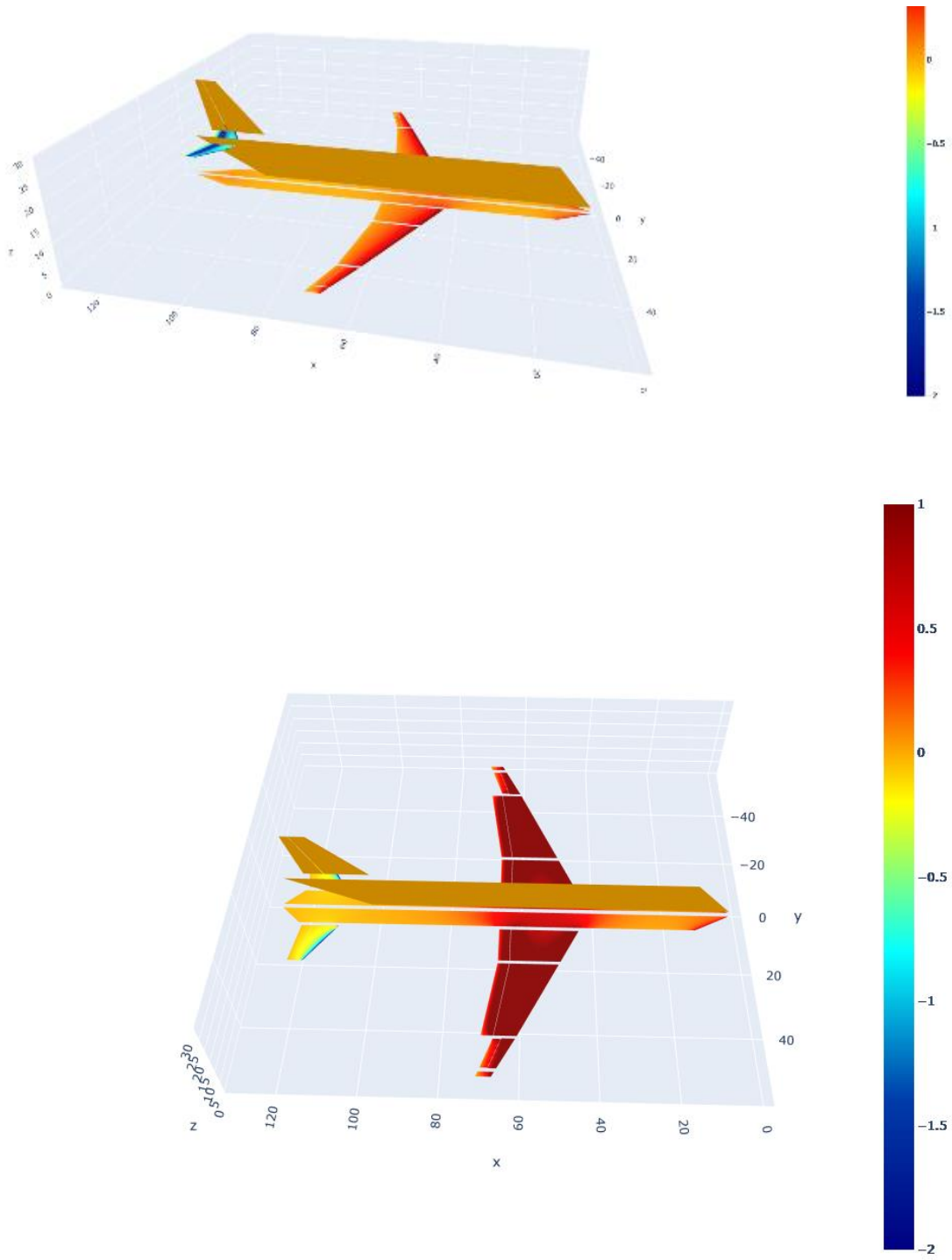


FIGURE 2 – Pressure Plot, A320 VORLAX Model with Elevators Deflected (Top) and with flaps extended (Bottom)

Using VORLAX, I developed aerodynamic databases for configurations of interest. For example, the basic low-speed (Mach = 0.2) controls-neutral database for the reverse engineered A320 – with flaps extended to the landing position ( $\delta_F=35$ -deg) and retracted – is seen in Figures 3 through 6. Data like this was generated for each vehicle, from which the aerodynamic derivatives that comprise the control effectiveness matrices are determined.

This sort of data reveals some interesting characteristics. As was expected, Figure 3 showed an increase in the zero-angle-of-attack lift coefficient from negligible at flaps zero to  $CL \sim 1.3$  when the flaps are extended. The extra lifting area of the CONF FULL deflected and extended Fowler flaps increases the slope of lift vs  $\alpha$  as well. Turning next to Figure 4, the baseline aircraft is  $\sim 20\%$  stable and self-trims around  $CL \sim 0$ ; with the landing flaps extended the vehicle develops a strong nose-down pitching moment.

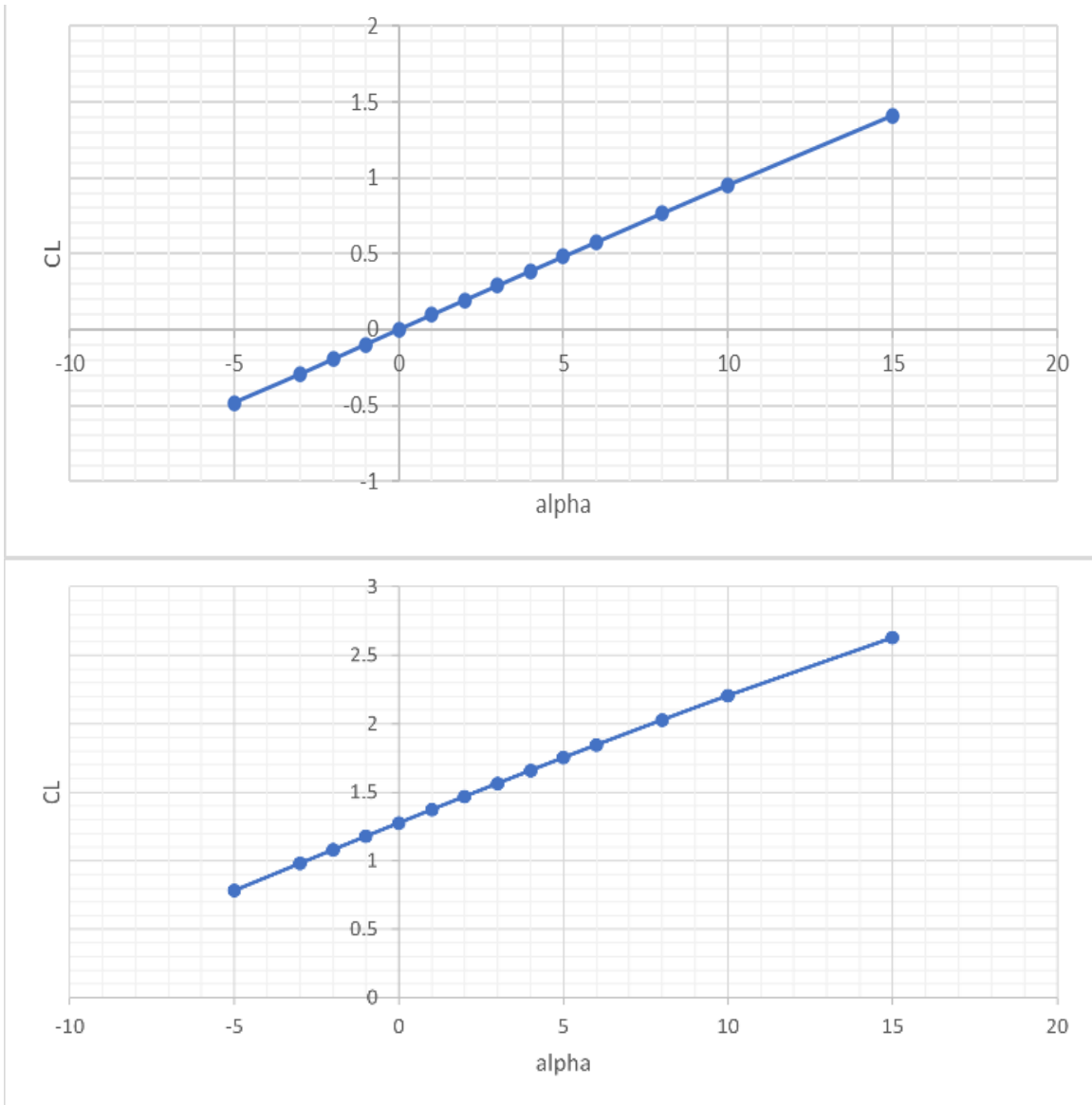


FIGURE 3 – Reverse-Engineered A320 – CL vs Alpha – flaps retracted (TOP) and CONF FULL flaps extended (BOTTOM)

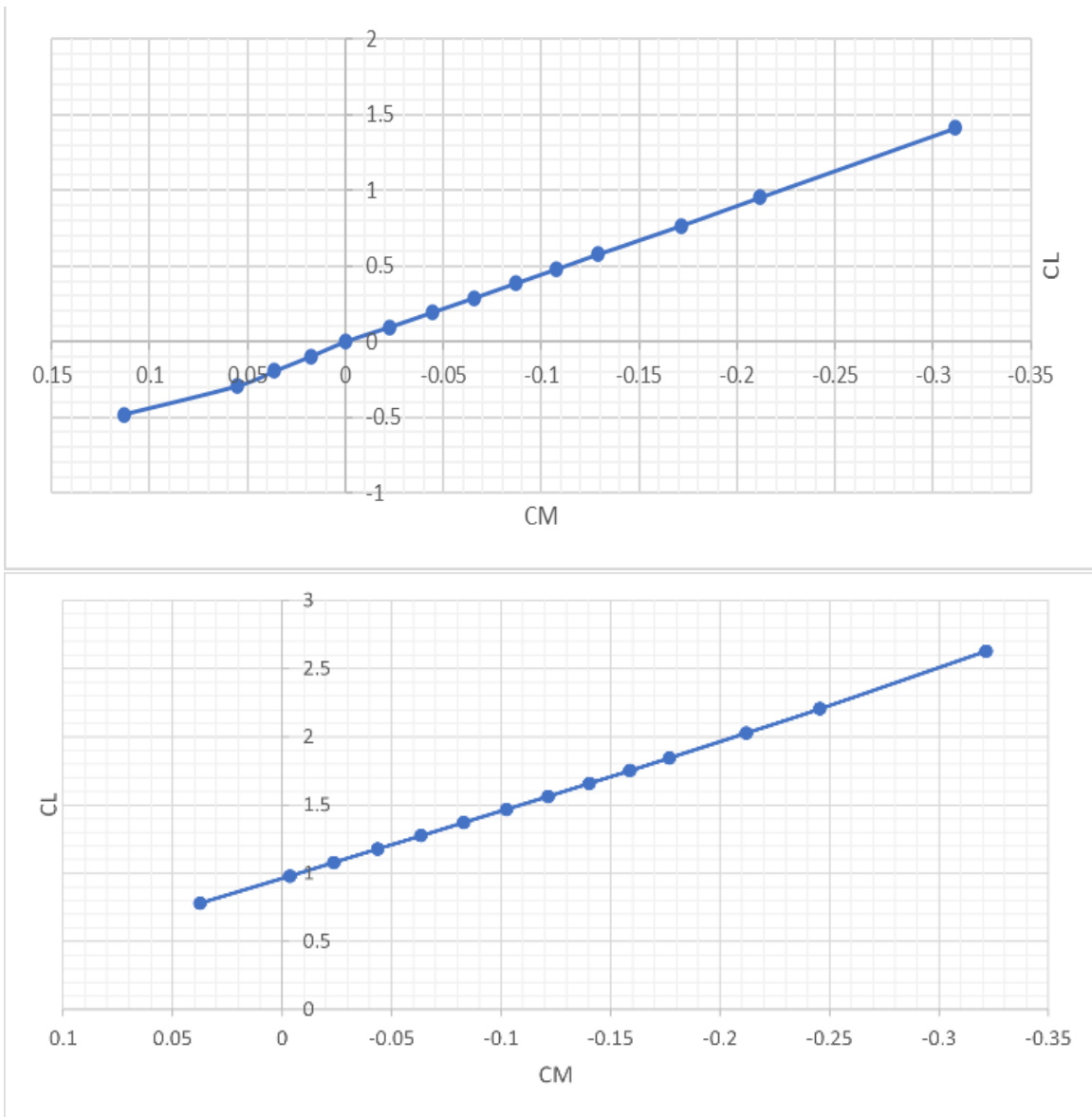


FIGURE 4 - Reverse-Engineered A320 – Longitudinal Stability - CL vs Cm –flaps retracted (TOP), CONF FULL flaps (BOTTOM)

Turning next to Figures 5 and 6, extending the flaps marginally increases the directional stability, while the dihedral effect is approximately 4 times as strong at negative angles of attack and decreases to 1.5 times as strong at the highest angles of attacks compiled.

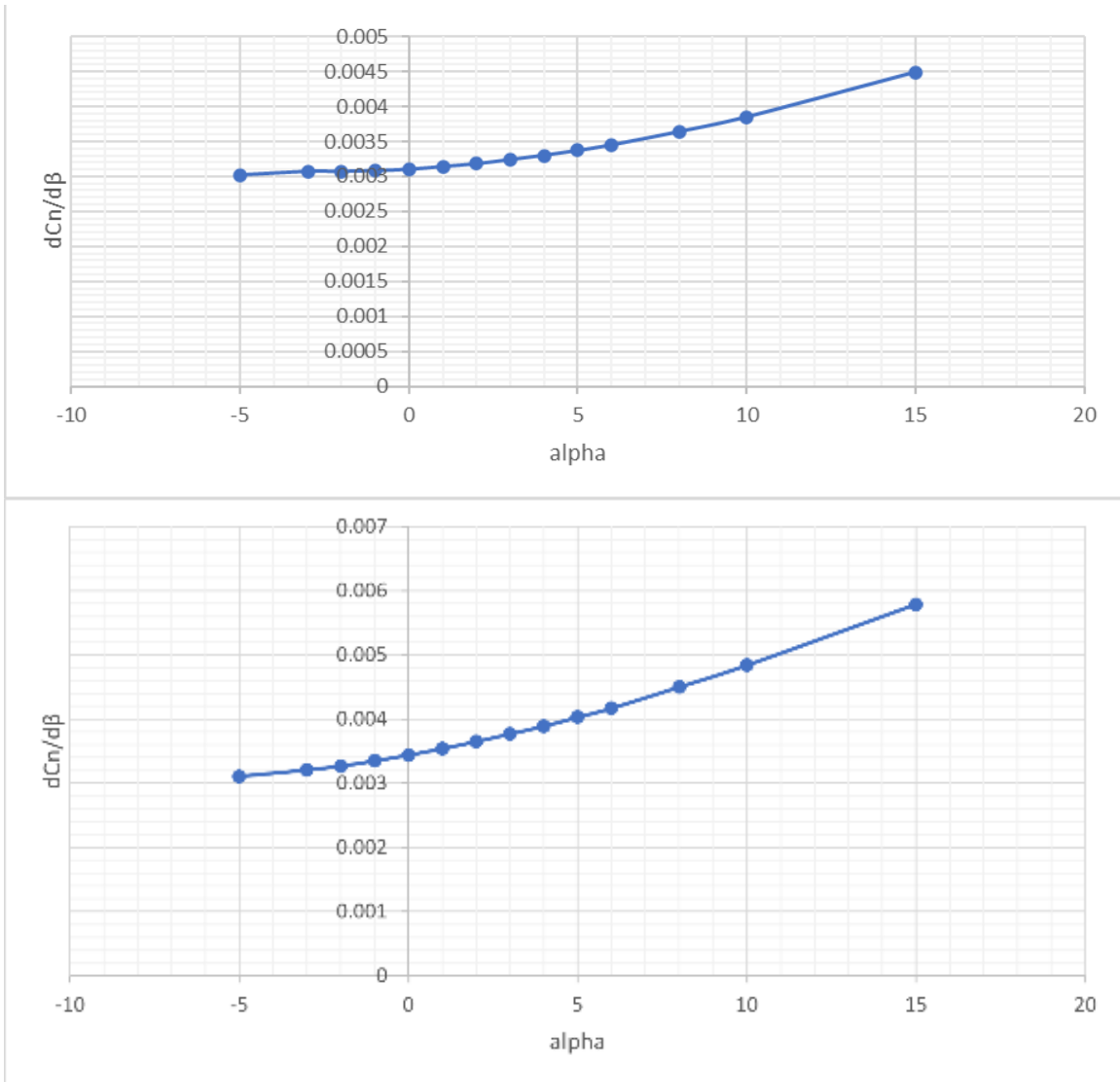


FIGURE 5 - Reverse-Engineered A320 – Directional Stability -  $C_n\beta$  vs Alpha – flaps retracted (TOP), CONF FULL flaps (BOTTOM)

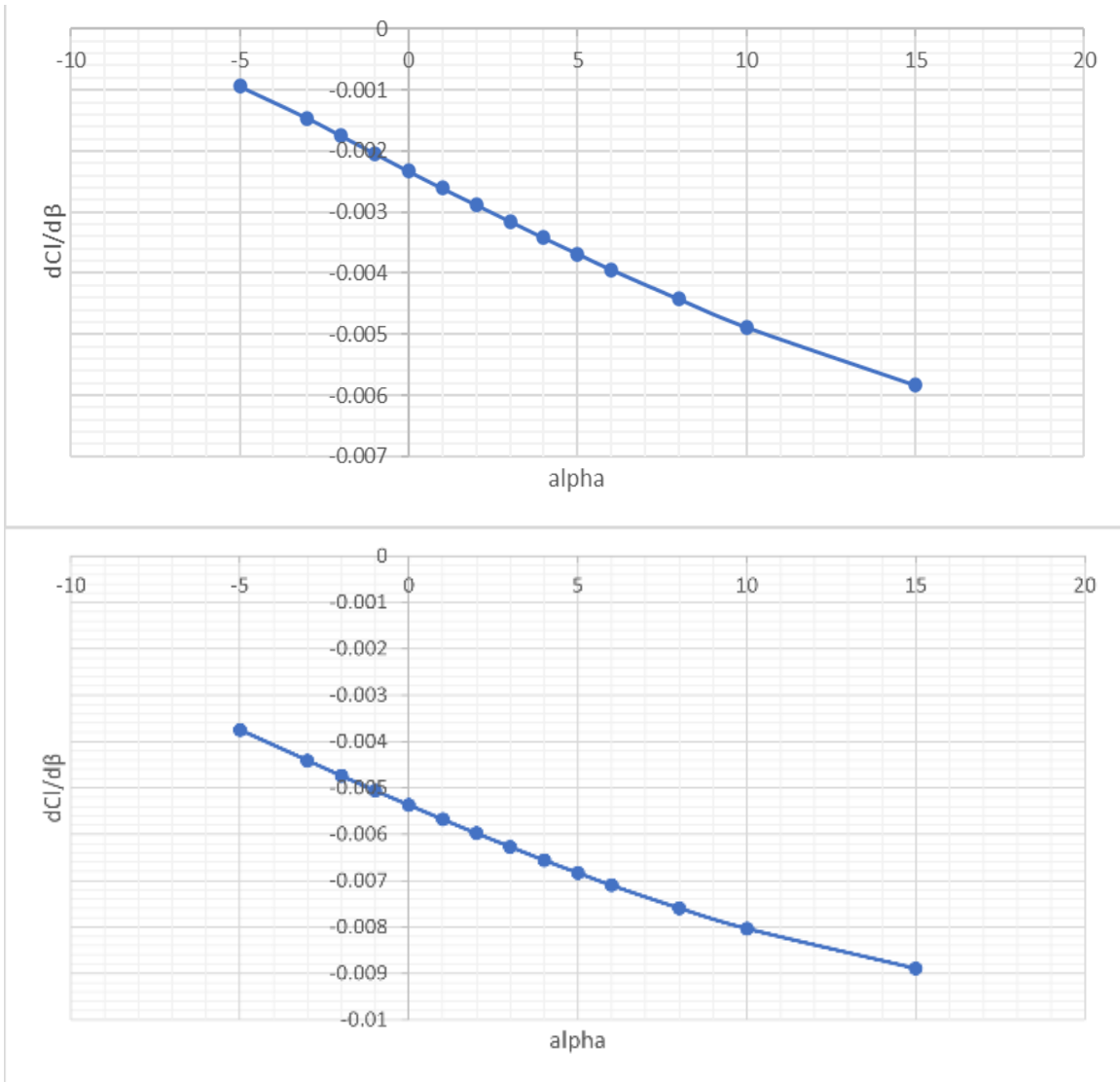


FIGURE 6 - Reverse-Engineered A320 – Dihedral Effect -  $Cl_\beta$  vs Alpha –flaps retracted (TOP), CONF FULL flaps (BOTTOM)

### A. Pre-Mix Model

The “Pre-mix” model used in this study takes the existing model for a vehicle, and schedules pairs of control surfaces, such as ailerons or elevators, as antisymmetric in their deflections. For the A320 and the X-2, I consider the aileron control to be the physical wing mounted control surfaces. A VORLAX visualization of the Bell X-2 Pre-Mix model can be seen in Figure 7. In this paradigm, when the right aileron deflects

trailing edge up ten degrees, the left aileron will deflect trailing edge down ten degrees. For the X-15 configuration, I consider a derivative of the actual flown aircraft – one with articulated trailing-edge “aileron” surfaces on the main wing. Recall that the actual X-15 used its wing trailing edge surfaces purely as flaps for landing and that all roll control in flight was developed using differential movements of its all-moving horizontal tail fins.

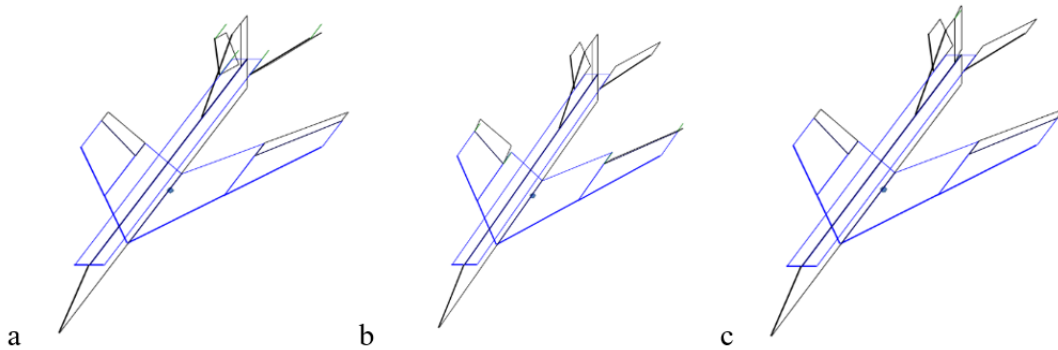


FIGURE 7 – Example Control Surface Deflections for a “Pre-Mix Model” – a) collective elevator, b) anti-symmetric aileron, c) rudder

The panel method VORLAX generated the aerodynamic database from which the control effectiveness matrix was procedurally generated. Several cases were needed to provide sufficient data to construct a CEM: A controls-neutral case at zero sideslip, a controls-neutral case at a non-zero sideslip, and case for each control surface deflected at some controlled value. These cases in combination with each other allowed for a determination of the change in Pitch, Roll, and Yawing moment coefficient due to an arbitrary deflection of any control surface deflection, resulting in the CEM seen below in Equation 4. It is noteworthy that this matrix is only applicable to a single flight condition, a combination of Mach, Alpha, and  $\beta$  (sideslip). This iteration of the modeling process assumes a linear relationship between the control surface deflection angle, and the change in moment coefficient generated, so linear interpolation was utilized between the



maximum value and the controls neutral case in order to fully inform the CEM at all control surface deflections.

$$\begin{bmatrix} CPM \\ CYM \\ CRM \end{bmatrix} = \begin{bmatrix} C_m & 0 & C_{m\delta_r} & C_{m\delta_a} & C_{m\delta_e} \\ 0 & C_{n\beta} & C_{n\delta_r} & C_{n\delta_a} & C_{n\delta_e} \\ 0 & C_{l\beta} & C_{l\delta_r} & C_{l\delta_a} & C_{l\delta_e} \end{bmatrix} \begin{bmatrix} 1 \\ \beta \\ \delta_r \\ \delta_a \\ \delta_e \end{bmatrix} \quad (4)$$

Classical configurations such as the Airbus A320 often require the use of flaps in takeoff and landing scenarios, and their use can have a significant impact on control surface effectiveness. To capture this, a model was made using VORLAX for the A320 both with and without flaps. Below in Figures 8-11 are some comparisons between the models. It was expected that the two models should exhibit similar trends for their control surface effectiveness, which was the case, with only marginal differences between them. The control power from the collective elevator is shown in Figure 8, and while the extremely negative angles of attack show a decreased ability to generate pitching moment for the flaps retracted, at all other alphas the values were virtually the same. The greatest difference between the two models was seen in the roll control from the aileron, shown in Figure 9, where there was an approximately 14% increase in the rolling moment due to aileron deflection at all angles of attack. Figures 10-11 again showed only marginal differences between the model types, however the adverse yaw from the aileron deflection noticeably was always negative when the flaps were retracted, however when the flaps were full some positive values were seen.

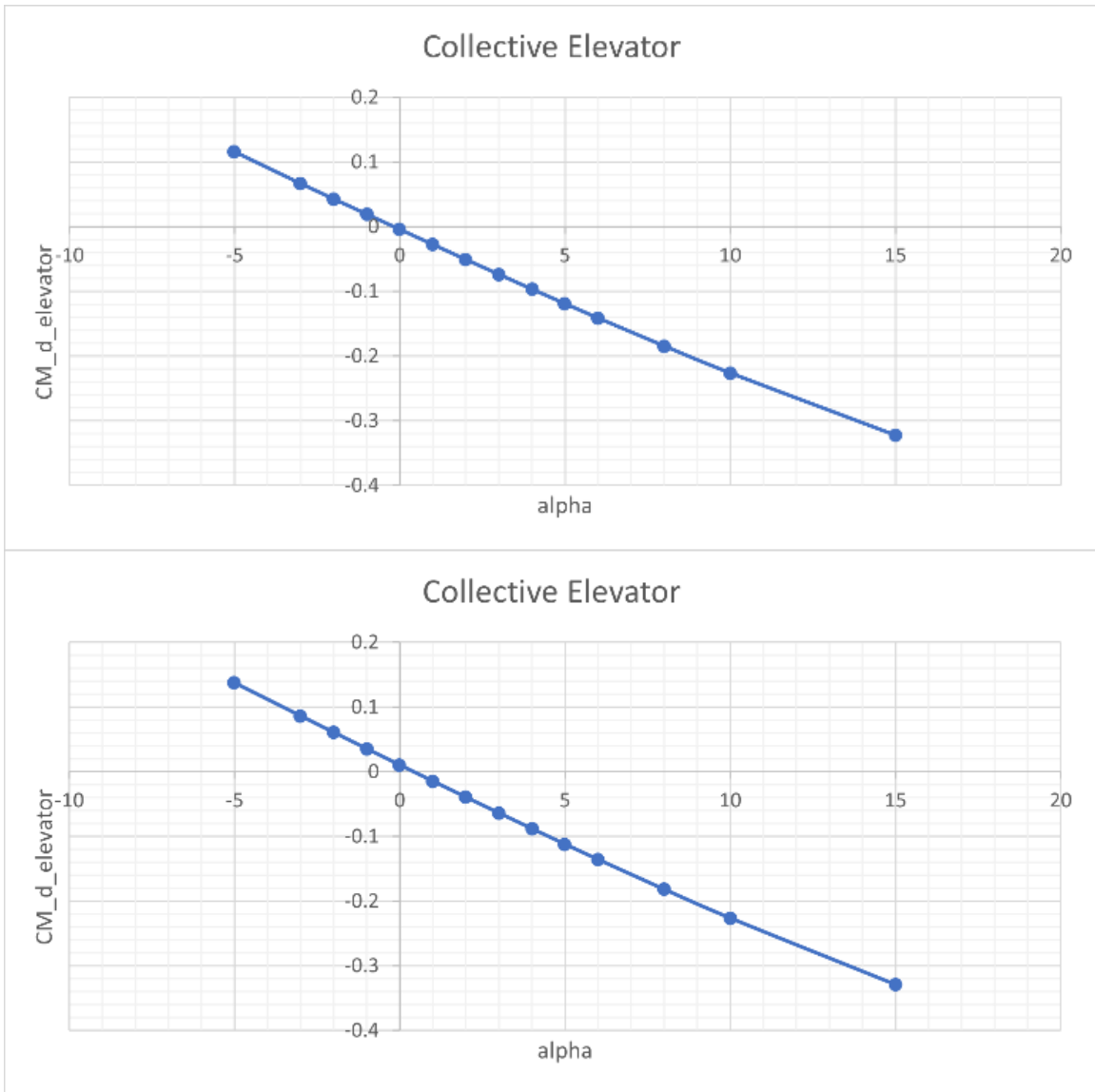


FIGURE 8 - Reverse-Engineered A320 – “Collective Elevator” control power –  $Cm_{\delta_e}$  vs Alpha – flaps retracted (TOP), CONF FULL (BOTTOM)

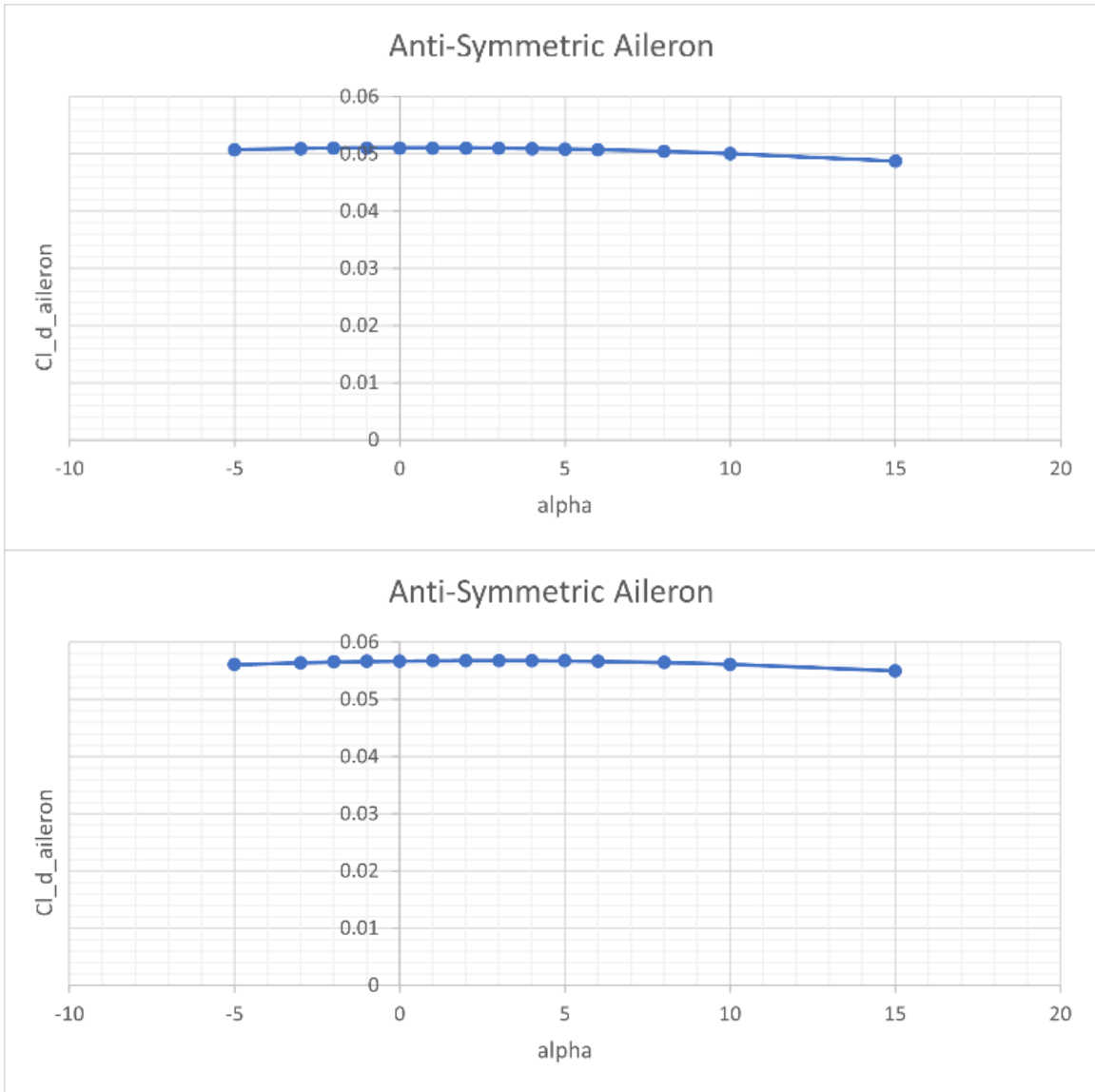


FIGURE 9 - Reverse-Engineered A320 – “Anti-Symmetric Aileron” control power –  $Cl_{\delta a}$  vs Alpha – flaps retracted (TOP), CONF FULL (BOTTOM)

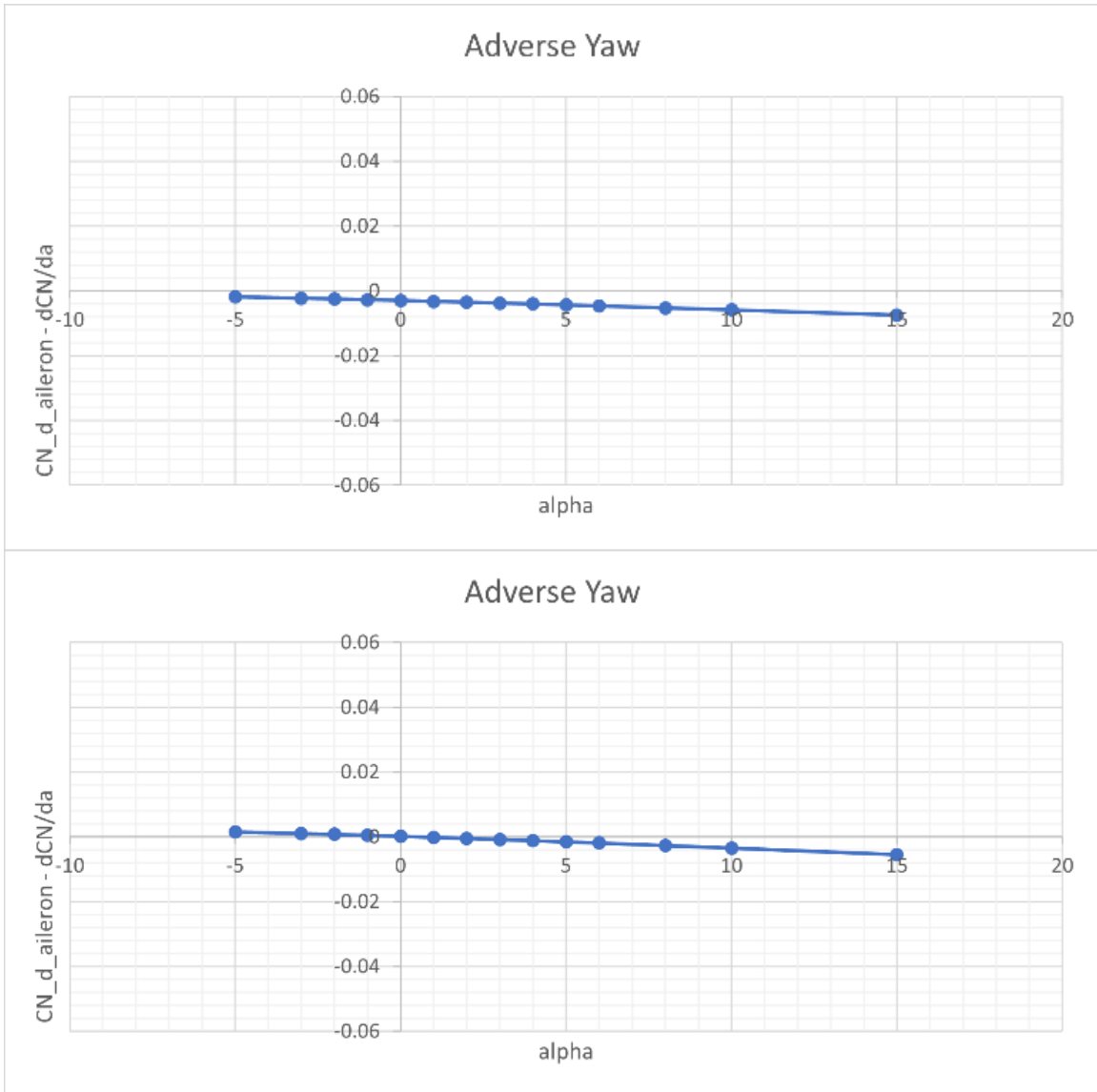


FIGURE 10 - Reverse-Engineered A320 – Adverse Yaw from “Anti-Symmetric Aileron” control power –  $Cn_{\delta a}$  vs Alpha, flaps retracted (TOP), CONF FULL (BOTTOM)

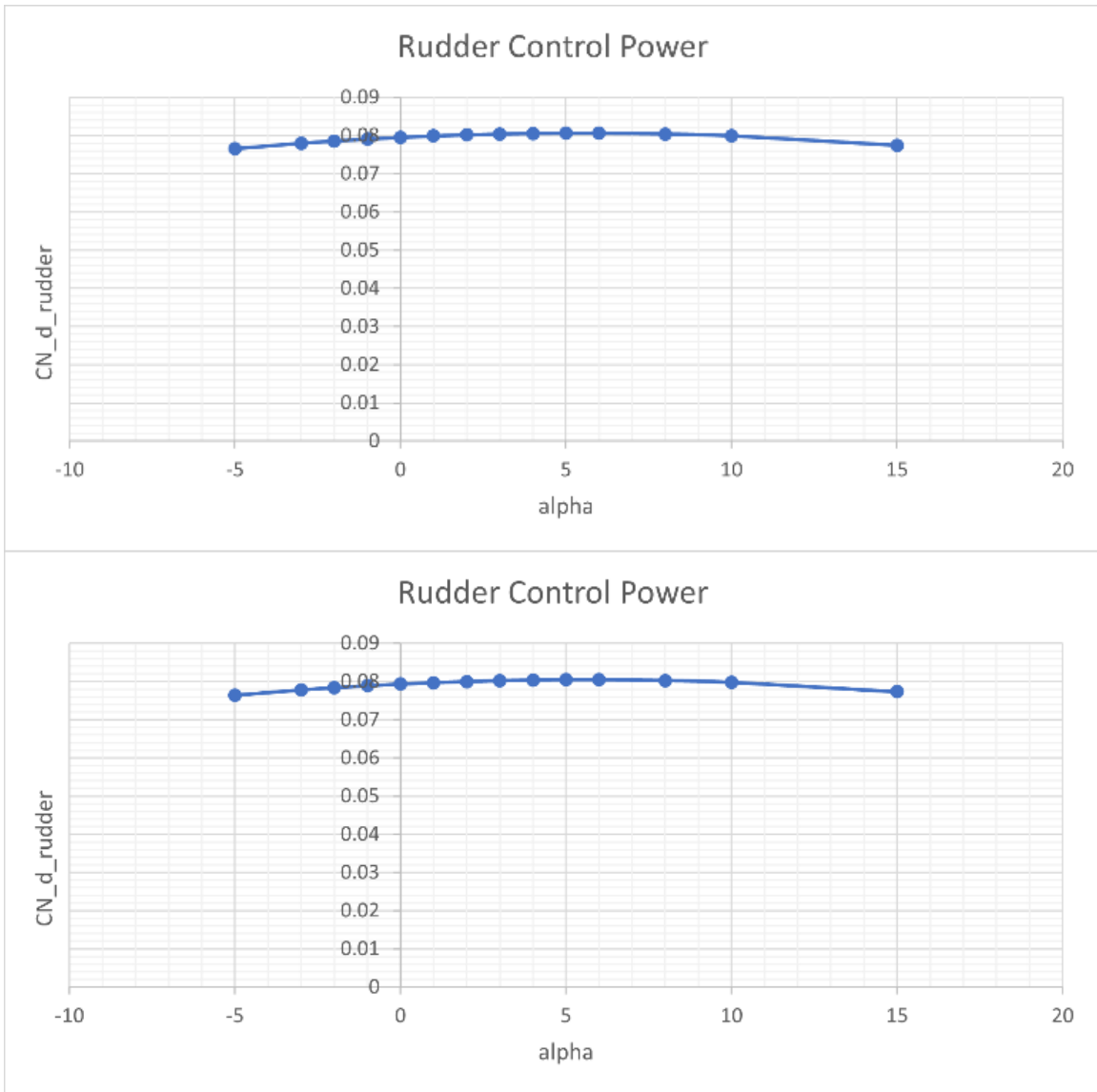


FIGURE 11 - Reverse-Engineered A320 – “Rudder” control power –  $Cn_{\delta}$  vs Alpha, flaps retracted (TOP), CONF FULL (BOTTOM)

### B. Independent Single Panel Model

Differing slightly from the Pre-Mix model discussed above, the Independent Single Panel (ISP) model allows the elevators and ailerons to independently deflect from one another. This allows for scheduling of the control surfaces to provide a wider range of moments generated to trim, counteract adverse effects of other control surface deflections, and account for the variation in rolling moment generated by a positive

deflection compared to a negative deflection. The latter is likely the most relevant, since a trailing edge down deflection of the aileron has a significantly different effect on the rolling moment compared to the trailing edge up case due to the change in the aerodynamic center location due to a negative deflection.

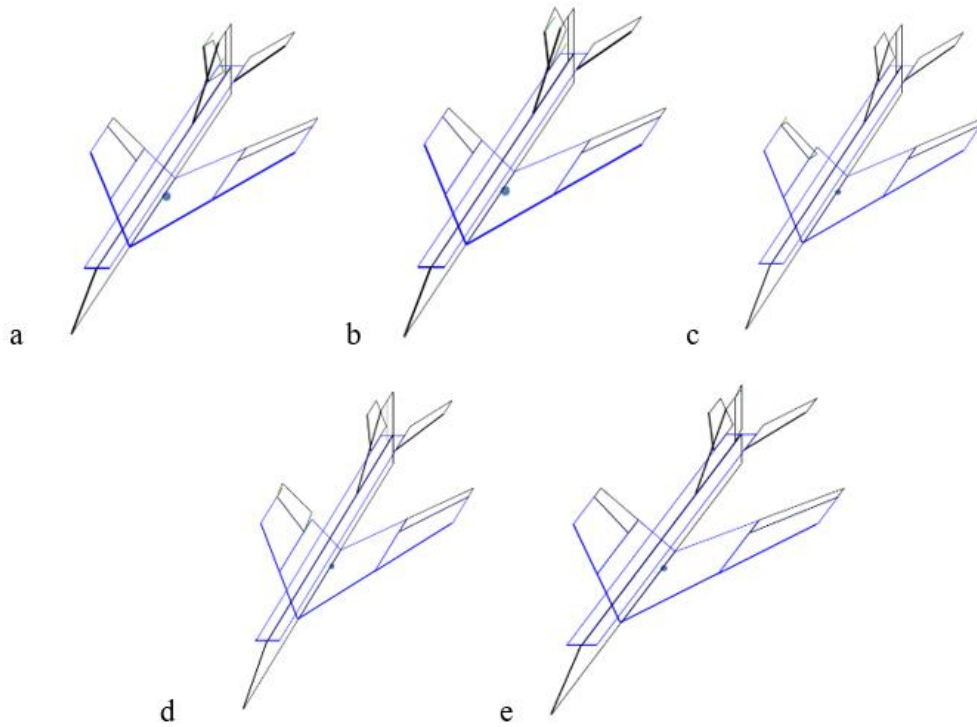


FIGURE 12 – Example Control Surface Deflections for an “Independent-Single-Panel Model” – a) RH elevator down, b) RH elevator up, c) RH Aileron down, d) RH Aileron up, e) rudder

As with the Pre-mix Model, several VORLAX cases were used to develop the CEM, with the notable difference being that in addition to all those referenced in the Pre-Mix Model process the aileron case is split into a single sided aileron deflected both up and down rather than a single antisymmetric case. This change resulted in a CEM seen in Equation 5 for each flight condition desired. Equation 5 is representative of the CEM for

the reverse-engineered A320, Bell-X2, as well as the “Son-of-X15.” These are examples of how this procedure is flexible enough to be utilized for generating attainable moment sets to account for whatever control surface configuration a vehicle uses.

$$\begin{bmatrix} CPM \\ CYM \\ CRM \end{bmatrix} = \begin{bmatrix} C_m & 0 & C_{m\delta_r} & C_{m\delta_{Right\ aileron}} & C_{m\delta_{Left\ aileron}} & C_{m\delta_{Right\ elevator}} & C_{m\delta_{Left\ elevator}} \\ 0 & C_{n\beta} & C_{n\delta_r} & C_{n\delta_{Right\ aileron}} & C_{n\delta_{Left\ aileron}} & C_{n\delta_{Right\ elevator}} & C_{n\delta_{Left\ elevator}} \\ 0 & C_{l\beta} & C_{l\delta_r} & C_{l\delta_{Right\ aileron}} & C_{l\delta_{Left\ aileron}} & C_{l\delta_{Right\ elevator}} & C_{l\delta_{Left\ elevator}} \end{bmatrix} \begin{bmatrix} 1 \\ \beta \\ \delta_r \\ \delta_{Right\ a} \\ \delta_{Left\ a} \\ \delta_{Right\ e} \\ \delta_{Left\ e} \end{bmatrix} \quad (5)$$

The reader should note that a single data set for both ailerons and elevators in this configuration. Each single panel was captured moving both up and down to develop a piecewise linear understanding of control power; pitch, roll and yaw responses may differ between the trailing-edge up and the trailing-edge down conditions. Since the reference independent-single-panel model is a “right-handed” model, I mapped the effects of moments across the line of symmetry of the vehicle. The left-hand control surface will have opposite “sign” moments and side-forces compared to the right-hand surface. Equations 6-9 show the definition of values for the left-hand aileron (LHA) in relation to the right-hand aileron (RHA) used to calculate the aerodynamic derivatives.

$$CY_{LHA} = -1 * CY_{RHA} \quad (6)$$

$$CYM_{LHA} = -1 * CYM_{RHA} \quad (7)$$

$$CRM_{LHA} = -1 * CRM_{RHA} \quad (8)$$

$$CPM_{LHA} = CPM_{RHA} \quad (9)$$

Similarly, Equations 10-13 show the definitions of values for the left-hand elevator (LHE) in relation to the right-hand elevators.

$$CY_{LHE} = -1 * CY_{RHE} \quad (10)$$

$$CYM_{LHE} = -1 * CYM_{RHE} \quad (11)$$

$$CRM_{LHE} = -1 * CRM_{RHE} \quad (12)$$

$$CPM_{LHE} = CPM_{RHE} \quad (13)$$



## CHAPTER 4

### RESULTS

In this section, the Attainable Moment Sets are generated using Equations 4-5 are shown for four different vehicles. The aerodynamic derivatives calculated have been normalized to the effectiveness of each control surface per degree of control surface deflection. The solution to these equations were calculated for each possible deflection of the control surfaces up to their respective limits for each vehicle using a linear approximation of the control surface effectiveness, and thus generate a 3-D volume of attainable moments. Each plot displays the capabilities of the pitching moment coefficient ( $CPM$ ), yawing moment coefficient ( $CYM$ ), and the rolling moment coefficient ( $CRM$ ). Also noted on each plot in the form of a red dot is the trim point (the origin) as this represents zero effective rate of change in the orientation of the aircraft in this analysis. I have done my best to represent these 3-D results as effectively as possible in this 2-D format, though at some points it may be difficult to discern the location of the trim point relative to the AMS volume. In cases where this is true, the respective discussion for that figure makes the results clear. Also presented below will be a case of the attainable moment set with the planes of zero deflection for each control surface overlaid, and while this may make the figure overly busy it does provide insight into the saturation of control surfaces to provide trim.

It should be noted that control surfaces on a vehicle are not simply used to trim a vehicle, they also provide the moments necessary to perform maneuvers, augment stability characteristics, and reject deviations in orientation due to wind gusts. The results

below do not incorporate a margin for a design to deem what would be acceptable performance.

## **1. Bell X-2**

The Bell X-2 is a very well-known aircraft for being an unassuming, yet deadly experimental aircraft in pursuit of supersonic flight. The flight characteristics – and limitations in the flight envelope – are well established in the literature, which led to this aircraft being an excellent choice for validation of the methods discussed in this thesis. Both Pre-Mix and Independent Single Panel models were developed, from which the AMS were generated for several relevant flight conditions; see Figure 13. A low Mach / high alpha case was tested, both at no side slip and at high sideslip, as is shown in Figures 14-15 to determine the performance of the Bell X-2 in landing scenarios. We also consider a subsonic and supersonic level flight case and a supersonic maneuvering flight case, all at modest sideslips; see Figures 16-19. The use of the Independent Single Panel model, as will hold true for all cases, provides an increased volume of the Attainable Moment Set, allowing more possible commanded moment combinations in the principal axes.

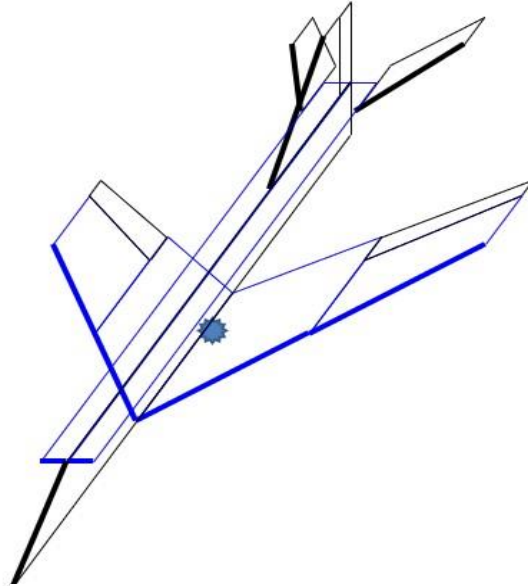


FIGURE 13 Line art of Bell X-2

Sub surfaces of the attainable moment set are shown in Figure 17, showing moment capabilities of the X-2 model when a control surface is held constant at zero. In the Pre-Mix Model these surfaces take the form of planes within the volume of the total attainable moment set. In the Independent Single Panel model, these surfaces were necessarily more complex than a flat plane due to the nature of the data they are derived from. In the ISP model, the elevators and ailerons acting independently cause an increase in the surface of zero deflection for any of the surfaces. Instead of holding one variable (control surface) constant in a three variable system we are holding either one variable (in the case of the rudder) or two variables (in the case of the elevators or ailerons) constant in a five-variable system. While this view certainly makes the visualization much more cluttered, it does demonstrate the contribution of each of the control surfaces more clearly than the attainable moment set alone.

Sideslip has a drastic impact on the X-2's ability to perform maneuvers while maintaining trim capability. For both models, the AMS moves from firmly centered

around the origin in the case of low sideslip to the point where trim requires a majority of the control surface's possible deflection. (Figures 14-15) The next flight condition represents the aircraft in approach to land at a moderate speed and angle of attack. Figures 16-17 show the AMS for this condition, and maintains the same overall shape and trim capability, though does exhibit a larger volume than the first case. With the approach case being flown at a moderate speed of Mach 0.8, the effectiveness of the control surfaces is clearly greater than at low speeds. For both initial cases the Pre-mix model AMS is box-like; the capabilities in each axis do not strongly depend on the other axes. The Independent Single Panel model maintains the same general trends as the Pre-mix model; the utilization of the control surfaces independently yields a much greater volume of attainable moments. For both, the ability to generate a positive rolling moment (*CRM*) decreases as the yawing moment (*CYM*) increases, and vice versa. Both models predict no issues with the trim condition, though the set of maneuvers that the X-2 will be able to perform are implied to be quite different depending on the control allocation.

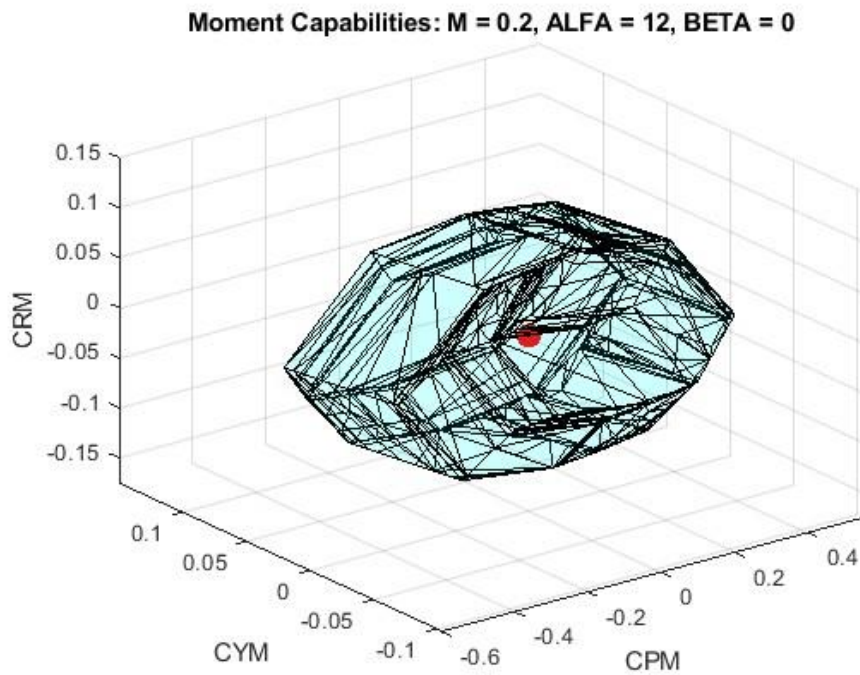
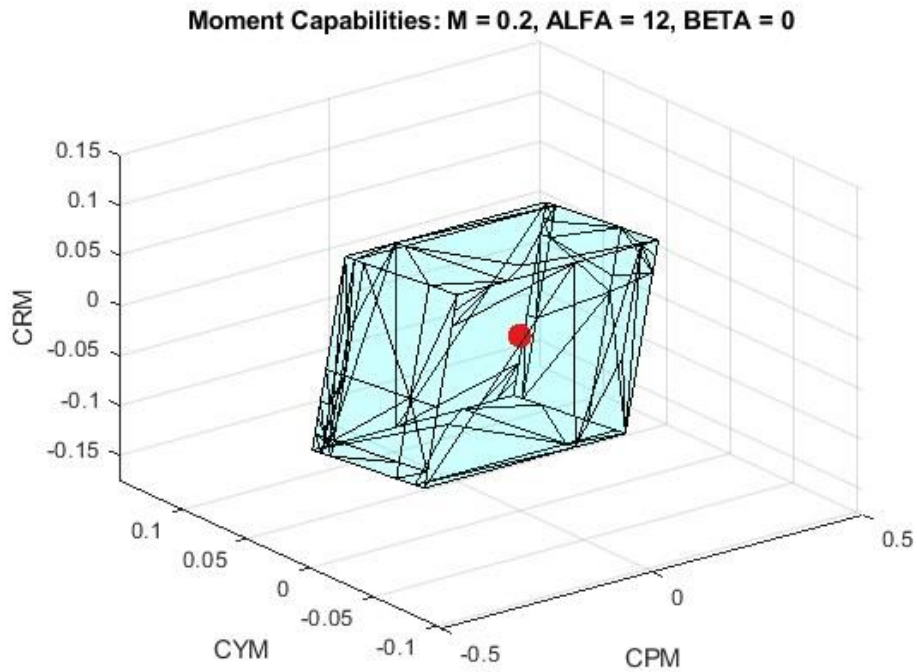


FIGURE 14 - Bell X-2 Attainable Moment Set during Landing at Mach = 0.2, Alpha = 12°,  $\beta = 0^\circ$ . Pre-Mix (TOP), Independent Single Panel (BOTTOM)

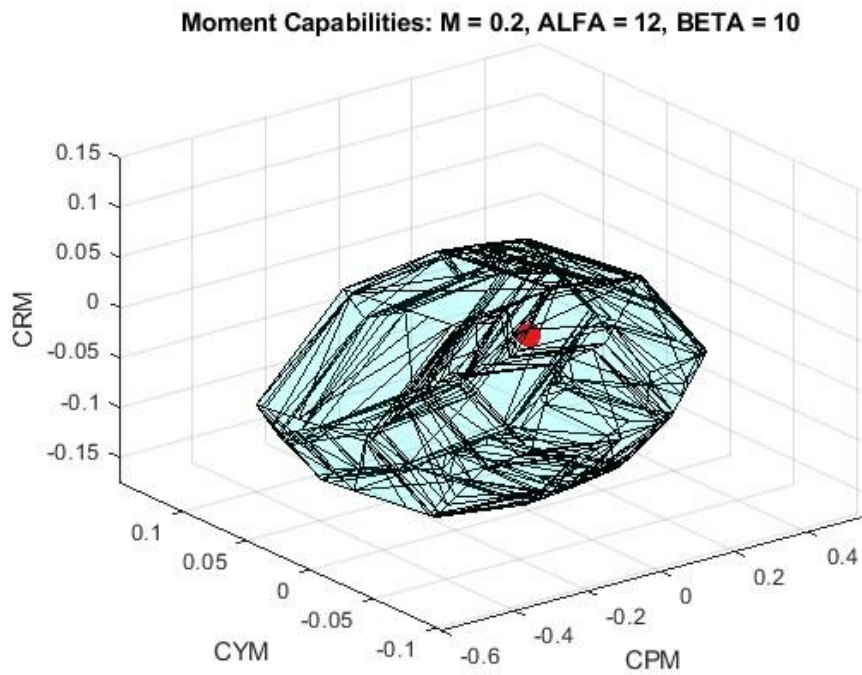
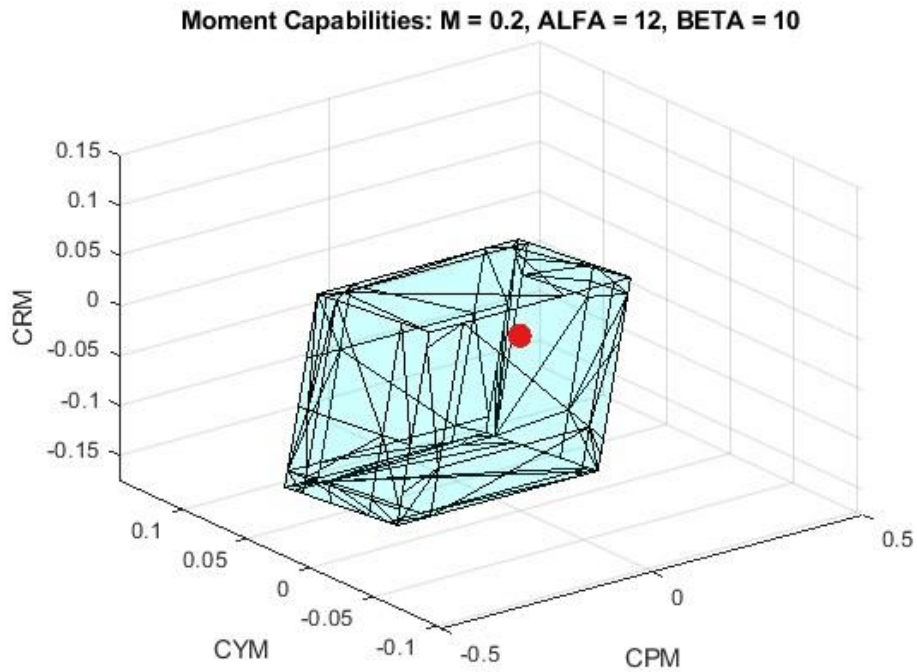
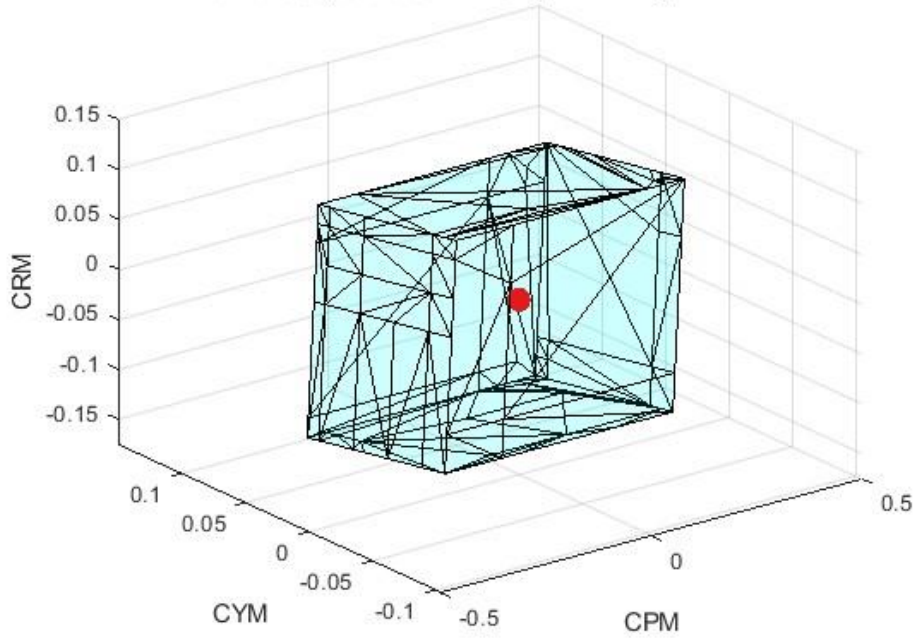


FIGURE 15 - Bell X-2 Attainable Moment Set During Crosswind Landing at Mach = 0.2,  $\alpha = 12^\circ$ ,  $\beta = 10^\circ$ . Pre-Mix (TOP), Independent Single Panel (BOTTOM)

**Moment Capabilities: M = 0.8, ALFA = 6, BETA = 1**



**Moment Capabilities: M = 0.8, ALFA = 6, BETA = 1**

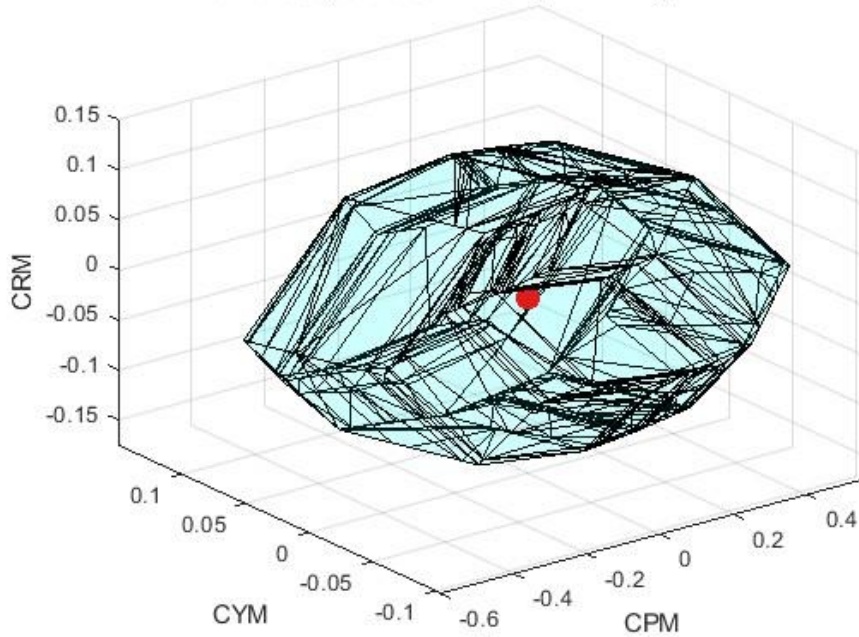
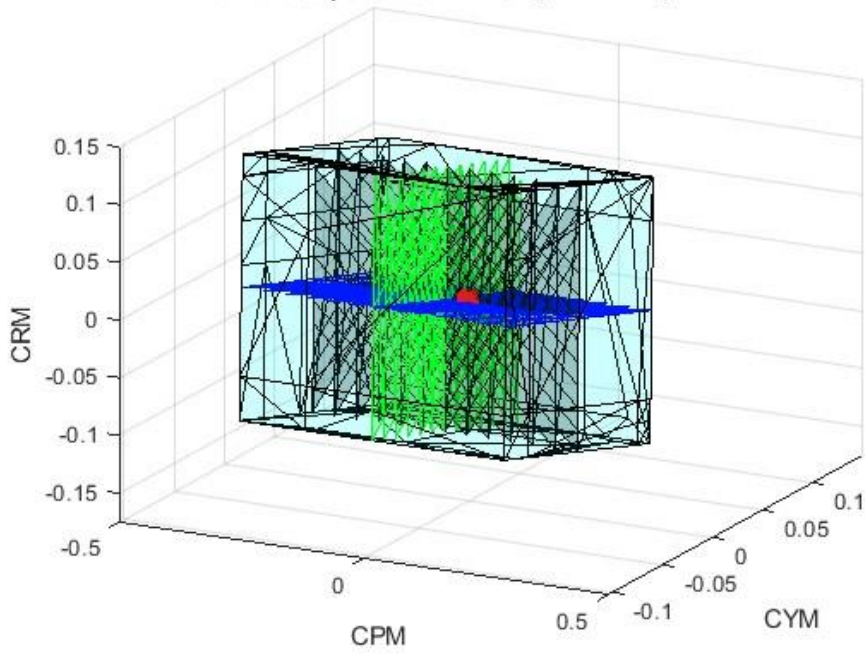


FIGURE 16 - Bell X-2 Attainable Moment Set During Subsonic Gliding Flight at Mach = 0.8, Alpha = 6°,  $\beta$  = 1°. Pre-Mix (TOP), Independent Single Panel (BOTTOM)

Moment Capabilities:  $M = 0.8$ ,  $\text{ALFA} = 6$ ,  $\text{BETA} = 1$



Moment Capabilities:  $M = 0.8$ ,  $\text{ALFA} = 6$ ,  $\text{BETA} = 1$

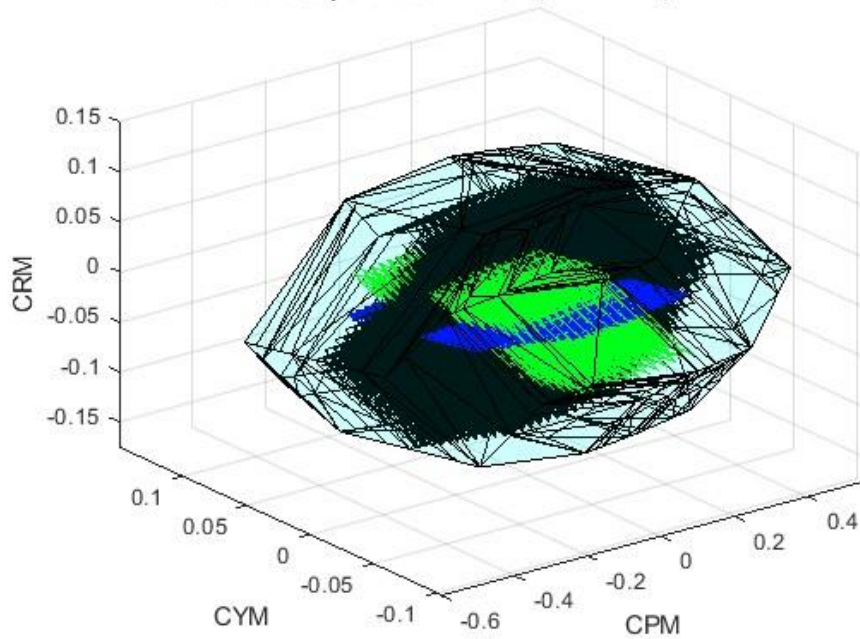


FIGURE 17 - Bell X-2 Attainable Moment Set During Subsonic Gliding Flight at Mach = 0.8,  $\text{Alpha} = 6^\circ$ ,  $\beta = 1^\circ$  with Zero-deflection Planes with volumes of zero deflection. Pre-Mix (TOP), Independent Single Panel (BOTTOM)



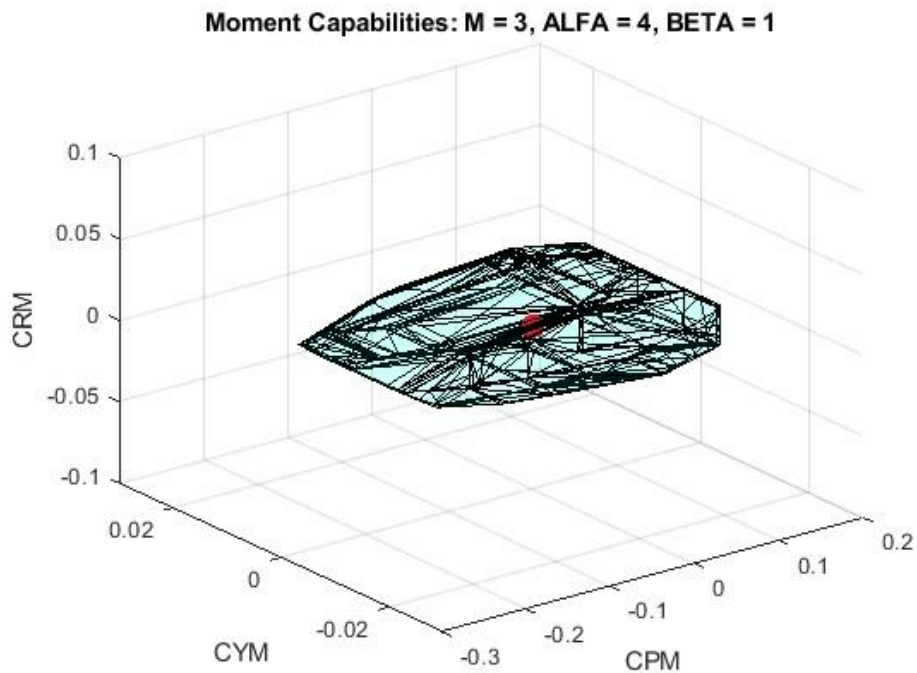
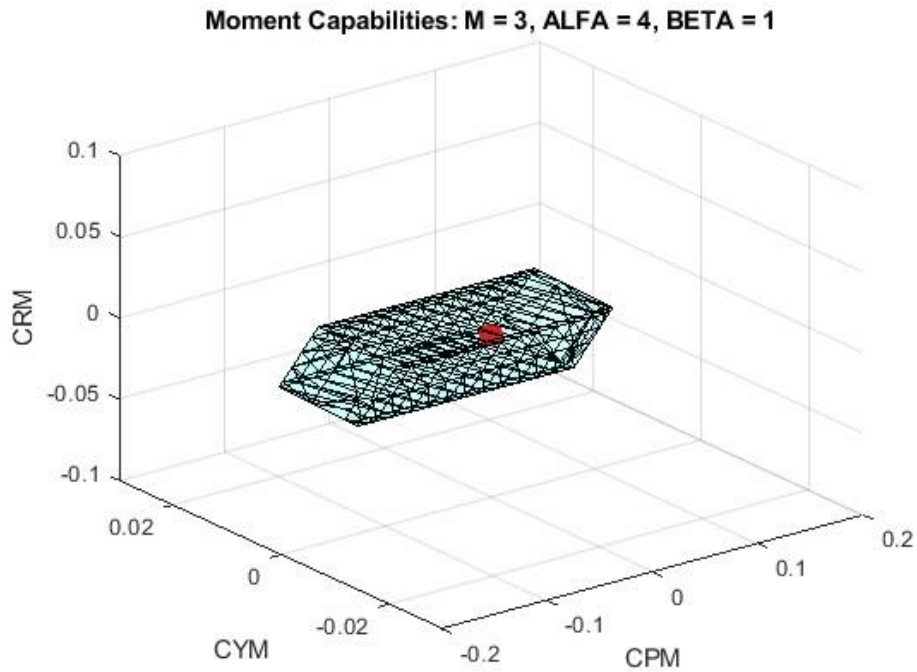


FIGURE 18 - Bell X-2 Attainable Moment Set During Supersonic Flight Mach = 3.0, Alpha = 4°,  $\beta$  = 1°. Pre-Mix (TOP), Independent Single Panel (BOTTOM)

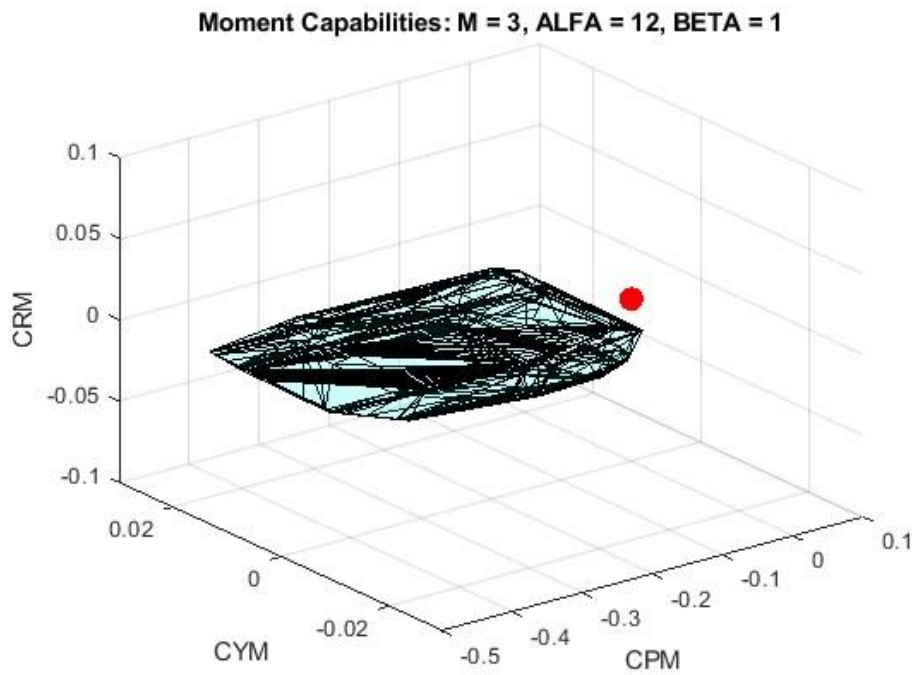
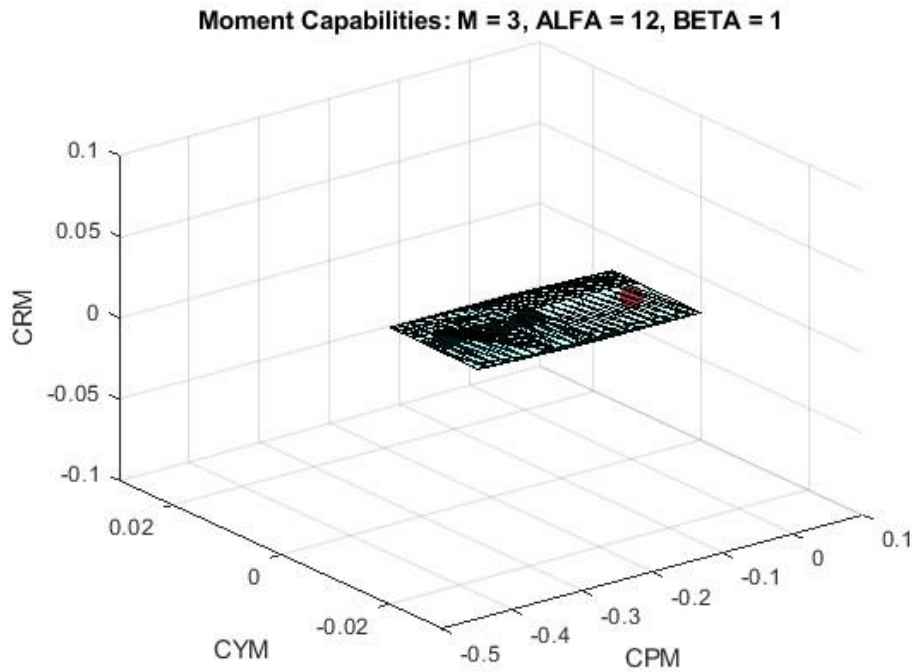


FIGURE 19 - Bell X-2 Attainable Moment Set During Supersonic Flight Mach = 3.0, Alpha = 12°,  $\beta = 1^\circ$ . Pre-Mix (TOP), Independent Single Panel (BOTTOM)

The Bell X-2 was designed for the sole purpose of pushing the boundaries of speed capability, so the peak speed point AMS are shown in Figures 18-19. Above it can be observed that the Independent Single Panel model extends the boundaries of the “box” generated by the Pre-Mix model, but the extension is much more pronounced than was seen in the low-speed cases. The axes were kept constant for all cases to demonstrate the variation in the size of the AMS as speed varies, and it is clear that as the speed increases into the supersonic regime that the attainable moment sets decrease drastically in size. For example, the high-speed Pre-Mix model case shown in Figure 18 is approximately 90 times smaller than the low-speed landing AMS of Figure 14. While the total volume is indeed smaller at high speed, it is even more clear that with an ISP model, the Bell X-2 has a larger subset of attainable moments when compared to the same flight case using the Pre-mix model due to the increased number of combinations of control surface deflections.

My modeling predicts favorable trim capability for the X-2 at moderate angle of attacks and Mach 3, for both models. That changes when the angle of attack is increased drastically as was shown in Figure 19, as neither model predicts trim is possible for this vehicle. While the increased volume of the attainable moment set due to the Independent Single Panel model surely increases the number of flight conditions where trim is possible, the tested case is not possible. When comparing the likes of the low-speed cases to the high-speed ones, the negative effect that increasing speed has on the moment coefficients are not equal. The pitching moment decreases from low to high speed by approximately half, while the rolling and yawing moments decrease by approximately an order of magnitude. This effect will be seen in later vehicles discussed in this thesis as

well, and the volumes of the attainable moment sets grow increasingly small as the speed increases.

The addition of the Independent Single Panel model to the Bell X-2 shows a marked improvement in the total volume of moments attained, as is shown in Table 1. In what may be the most important flight condition for the trim performance of the X-2, landing scenarios, the incorporation of independently scheduled control surfaces yields an approximately 55% increase of attainable moments, which would translate to a greater set of sideslips that the X-2 could handle and still land safely. There is a distinct difference in the results of the total volume comparisons between the low-speed and high-speed cases, as the SPM provides over double the attainable moments as the Pre-Mix model at Mach 3. While this may be a drastic improvement in size, it may not be sufficient alone to justify the extra time it may take in the design process to utilize a SPM control scheme in conceptual or preliminary design.

Table 1. Attainable Moment Set, Volume Comparison for Bell X-2

<b>Case</b>	<b>Pre-Mix Volume</b>	<b>Independent Single-Panel Volume</b>	<b>Difference (%)</b>
M = 0.2, Alpha = 12	0.009	0.016	54.7
M = 0.8, Alpha = 6	0.016	0.028	58.3
M = 3, Alpha = 4	0.0001	0.0005	124.5
M = 3, Alpha = 12	0.0001	0.0004	112.5

## 2. North American X-15

One of the most famous “X-planes,” the North American X-15 has captured the mind of many an aerospace enthusiast. Boasting a configuration that is atypical from a classical standpoint and an operational envelope larger than any other plane to have existed, this vehicle was a perfect choice for a case study in determining its Attainable Moment Set. Shown below is the VORLAX model of my rendition of the X-15, the “Son-of-X15.” The model was configured with the same all-moving vertical rudder, as well as the all-moving horizontal stabilizers of the original X15. What differs between the original vehicle and this model was the implementation of an aileron spanning the width of each wing. This was done to demonstrate more clearly the additional capability the independently scheduled surfaces would provide.

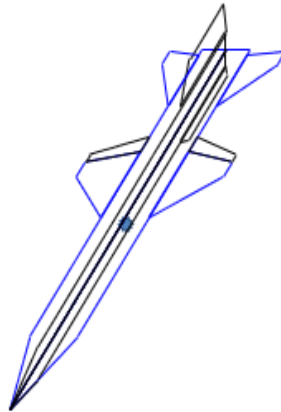


FIGURE 20 – “Son-of-X15”  
VORLAX Model

As was done for the Bell X-2, an analysis of the landing condition for the X-15 was requisite. The X-15 landed at a high angle of attack, so Figures 21-22 are representative of those conditions at zero and high sideslip. While the X-15 clearly demonstrates the ability to trim while landing without sideslip, it struggles with high

sideslip case for the Pre-Mix model where the trim point peaks through the boundary of the attainable moment set. The Independent Single Panel model solved this inability to trim in the landing condition, as in Figure 22 the trim point is completely bound by the AMS. In the landing condition the ISP model provides an additional 60% volume to the AMS over the Pre-Mix model, allowing much higher sideslips to be tolerated as shown in Table 2.

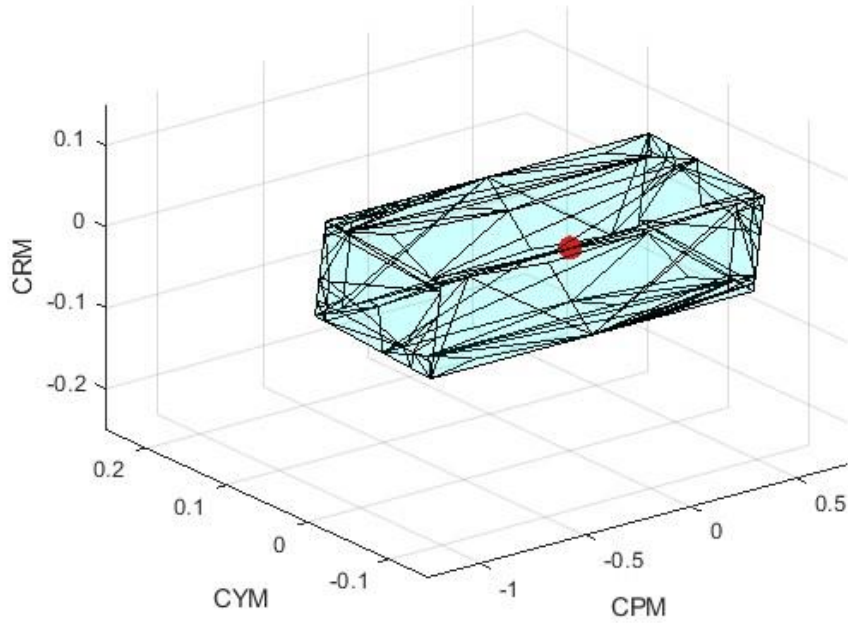
The purpose of the X-15 was to fly faster than ever before, thus multiple cases at high Mach numbers are shown in Figures 23-26. At low angles of attack, the X-15 demonstrates a strong ability to trim. As the sideslip increases, the axis of failure for trim seemed to be in roll. With the addition of the aileron action of the ISP model this is a non-issue for reasonable sideslips since the increase in volume for the ISP over the Pre-Mix model is primarily in the rolling capabilities for this vehicle. As was seen in the low-speed case, the ISP model provides significantly more control authority for the airframe at reasonable sideslips, which helps to avoid control saturation for trim alone.

At high angle of attacks paired with high speeds, the Pre-Mix model predicts that almost all the ability to generate pitching moment is used to trim, and while the results are similar for the ISP model, there is still a relatively large amount of capability left after achieving trim. This is even more apparent when comparing the effect that sideslip has on the vehicle at this extreme flight condition, as is shown in Figure 26, where the trim point is on the cusp of the edge for the Pre-Mix model at even 1-deg of sideslip, while the ISP model remains similarly placed with additional range for trim.

The X-15, or rather my modeling of it, continues to demonstrate the success of its design when considering this analysis. The Bell X-2 results above was unable to trim at

the same speeds and lower angles of attack than the “Son-of-X15,” which was able to even continue to trim at an appreciable sideslip which was not seen for the aforementioned vehicle. With the current fascination with the development of hypersonic vehicles, there is already a blueprint from which to build from. Currently, there seems to be a push for the development of a slender-bodied vehicle with little control authority, and the use of an attainable moment set cautions against such an approach. Significant control authority will be necessary for any form of maneuverability at extremely high speeds; control surfaces relative effectiveness decrease rapidly as the speed of travel increases.

**Moment Capabilities: M = 0.3, ALFA = 12, BETA = 0**



**Moment Capabilities: M = 0.3, ALFA = 12, BETA = 0**

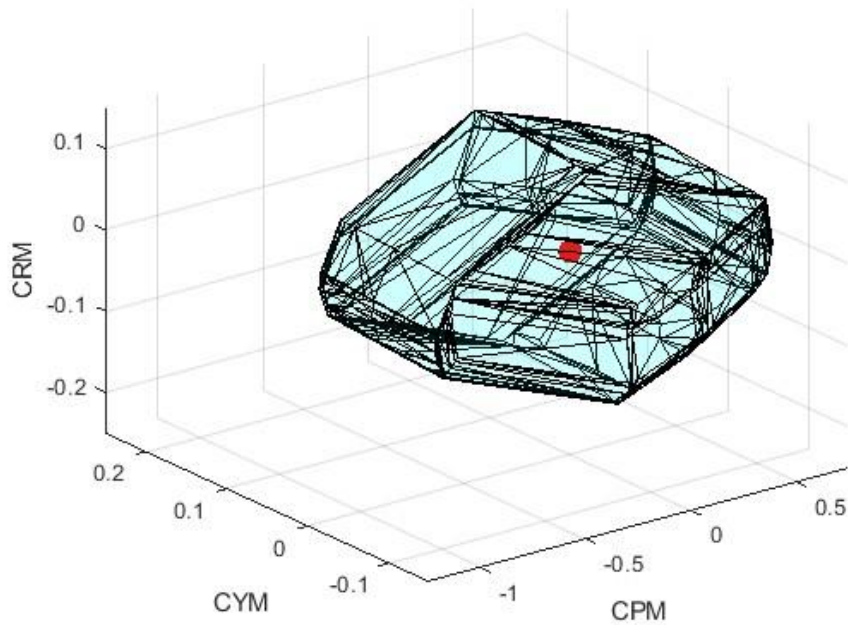
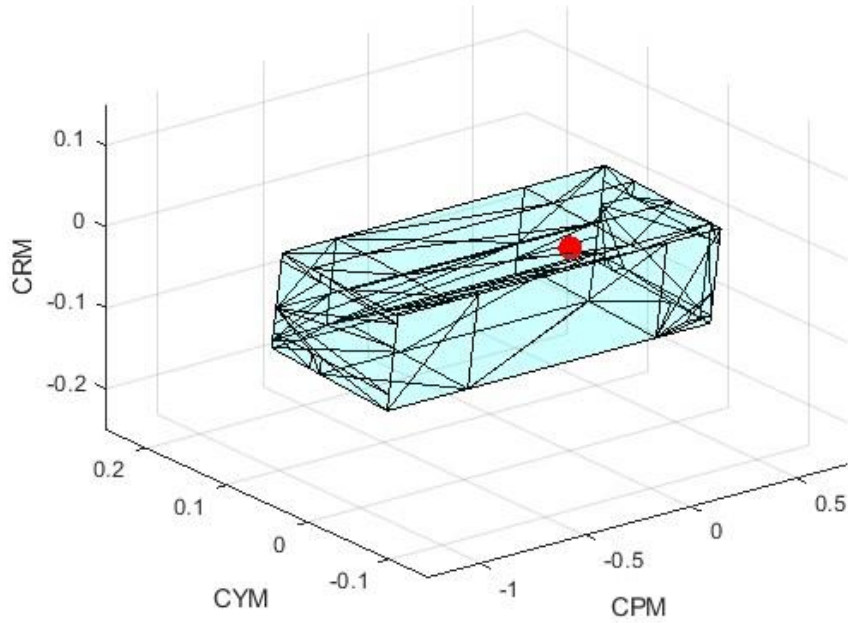


FIGURE 21 - "Son-of-X-15" Attainable Moment Set during Landing at Mach = 0.3, Alpha =  $12^\circ$ ,  $\beta = 0^\circ$ . Pre-Mix (TOP), Independent Single Panel (BOTTOM)



Moment Capabilities:  $M = 0.3$ ,  $\text{ALFA} = 12$ ,  $\text{BETA} = 10$



Moment Capabilities:  $M = 0.3$ ,  $\text{ALFA} = 12$ ,  $\text{BETA} = 10$

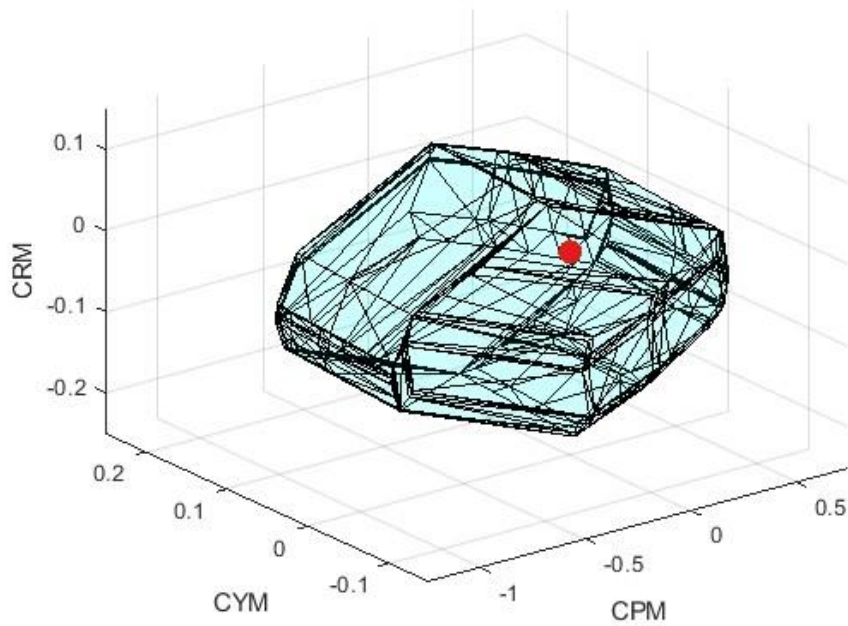


FIGURE 22 - "Son-of-X-15" Attainable Moment Set During Crosswind Landing at Mach = 0.3,  $\text{Alpha} = 12^\circ$ ,  $\beta = 10^\circ$ . Pre-Mix (TOP), Independent Single Panel (BOTTOM)

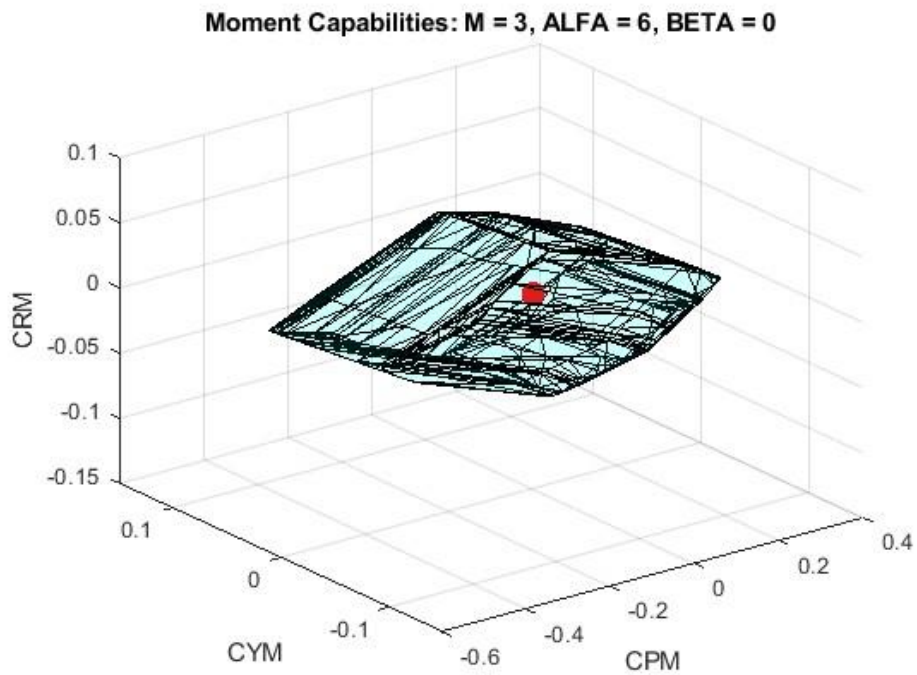
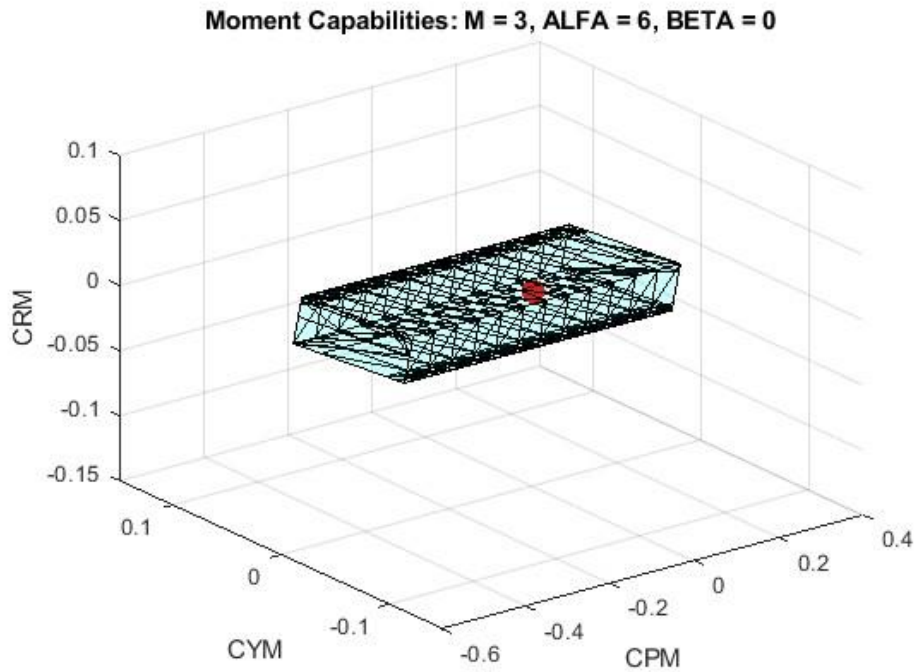


FIGURE 23 - “Son-of-X-15” Attainable Moment Set During Supersonic Level Flight at Mach = 3.0, Alpha = 6°,  $\beta = 0^\circ$ . Pre-Mix (TOP), Independent Single Panel (BOTTOM)

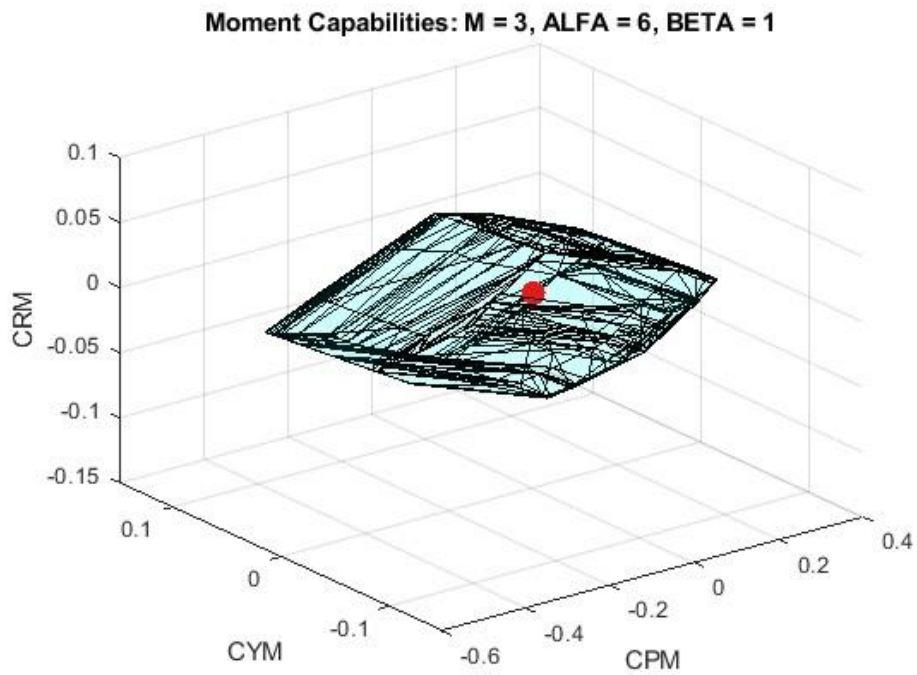
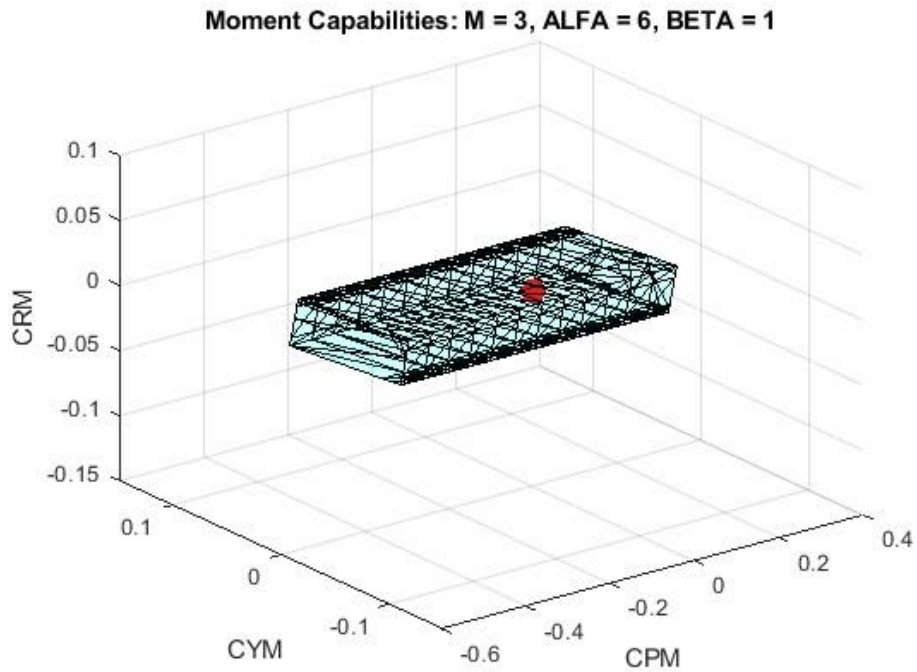


FIGURE 24 - “Son-of-X-15” Attainable Moment Set During Supersonic Level Flight at Mach = 3.0,  $\alpha = 6^\circ$ ,  $\beta = 1^\circ$ . Pre-Mix (TOP), Independent Single Panel (BOTTOM)

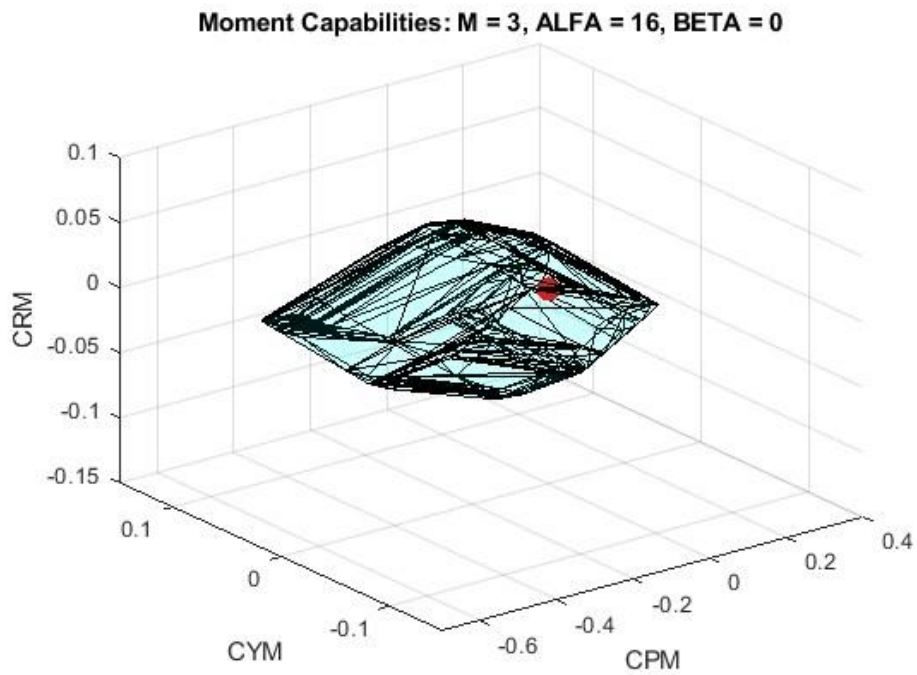
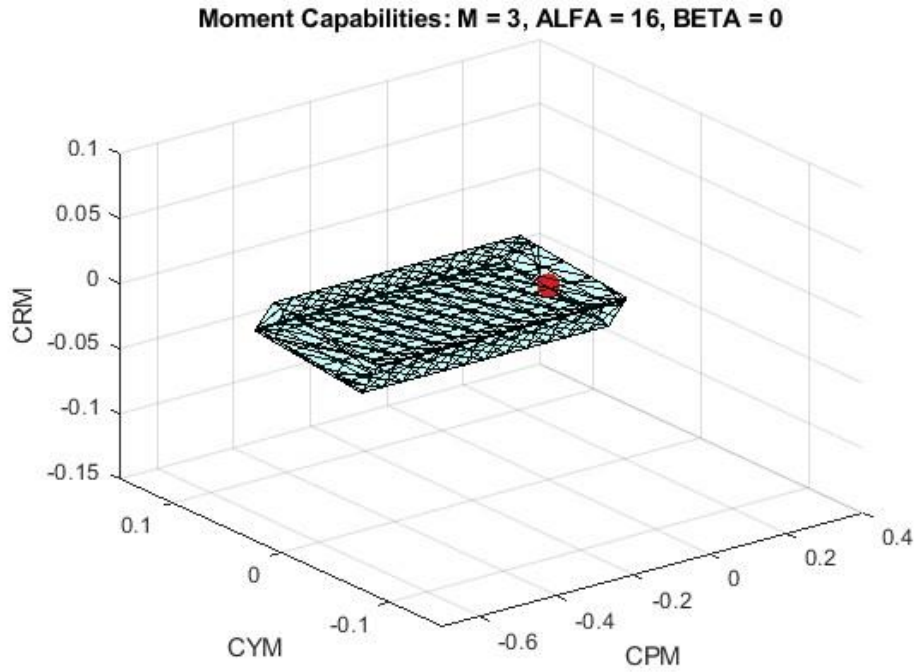


FIGURE 25 - “Son-of-X-15” Attainable Moment Set During Supersonic Re-Entry Mach = 3.0,  $\alpha = 16^\circ$ ,  $\beta = 0^\circ$ . Pre-Mix (TOP), Independent Single Panel (BOTTOM)

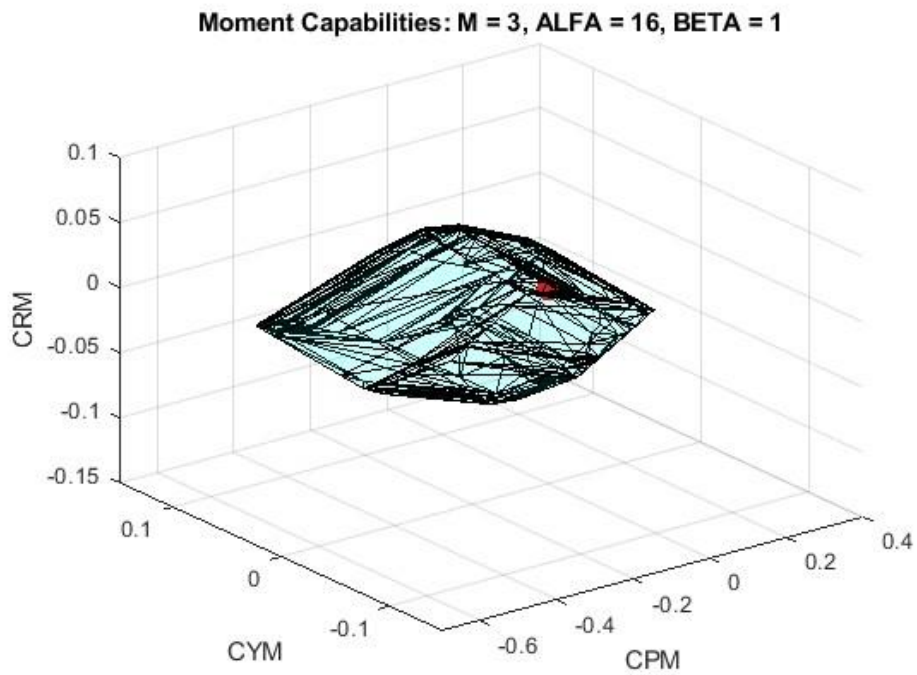
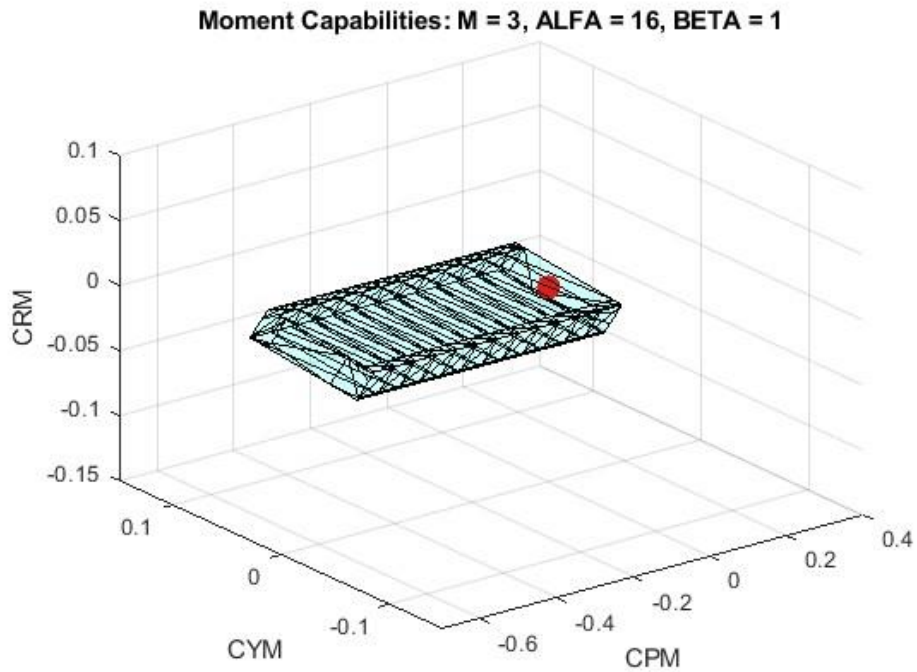


FIGURE 26 - “Son-of-X-15” Attainable Moment Set During Supersonic Re-Entry Mach = 3.0,  $\alpha = 16^\circ$ ,  $\beta = 1^\circ$ . Pre-Mix (TOP), Independent Single Panel (BOTTOM)

Table 2. Attainable Moment Set, Volume Comparison for “Son-of-X15”

Case	Pre-Mix Volume	Independent Single-Panel Volume	Difference (%)
M = 0.3, Alpha = 12	0.0286	0.0535	60
M = 3, Alpha = 6	0.00295	0.00716	83
M = 3, Alpha = 16	0.00247	0.00576	80

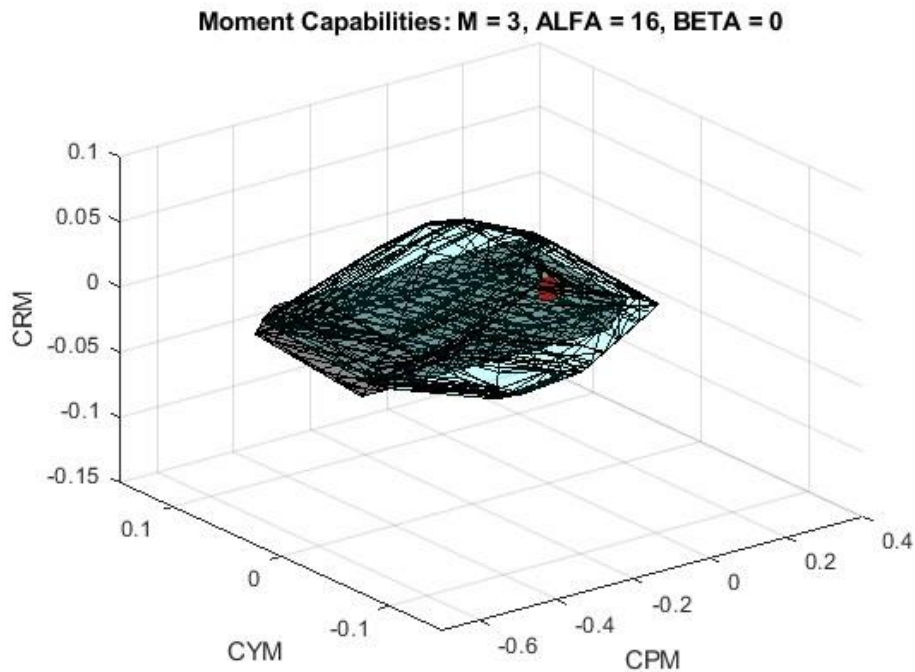


FIGURE 27 - “Son-of-X-15” Attainable Moment Set During Supersonic Re-Entry Mach = 3.0, Alpha = 16°,  $\beta = 1^\circ$ . Pre-Mix (BLACK) and Independent Single Panel (BLUE)

The introduction of the Independent Single Panel model shows an increase in total volume of the AMS, with an average of about 75% improvement over the Pre-Mix model, as is shown in Table 1 and Figure 27. These are somewhat smaller than the improvement shown by the X-2 modeling for the similar high-speed cases. It is also worth noting that the total volume of the AMS for the “Son-of-X15” is on an order of

magnitude larger than that of the Bell X-2, which indicates a much more ideal control surface sizing and placement for this vehicle from this perspective.

### 3. Airbus A320

Thus far the results for experimental, non-classically configured airplanes have been shown. It is my desire to also demonstrate the concept of Attainable Moment Sets on a familiar, classically configured vehicle. The Airbus A320 is one of the widest used vehicles in commercial aviation, and while its flight envelope is not as extreme as the X-2 or the X-15 it must still be trimmed within its operating range, as all successful air vehicles must. Unlike the previous airframes, the A320 utilizes flaps during takeoff and landing, which required the development of four separate VORLAX model sets, Pre-Mix and ISP models both with and without flaps, one of which is visualized in Figure 28.

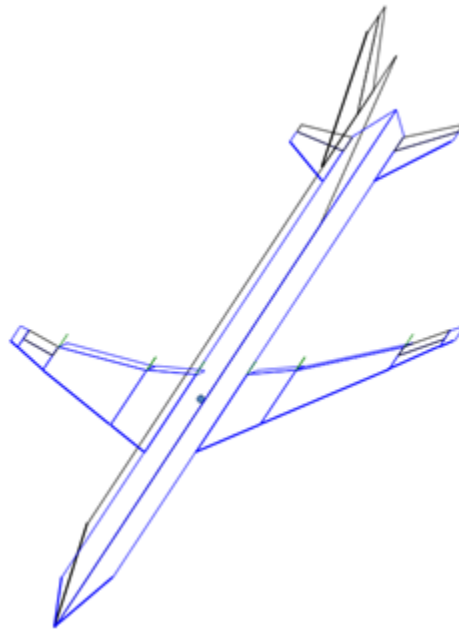


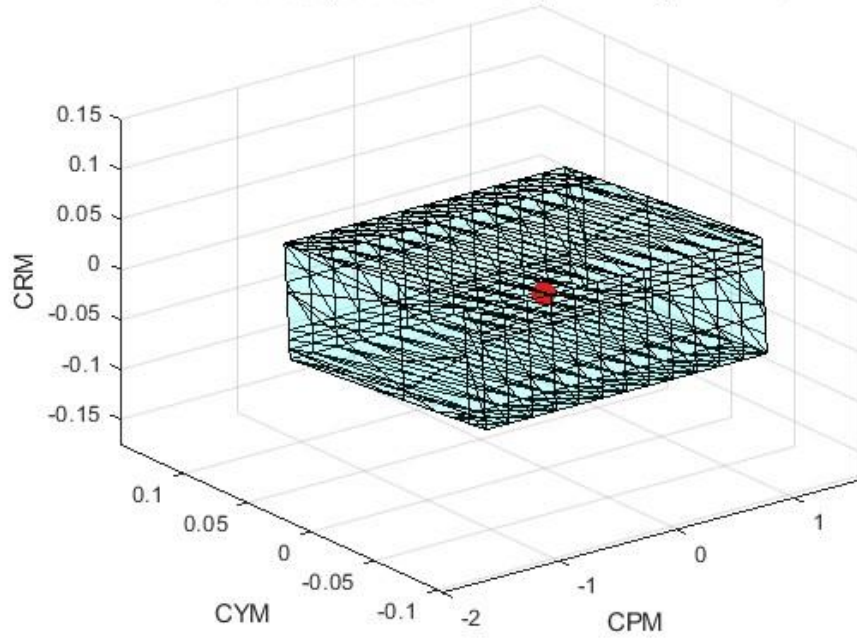
FIGURE 28 – Reverse Engineered  
A320 VORLAX Model

Figures 29-34 show the Attainable Moment Sets for the model of the Airbus A320 with flaps extended in takeoff and landing scenarios. As was expected, the A320 demonstrates more than adequate control power to trim at takeoff and landing without sideslip. The trim point at high sideslip does not lie within the AMS for the high sideslip case for the Pre-Mix model, however the increased volume from the Independent Single Panel model makes up the difference to provide trim capability past 7.5-deg of sideslip. This was a curious finding since the control allocation of the A320 is more similar to the Pre-Mix model than the Independent Single Panel model, and the airframe has repeatedly proven the ability to land at high sideslips. The inconsistency is attributed to the lack of spoilers modeled, a drawback from VORLAX as this is not possible to implement in its current form. Inspection of the A320 Operation Manual [21] shows that spoilers are paramount at this flight condition, which is confirmed by the Attainable Moment Set that is calculated from aerodynamic derivatives not including effects from these spoilers.

Takeoff and landing are typically the most difficult areas of flight to achieve peak performance for commercial aircraft such as the A320. The spoilers used on the aircraft to provide adequate performance currently, though it is important to note that for these areas of flight that independently scheduling the control surfaces does provide the same trim limits without the use of spoilers.



**Moment Capabilities: M = 0.2, ALFA = 6, BETA = 0**



**Moment Capabilities: M = 0.2, ALFA = 6, BETA = 0**

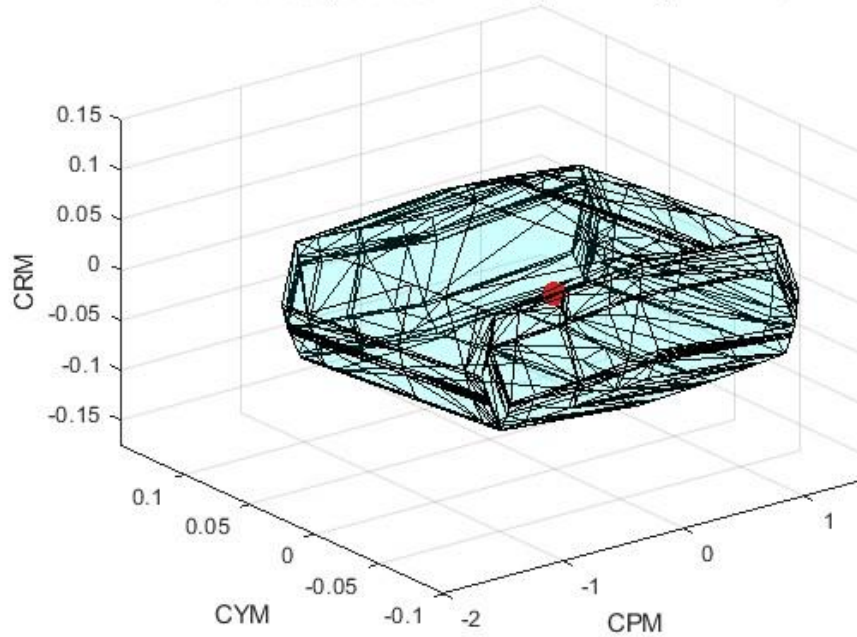


**FIGURE 29 - A320 flaps full Attainable Moment Set during Takeoff at Mach = 0.2, Alpha = 6°,  $\beta$  = 0°. Pre-Mix (TOP), Independent Single Panel (BOTTOM)**

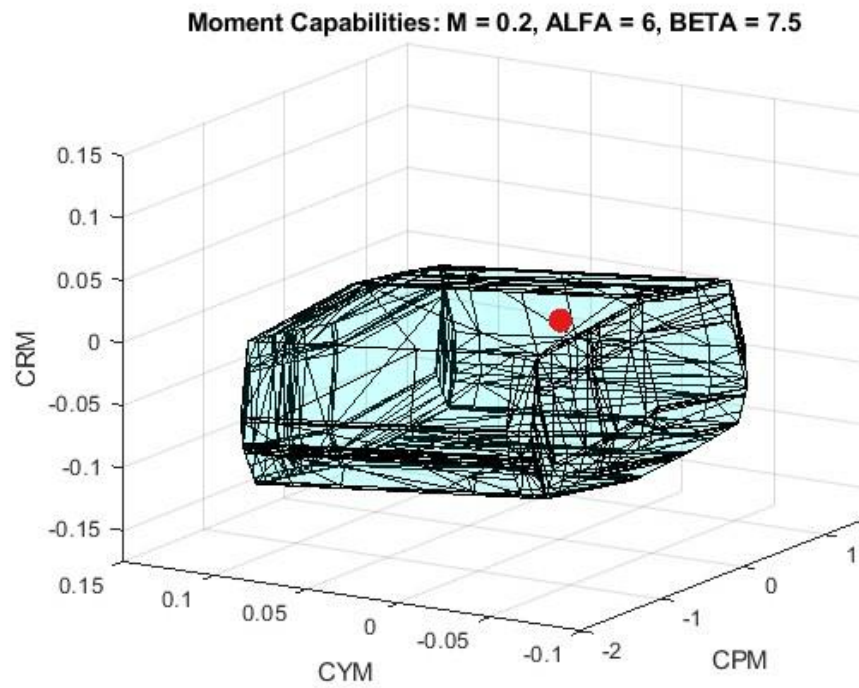
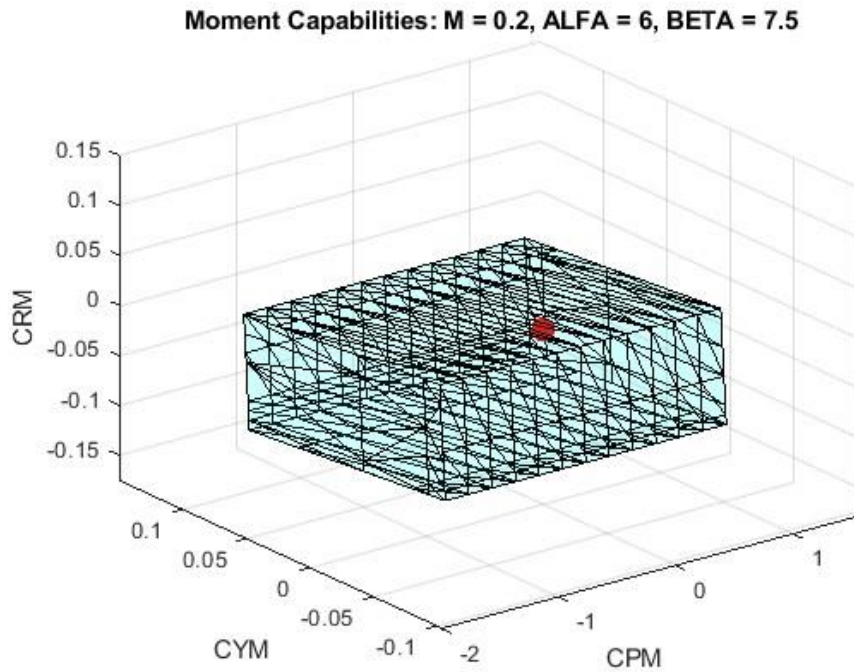
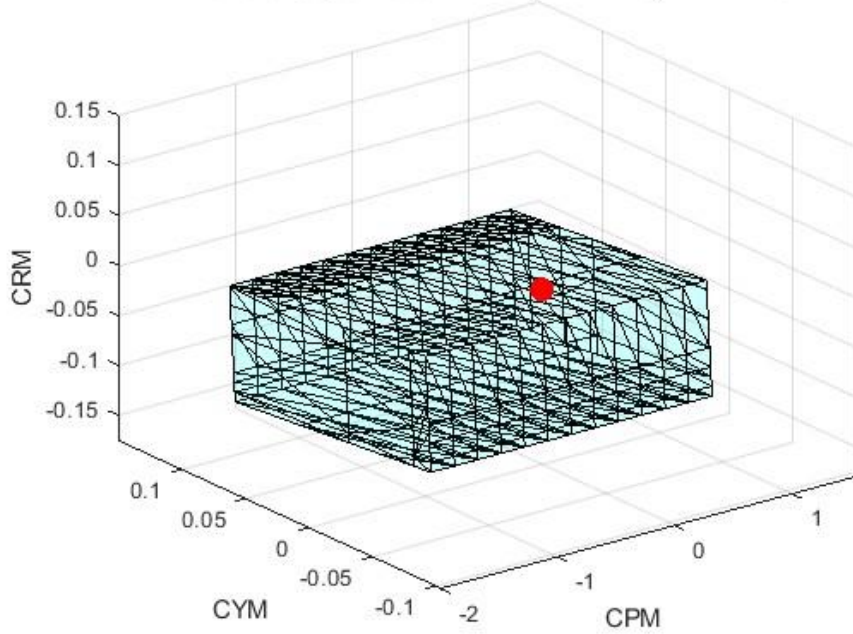


FIGURE 30 - A320 flaps full Attainable Moment Set during Takeoff at Mach = 0.2, Alpha =  $6^\circ$ ,  $\beta = 7.5^\circ$ . Pre-Mix (TOP), Independent Single Panel (BOTTOM)

Moment Capabilities:  $M = 0.2$ ,  $\text{ALFA} = 6$ ,  $\text{BETA} = 10$



Moment Capabilities:  $M = 0.2$ ,  $\text{ALFA} = 6$ ,  $\text{BETA} = 10$

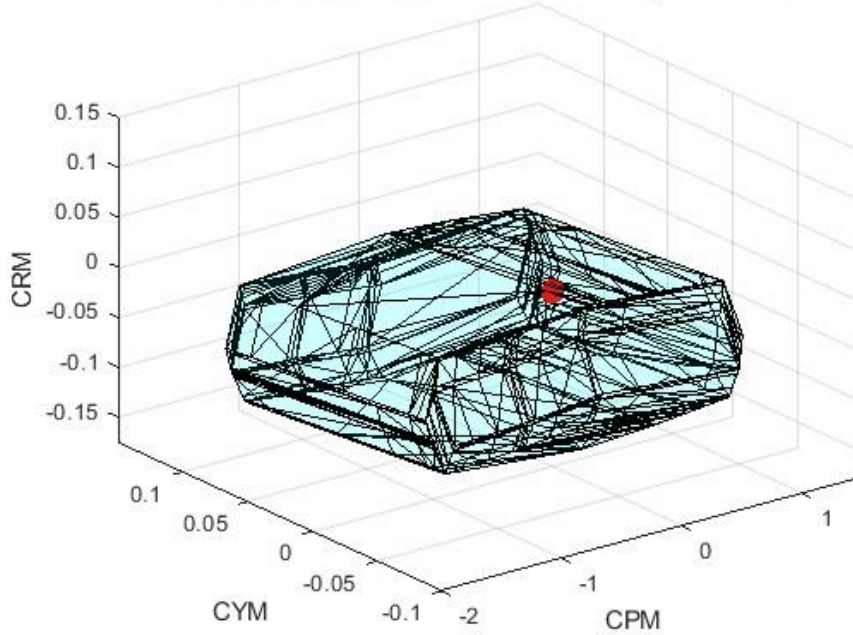
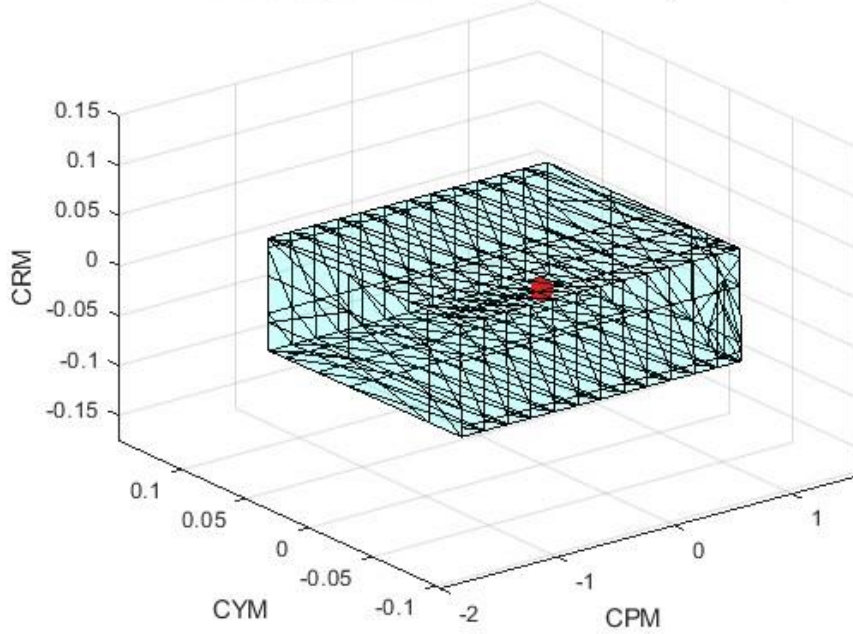


FIGURE 31 - A320 flaps full Attainable Moment Set during Takeoff at Mach = 0.2, Alpha = 6°,  $\beta = 10^\circ$ . Pre-Mix (TOP), Independent Single Panel (BOTTOM)

**Moment Capabilities: M = 0.2, ALFA = 12, BETA = 0**



**Moment Capabilities: M = 0.2, ALFA = 12, BETA = 0**

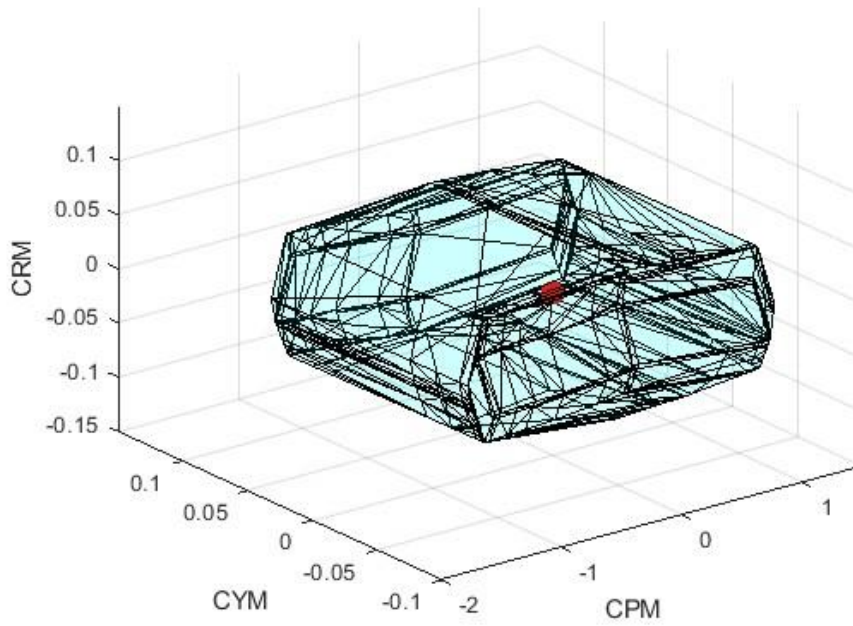
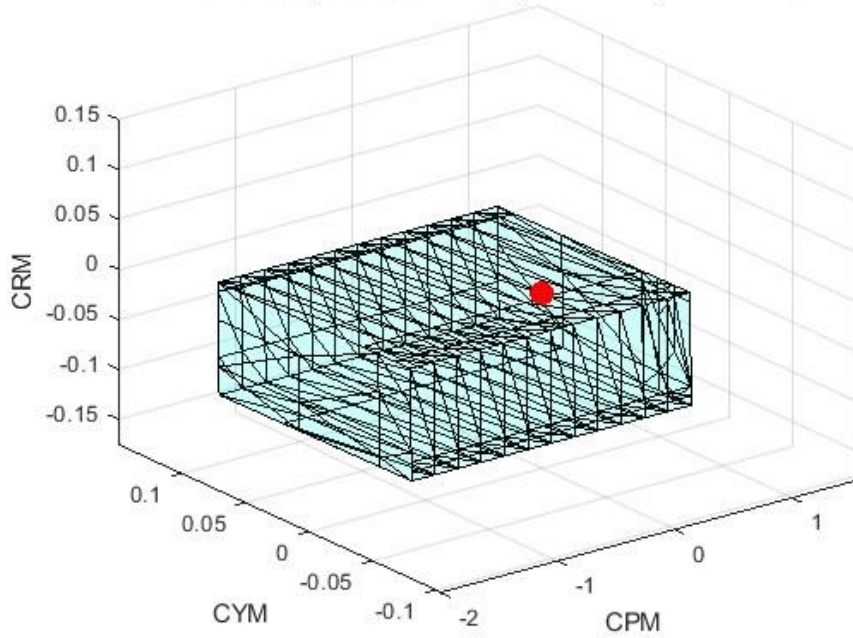


FIGURE 32 - A320 flaps full Attainable Moment Set During Landing at Mach = 0.2, Alpha = 12°,  $\beta = 0^\circ$ . Pre-Mix (TOP), Independent Single Panel (BOTTOM)

**Moment Capabilities: M = 0.2, ALFA = 12, BETA = 7.5**



**Moment Capabilities: M = 0.2, ALFA = 12, BETA = 7.5**

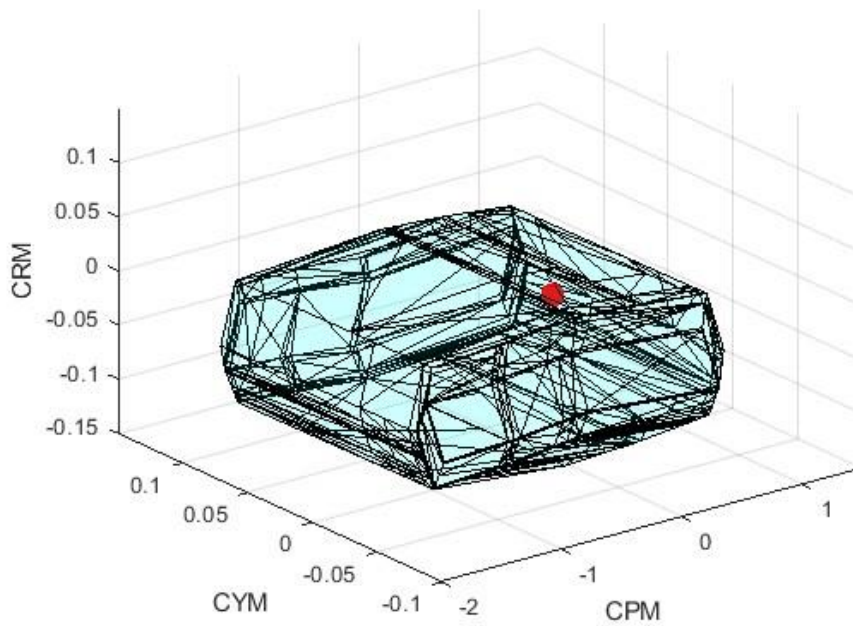
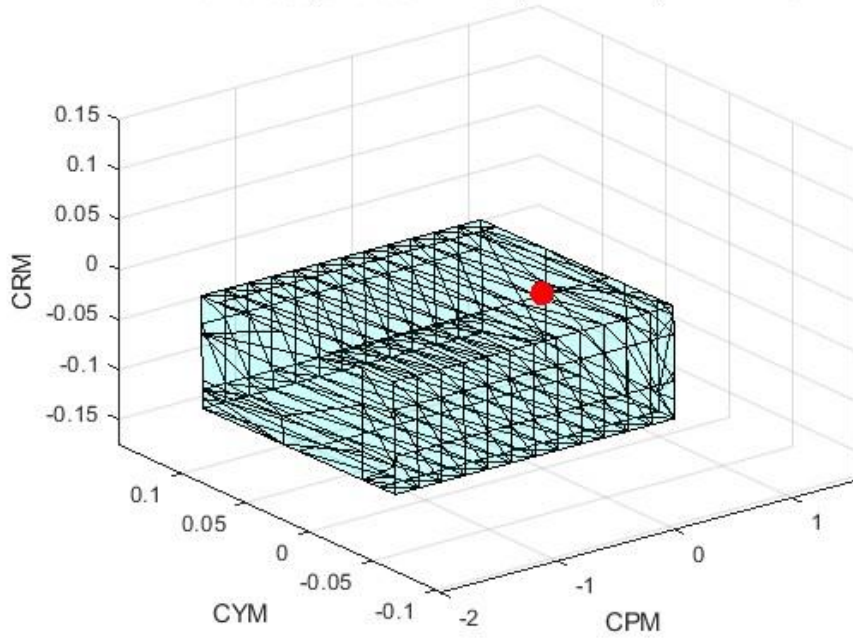


FIGURE 33 - A320 flaps full Attainable Moment Set during Crosswind Landing at Mach = 0.2, Alpha = 12°,  $\beta$  = 7.5°. Pre-Mix (TOP), Independent Single Panel (BOTTOM)

**Moment Capabilities: M = 0.2, ALFA = 12, BETA = 10**



**Moment Capabilities: M = 0.2, ALFA = 12, BETA = 10**

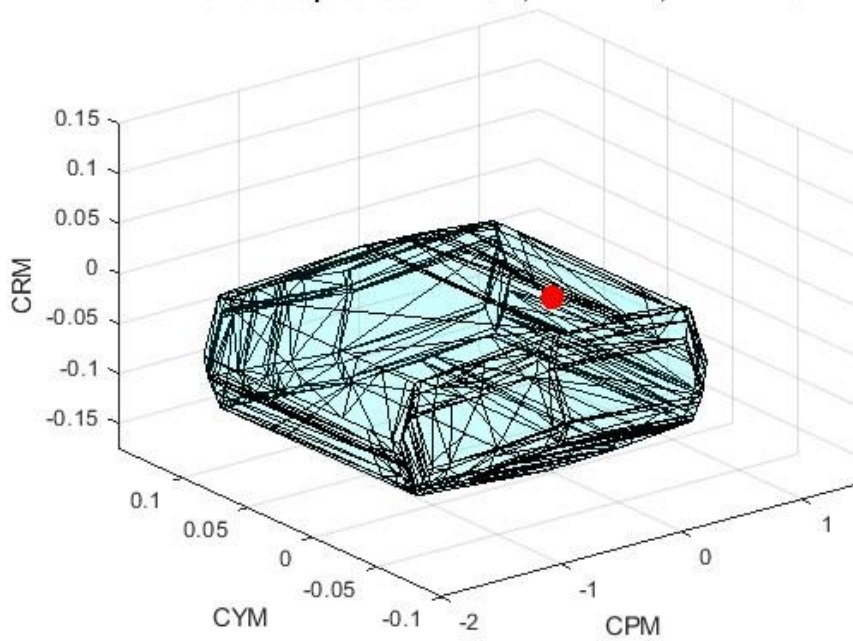
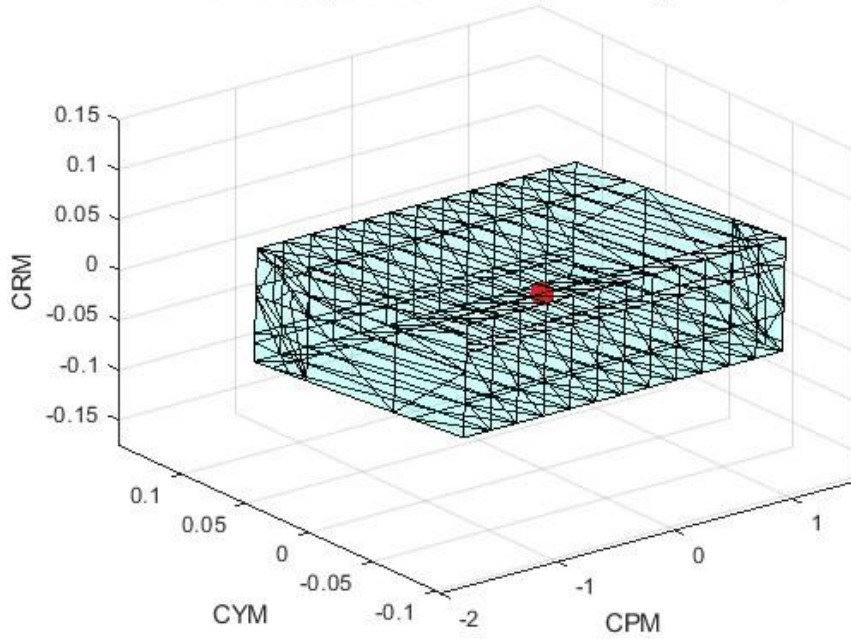


FIGURE 34 - A320 landing flaps Attainable Moment Set During Crosswind Landing at Mach = 0.2, Alpha = 12°,  $\beta$  = 10°. Pre-Mix (TOP), Independent Single Panel (BOTTOM)

**Moment Capabilities: M = 0.6, ALFA = 6, BETA = 0**



**Moment Capabilities: M = 0.6, ALFA = 6, BETA = 0**

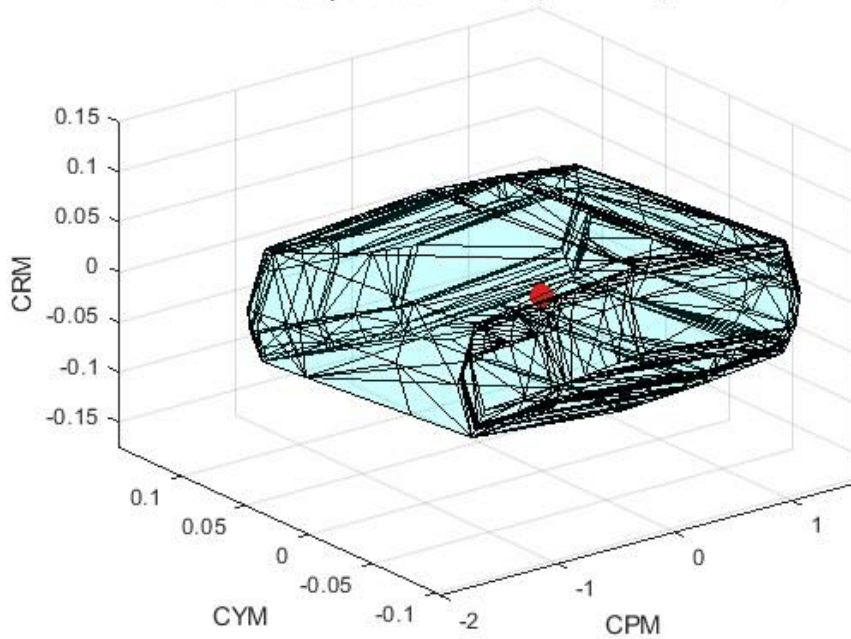
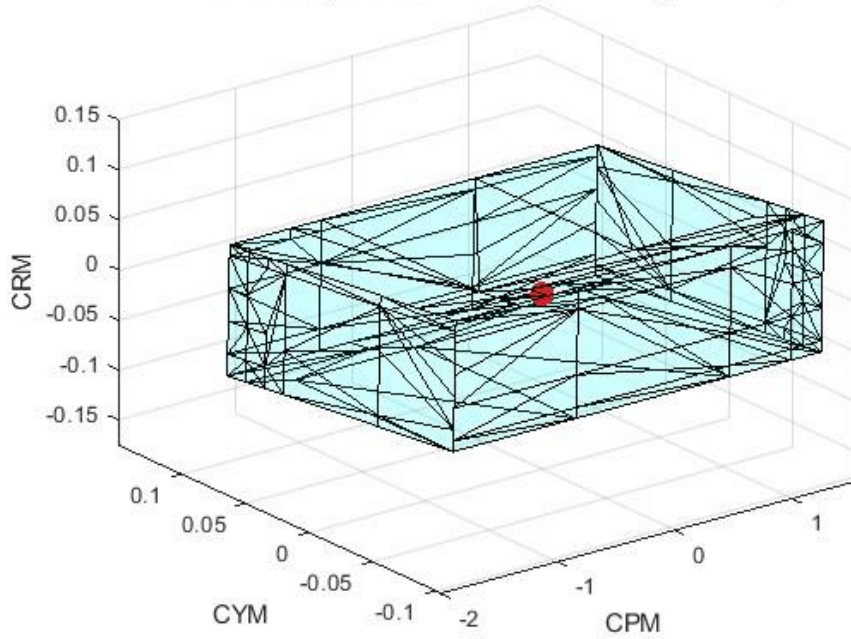


FIGURE 35 - A320 flaps up Attainable Moment Set During Subsonic Flight at Mach = 0.6, Alpha = 6°,  $\beta = 0^\circ$ . Pre-Mix (TOP), Independent Single Panel (BOTTOM)

**Moment Capabilities:  $M = 0.8$ ,  $\text{ALFA} = 4$ ,  $\text{BETA} = 0$**



**Moment Capabilities:  $M = 0.8$ ,  $\text{ALFA} = 4$ ,  $\text{BETA} = 0$**

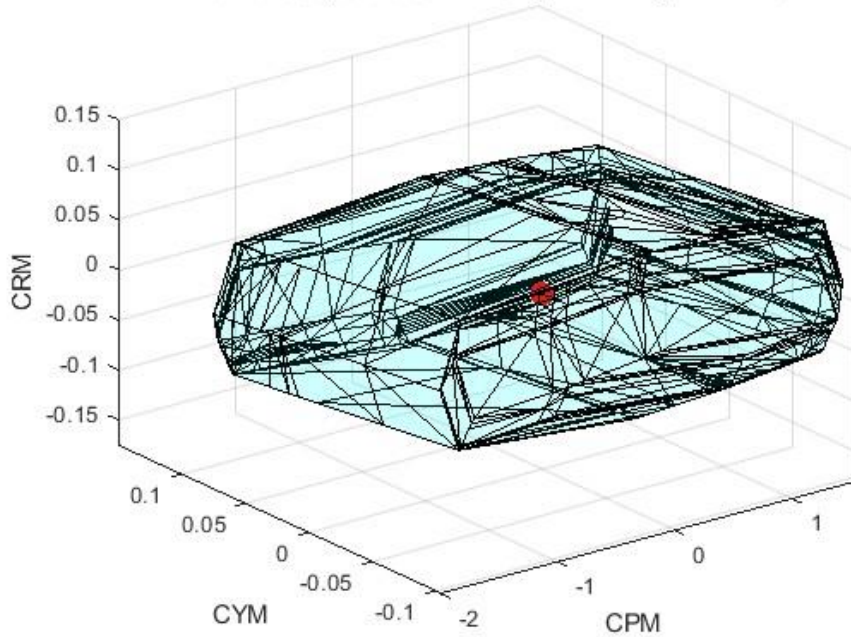


FIGURE 36 - A320 flaps up Attainable Moment Set During Subsonic Flight at Mach = 0.8,  $\text{Alpha} = 4^\circ$ ,  $\beta = 0^\circ$ . Pre-Mix (TOP), Independent Single Panel (BOTTOM)



With the takeoff and landing covered, the next flight conditions for the A320 are enroute climb (Figure 35) and at cruise (Figure 36). Both models exhibit the expected ability to trim, although there are some key differences between the two. As discussed earlier, there is a decreased ability to produce positive rolling moment as the yawing moment increases. Noticeably, the pitching moment is completely decoupled from the lateral-directional axes. That is to say that the range of pitching moments generated is not dependent on the yawing moment or rolling moment generated by the vehicle. This indicates a miniscule effect of the ailerons and rudder in pitch, which was expected of a configuration such as the A320. The dependence of rolling moment and yawing moment in turn indicate the adverse yaw or the ailerons and the adverse roll of rudder action, as minor as these effects are at this flight condition for this classical configuration.

The A320, like the previous airframes, displayed a significant increase in the volume attainable moment sets for the Independent Single Panel model compared to the Pre-Mix model. The increased volume, and again the range of commandable moments is not quite as pronounced compared to the previous airframes discussed, with the average increase being approximately 21%. The difference of these scheduling methods for the X-2 and “Son-of-X15” were in the range of 55-125% depending on the flight regime. While the increased performance is certainly not as great for this classical configuration as the experimental planes discussed, the ability to generate a twenty-percent increase in commandable moments by simply allocating the controls that already exist on a vehicle is invaluable. Through a more in-depth analysis of this configuration with greater fidelity it could be shown that spoilers are not necessary for the A320, which would result in

weight savings, reduced mechanical complexity, and countless other benefits in the commercial space.

Table 3. Attainable Moment Set, Volume Comparison for A320

Case	Pre-Mix Volume	Independent Single-Panel Volume	Difference (%)
M = 0.2, Alpha = 6 (Flaps)	0.044	0.055	21.5
M = 0.2, Alpha = 12 (Flaps)	0.042	0.051	19.0
M = 0.6, Alpha = 6 (No Flaps)	0.053	0.066	21.0
M = 0.8, Alpha = 4 (No Flaps)	0.077	0.097	22.3

#### 4. Air Force GHV

As modern interest in maneuvering hypersonic vehicles increases, the necessity to develop an airframe capable of controlled flight in that regime does as well. The hypersonic flight regime is not a friendly one to the engineer, as issues concerning the material properties and propulsion capability are pushed to the limit of current technology, and often surpass them. The above issues are only compounded by the need for a stable and controllable aircraft, which in many cases require a design that is suboptimal for one aspect of the project. The Air Force Institute of Technology (AFIT), in conjunction with graduate students and professors from across the United States and the Air Force Research Lab (AFRL), have developed a General Hypersonic Vehicle (GHV) on which design optimization is performed and assessment tools for hypersonic vehicles developed. My work with AFIT has included the trim analysis method using attainable moment sets shown above in this paper.

Common thought on the design of a hypersonic airframe has pushed line-art towards a very slender, body-heavy design that can be seen in the VORLAX

representation of the GHV (Figure 37). Material property concerns with the aerodynamic heating that occurs at such high speeds drives the necessity for as little surface area protruding into the free-stream as possible. This provides concerns for the stability of such a vehicle, as this severely limits the available control surface area on the vehicle, in addition to atypical mass moments of inertia. Advancements around propulsion systems that could achieve sustained hypersonic speeds, namely the use of a supersonic combustion ramjet engine (scram jet), are also being made by the previously mentioned research groups and others, but the efficacy of those systems are somewhat dubious when it is also considered that the operational envelope of angle of attack is quite limited. A deviation from the angle of attack that the design could withstand could cause unstart in the engine, which would render the airframe incapable of continued flight. The propulsion issue noted above poses a challenge to the design of the stability and control system of a hypersonic vehicle. The range of allowable angle of attacks may be so small that the longitudinal stability would need to be exceptionally high such that even exceptionally small perturbations in pitch do not push the angle of attack outside the operational range. While these issues to overcome are outside the scope of this thesis in terms of addressing a solution, they are noted since they are intrinsic to the design space.

The GHV used by AFIT as a research geometry for hypersonic research does not have any specific control surfaces prescribed, which left the addition of any control surfaces to an arbitrary design decision. In the case of the geometry for which attainable moment sets were generated in this thesis for the GHV, it was decided that a pair of elevons and a pair of rudders should be a reasonable configuration for the vehicle; see Figure 37. This was largely due to the inability to incorporate a separate horizontal

stabilizer in the vehicle. While this meant that an entirely different control scheme was necessary for the generation of an attainable moment set, it was made simple due to the flexibility of the procedure. The method for generating an AMS is largely agnostic to the total number and the orientation of control surfaces since each control surfaces contributions to any of the principal moments are accounted for regardless of size. In this case, due in part to the lower number of control surfaces and the high speed at which aerodynamic data was to be generated, positive and negative deflection of each individual control surface were generated. The results of this increased number of files yielded the expected result, i.e., a mirroring of a positive elevon deflection across the centerline would have provided the same result as generating the aerodynamic data from VORLAX.

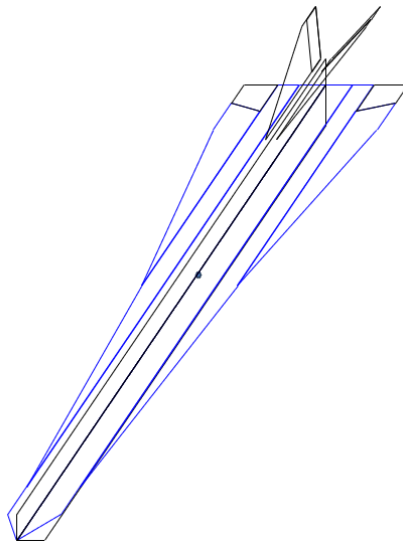
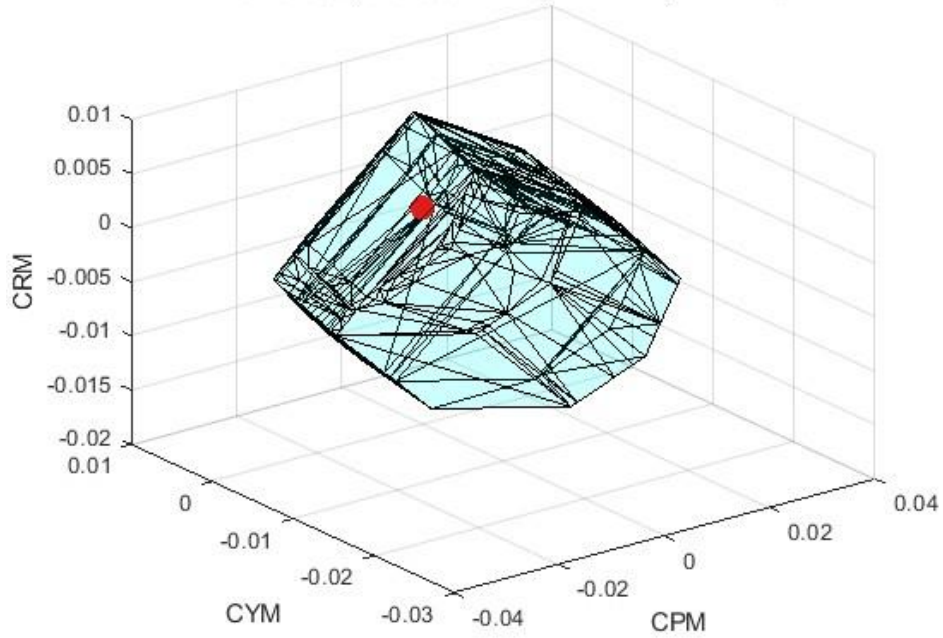


FIGURE 37 – GHV VORLAX Model

Attainable moment sets were generated over a wide variety of Mach numbers, while the ranges of angle of attacks were kept low for reasons mentioned above.

**Moment Capabilities: M = 3, ALFA = 4, BETA = 0**



**Moment Capabilities: M = 3, ALFA = 4, BETA = 1**

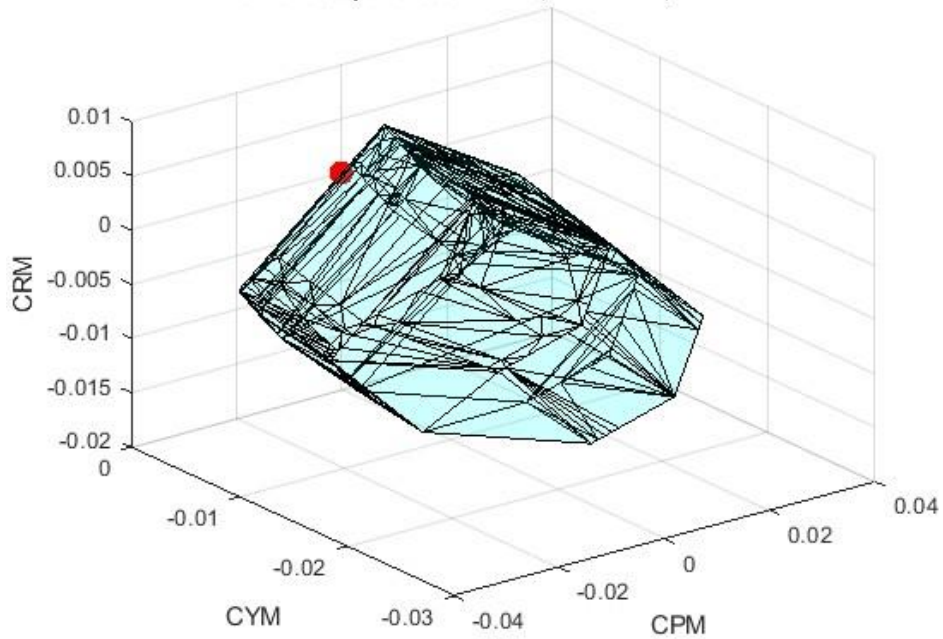


**FIGURE 38 - GHV Attainable Moment Set, Mach = 3, Alpha = 4°,  $\beta = 0^\circ$  (TOP),  $\beta = 1^\circ$  (BOTTOM)**

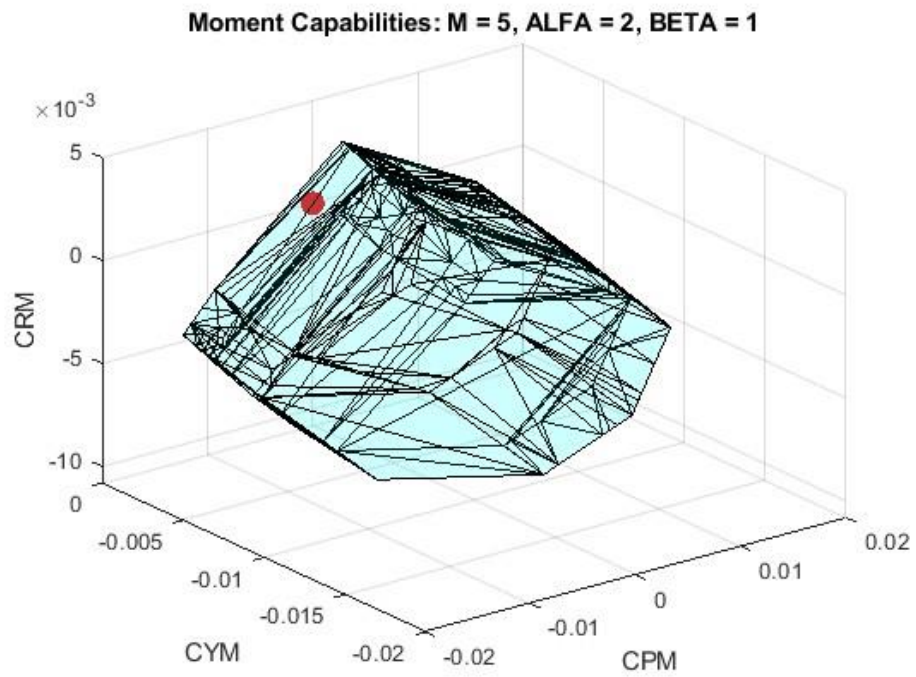
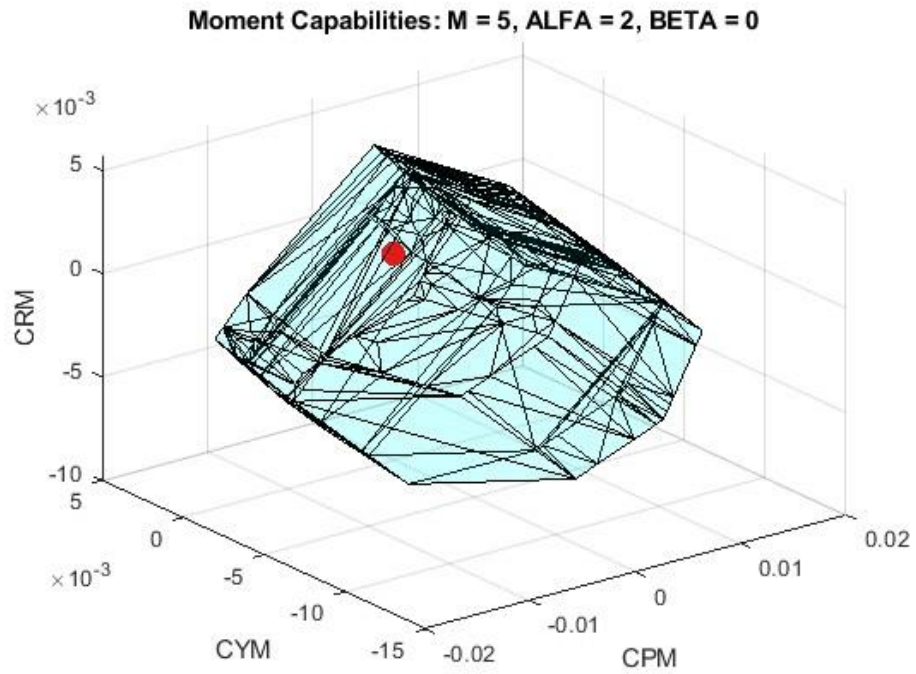


FIGURE 39 - GHV Attainable Moment Set, Mach = 5, Alpha =  $2^\circ$ ,  $\beta = 0^\circ$  (TOP),  $\beta = 1^\circ$  (BOTTOM)

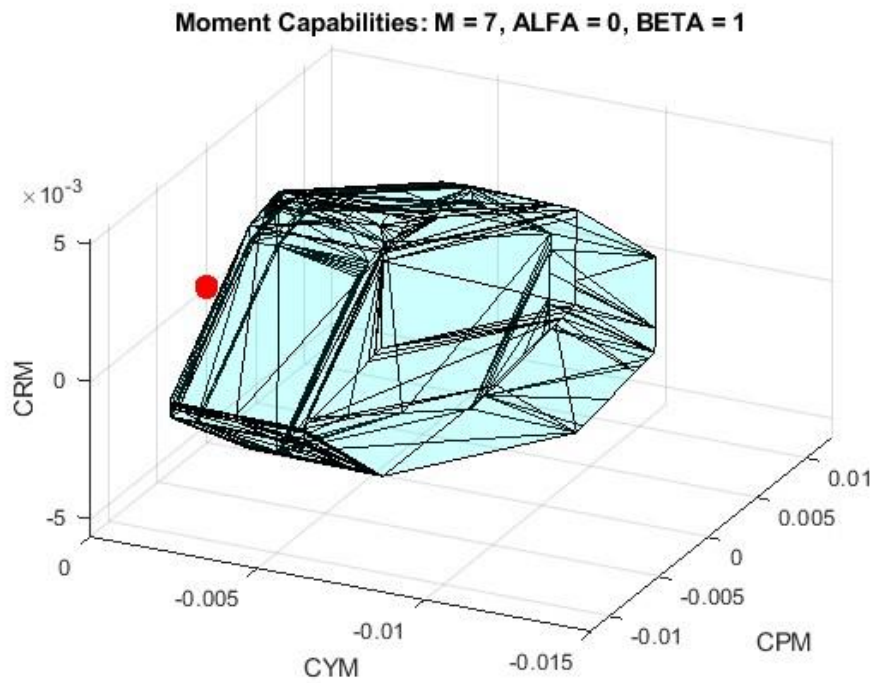
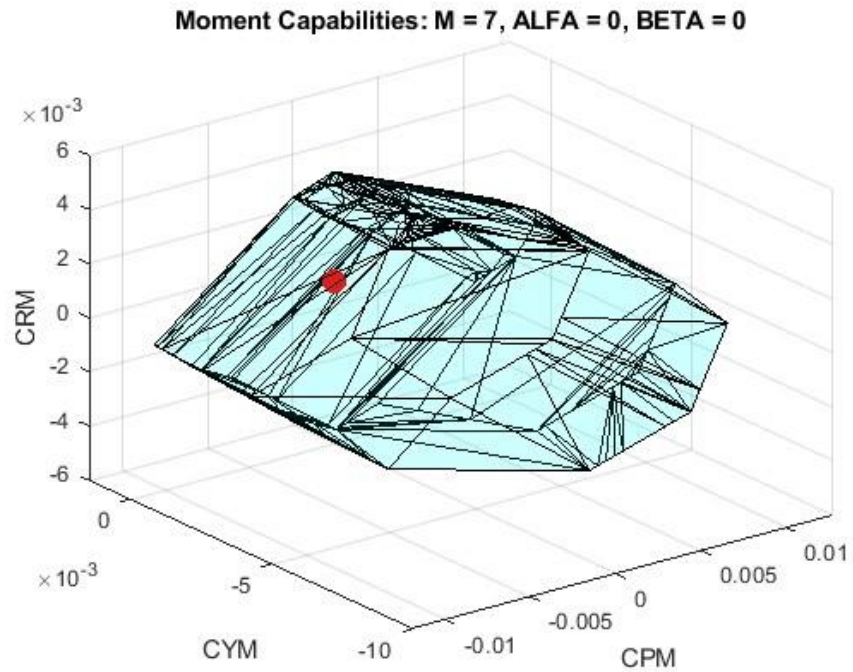


FIGURE 40 - GHV Attainable Moment Set, Mach = 7,  $\alpha = 0^\circ$ ,  $\beta = 0^\circ$  (TOP),  $\beta = 1^\circ$  (BOTTOM)

Figures 38-40 show clearly that at this fidelity of study the GHV is incapable of tolerating any amount of sideslip, as even a single degree of sideslip pushes the trim point outside the bound of the volume. The asymmetric results of the yawing moment called into question the assumption of a linear relationship between the moments generated by a control surface and their degree of deflection, which will be discussed in more detail below. The reliability of this analysis of the attainable moment set may be quantitatively questionable, however there is some insight to be drawn. A linear interpolation between the maximum deflection and zero is likely to provide an overly optimistic view of the abilities of each degree of deflection in between, which should lead to an overestimate of the total volume of the attainable moment set. The total volume of the AMS shown in Figure 38, which is the largest, is only  $1.66e-5$ . This is approximately 1,500 times smaller than even the smallest volume found during the analysis of the “Son-of-X15.”

The miniscule volume of the attainable moment sets for the GHV reveals a larger problem in the hypersonic regime, that there simply is not enough control surface available, at least in this geometry, to generate enough moments to reasonably denote this vehicle as maneuvering. This thesis has not delved into the topic of determining what moments are required to perform specific maneuvers, such as confirming an aircraft’s time to roll, but the volume of moments suggested by this analysis suggests to me that an analysis on maneuvering performance points would yield extremely unsatisfactory results.



## CHAPTER 5

### DISCUSSION AND FUTURE DEVELOPMENT

The above discussion has shown that there are many observations about a configuration that can be made using the Attainable Moment Set. The differences between the results shown for the Pre-Mix and the Independent Single Panel models were often small, with most of the added volume being added to the attainable moment set away from the area of concern for trim. In some cases that difference is enough to demonstrate the ability to trim with the Independent Single Panel model where the Pre-Mix model could not. The process for generating a valid attainable moment set is not trivial, though it does benefit from the fact that it does not need more information than generally is already determined in the design process of a vehicle. The control effectiveness matrices for the vehicles in this study were determined using VORLAX, however any valid approximation of its terms should provide the same result. As was seen in the above examples, the linear approximation of the control effectiveness is not sufficient at extremely high speeds, and more work is yet to be done to refine the process.

Consideration of other aspects of the design of an aircraft could be included in the analysis of attainable moment sets. For example, the effects of decoupled control surfaces on structural requirements. As controls are allowed to deflect independently of each other they can provide a wider range of moments in pitch, roll, and yaw but they may also generate unfavorable forces on the torque box and body of the vehicle. An extension of this work could address these concerns by placing limits on the deflection ranges of matched control surfaces.

In this thesis minimal effectiveness terms were found for each control surface deflection; one at zero, and one at its maximum value. In order to produce an attainable moment set more reasonable for high fidelity design, it would be necessary to increase the number of terms extensively. Instead of approximating the effectiveness at each deflection case by linearly interpolating between the zero and maximum it would be far more reasonable to have a modeled value every one or two degrees and use that data to construct the attainable moment set. This would certainly lead to a more accurate representation of the data for non-classical configurations, especially those traveling at particularly high speeds. That said for classical configurations like the A320 discussed above, the procedure in place is likely sufficient for preliminary design purposes, since the effects non-linearity in high speeds are not present.

A simple approach such as the one described in this paper should prove more than reasonable, especially considering the difference in effectiveness of positive versus negative aileron deflection that was done for the Independent Single Panel model. Design philosophies are ever changing as technology advances, and the use of attainable moment sets may well be a contribution to preliminary design assessment, both for classical and non-classical configurations. A goal of this method, among others, would be that its inclusion in the design process would facilitate rapid testing of various airframes performance in order to assure compliance to objective specifications. I have made no attempt at determining the specifications for which a specific airframe may be judged by using the procedure outlined in this thesis due to their unique nature depending on the type of aircraft and its intended mission set.

The procedure of generating and analyzing attainable moment sets is in the spirit of a paper written by Leggett & Black entitled “MIL-STD-1797 IS NOT A COOKBOOK.” [22] The development of objective requirements for engineers to base their design decisions on and verify their performance is paramount. As those authors noted in the development of a design it would be easy to determine a requirement to be “the plane will fly well,” which would certainly be a desirable outcome yet does not provide any indication of how to make a plane fly well or accomplish its mission. One aspect of ensuring an air vehicles success would of course be the ability to trim while maintaining enough control authority to ensure that maneuvers can be made from any attitude during any realized flight condition. The objective requirement of trim capability and the control authority available after trim can easily be confirmed using the analysis of the vehicle’s attainable moment sets. This thesis addressed the trim performance aspect of that requirement, but with extension a quantitative value of the control surface saturation could be made to concretely determine the remaining control authority after trimming the vehicle.

## REFERENCES

- [1] See: <https://www.nasa.gov/consortium/ModelBasedSystems>
- [2] See: [https://www.phoenix-int.com/wp-content/uploads/2021/01/Kolonay\\_PIMDAOEvent2021Rev3.pdf](https://www.phoenix-int.com/wp-content/uploads/2021/01/Kolonay_PIMDAOEvent2021Rev3.pdf)
- [3] See: <https://aerospaceamerica.aiaa.org/year-in-review/hypersonic-work-escalates-on-multiple-fronts/>
- [4] Takahashi, T.T., Griffin, J.A. and Grandhi, R.V., “A Review of High-Speed Aircraft Stability and Control Challenges,” AIAA 2023-3231, 2023.
- [5] Day, R.E., "Coupling Dynamics in Aircraft Design: A Historical Perspective," NASA SP-532, NASA, 1997.
- [6] Day, R. and Reisert, D., “Flight Behavior of the X-2 Research Airplane to a Mach Number of 3.20 and a Geometric Altitude of 126,200 Feet,” NASA TM X-137, 1959.
- [7] Holleman, E.C. and Reisert, D., “Controllability of the X-15 Research Airplane with Interim Engines During High-Altitude Flight,” NASA TM X-51A4, 1961.
- [8] Hoey, R.G., “Flight Test Handling Qualities of the X-24A Lifting Body,” AFFTC TD-71-11, 1971.
- [9] Moes, T. and Iliff, K., “Stability and Control Estimation Flight Test Results for the SR-71 Aircraft with Externally Mounted Experiments,” NASA/TP 2002-210718, 2002.
- [10] Scheiss, J.R., “Lateral Stability and Control Derivatives Extracted from Space Shuttle Challenger Flight Data,” N88-16788, NASA TM 100520, 1988.
- [11] Wolowicz, C. H., and Yancey, R.B., “Summary of Stability and Control Characteristics of the XB-70 Airplane,” NASA TM X-2933, 1973.
- [12] Kirsten, P.W., Richardson, D.F., and Wilson, C.M., “Predicted and Flight Test Results of the Performance, Stability and Control of the Space Shuttle from Reentry to Landing,” NASA CP-2283 Vol. I, 1983.
- [13] Takahashi, T.T., Aircraft Performance and Sizing, Volume II: Applied Aerodynamic Design, Momentum Press, New York, 2016.
- [14] Schulz, C. and Wetherall, R., “Falcon Hypersonic Technology Vehicle (HTV-2) Industry Team Expo Briefing,” DISTAR Case 16757, May 24, 2011.

- [15] Yechout, T.R., Introduction to Aircraft Flight Mechanics, Second Edition, AIAA, 2014.
- [16] Bordignon, K. *Constrained Control Allocation for Systems with Redundant Control Effectors*. Doctoral dissertation, Virginia Polytechnic Institute and State University, 1996.
- [17] Durham, W., Bordignon, K. A., and Beck, R., Aircraft Control Allocation. Wiley, 2017.
- [18] Zhang, J., Söpper, M. and Holzapfel, F., "Attainable Moment Set Optimization to Support Configuration Design: A Required Moment Set Based Approach" *Applied Sciences* 11, No. 8, 2021. pp. 3685.
- [19] Miranda, L. R., Baker, R. D., and Elliott, W. M., "A Generalized Vortex Lattice Method for Subsonic and Supersonic Flow," NASA CR 2875, 1977.
- [20] Souders, T.J. and Takahashi, T.T., "VORLAX 2020: Making a Potential Flow Solver Great Again," AIAA 2021-2458, 2021.
- [21] See: [https://www.smartcockpit.com/docs/A320-Flight\\_Controls.pdf](https://www.smartcockpit.com/docs/A320-Flight_Controls.pdf)
- [22] Leggett, D.B., and Black, G.T., "MIL-STD-1797 is Not a Cookbook," *Flying Qualities*, AGARD-CP-508, Feb. 1991, pp. 7-1 through 7-19.

APPENDIX A  
VORLAX INPUT FILES

X-2\_Stability\_Case\_withB\_Deflected\_at0Deg (Standard File Base Case with No Sideslip)

\*000000001111111111222222222233333333334444444444555555555566666666667777777777

\*23456789012345678901234567890123456789012345678901234567890123456789012345678901234567890

\*ISOLV LAX LAY REXPAR HAG FLOATX FLOATY ITRMAX

0.0 0.0 0.0 0.2 0.0 0.0 0.0 399

\*NMACH  
3 0.2 0.8 3.0

\*NALFA  
3 4 6 12

\*LATRL PSI PITCHQ ROLLQ YAWQ VINP

1.0 0.0 0.0 0.0 0.0 1.0

\*NPAN SREF CBAR XBAR ZBAR WSPAN

10 000258.04 008.32 008.58 000.00 0032.17

-----

\* Plate #1 wing 1

\*X1 Y1 Z1 CORD1 Comment:

0000.00 0000.00 0000.00 0010.70

0007.35 0007.97 0000.00 0008.05

\*NVOR RNCV SPC PDL

025.0 015.0 1.0 0.0

\*AINC1 AINC1 ITS NAP IQUMENT ISYNT NPP

0.00000 0.00000 0.0 00.0 2.0 0.0 00.0

-----

\* Plate #2 wing 2

\*X1 Y1 Z1 CORD1 Comment:

0007.35 0007.97 0000.00 0006.13

0014.83 0016.08 0000.00 0004.05

\*NVOR RNCV SPC PDL

025.0 010.0 1.0 0.0

\*AINC1 AINC1 ITS NAP IQUMENT ISYNT NPP

0.00000 0.00000 0.0 00.0 2.0 0.0 00.0

-----

\* Plate #3 Aileron\_R

\*X1 Y1 Z1 CORD1 Comment:

0013.48 0007.97 0000.00 0001.92

0018.88 0016.08 0000.00 0001.29

\*NVOR RNCV SPC PDL

025.0 005.0 0.0 0.0

\*AINC1 AINC1 ITS NAP IQUMENT ISYNT NPP

0.00000 0.00000 0.0 00.0 1.0 0.0 00.0

-----

\* Plate #4 Aileron\_L

\*X1 Y1 Z1 CORD1 Comment:

0013.48 -0007.97 0000.00 0001.92

0018.88 -0016.08 0000.00 0001.29

\*NVOR RNCV SPC PDL

025.0 005.0 0.0 0.0

\*AINC1 AINC1 ITS NAP IQUMENT ISYNT NPP

0.00000 0.00000 0.0 00.0 1.0 0.0 00.0

-----

\* Plate #5 Horizontal\_Tail\_R

\*X1 Y1 Z1 CORD1 Comment:

0021.40 0002.00 0004.45 0003.85

0027.01 0006.38 0004.45 0002.28

\*NVOR RNCV SPC PDL

010.0 010.0 1.0 0.0

\*AINC1 AINC1 ITS NAP IQUMENT ISYNT NPP

0.00000 0.00000 0.0 00.0 1.0 0.0 00.0

-----

\* Plate #6 Horizontal\_Tail\_L

\*X1 Y1 Z1 CORD1 Comment:

0021.40 -0002.00 0004.45 0003.85

0027.01 -0006.38 0004.45 0002.28

\*NVOR RNCV SPC PDL

010.0 010.0 1.0 0.0

\*AINC1 AINC1 ITS NAP IQUMENT ISYNT NPP

0.00000 0.00000 0.0 00.0 1.0 0.0 00.0

-----

\* Plate #7 Vertical Tail

\*X1 Y1 Z1 CORD1 Comment:

0014.91 0000.00 0004.45 0007.75

0021.00 0000.00 0011.12 0001.65

\*NVOR RNCV SPC PDL

010.0 010.0 1.0 0.0

\*AINC1 AINC1 ITS NAP IQUMENT ISYNT NPP

0.00000 0.00000 0.0 00.0 1.0 0.0 00.0

-----

```

* Plate #8 Rudder
*X1      Y1      Z1      CORD1      Comment:
0022.66  0000.00  0004.45  0001.24
0022.66  0000.00  0011.12  0001.24
*NVOR    RNCV    SPC      PDL
010.0    005.0      0.0      0.0
*AINC1   AINC1   ITS      NAP      IQANT    ISYNT    NPP
0.00000  0.00000  0.0      00.0     1.0      0.0      00.0
*-----
* Plate #9 Horizontal_Fuselage_1
*X1      Y1      Z1      CORD1      Comment:
-0007.80  0000.05  0004.45  0031.65
-0007.80  0002.00  0004.45  0031.65
*NVOR    RNCV    SPC      PDL
005.0    050.0     1.0      0.0
*AINC1   AINC1   ITS      NAP      IQANT    ISYNT    NPP
0.00000  0.00000  0.0      00.0     2.0      0.0      00.0
*-----
* Plate #10 Upper Vertical
*X1      Y1      Z1      CORD1      Comment:
-0007.75  0000.00  0004.45  0031.65
-0013.75  0000.00  0000.00  0037.65
*NVOR    RNCV    SPC      PDL
005.0    050.0     1.0      0.0
*AINC1   AINC1   ITS      NAP      IQANT    ISYNT    NPP
0.00000  0.00000  0.0      00.0     1.0      0.0      00.0
*-----
* NXS      NYS      NZS
00.0      00.0     00.0
*
* END

```





```

5      10      1      0
*AINC1 ANINC2 ITS  NAP      IQUNT  ISYNT  NPP
0      0      0      0      1      0      0
*-----*
*Panel #6 All Moving Vertical Tail Panel
*X      Y      Z      CORD
39.92  0      3.909  9.378
41.243 0      7.018  7.598
*NVOR   RNCV   SPC   PDL
5      10     1     0
*AINC1 ANINC2 ITS  NAP      IQUNT  ISYNT  NPP
-0.0000 -0.0000 0      0      1      0      0
*-----*
*Panel #7 Ventral Tail Panel
*X      Y      Z      CORD
39.26  0.00   -2.355 10.267
40.966 0.00   -3.845 9.0
*NVOR   RNCV   SPC   PDL
5      10     1     0
*AINC1 ANINC2 ITS  NAP      IQUNT  ISYNT  NPP
0      0      0      0      1      0      0
*-----*
*Panel #8 Horizontal Tail Panel
*X      Y      Z      CORD
41.82  3.665  0      6.94
48.22  8.82  -0.644 1.69
*NVOR   RNCV   SPC   PDL
10     6      1     0
*AINC1 ANINC2 ITS  NAP      IQUNT  ISYNT  NPP
0.000  0.000  0      0      1      0      0
*Panel #9 Horizontal Tail Panel
*X      Y      Z      CORD
41.82  -3.665 0      6.94
48.22  -8.82  -0.644 1.69
*NVOR   RNCV   SPC   PDL
10     6      1     0
*AINC1 ANINC2 ITS  NAP      IQUNT  ISYNT  NPP
0.000  0.000  0      0      1      0      0
* NXS   NYS   NZS
* 00    00    00
*
* END

```

AIRBUS\_A320\_base (Standard File Base Case with No Flaps and No Sideslip)

```

*
*
*ISOLV    LAX      LAY      REXPAR    HAG      FLOATX    FLOATY    ITRMAX
0.0      0.0      1.0      0.2      0.0      0.0      0.0      399
*
*NMACH
3      0.2 0.6 0.8
*NALFA
3      4 6 12
*
*LATRL    PSI      PITCHQ    ROLLQ     YAWQ      VINF
0      -0.00    0.00     0.00     0.00     1.00
*
*NPAN     SREF      CBAR      XBAR      ZBAR      WSPAN
13     1320    11.8     55.46    2.50     111.88
*
*
*                AIRCRAFT PANEL LAYOUT
*123456789!123456789!123456789!123456789!123456789!123456789!123456789!
*      !      !      !      !      !      !      !
*
*-----X1!-----Y1!-----Z1!-----CORD1!
*      0.00      0.00      0.00      100
*      12.475    0.00      13.583    116.775
*
*-----NVOR!-----RNCV!-----SPC!-----PDL!
*      5.00      50.0      1.00      0.00
*
*-----AINC1!-----AINC2!-----ITS!-----NAP!-----IQUANT!-----ISYNT!-----NPP!
*      0.0      0.0      0      0      1      0      0
*
*-----X1!-----Y1!-----Z1!-----CORD1!
*      0.00      0.00      0.00      129.25
*      12.475    6.475     0.00      110
*
*-----NVOR!-----RNCV!-----SPC!-----PDL!
*      5.00      50.0      1.00      0.00
*
*-----AINC1!-----AINC2!-----ITS!-----NAP!-----IQUANT!-----ISYNT!-----NPP!
*      0.0      0.0      0      0      2      0      0
*
*-----X1!-----Y1!-----Z1!-----CORD1!
*      43.710    6.475     0.00      19.357
*      49.470    18.833    1.08      13.597
*
*-----NVOR!-----RNCV!-----SPC!-----PDL!
*      12.00     15.0      1.00      0.00
*
*-----AINC1!-----AINC2!-----ITS!-----NAP!-----IQUANT!-----ISYNT!-----NPP!
*      0.0      0.0      0      0      2      0      0
*
*-----X1!-----Y1!-----Z1!-----CORD1!
*      63.067    6.475     0.00      3.333
*      63.067    18.833    1.08      3.333
*
*-----NVOR!-----RNCV!-----SPC!-----PDL!
*      12.00     5.0       0.00      0.00
*
*-----AINC1!-----AINC2!-----ITS!-----NAP!-----IQUANT!-----ISYNT!-----NPP!
*      -0.700    -0.700     0      0      2      0      0
*
*-----X1!-----Y1!-----Z1!-----CORD1!
*      49.470    18.833    1.08      13.597
*      61.006    43.573    3.24      5.7665
*
*-----NVOR!-----RNCV!-----SPC!-----PDL!
*      25.00     15.0      1.00      0.00
*
*-----AINC1!-----AINC2!-----ITS!-----NAP!-----IQUANT!-----ISYNT!-----NPP!
*      0.0      0.0      0      0      2      0      0
*
*-----X1!-----Y1!-----Z1!-----CORD1!
*      63.067    18.833    1.08      3.333

```

```

*      66.772    43.573    3.24    3.333
*
*-----NVOR!-----RNCV!-----SPC!-----PDL!
*      25.00     5.0      0.00    0.00
*
*-----AINC1!-----AINC2!-----ITS!-----NAP!-----IQUANT!-----ISYNT!-----NPP!
*     -0.700    -0.700     0      0      2      0      0
*
*-----X1!-----Y1!-----Z1!-----CORD1!
*      61.006    43.573    3.24    3.5995
*      65.843    53.143    4.08    2.0519
*
*-----NVOR!-----RNCV!-----SPC!-----PDL!
*      15.00     10.0     1.00    0.00
*
*-----AINC1!-----AINC2!-----ITS!-----NAP!-----IQUANT!-----ISYNT!-----NPP!
*      0.0      0.0      0      0      2      0      0
*
*-----X1!-----Y1!-----Z1!-----CORD1!
*      64.605    43.573    3.24    2.167
*      67.8949   53.143    4.08    2.167
*
*-----NVOR!-----RNCV!-----SPC!-----PDL!
*      10.00     5.0      0.00    0.00
*
*-----AINC1!-----AINC2!-----ITS!-----NAP!-----IQUANT!-----ISYNT!-----NPP!
*      0.0      0.0      0      0      1      0      0
*
*-----X1!-----Y1!-----Z1!-----CORD1!
*      64.605   -43.573    3.24    2.167
*      67.8949  -53.143    4.08    2.167
*
*-----NVOR!-----RNCV!-----SPC!-----PDL!
*      10.00     5.0      0.00    0.00
*
*-----AINC1!-----AINC2!-----ITS!-----NAP!-----IQUANT!-----ISYNT!-----NPP!
*      0.0      0.0      0      0      1      0      0
*
*-----X1!-----Y1!-----Z1!-----CORD1!
*      65.843    53.143    4.08    4.2189
*      67.225    55.940    4.327   3.75
*
*-----NVOR!-----RNCV!-----SPC!-----PDL!
*      2.00     15.0     1.00    0.00
*
*-----AINC1!-----AINC2!-----ITS!-----NAP!-----IQUANT!-----ISYNT!-----NPP!
*      0.0      0.0      0      0      2      0      0
*
*-----X1!-----Y1!-----Z1!-----CORD1!
*      111.30    6.475     0.1     7.527
*      119.80   20.425    1.566   2.403
*
*-----NVOR!-----RNCV!-----SPC!-----PDL!
*      14.00     10.0     1.00    0.00
*
*-----AINC1!-----AINC2!-----ITS!-----NAP!-----IQUANT!-----ISYNT!-----NPP!
*      0.0      0.0      0      0      2      0      0
*
*-----X1!-----Y1!-----Z1!-----CORD1!
*      118.827    6.475     0.1     3.333
*      122.203   20.425    1.566   1.667
*
*-----NVOR!-----RNCV!-----SPC!-----PDL!
*      14.00     5.0      0.00    0.00
*
*-----AINC1!-----AINC2!-----ITS!-----NAP!-----IQUANT!-----ISYNT!-----NPP!
*      0.0      0.0      0      0      1      0      0
*
*-----X1!-----Y1!-----Z1!-----CORD1!
*      118.827   -6.475     0.1     3.333
*      122.203  -20.425    1.566   1.667
*

```

```

*-----NVOR!-----RNCV!-----SPC!-----PDL!
      14.00      5.0      0.00      0.00
*
*-----AINC1!-----AINC2!-----ITS!-----NAP!----IQUANT!-----ISYNT!-----NPP!
      0.0      0.0      0      0      1      0      0
*
*-----X1!-----Y1!-----Z1!-----CORD1!
      101.30      0.000      13.583      13.08
      118.62      0.000      30.166      4.045
*
*-----NVOR!-----RNCV!-----SPC!-----PDL!
      10.00      10.0      1.00      0.00
*
*-----AINC1!-----AINC2!-----ITS!-----NAP!----IQUANT!-----ISYNT!-----NPP!
      0.0      0.0      0      0      1      0      0
*
*-----X1!-----Y1!-----Z1!-----CORD1!
      114.38      0.000      13.583      6.000
      122.665      0.000      30.166      2.167
*
*-----NVOR!-----RNCV!-----SPC!-----PDL!
      10.00      5.0      0.00      0.00
*
*-----AINC1!-----AINC2!-----ITS!-----NAP!----IQUANT!-----ISYNT!-----NPP!
      0.000      0.000      0      0      1      0      0
*
*NXS   NYS   NZS
      0     0     0
* END

```

AIRBUS\_A320\_flaps3\_base (Standard File Base Case with Flaps and No Sideslip)

```

*
*
*ISOLV      LAX      LAY      REXPAR      HAG      FLOATX      FLOATY      ITRMAX
0.0        0.0        1.0        0.2         0.0         0.0         0.0         399
*
*NMACH
3          0.2 0.6 0.8
*NALFA
3          4 6 12
*
*LATRL      PSI      PITCHQ      ROLLQ      YAWQ      VINFL
0          -0.00     0.00       0.00       0.00       1.00
*
*NPAN      SREF      CBAR      XBAR      ZBAR      WSPAN
15         1320     11.8       55.46      2.50       111.88
*
*
*                AIRCRAFT PANEL LAYOUT
*123456789!123456789!123456789!123456789!123456789!123456789!123456789!
*          !          !          !          !          !          !          !
*
*-----Fuselage Body Vertical-----
*-----X1!-----Y1!-----Z1!-----CORD1!
0.00      0.00      0.00      100
12.475    0.00     13.583    116.775
*
*-----NVOR!-----RNCV!-----SPC!-----PDL!
5.00     50.0     1.00     0.00
*
*-----AINC1!-----AINC2!-----ITS!-----NAP!-----IQUANT!-----ISYNT!-----NPP!
0.0       0.0       0         0         1         0         0
*
*-----Fuselage Body Horizontal-----
*-----X1!-----Y1!-----Z1!-----CORD1!
0.00      0.00      0.00     129.25
12.475    6.475    0.00     110
*
*-----NVOR!-----RNCV!-----SPC!-----PDL!
5.00     50.0     1.00     0.00
*
*-----AINC1!-----AINC2!-----ITS!-----NAP!-----IQUANT!-----ISYNT!-----NPP!
0.0       0.0       0         0         2         0         0
*
*-----Wing Inboard-----
*-----X1!-----Y1!-----Z1!-----CORD1!
43.710    6.475    0.00     19.357
49.470    18.833   1.08     13.597
*
*-----NVOR!-----RNCV!-----SPC!-----PDL!
12.00     15.0     1.00     0.00
*
*-----AINC1!-----AINC2!-----ITS!-----NAP!-----IQUANT!-----ISYNT!-----NPP!
0.0       0.0       0         0         2         0         0
*
*-----Inboard Flaps-----
*-----X1!-----Y1!-----Z1!-----CORD1!
63.067    6.475    0.00     3.333
63.067    18.833   1.08     3.333
*
*-----NVOR!-----RNCV!-----SPC!-----PDL!
12.00     5.0      0.00     0.00
*
*-----AINC1!-----AINC2!-----ITS!-----NAP!-----IQUANT!-----ISYNT!-----NPP!
-0.700    -0.700    0         0         2         0         0
*
*-----Wing Midspan-----
*-----X1!-----Y1!-----Z1!-----CORD1!
49.470    18.833   1.08     13.597
61.006    43.573   3.24     5.7665
*
*-----NVOR!-----RNCV!-----SPC!-----PDL!
25.00     15.0     1.00     0.00
*
*-----AINC1!-----AINC2!-----ITS!-----NAP!-----IQUANT!-----ISYNT!-----NPP!
0.0       0.0       0         0         2         0         0
*
*-----Midspan Flaps-----
*-----X1!-----Y1!-----Z1!-----CORD1!
63.067    18.833   1.08     3.333

```

```

*      66.772    43.573    3.24    3.333
*-----NVOR!-----RNCV!-----SPC!-----PDL!
*      25.00     5.0      0.00    0.00
*
*-----AINC1!-----AINC2!-----ITS!-----NAP!-----IQUANT!-----ISYNT!-----NPP!
*     -0.700    -0.700     0      0      2      0      0
*
*-----X1!-----Y1!-----Z1!-----CORD1!
*      61.006    43.573    3.24    3.5995
*      65.843    53.143    4.08    2.0519
*
*-----NVOR!-----RNCV!-----SPC!-----PDL!
*      15.00     10.0     1.00    0.00
*
*-----AINC1!-----AINC2!-----ITS!-----NAP!-----IQUANT!-----ISYNT!-----NPP!
*      0.0      0.0      0      0      2      0      0
*
*-----X1!-----Y1!-----Z1!-----CORD1!
*      64.605    43.573    3.24    2.167
*      67.8949   53.143    4.08    2.167
*
*-----NVOR!-----RNCV!-----SPC!-----PDL!
*      10.00     5.0      0.00    0.00
*
*-----AINC1!-----AINC2!-----ITS!-----NAP!-----IQUANT!-----ISYNT!-----NPP!
*      0.0      0.0      0      0      1      0      0
*
*-----X1!-----Y1!-----Z1!-----CORD1!
*      64.605   -43.573    3.24    2.167
*      67.8949  -53.143    4.08    2.167
*
*-----NVOR!-----RNCV!-----SPC!-----PDL!
*      10.00     5.0      0.00    0.00
*
*-----AINC1!-----AINC2!-----ITS!-----NAP!-----IQUANT!-----ISYNT!-----NPP!
*      0.0      0.0      0      0      1      0      0
*
*-----X1!-----Y1!-----Z1!-----CORD1!
*      65.843    53.143    4.08    4.2189
*      67.225    55.940    4.327   3.75
*
*-----NVOR!-----RNCV!-----SPC!-----PDL!
*      2.00     15.0     1.00    0.00
*
*-----AINC1!-----AINC2!-----ITS!-----NAP!-----IQUANT!-----ISYNT!-----NPP!
*      0.0      0.0      0      0      2      0      0
*
*-----X1!-----Y1!-----Z1!-----CORD1!
*     111.30    6.475     0.1     7.527
*     119.80   20.425    1.566    2.403
*
*-----NVOR!-----RNCV!-----SPC!-----PDL!
*      14.00     10.0     1.00    0.00
*
*-----AINC1!-----AINC2!-----ITS!-----NAP!-----IQUANT!-----ISYNT!-----NPP!
*      0.0      0.0      0      0      2      0      0
*
*-----X1!-----Y1!-----Z1!-----CORD1!
*     118.827    6.475     0.1     3.333
*     122.203   20.425    1.566    1.667
*
*-----NVOR!-----RNCV!-----SPC!-----PDL!
*      14.00     5.0      0.00    0.00
*
*-----AINC1!-----AINC2!-----ITS!-----NAP!-----IQUANT!-----ISYNT!-----NPP!
*      0.0      0.0      0      0      1      0      0
*
*-----X1!-----Y1!-----Z1!-----CORD1!
*     118.827   -6.475     0.1     3.333
*     122.203  -20.425    1.566    1.667
*

```

```

*-----NVOR!-----RNCV!-----SPC!-----PDL!
      14.00      5.0      0.00      0.00
*
*-----AINC1!-----AINC2!-----ITS!-----NAP!----IQUANT!-----ISYNT!-----NPP!
      0.0      0.0      0      0      1      0      0
*
*-----X1!-----Y1!-----Z1!-----CORD1!
      101.30      0.000      13.583      13.08
      118.62      0.000      30.166      4.045
*
*-----NVOR!-----RNCV!-----SPC!-----PDL!
      10.00      10.0      1.00      0.00
*
*-----AINC1!-----AINC2!-----ITS!-----NAP!----IQUANT!-----ISYNT!-----NPP!
      0.0      0.0      0      0      1      0      0
*
*-----X1!-----Y1!-----Z1!-----CORD1!
      114.38      0.000      13.583      6.000
      122.665      0.000      30.166      2.167
*
*-----NVOR!-----RNCV!-----SPC!-----PDL!
      10.00      5.0      0.00      0.00
*
*-----AINC1!-----AINC2!-----ITS!-----NAP!----IQUANT!-----ISYNT!-----NPP!
      0.000      0.000      0      0      1      0      0
*
*NXS   NYS   NZS
      0     0     0
* END

```



GHV VORLAX Model - Rev Dec 27, 2022 - TTT (Base Case with No Sideslip)  
 \*  
 \* This 100% scale reference geometry has an estimated launch mass of 5000-lbm  
 \* and an empty mass of 3000-lbm  
 \*

\* Estimated mass moment of inertias from X-15 are:  
 \* Ixx ~ 300 to 360 slug-ft^2 (empty --> full)  
 \* Iyy ~ 6000 to 8000 slug-ft^2 (empty --> full)  
 \* Izz ~ 6000 to 8000 slug-ft^2 (empty --> full)  
 \*

*ISOLV	LAX	LAY	REXPAR	HAG	FLOATX	FLOATY	ITRMAX
0	1	1	0.0	0	0	0	399
*NMACH	MACH						
3	3.0	5.0	7.0				
* 10	0.1	0.7	0.9	1.1	1.5	1.9	2.29 2.98 4.65 6.86
*NALPHA	ALPHA						
7	0	2	4	6	10	15	20
*LATRL	PSI	PITCHQ	ROLLQ	YAWQ	VINF		
0	0	0	0	0	1		
*NPAN	SREF	CBAR	XBAR	ZBAR	WSPAN		
11	5084.	84.733	100.0	0.0	60.0		

-----  
 \*0000000011111111222222223333333344444444555555556666666677777777778  
 \*234567890123456789012345678901234567890123456789012345678901234567890123456789012345678901234567890  
 \*

\*Panel #1 Horizontal Body Panel  
 \*X Y Z CORD  
 0.0 0.0 0.0 170.0  
 9.75 9.75 0.0 160.25  
 \*NVOR RNCV SPC PDL  
 4 50 0 0  
 \*AINC1 ANINC2 ITS NAP IQUANT ISYNT NPP  
 0 0 0 0 2 0 0  
 -----

\*Panel #2 Vertical Body Panel #1  
 \*X Y Z CORD  
 0 0 0 170.00  
 0.00 0 9.75 170.0  
 \*NVOR RNCV SPC PDL  
 4 50 0 0  
 \*AINC1 ANINC2 ITS NAP IQUANT ISYNT NPP  
 0 0 0 0 1 0 0  
 -----

\*Panel #3 Vertical Body Panel #2  
 \*X Y Z CORD  
 0 0 0 170.00  
 15.25 0 -15.25 154.75  
 \*NVOR RNCV SPC PDL  
 4 50 0 0  
 \*AINC1 ANINC2 ITS NAP IQUANT ISYNT NPP  
 0 0 0 0 1 0 0  
 -----

\*Panel #4 Inner wing Panel (84-deg sweep)  
 \*X Y Z CORD  
 20.0 9.75 0 150.00  
 95.0 17.6 0 75.00  
 \*NVOR RNCV SPC PDL  
 10 30 0 0  
 \*AINC1 ANINC2 ITS NAP IQUANT ISYNT NPP  
 0 0 0 0 2 0 0  
 -----

\*Panel #5 Outer wing Panel (73.3-deg sweep)  
 \*X Y Z CORD  
 95.0 17.6 0 65.00  
 153.0 30.0 0 10.0  
 \*NVOR RNCV SPC PDL  
 10 25 0 0  
 \*AINC1 ANINC2 ITS NAP IQUANT ISYNT NPP  
 0 0 0 0 2 0 0  
 -----

\* PANEL # 6 - ELEVON # 1  
 \*X Y Z CORD  
 160.0 17.6 0 10.00  
 163.0 30.0 0 7.0  
 \*NVOR RNCV SPC PDL  
 10 5 0 0

```

*AINC1  ANINC2  ITS      NAP      IQUNT  ISYNT  NPP
0        0        0        0        1      0      0
-----
*
*
* PANEL # 7 - ELEVON # 2
*X      Y      Z      CORD
160.0  -17.6  0      10.00
163.0  -30.0  0      7.0
*NVOR   RNCV   SPC   PDL
10      5      0      0
*AINC1  ANINC2  ITS      NAP      IQUNT  ISYNT  NPP
0        0        0        0        1      0      0
-----
*
*
*Panel # 8 Vertical Tail Panel # 1
*X      Y      Z      CORD
139.75  2.00  9.75  30.25
174.50  11.85 17.1  7.5
*NVOR   RNCV   SPC   PDL
10      10     0      0
*AINC1  ANINC2  ITS      NAP      IQUNT  ISYNT  NPP
0        0        0        0        1      0      0
-----
*
*
*Panel # 9 Vertical Tail Panel # 2
*X      Y      Z      CORD
139.75  -2.00  9.75  25.25
174.50  -11.85 17.1  2.5
*NVOR   RNCV   SPC   PDL
10      10     0      0
*AINC1  ANINC2  ITS      NAP      IQUNT  ISYNT  NPP
0        0        0        0        1      0      0
-----
*
*
*Panel # 10 Rudder # 1
*X      Y      Z      CORD
165.00  2.00  9.75  5.
177.00  11.85 17.1  5.
*NVOR   RNCV   SPC   PDL
10      5      0      0
*AINC1  ANINC2  ITS      NAP      IQUNT  ISYNT  NPP
0        0        0        0        1      0      0
-----
*
*
*Panel # 11 Rudder # 2
*X      Y      Z      CORD
165.00  -2.00  9.75  5.
177.00  -11.85 17.1  5.
*NVOR   RNCV   SPC   PDL
10      5      0      0
*AINC1  ANINC2  ITS      NAP      IQUNT  ISYNT  NPP
0        0        0        0        1      0      0
-----
*
* NXS      NYS      NZS
00        00        00
*
* END

```

APPENDIX B

BELL X-2 PRE-MIX MODEL AERODYNAMIC DATA

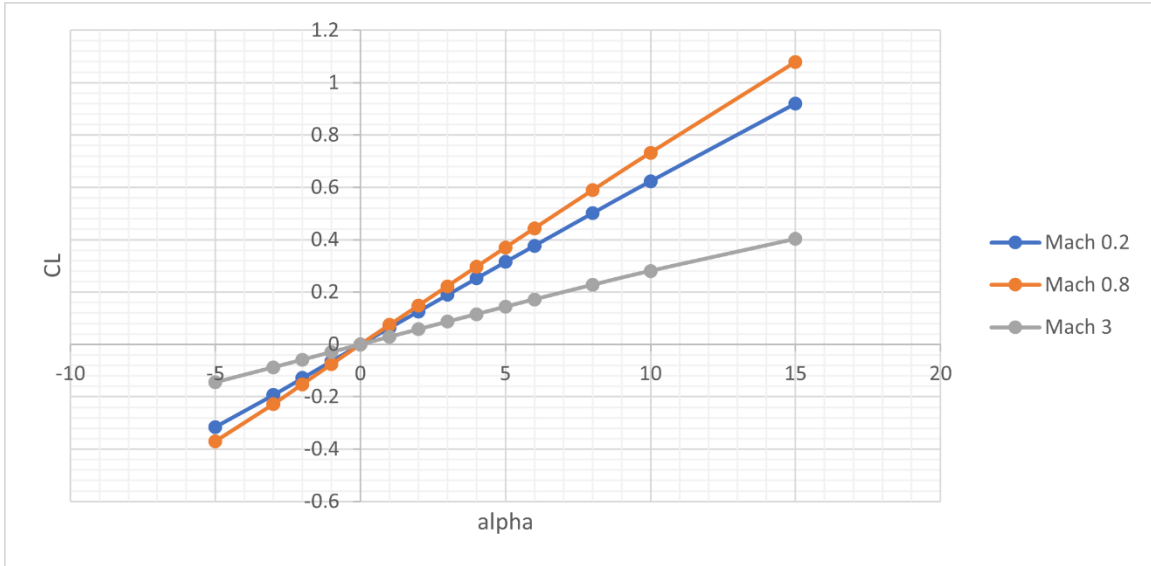


FIGURE B1 - CL vs alpha

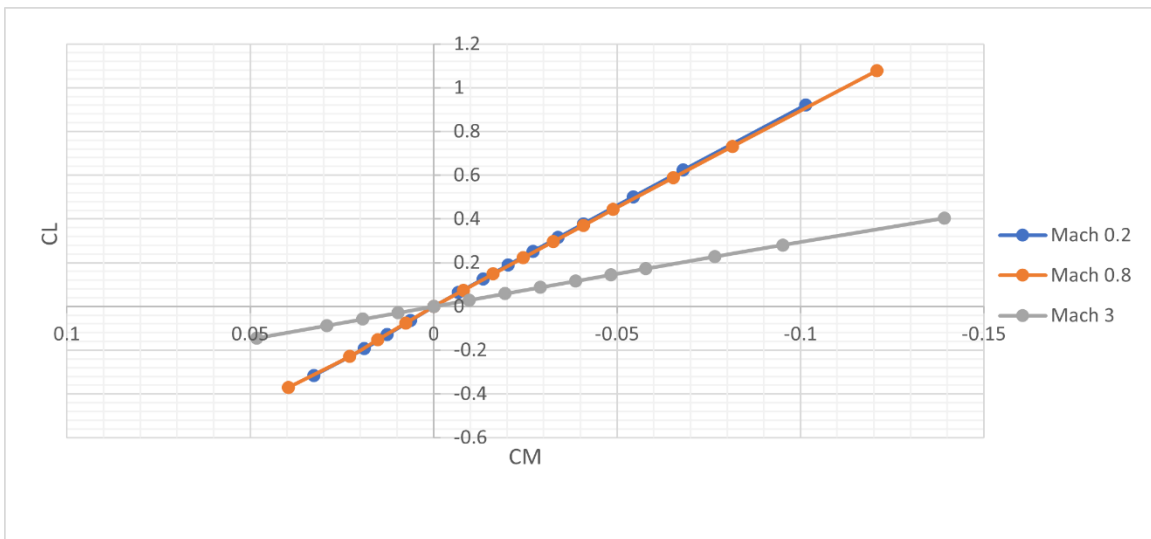


FIGURE B2 - CL vs CM

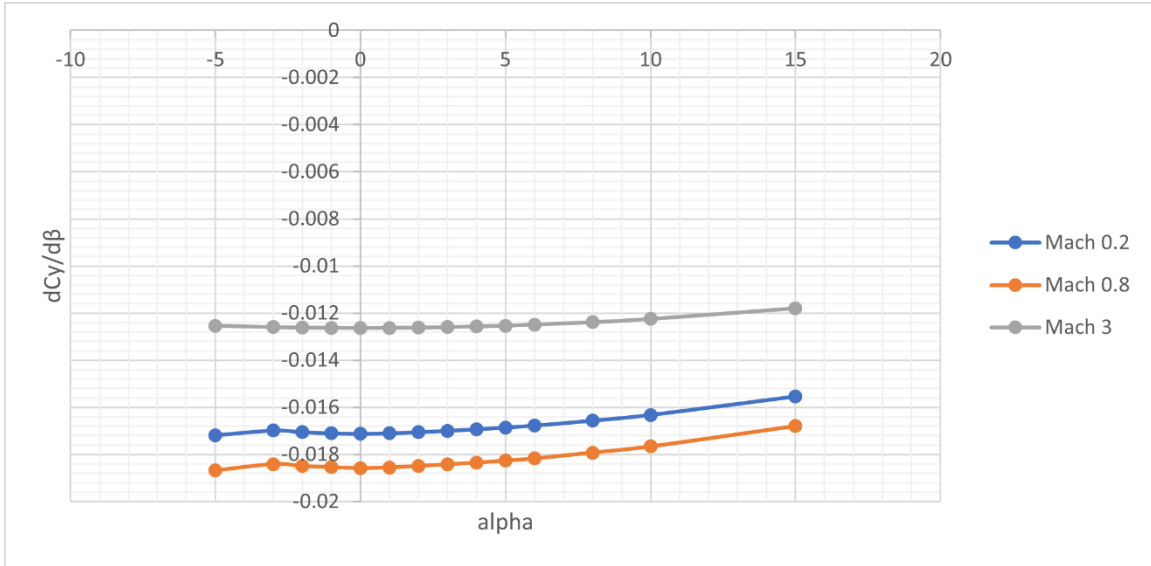


FIGURE B3 -  $C_\gamma\beta$  vs Alpha

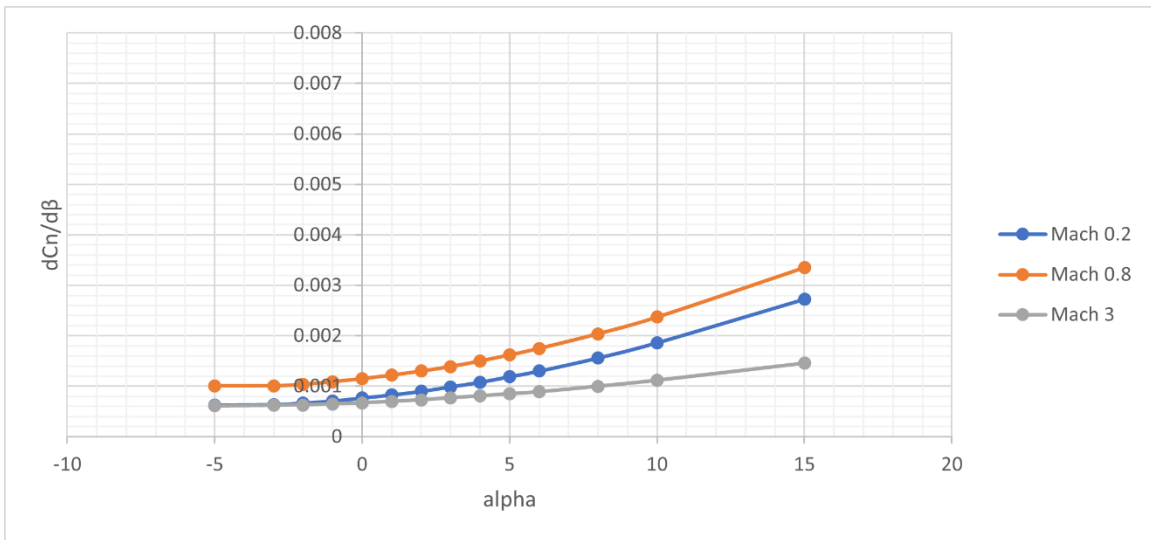


FIGURE B4 -  $C_n\beta$  vs Alpha

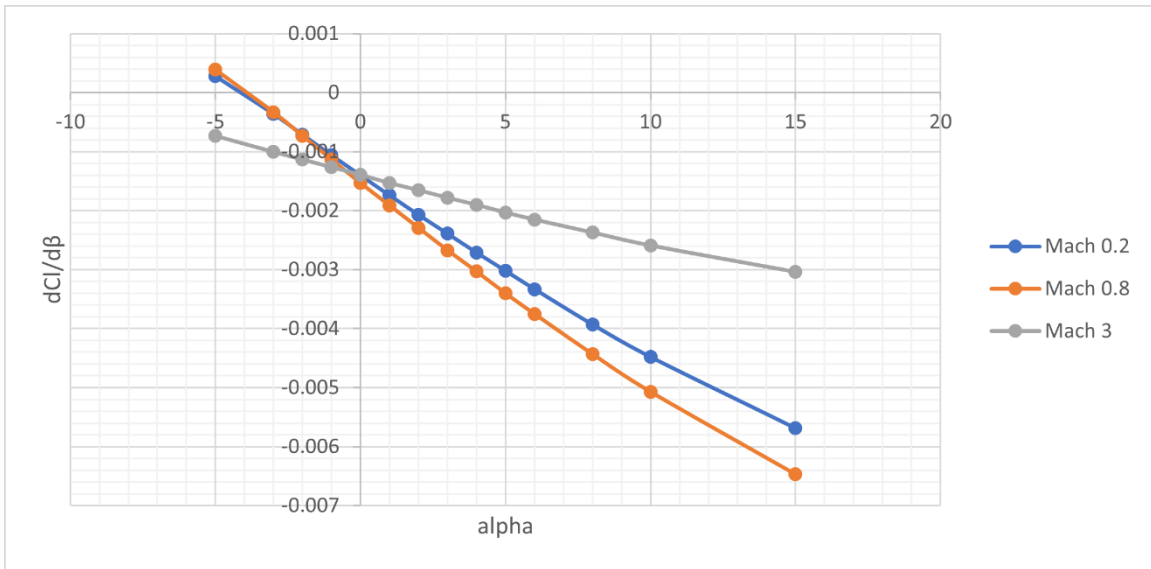


FIGURE B5 -  $C_l\beta$  vs Alpha

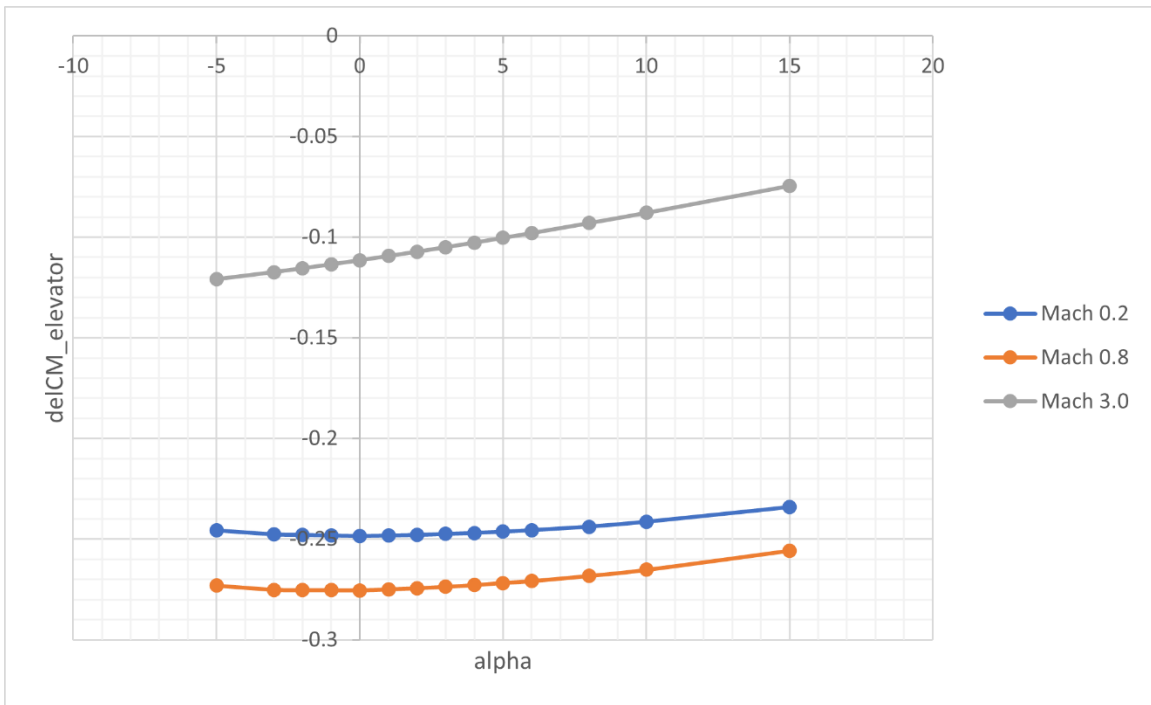


FIGURE B6 -  $C_{m\delta_e}$  vs Alpha

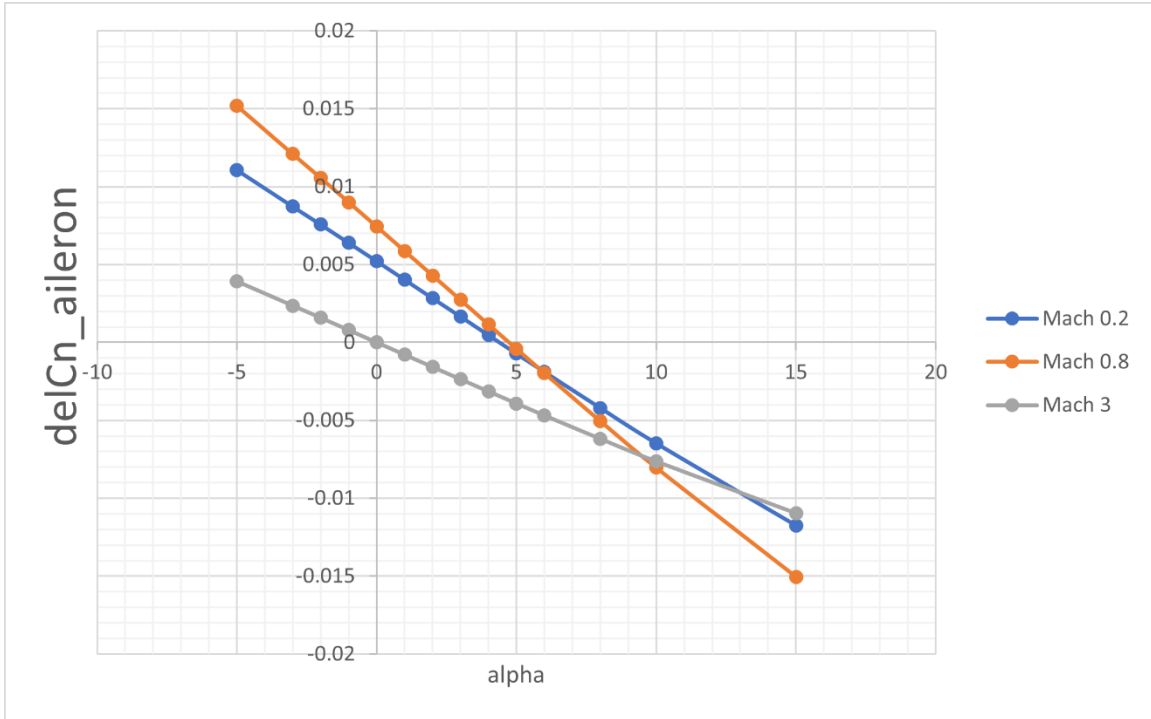


FIGURE B7  $-C_{n_{\delta a}}$  vs Alpha

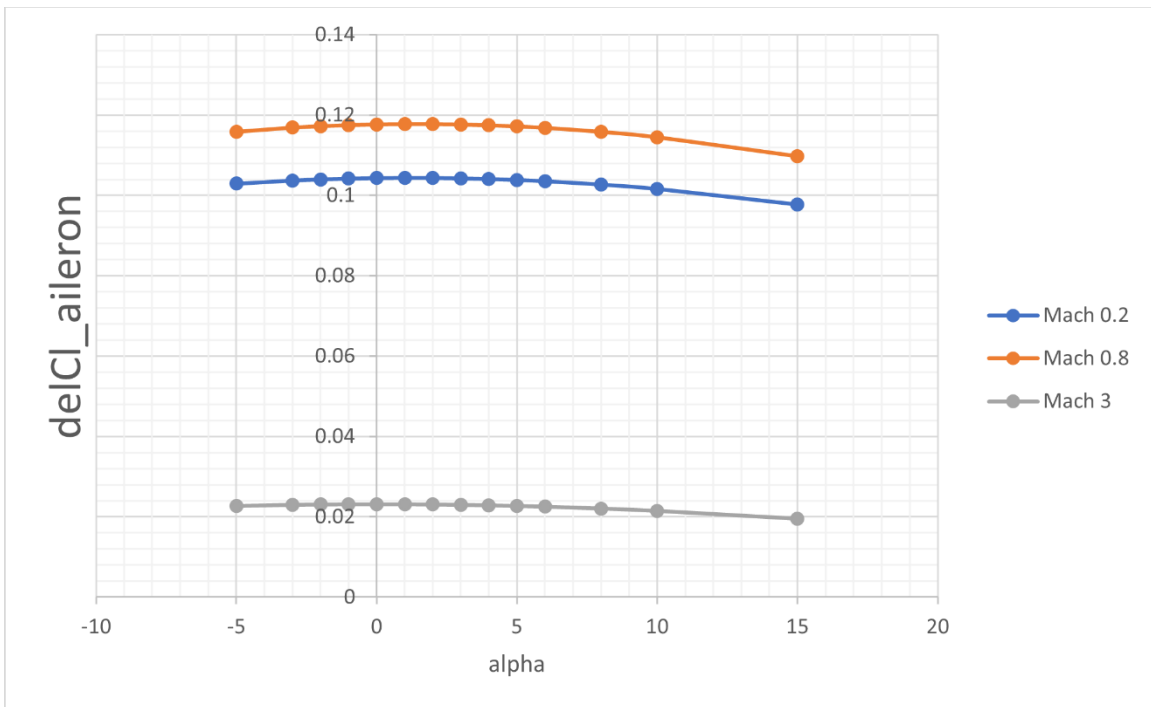


FIGURE B8  $-C_{l_{\delta a}}$  vs Alpha

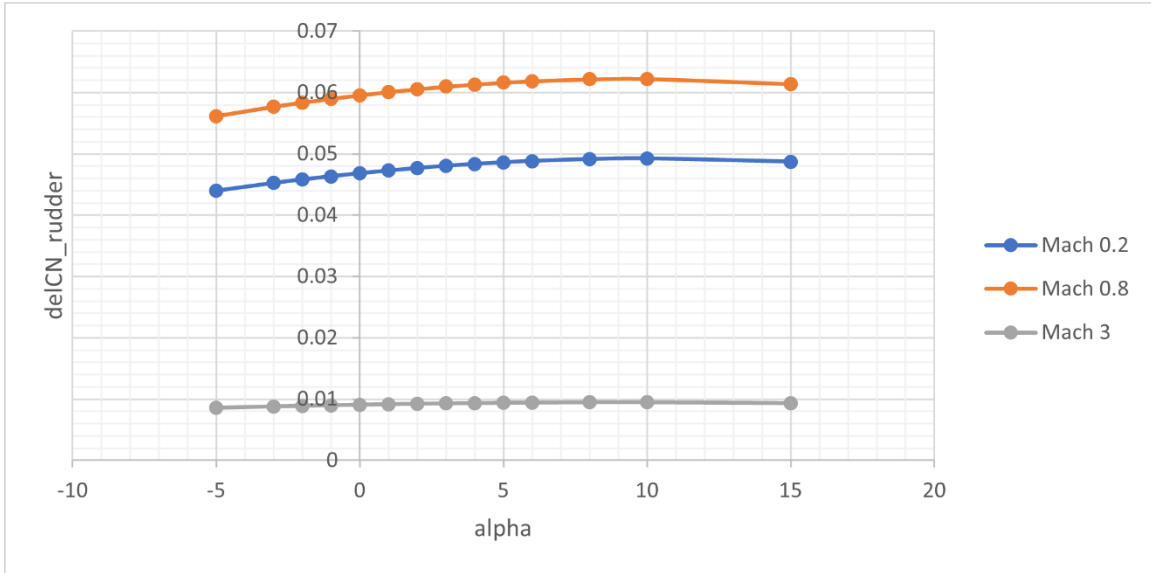


FIGURE B9 –  $C_{n_{\delta r}}$  vs Alpha

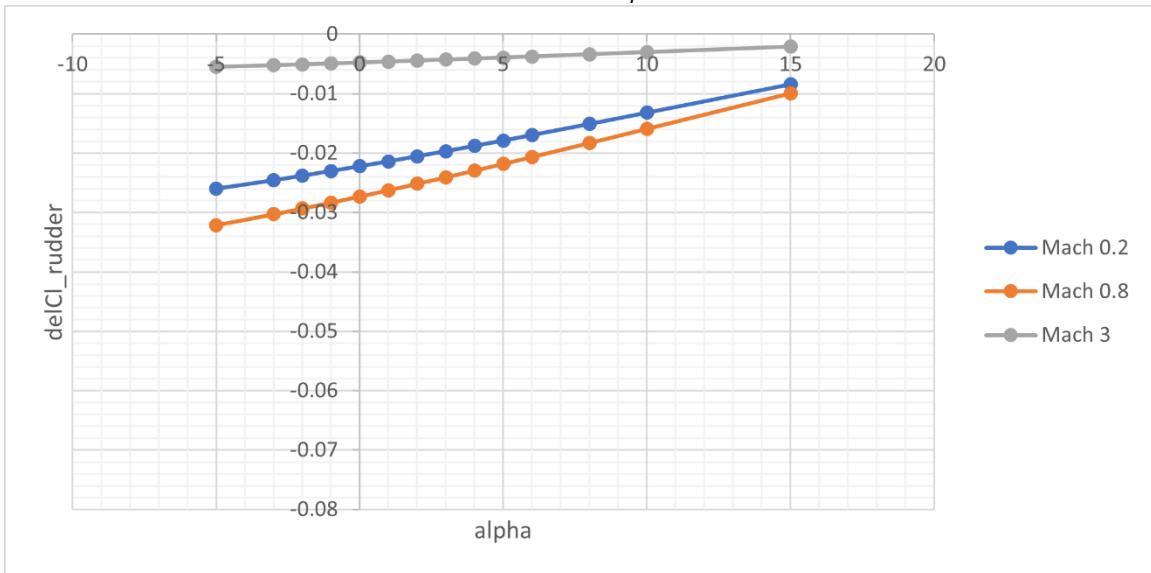


FIGURE B10 –  $C_{l_{\delta r}}$  vs Alpha



## APPENDIX C

### BELL X-2 INDEPENDENT SINGLE PANEL MODEL AERODYNAMIC DATA

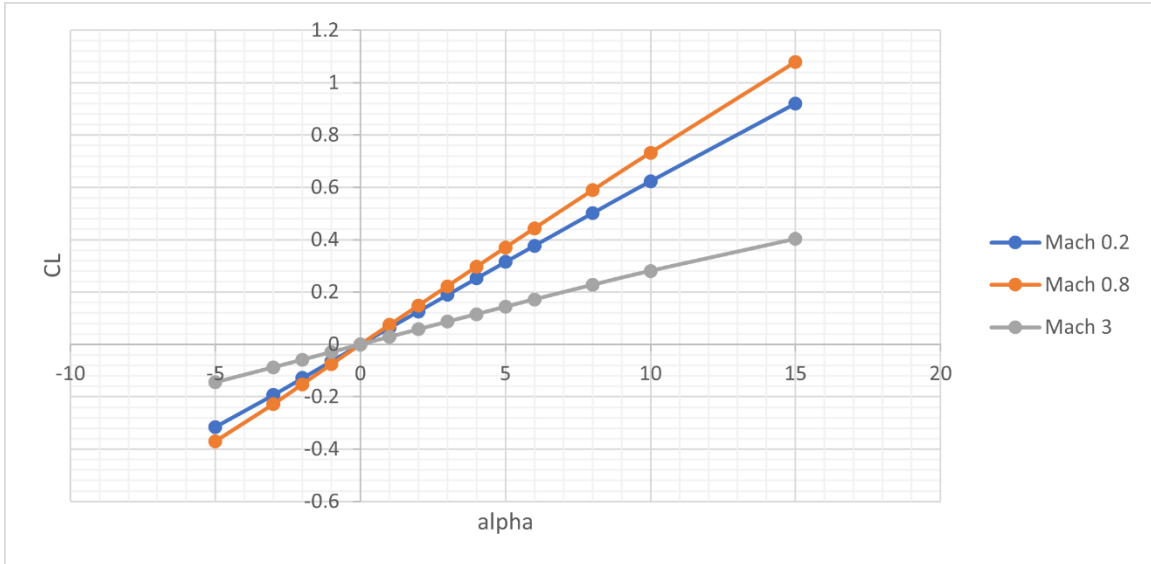


FIGURE C1 – CL vs Alpha

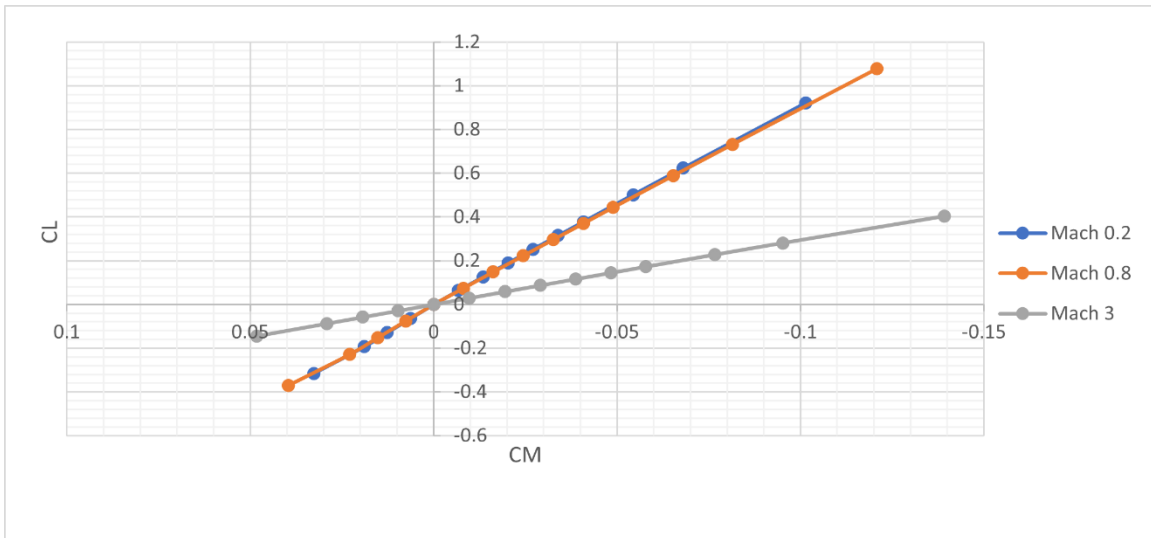


FIGURE C2 – CL vs CM

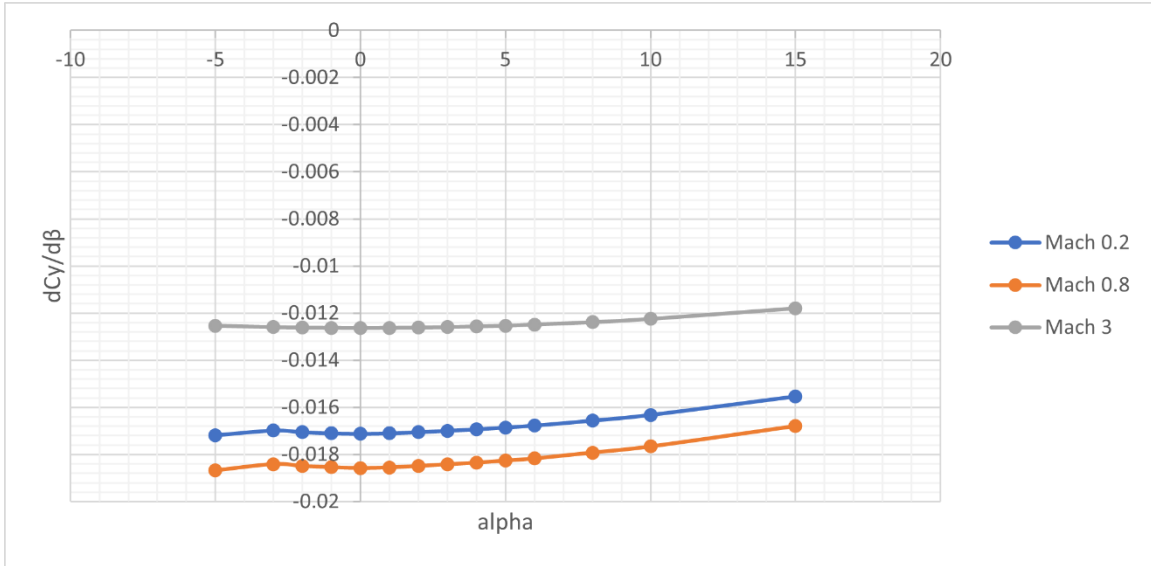


FIGURE C3 -  $C_{Y\beta}$  vs Alpha

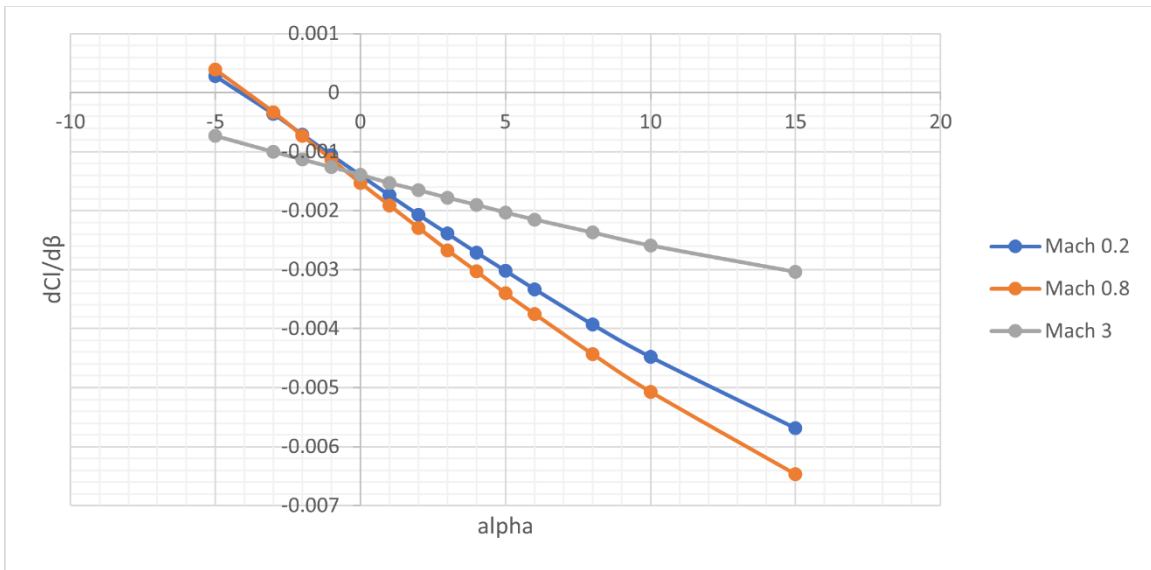


FIGURE C4 -  $C_{n\beta}$  vs Alpha

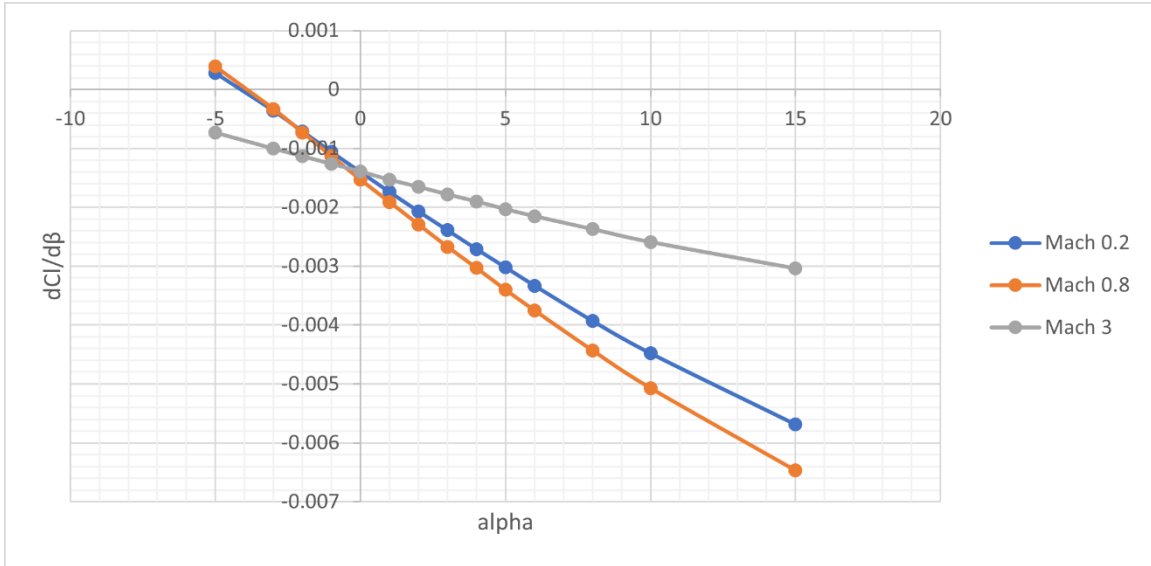


FIGURE C5 -  $C_l\beta$  vs Alpha

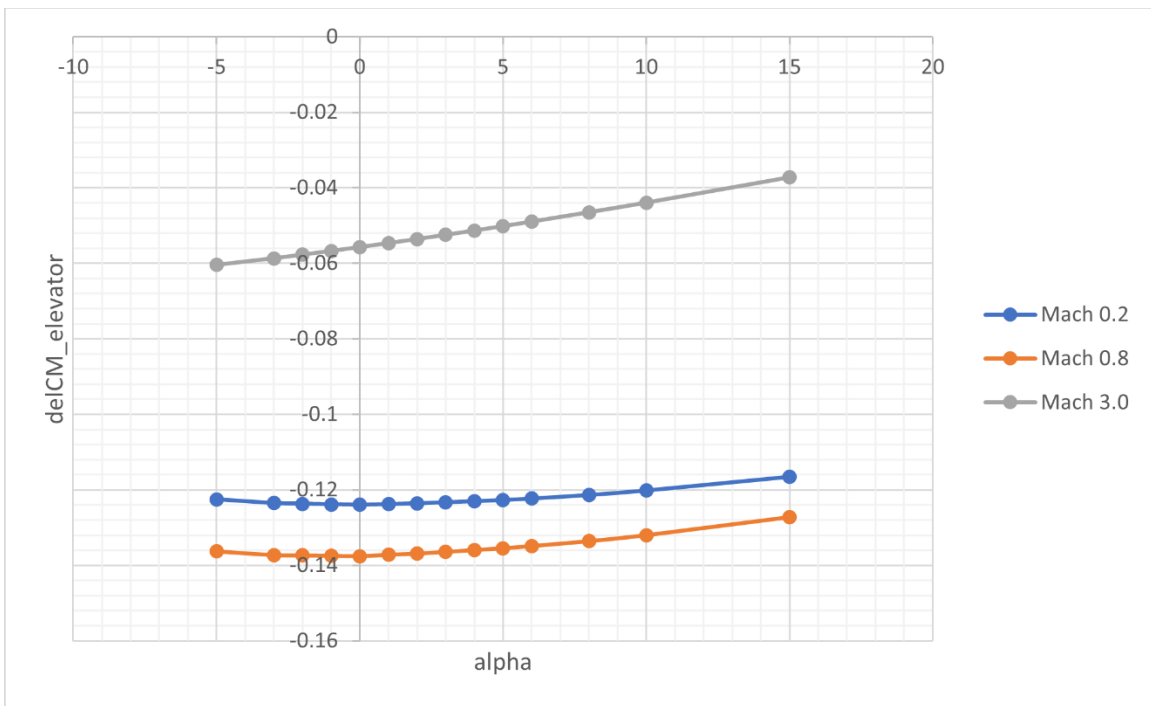


FIGURE C6 -  $C_{m\delta_e}$  vs Alpha, Positive Deflection

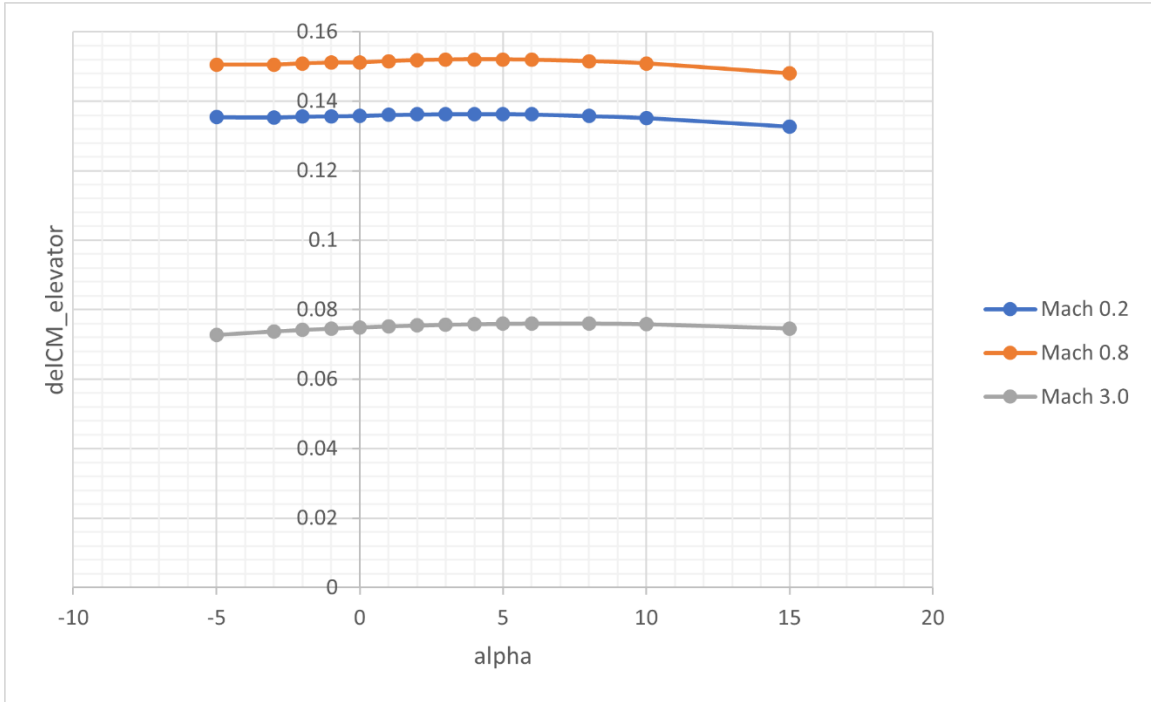


FIGURE C7 –  $C_{m_{\delta_e}}$  vs Alpha, Negative Deflection

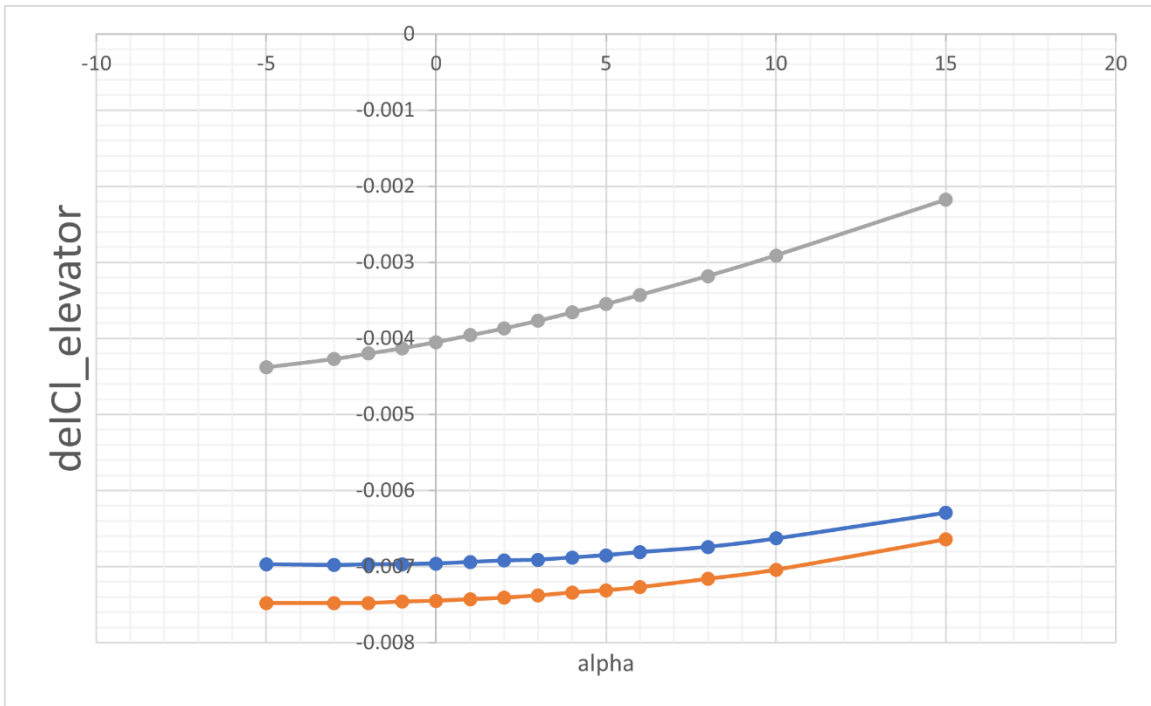


FIGURE C8 –  $C_{l_{\delta_e}}$  vs Alpha, Positive Deflection

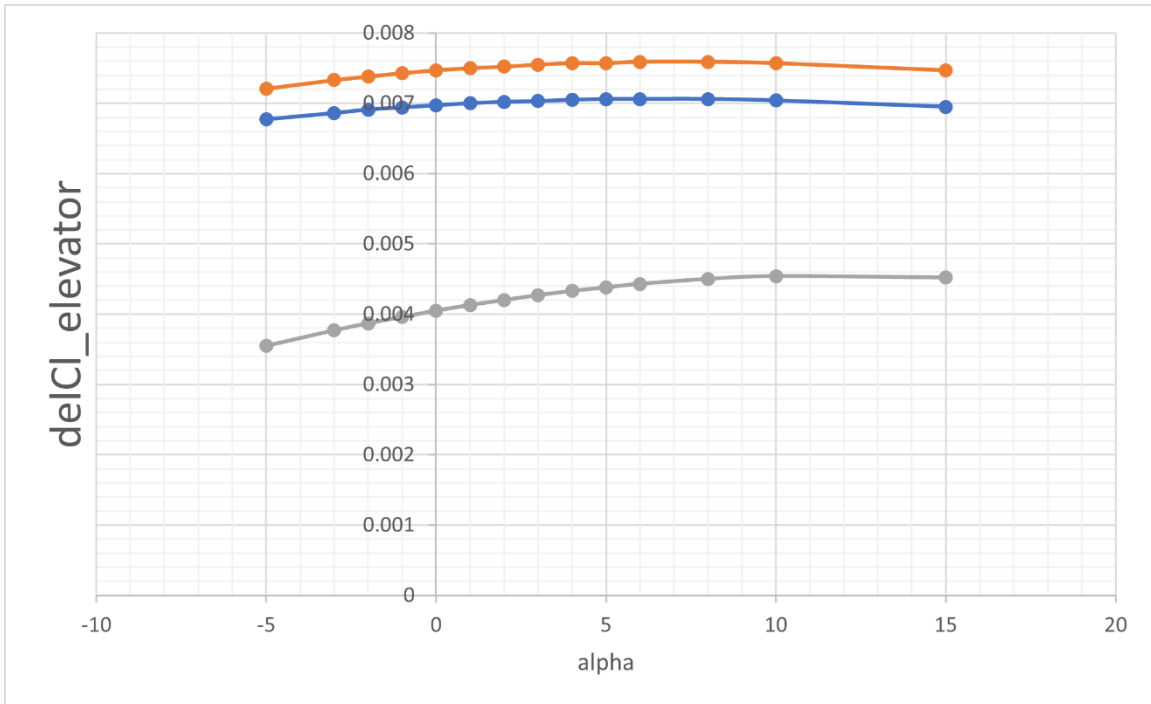


FIGURE C9 –  $C_{l_{\delta_e}}$  vs Alpha, Negative Deflection

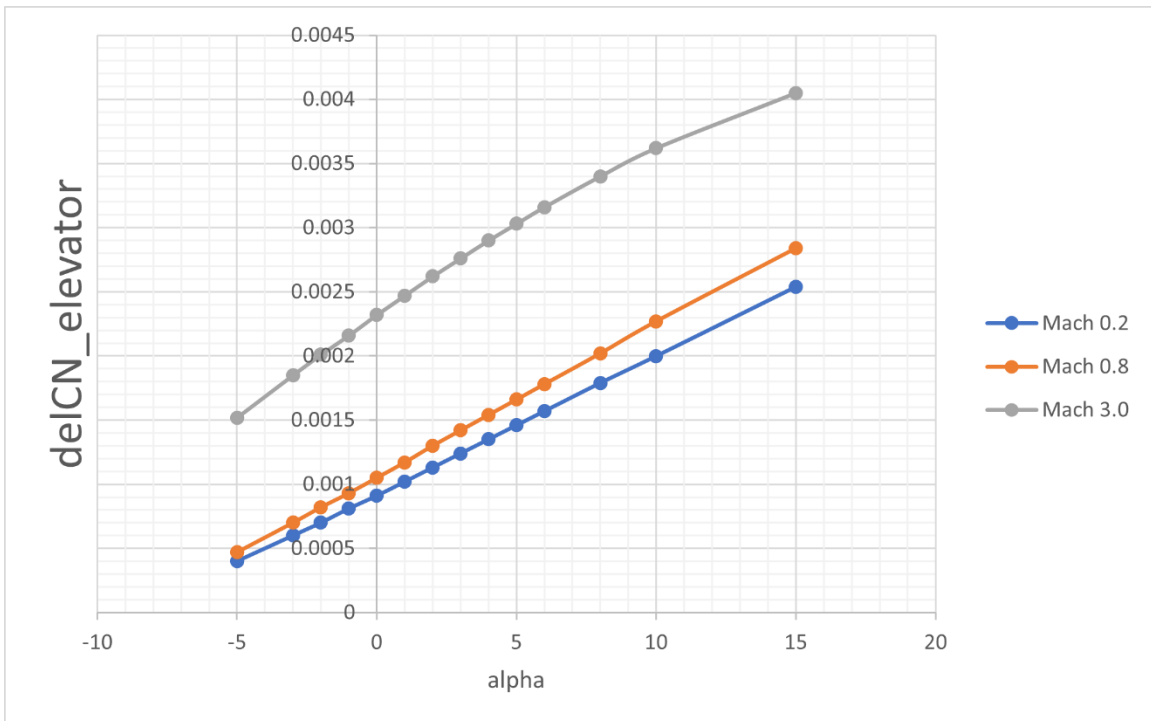


FIGURE C10 –  $C_{n_{\delta_e}}$  vs Alpha, Positive Deflection

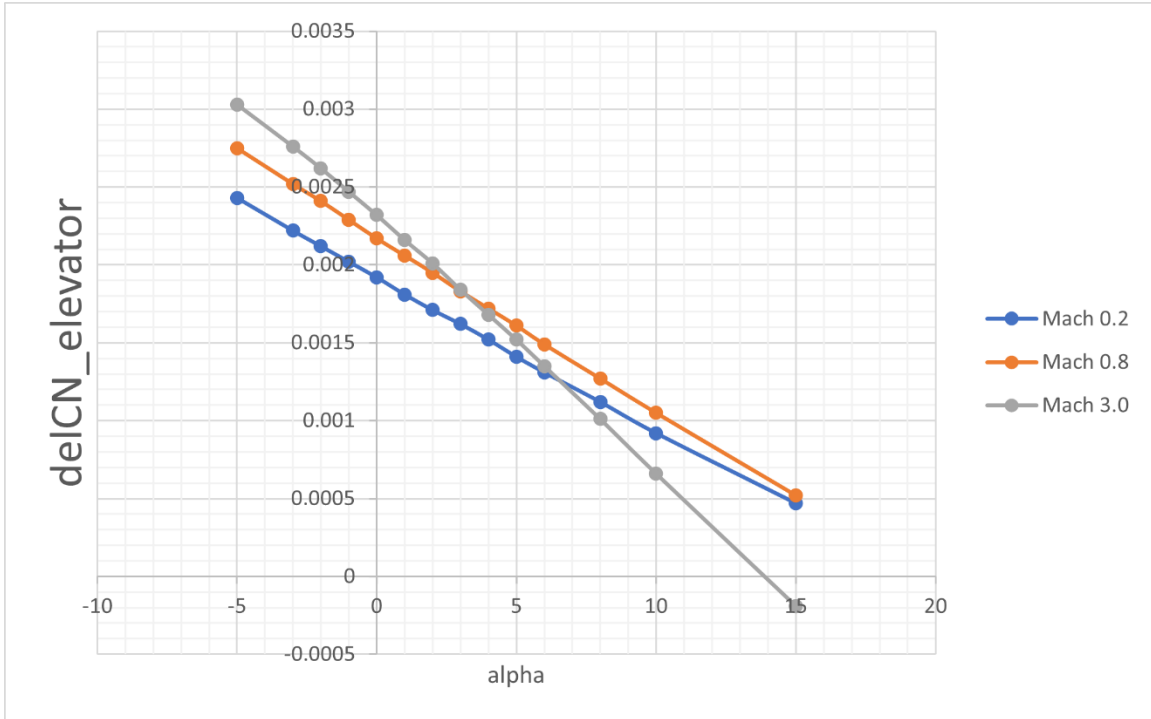


FIGURE C11 –  $C_{n_{\delta_e}}$  vs Alpha, Negative Deflection

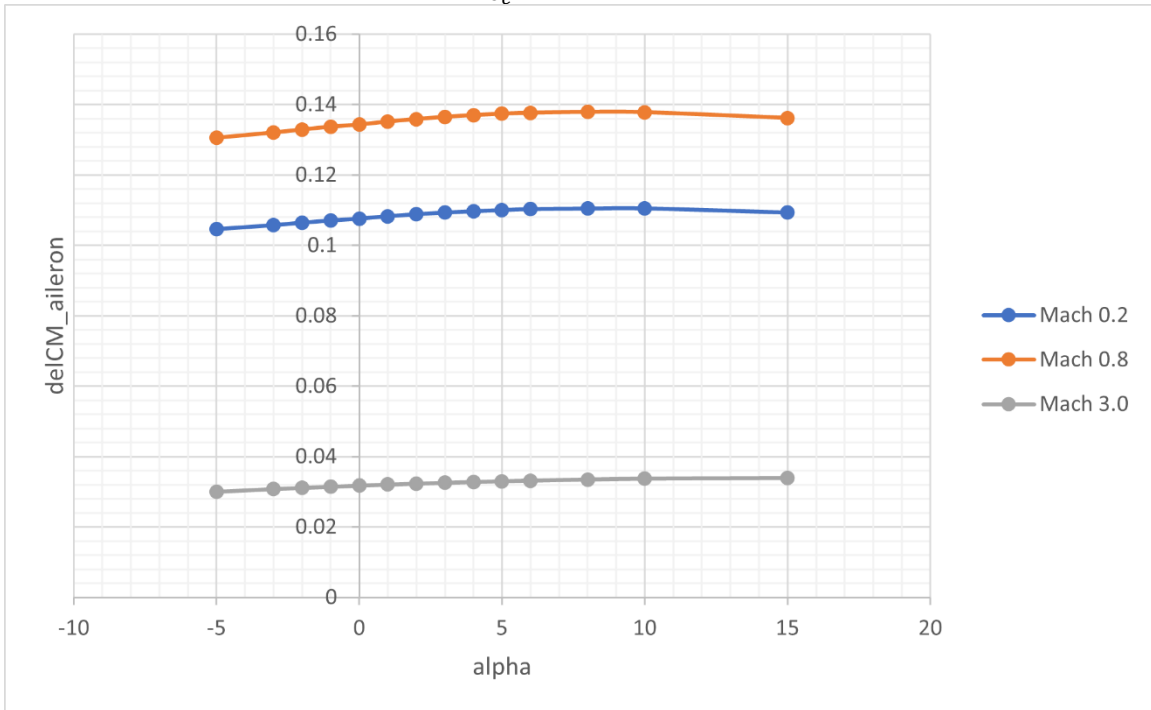


FIGURE C12 –  $C_{m_{\delta_a}}$  vs Alpha, Positive Deflection

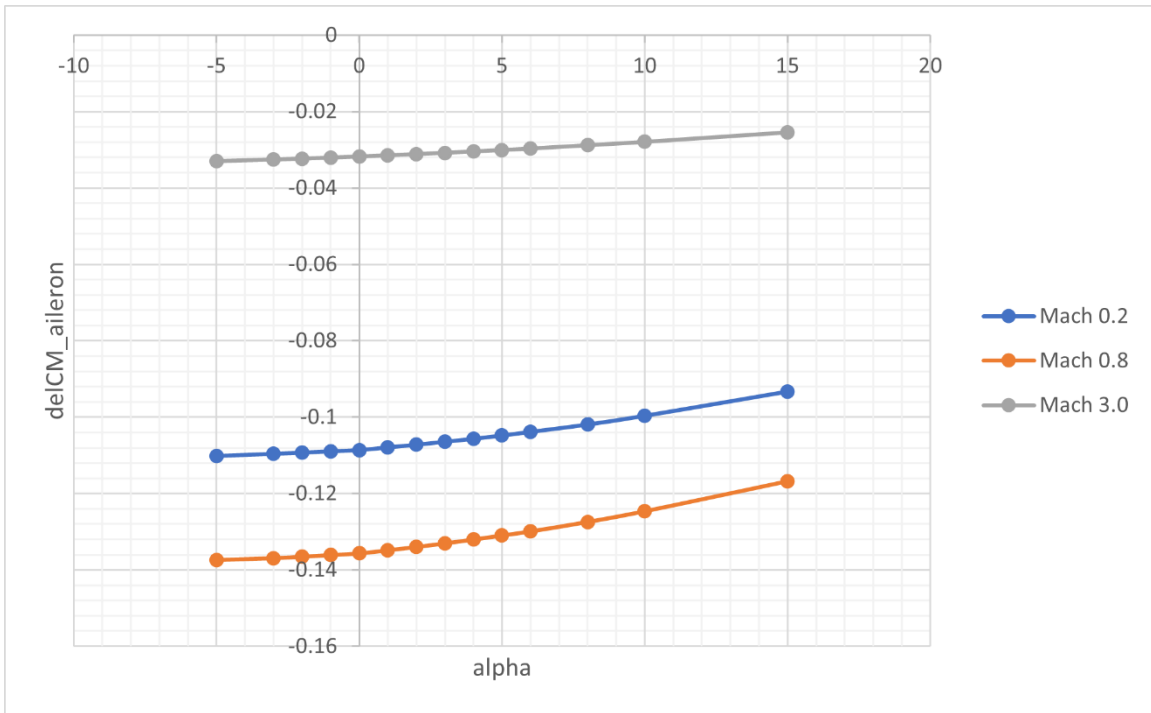


FIGURE C13  $-C_{m_{\delta a}}$  vs Alpha, Negative Deflection

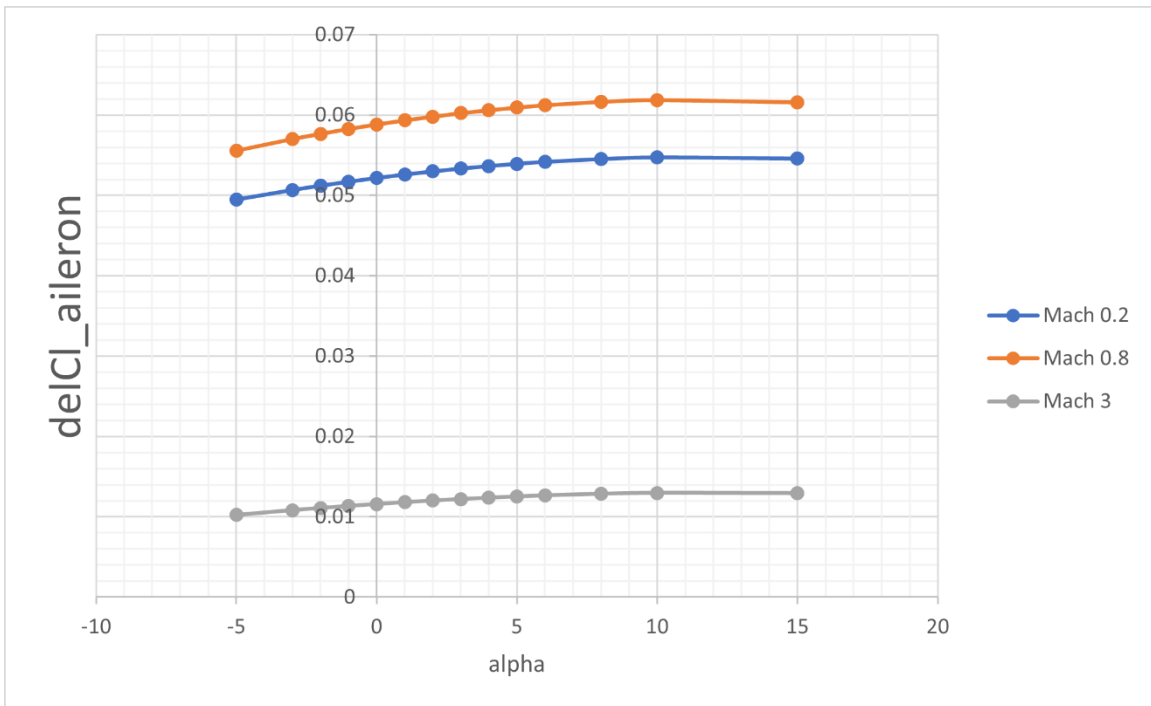


FIGURE C14  $C_{l_{\delta a}}$  vs Alpha, Positive Deflection



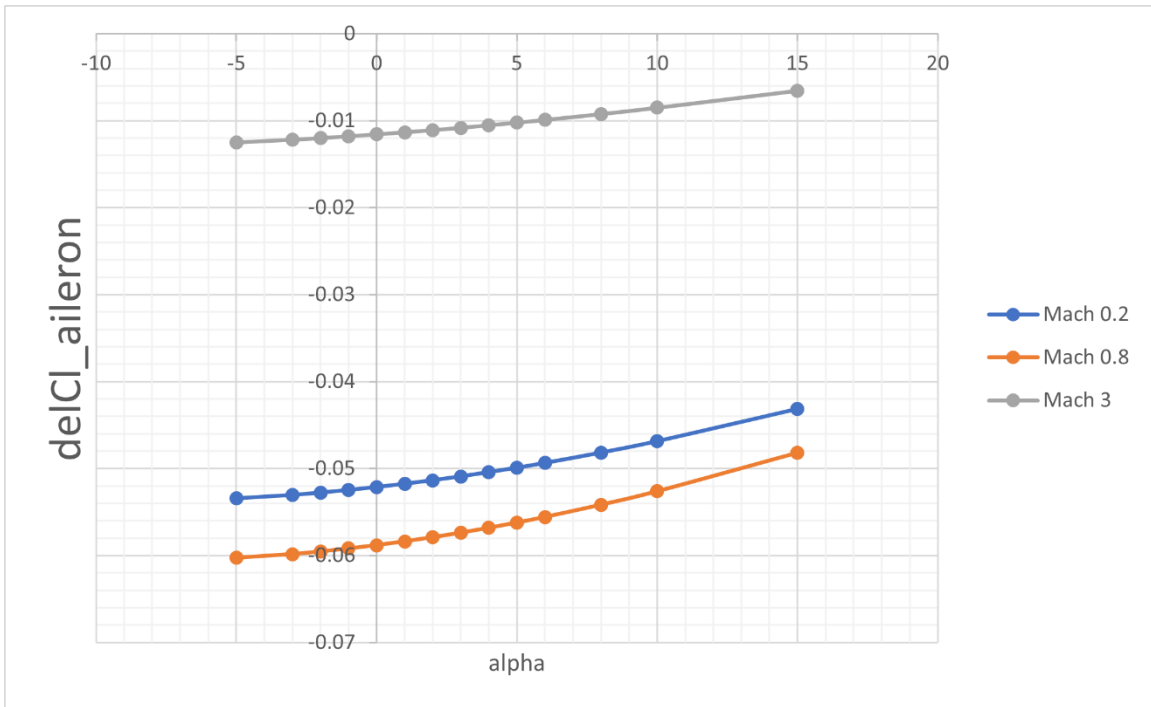


FIGURE C15 –  $C_{l_{\delta_a}}$  vs Alpha, Negative Deflection

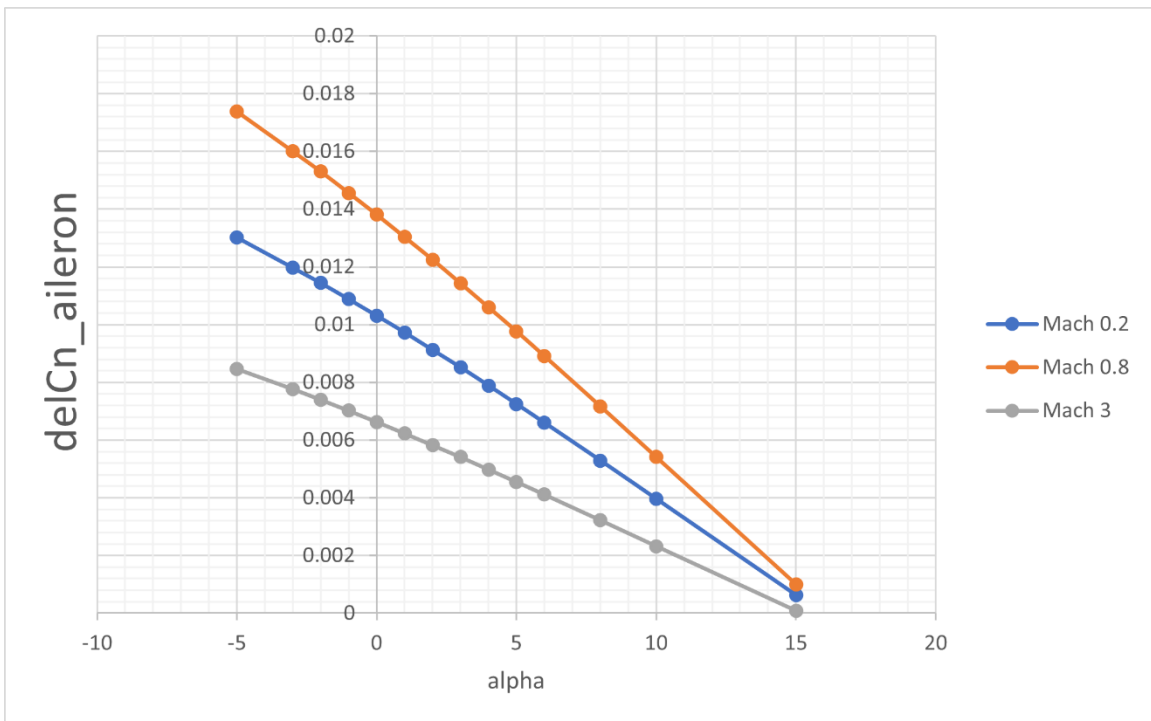


FIGURE C16 –  $C_{n_{\delta_a}}$  vs Alpha, Positive Deflection

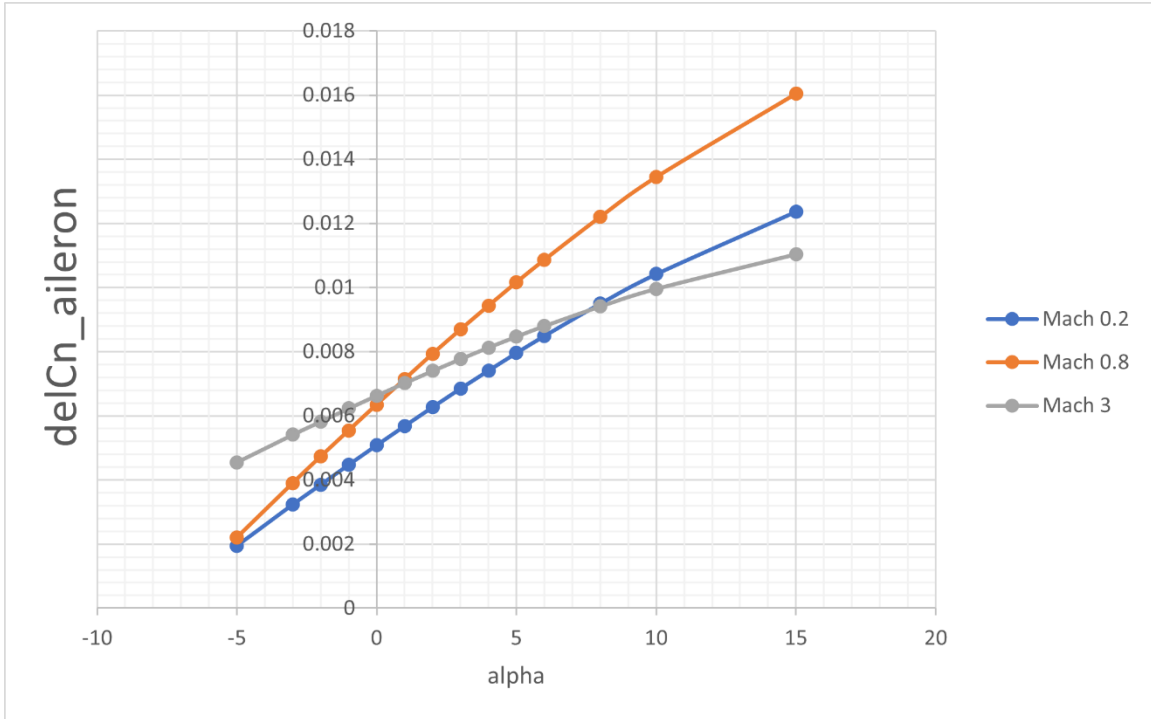


FIGURE C17 –  $C_{n_{\delta a}}$  vs Alpha, Negative Deflection

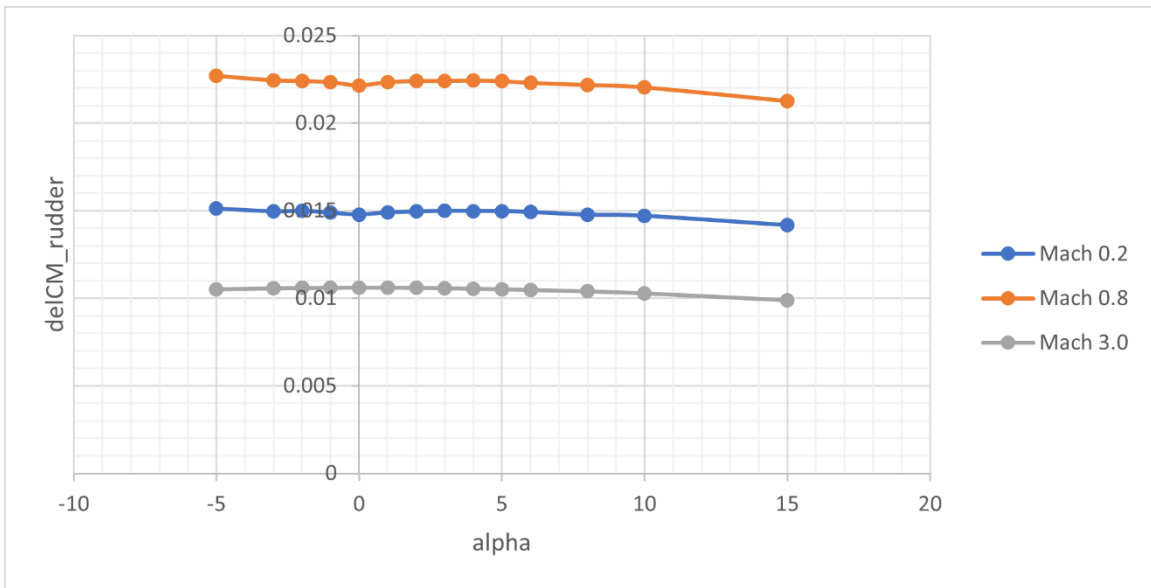


FIGURE C18 –  $C_{m_{\delta r}}$  vs Alpha

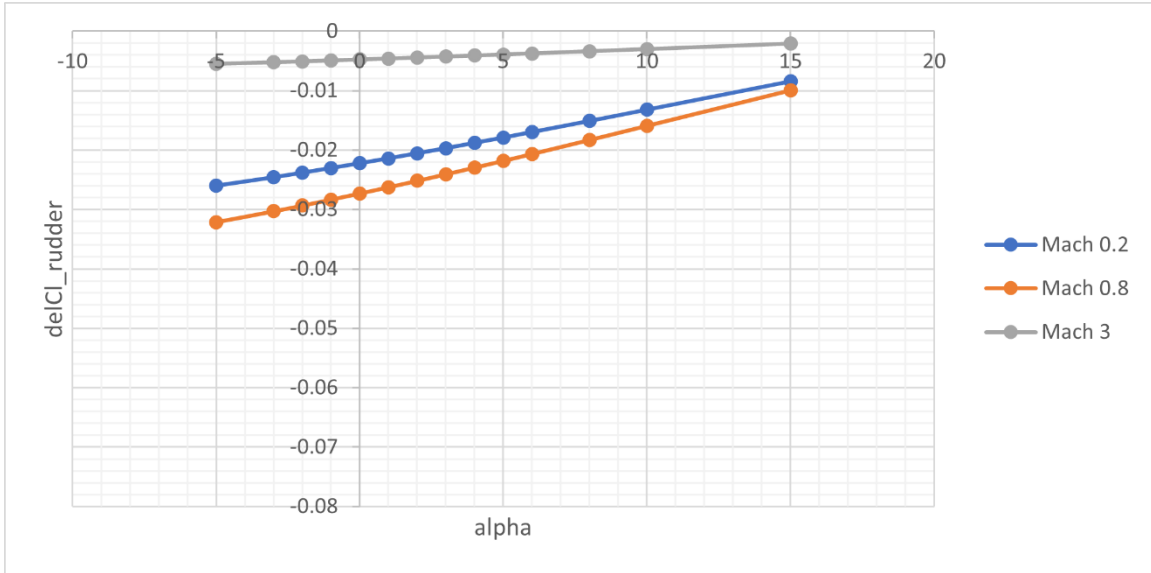


FIGURE C19 –  $C_{l_{\delta r}}$  vs Alpha

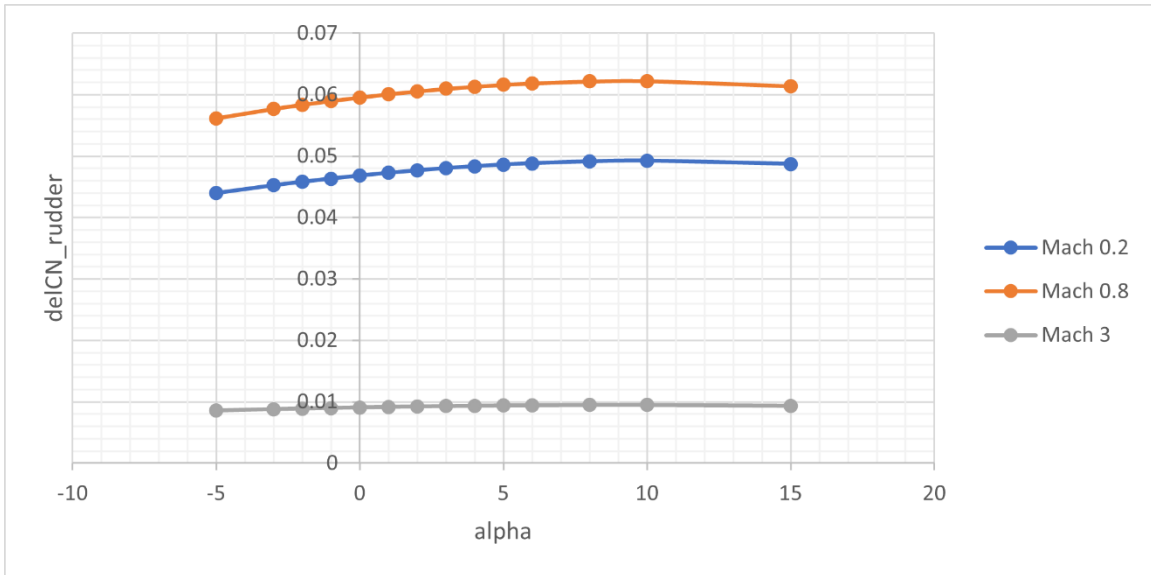


FIGURE C20 –  $C_{n_{\delta r}}$  vs Alpha

APPENDIX D

“SON-OF-X15” PRE-MIX MODEL AERODYNAMIC DATA

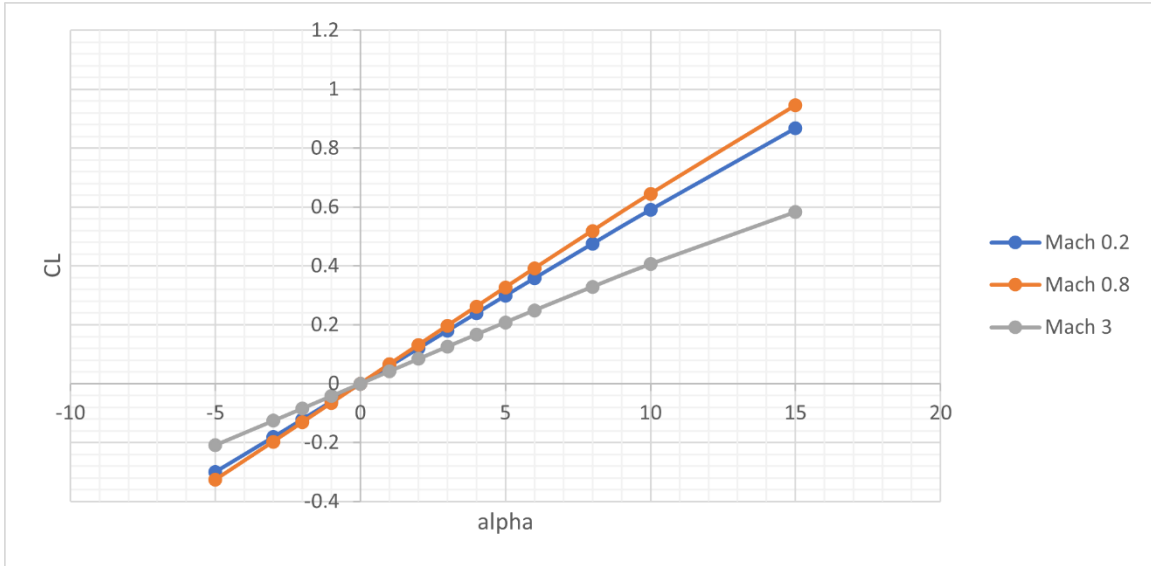


FIGURE D1 – CL vs Alpha

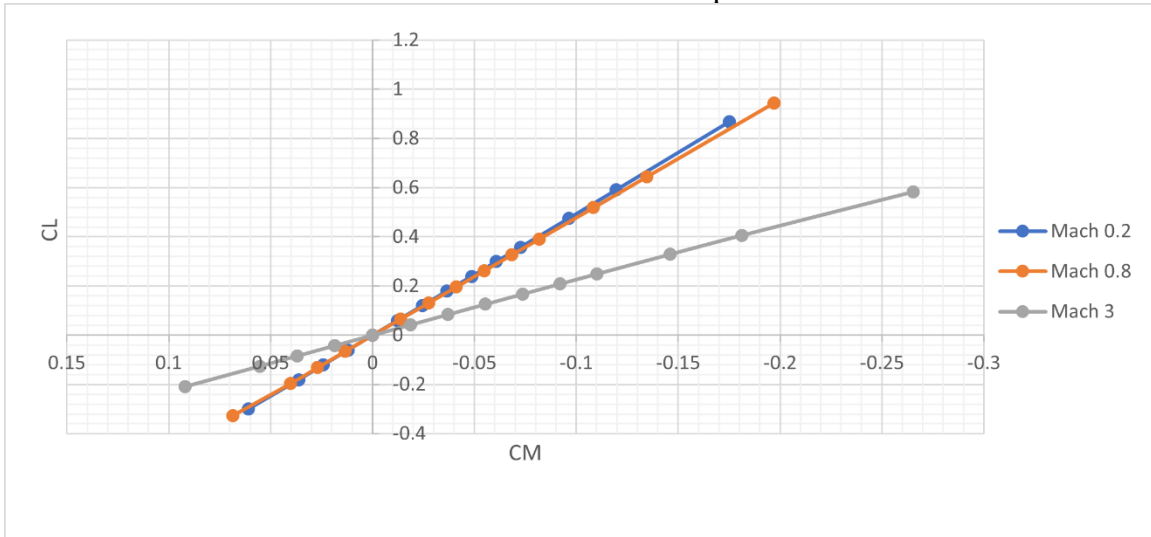


FIGURE D2 – CL vs CM

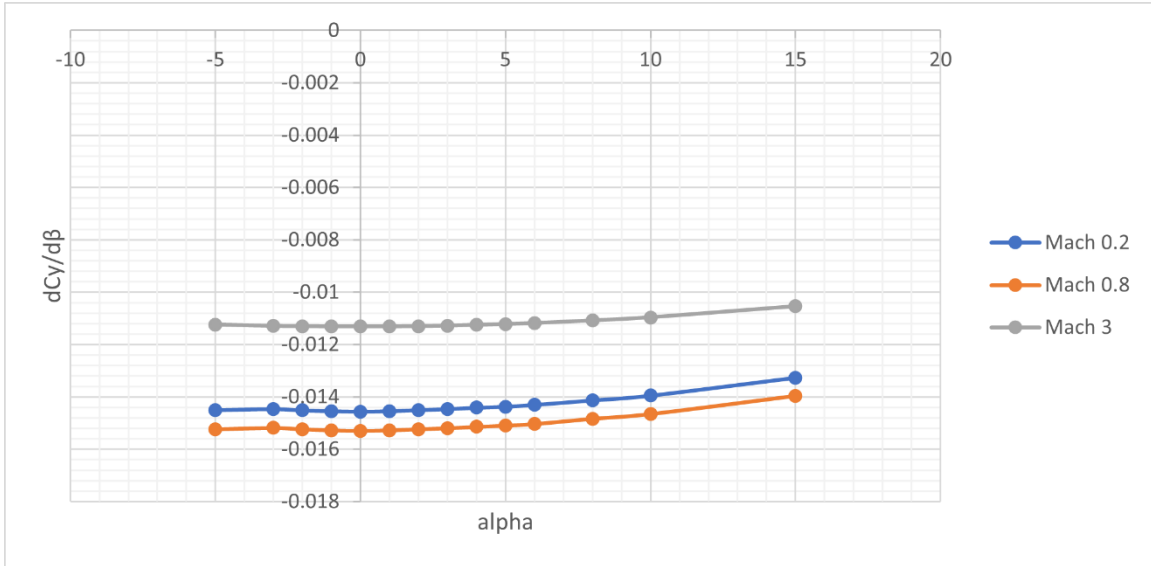


FIGURE D3 –  $C_Y\beta$  vs Alpha

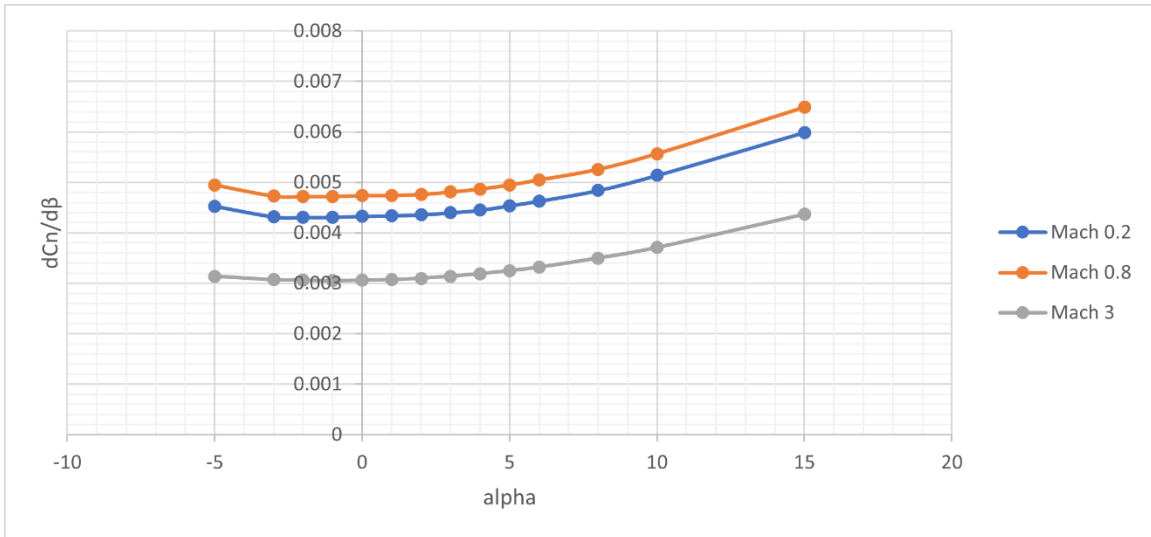


FIGURE D4 –  $C_n\beta$  vs Alpha

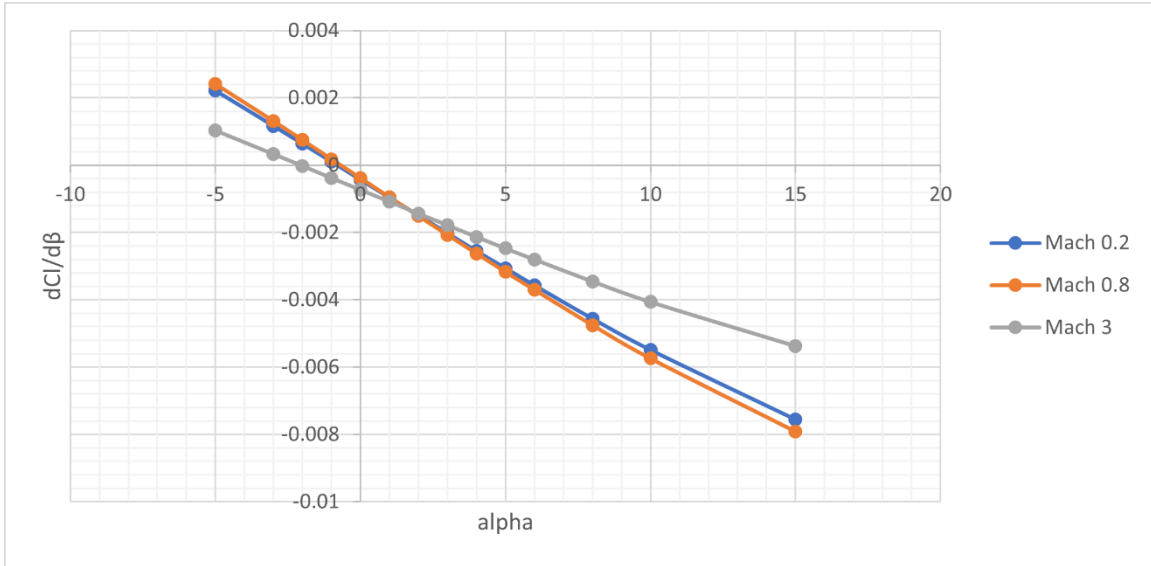


FIGURE D5 –  $C_l\beta$  vs Alpha

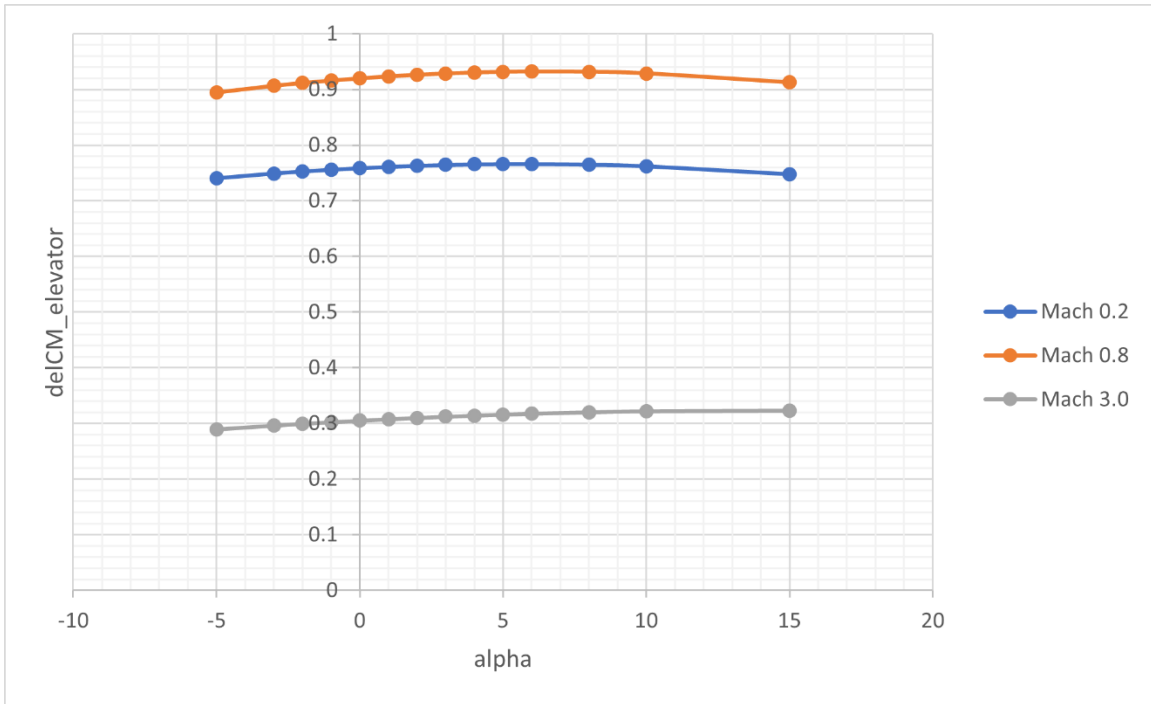


FIGURE D6 –  $C_{m\delta_e}$  vs Alpha

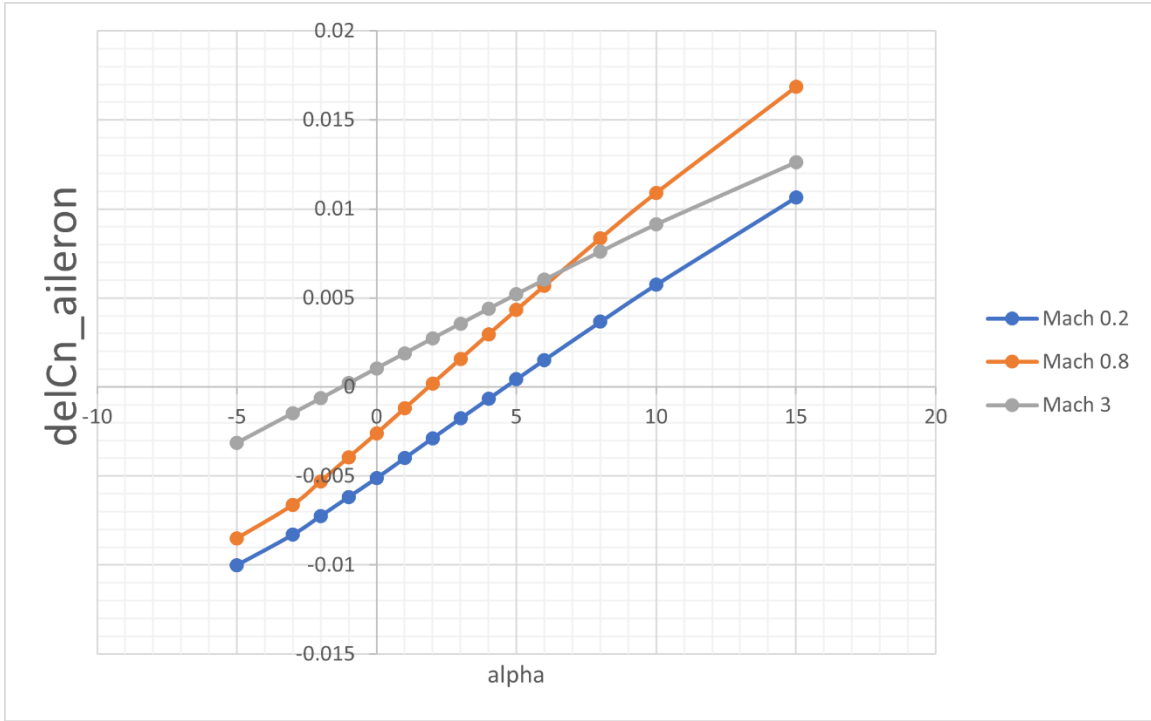


FIGURE D7 –  $C_{n_{\delta a}}$  vs Alpha

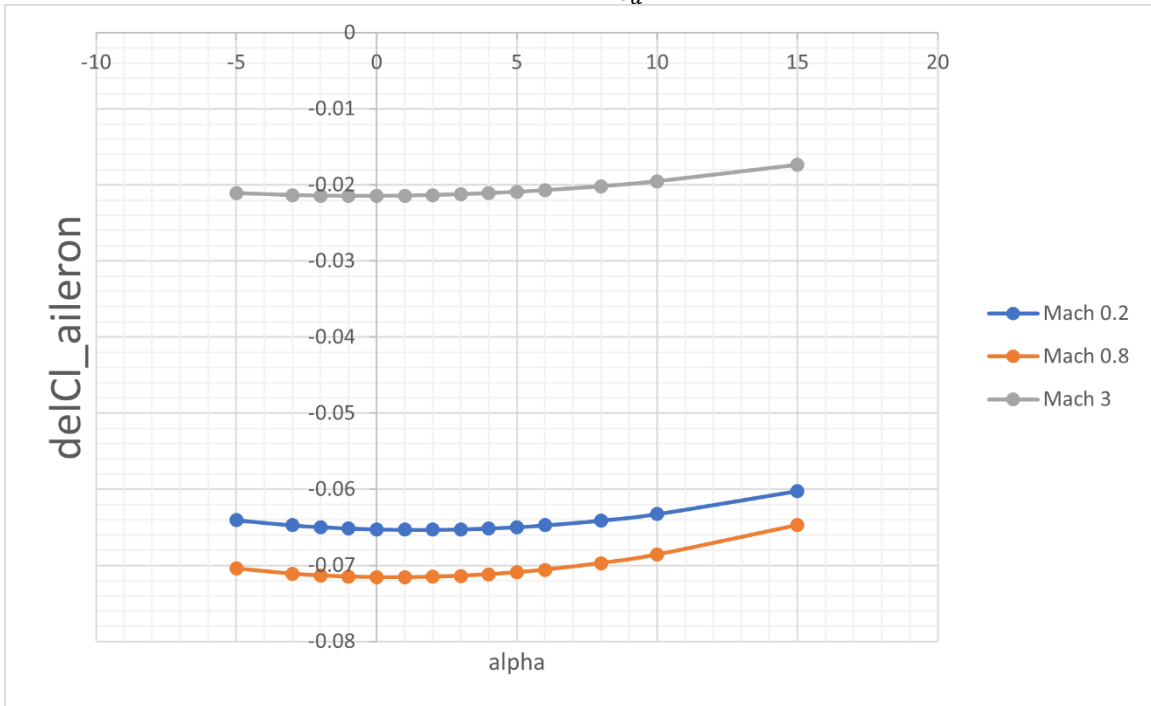


FIGURE D8 –  $C_{l_{\delta a}}$  vs Alpha



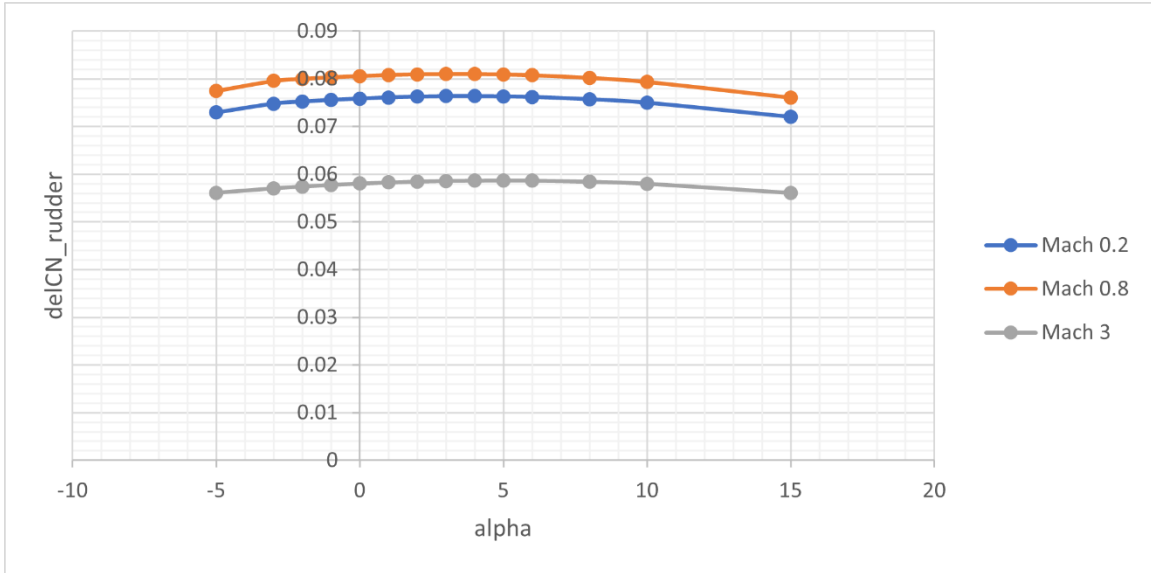


FIGURE D9 –  $C_{n_{\delta r}}$  vs Alpha

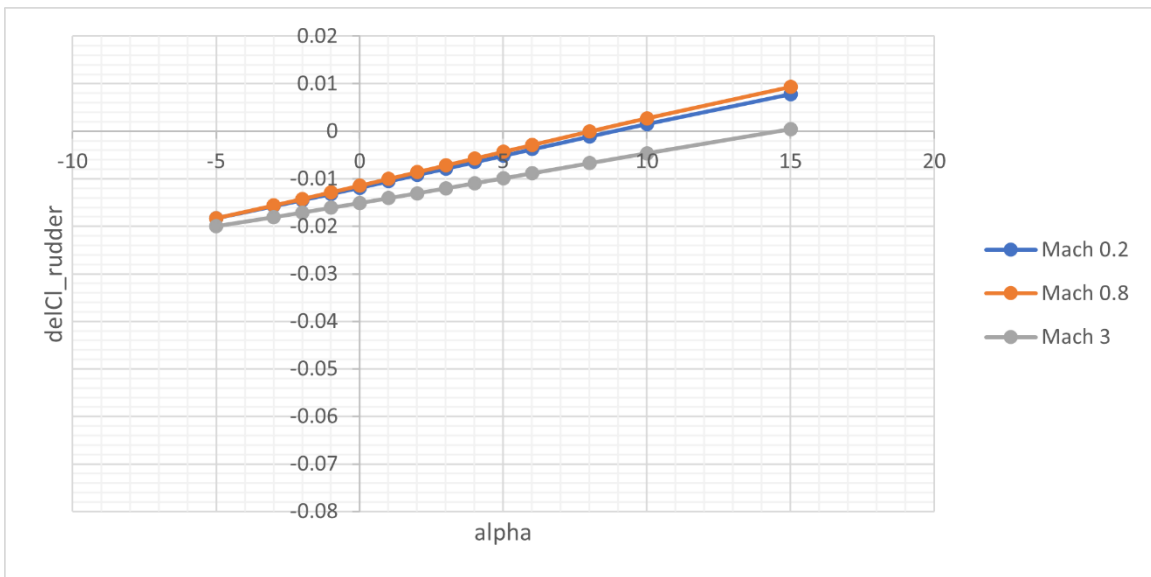


FIGURE D10 –  $C_{l_{\delta r}}$  vs Alpha

## APPENDIX E

### “SON-OF-X15” INDEPENDENT SINGLE PANEL MODEL AERODYNAMIC DATA

Note, the actual X-15 lacks wing mounted ailerons while this model includes wing mounted ailerons.

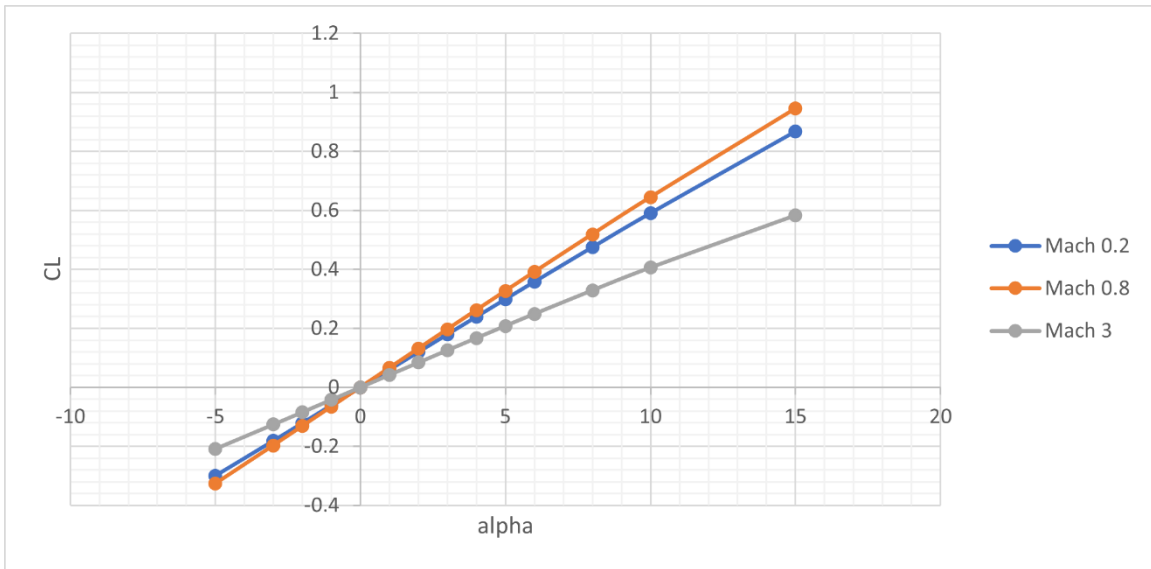


FIGURE E1- CL vs Alpha

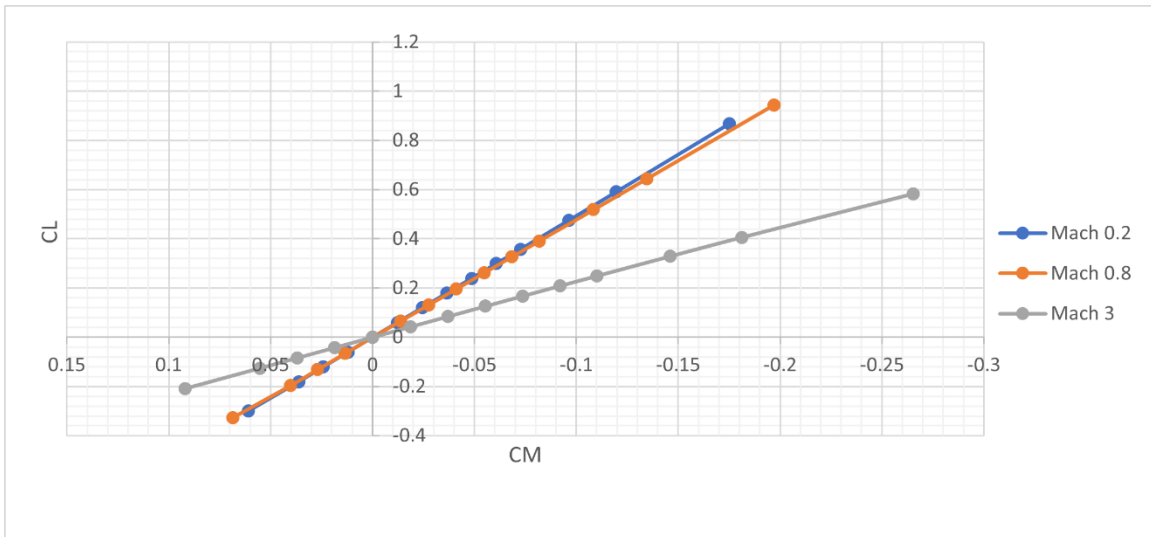


FIGURE E2- CL vs CM

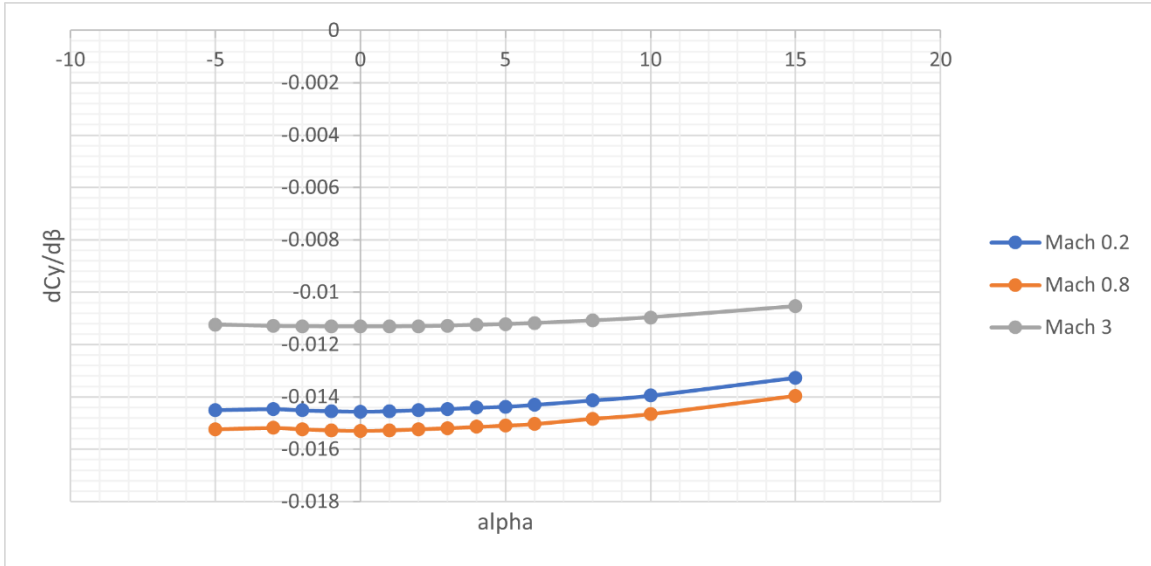


FIGURE E3-  $C_y\beta$  vs Alpha

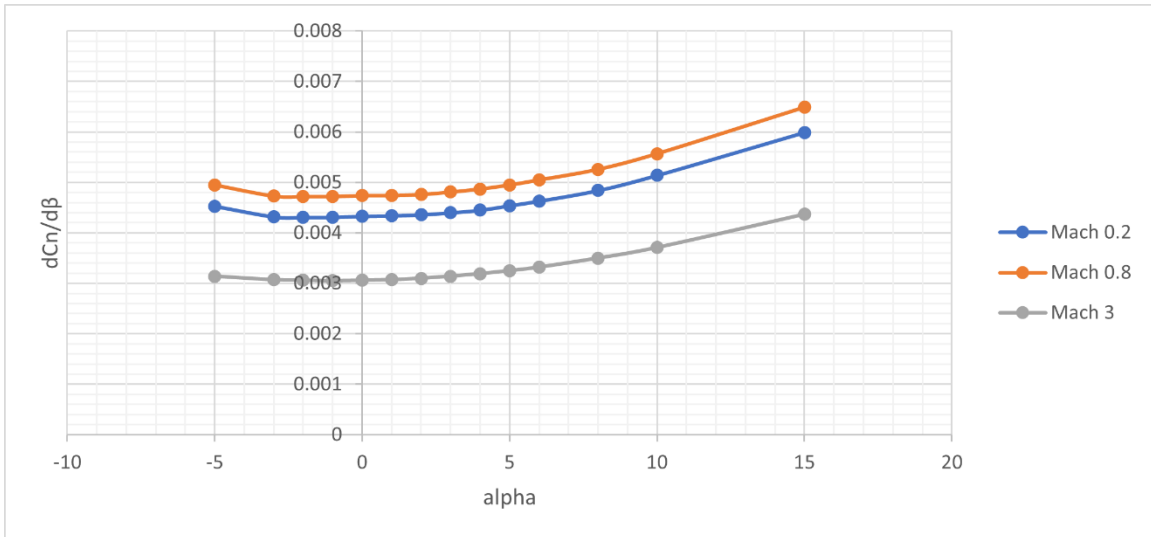


FIGURE E4-  $C_n\beta$  vs Alpha

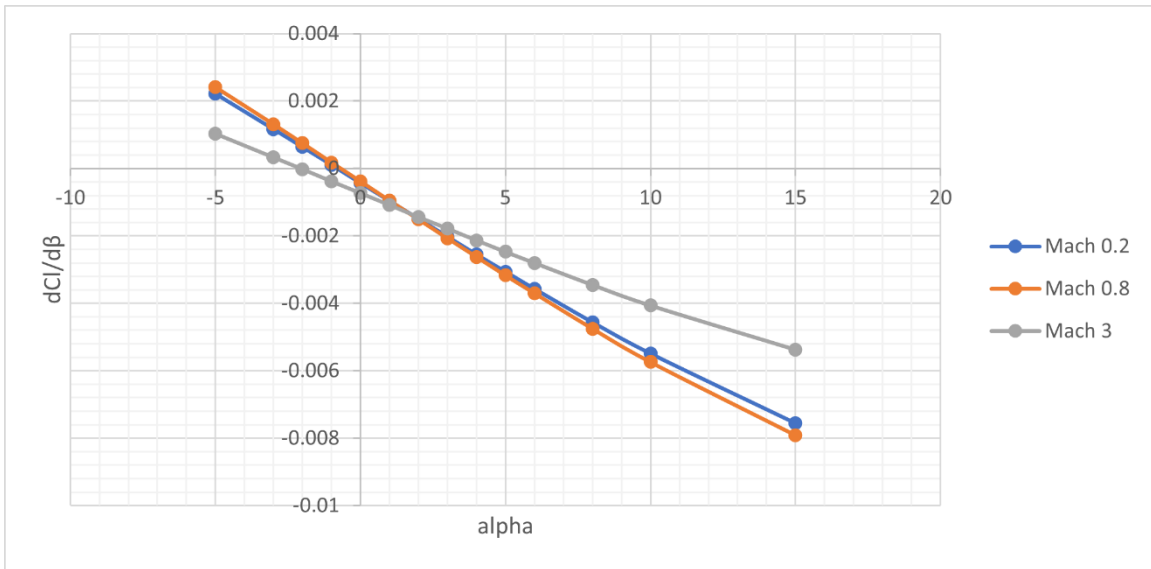


FIGURE E5-  $C_l\beta$  vs Alpha

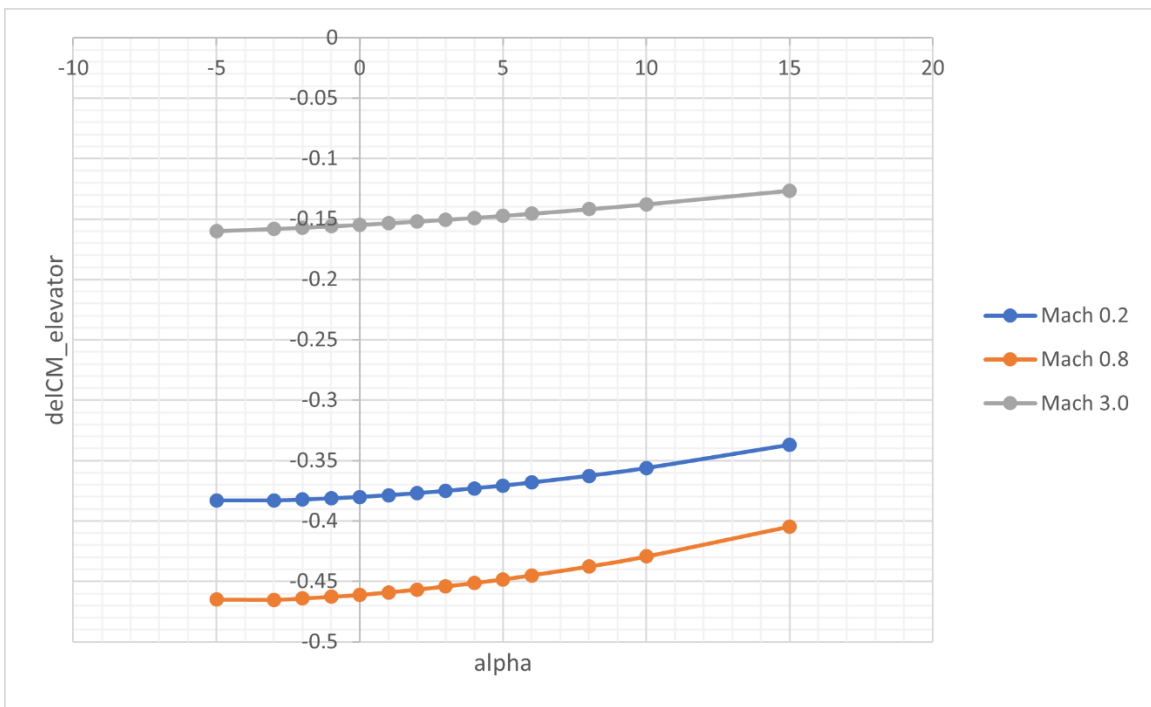


FIGURE E6-  $C_{m\delta_e}$  vs Alpha, Positive Deflection

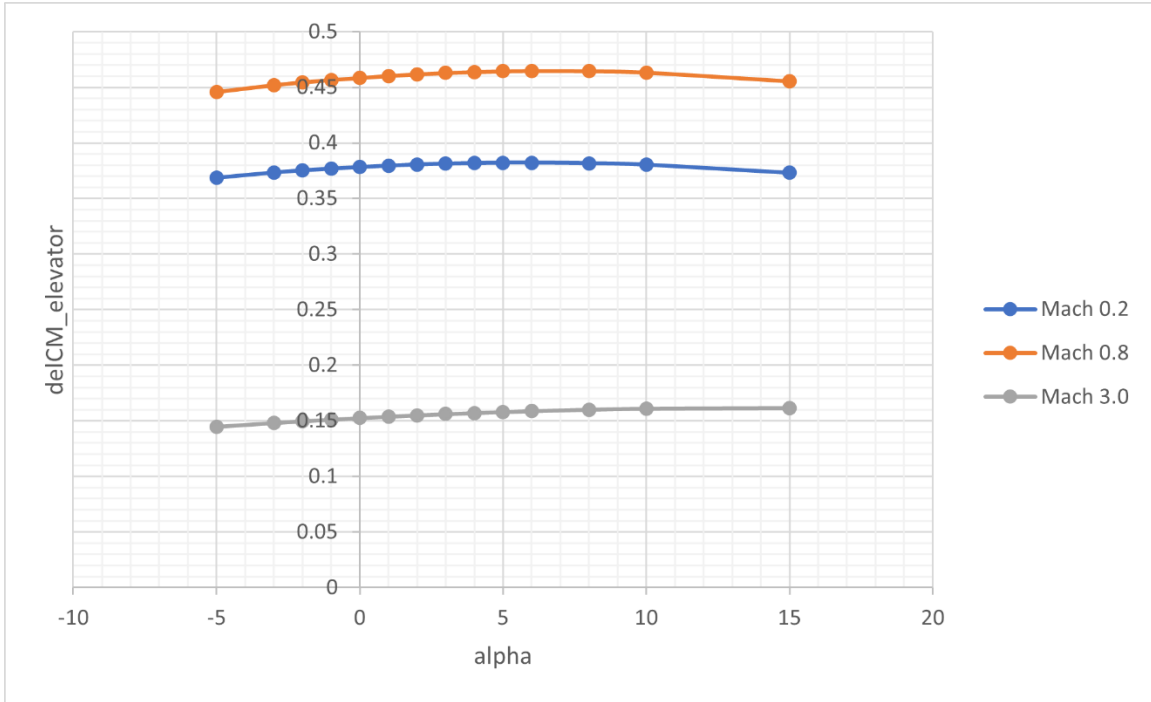


FIGURE E7-  $C_{m_{\delta_e}}$  vs Alpha, Negative Deflection

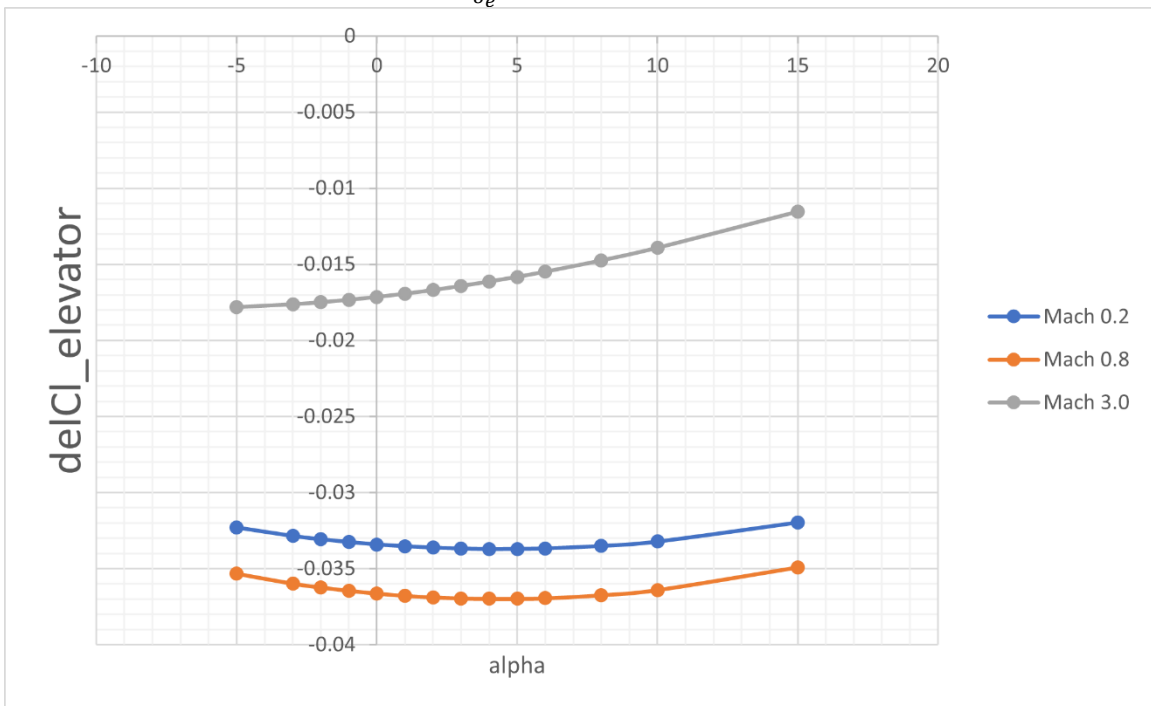


FIGURE E8-  $C_{l_{\delta_e}}$  vs Alpha, Positive Deflection

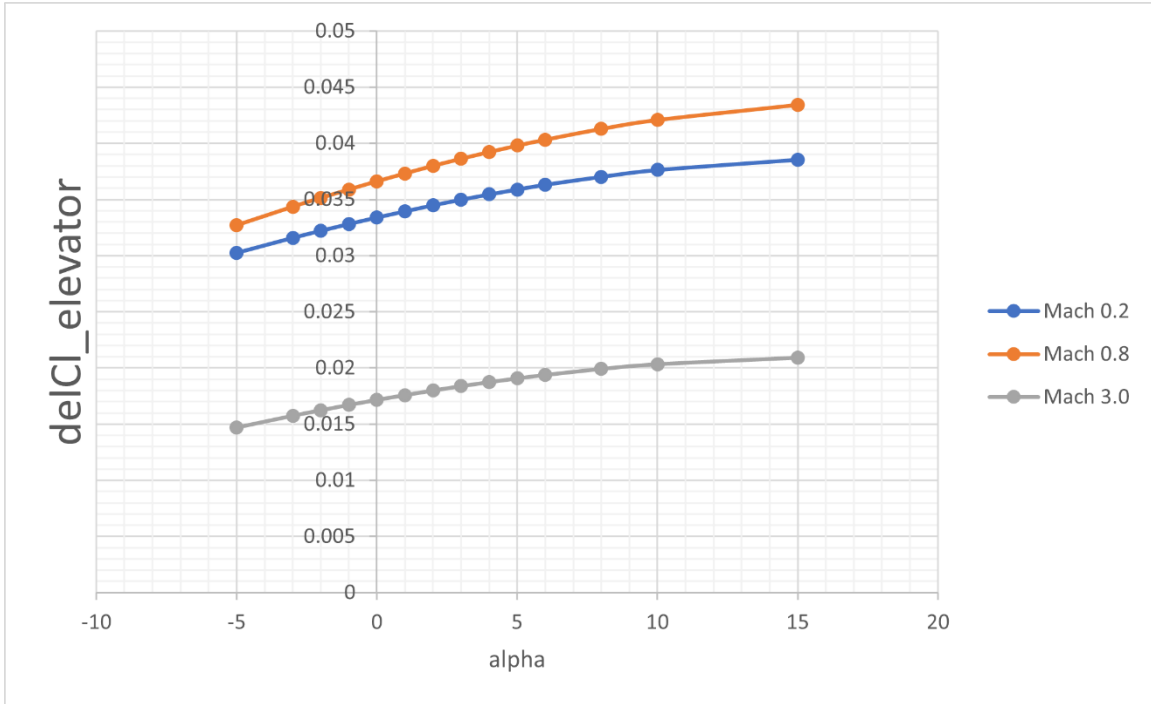


FIGURE E9-  $C_{l_{\delta_e}}$  vs Alpha, Negative Deflection

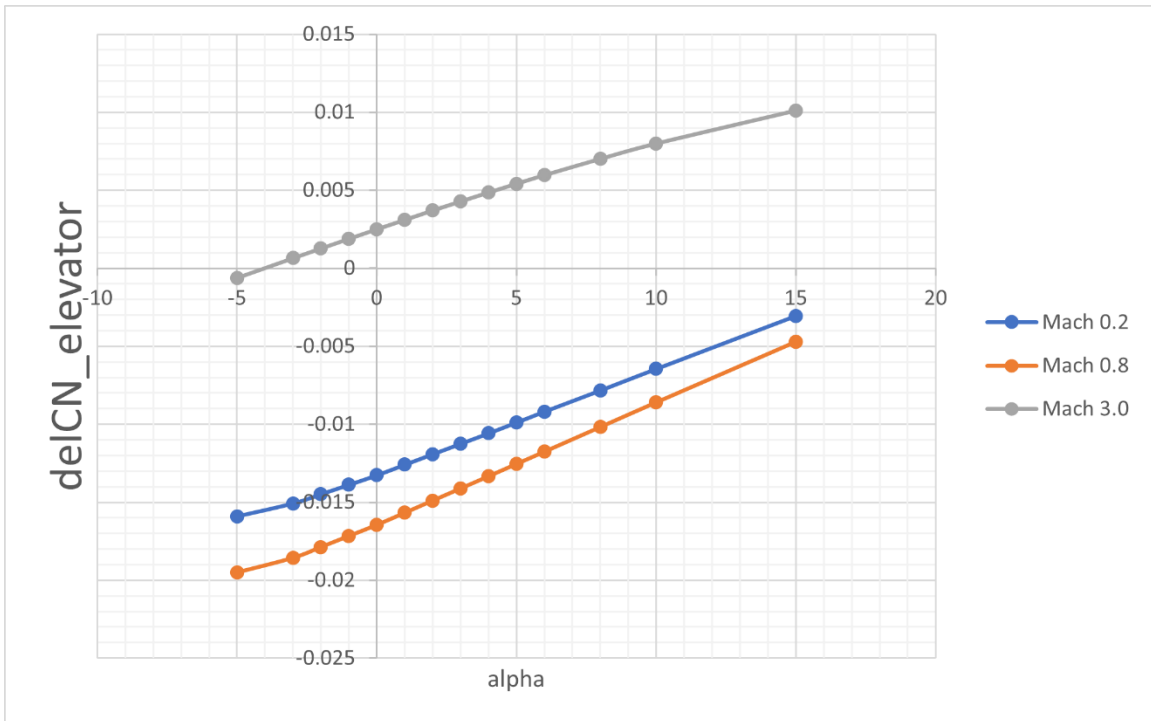


FIGURE E10-  $C_{n_{\delta_e}}$  vs Alpha, Positive Deflection

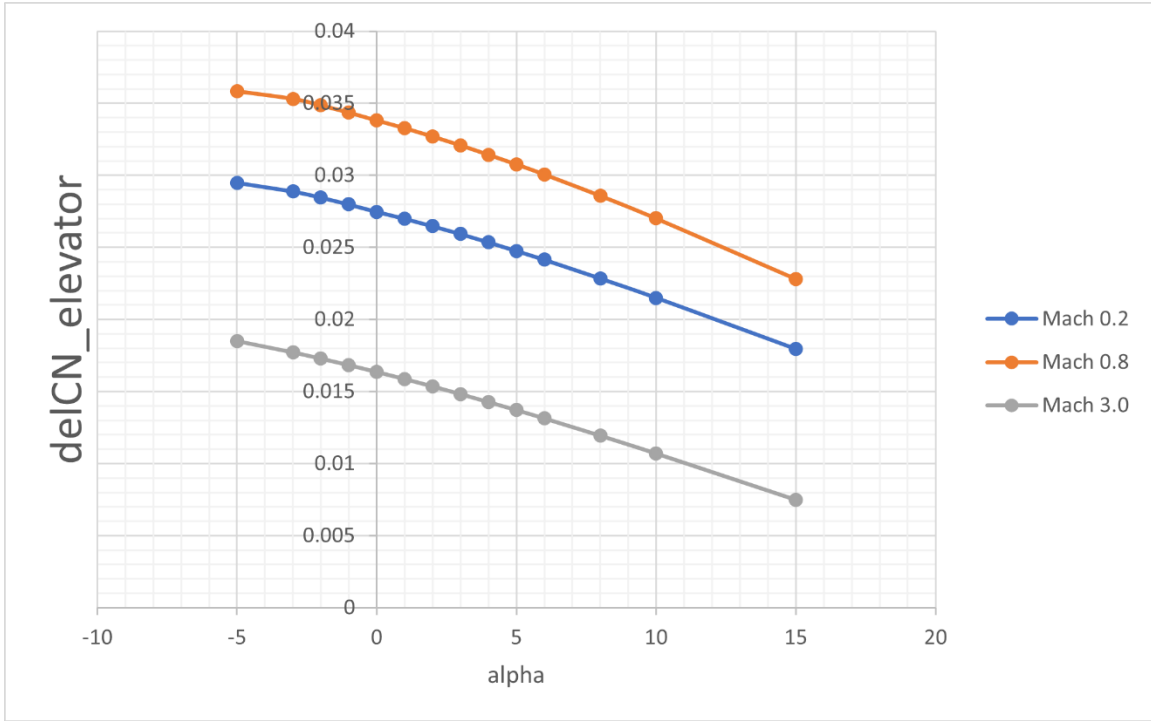


FIGURE E11-  $C_{n\delta_e}$  vs Alpha, Negative Deflection

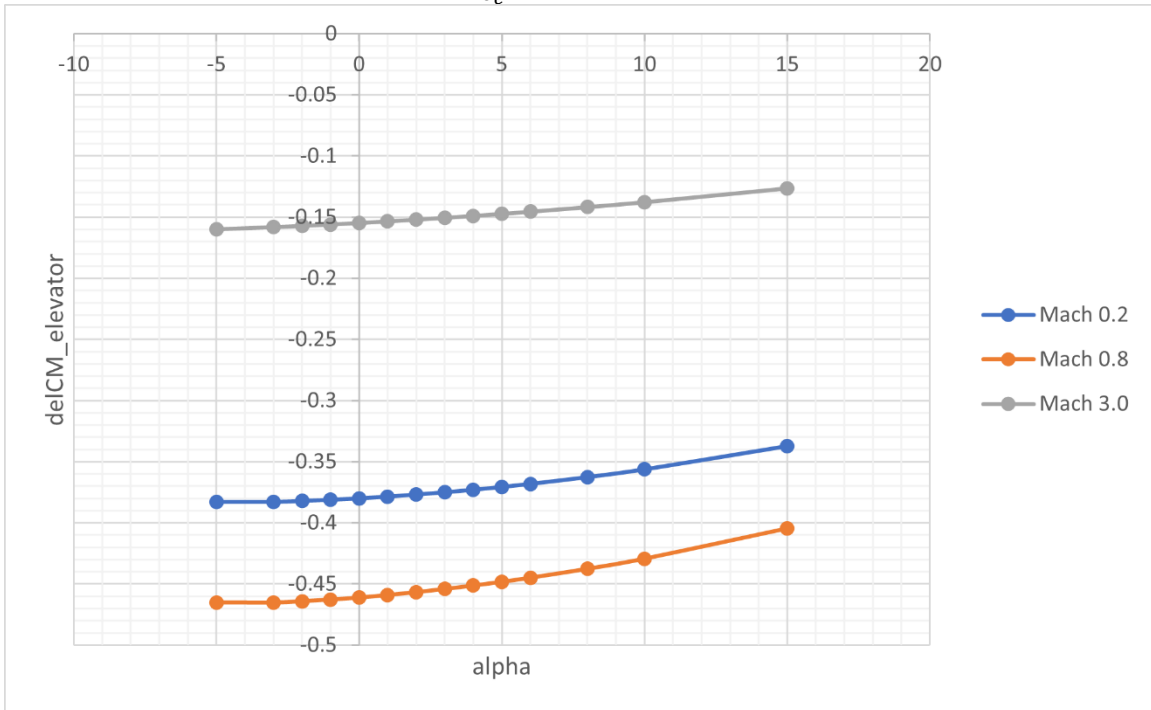


FIGURE E12-  $C_{m\delta_a}$  vs Alpha, Positive Deflection



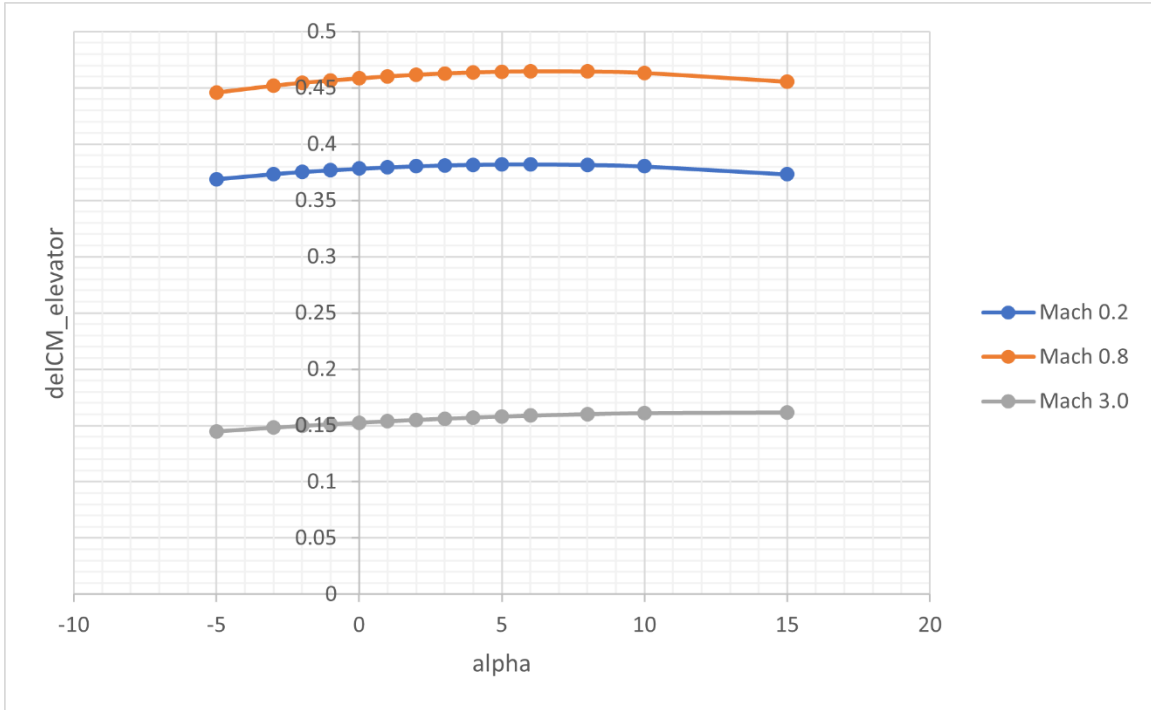


FIGURE E13-  $C_{m\delta_a}$  vs Alpha, Negative Deflection

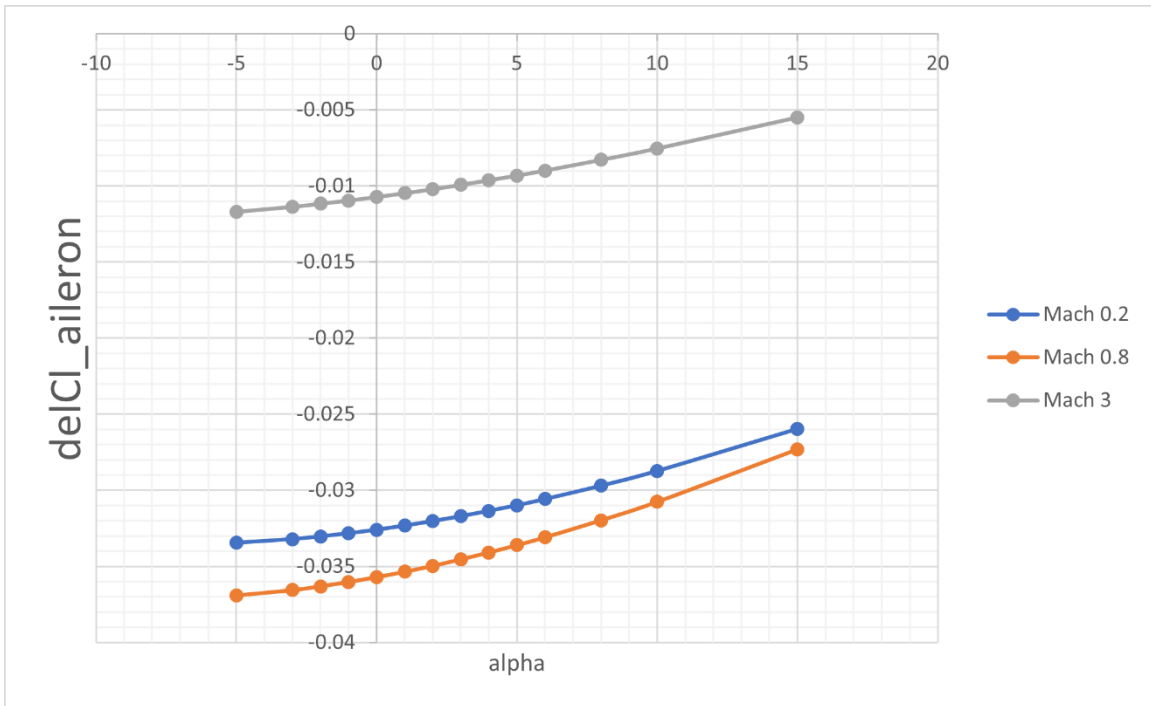


FIGURE E14-  $C_{l\delta_a}$  vs Alpha, Positive Deflection

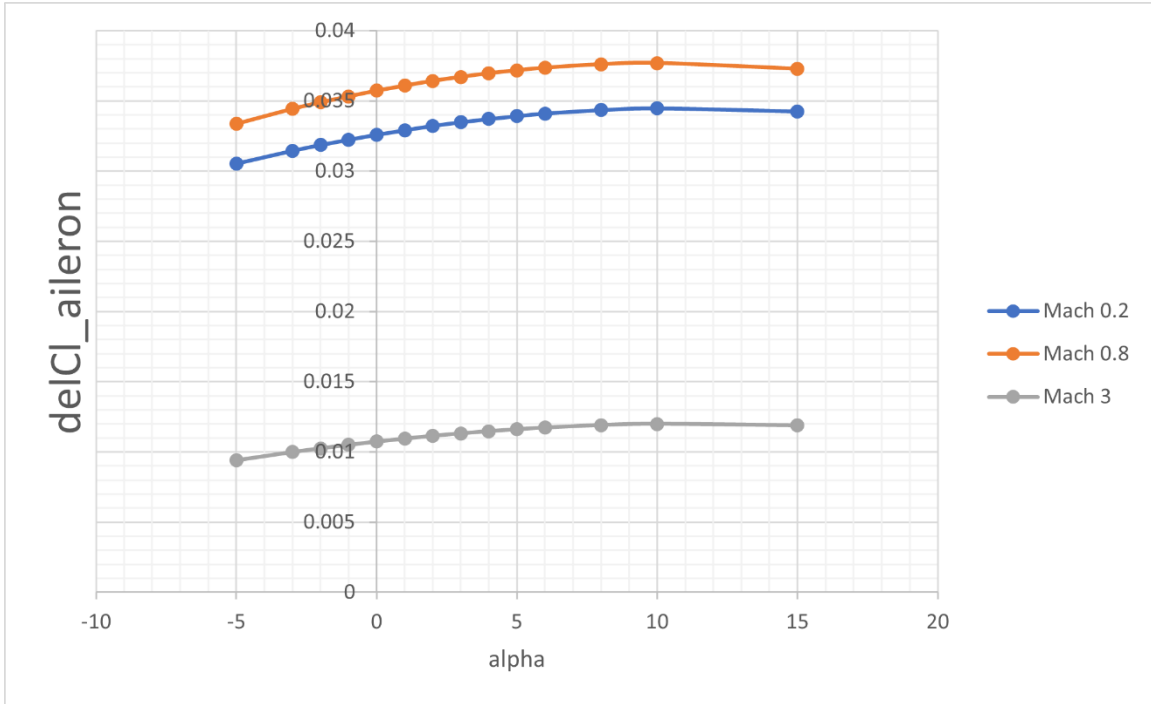


FIGURE E15-  $C_{l_{\delta\alpha}}$  vs Alpha, Negative Deflection

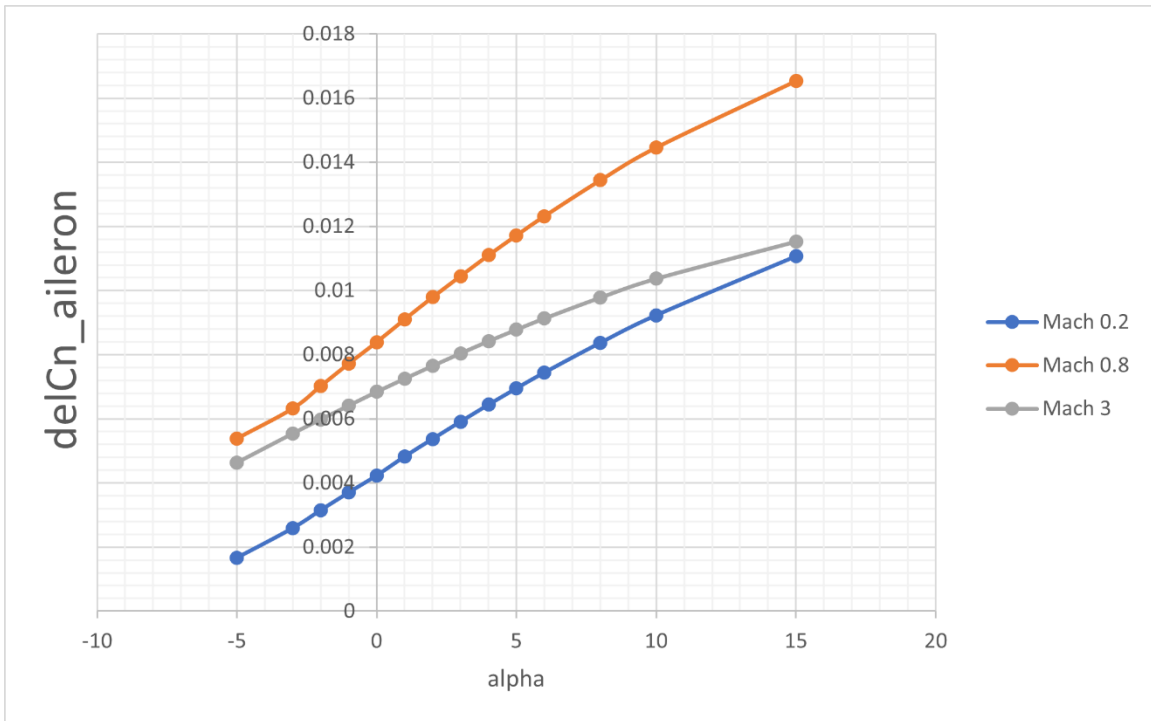


FIGURE E16-  $C_{n_{\delta\alpha}}$  vs Alpha, Positive Deflection

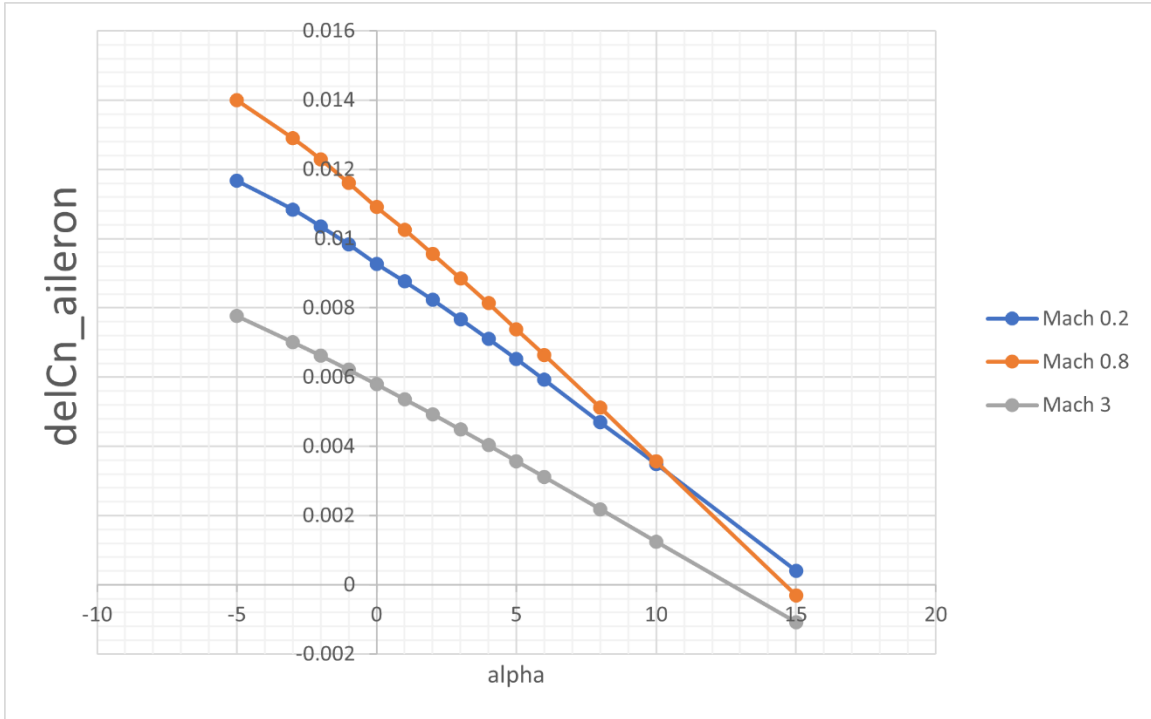


FIGURE E17-  $C_{n_{\delta a}}$  vs Alpha, Negative Deflection

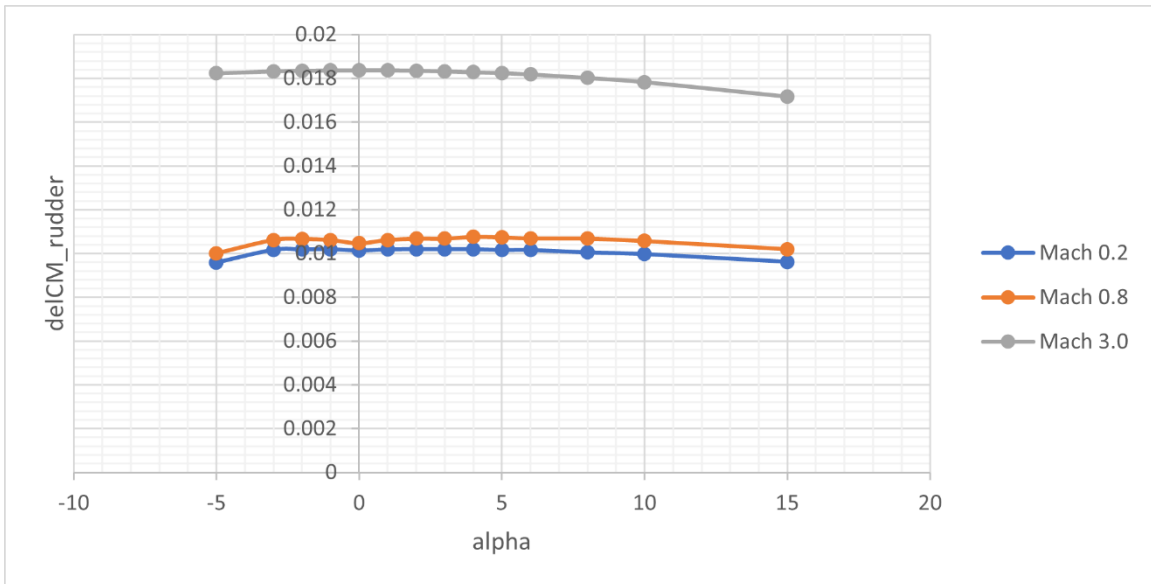


FIGURE E18-  $C_{m_{\delta r}}$  vs Alpha

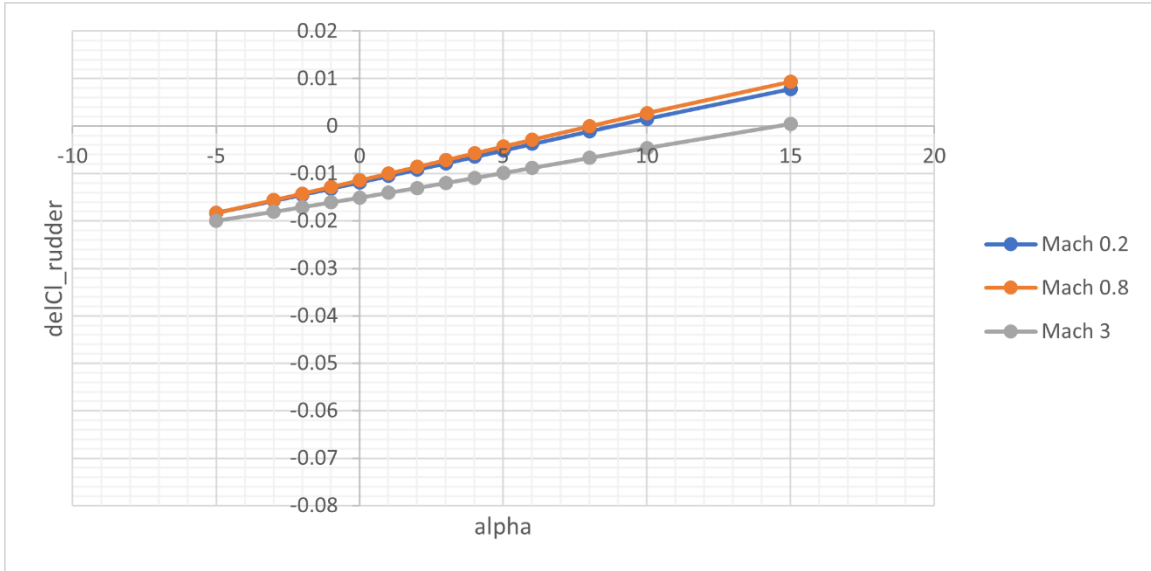


FIGURE E19-  $C_{l_{\delta_r}}$  vs Alpha

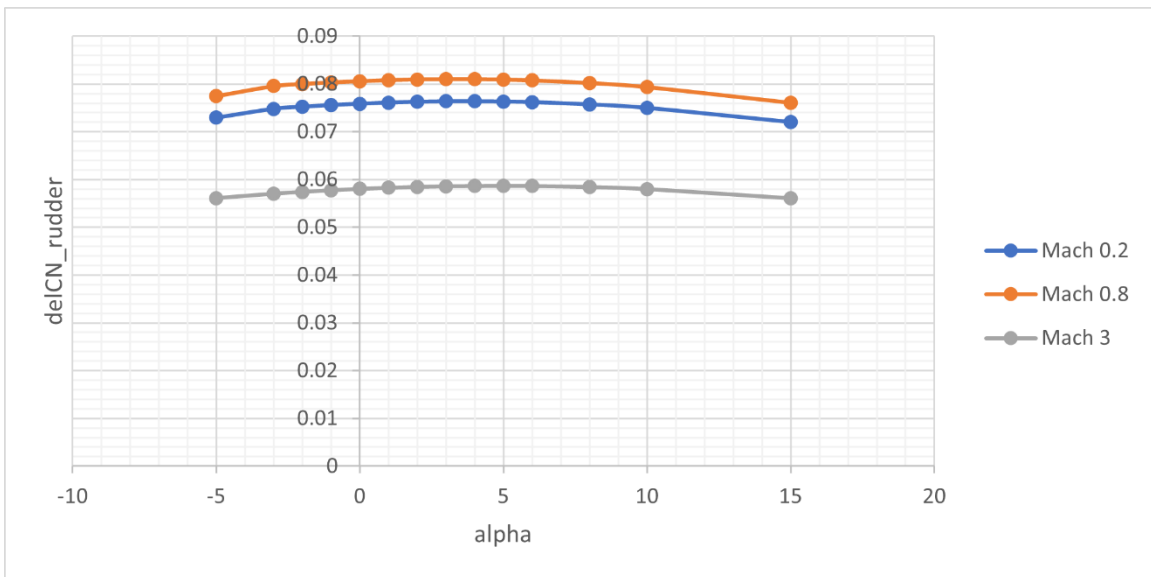


FIGURE E20-  $C_{n_{\delta_r}}$  vs Alpha

APPENDIX F

AIRBUS A320 PRE-MIX MODEL AERODYNAMIC DATA

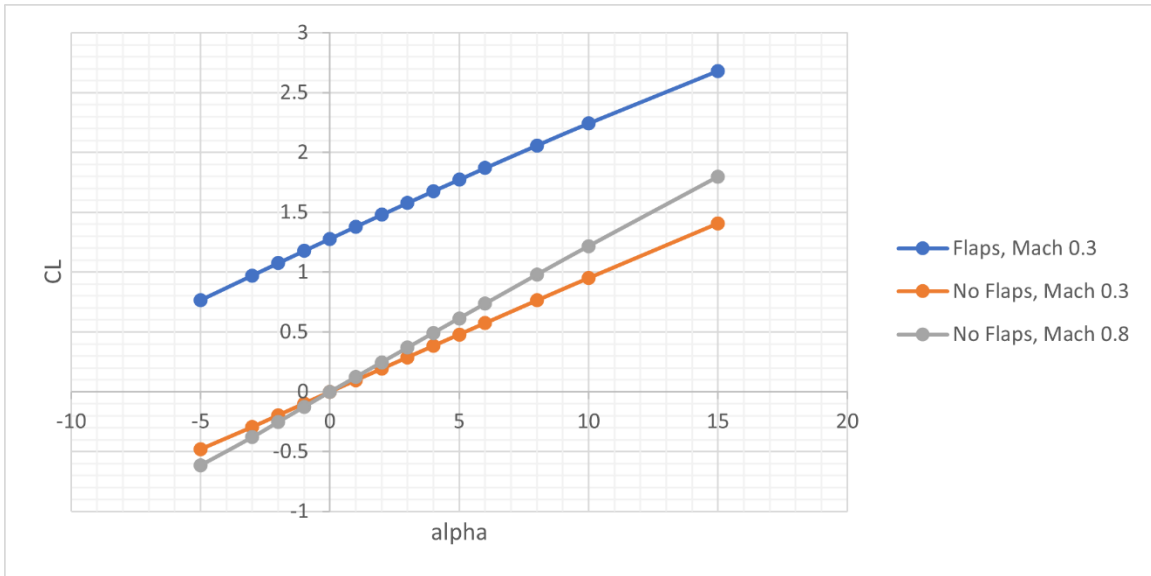


FIGURE F1 - CL vs Alpha

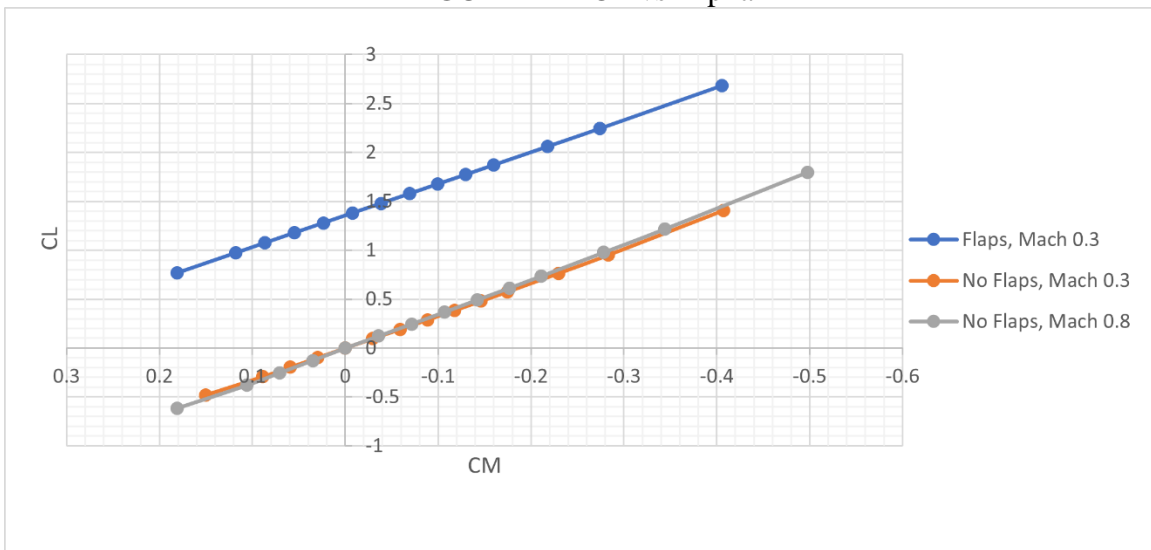


FIGURE F2 - CL vs CM

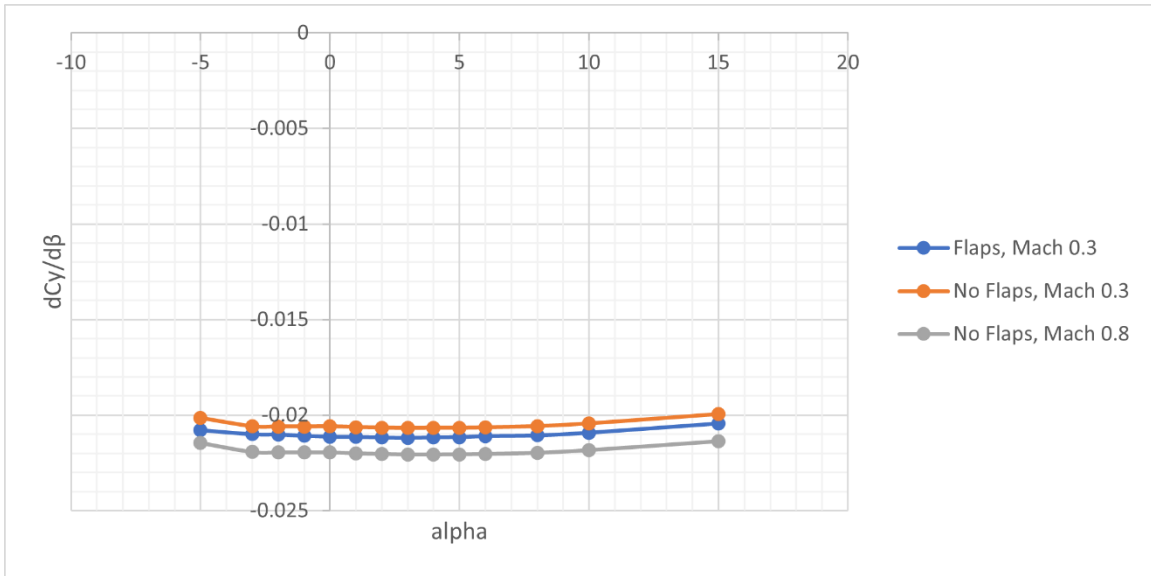


FIGURE F3 -  $C_y\beta$  vs Alpha

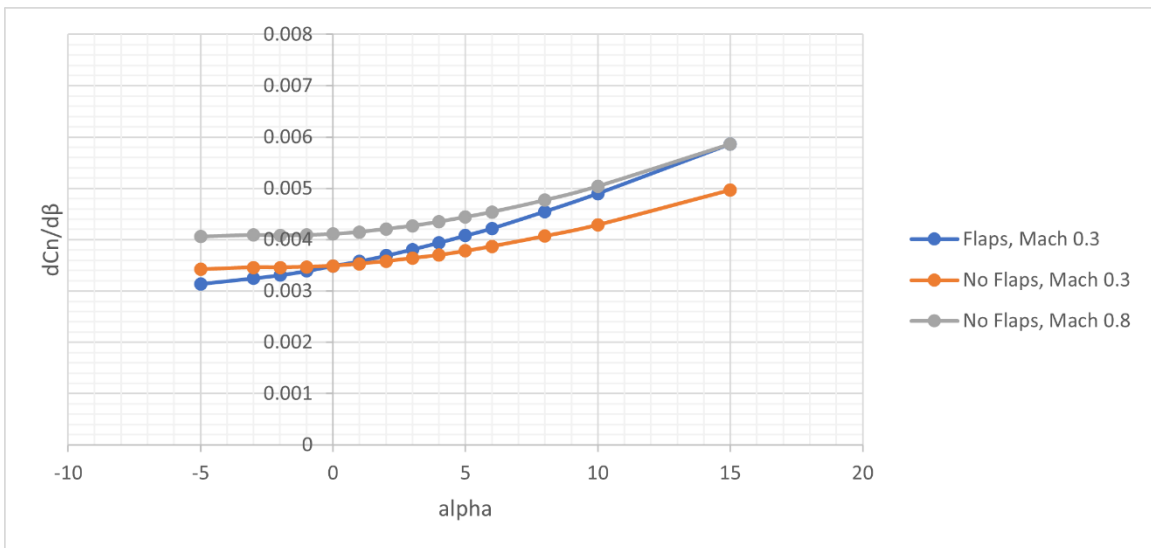


FIGURE F4 -  $C_n\beta$  vs Alpha

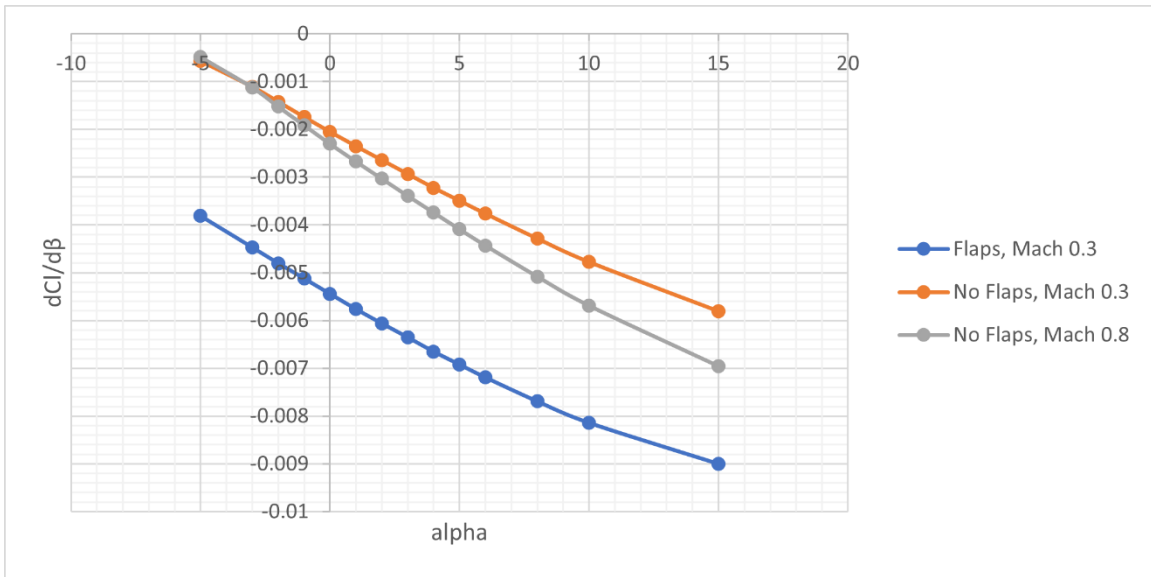


FIGURE F5 -  $C_l\beta$  vs Alpha

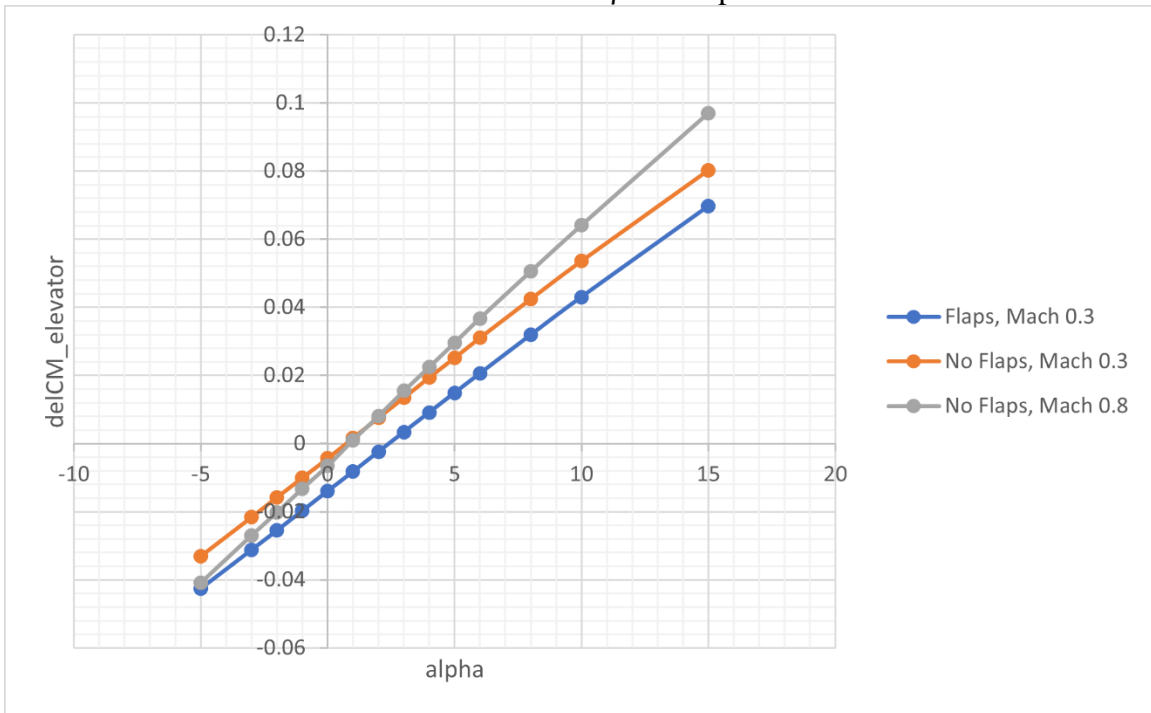


FIGURE F6 -  $C_{m_{\delta_e}}$  vs Alpha



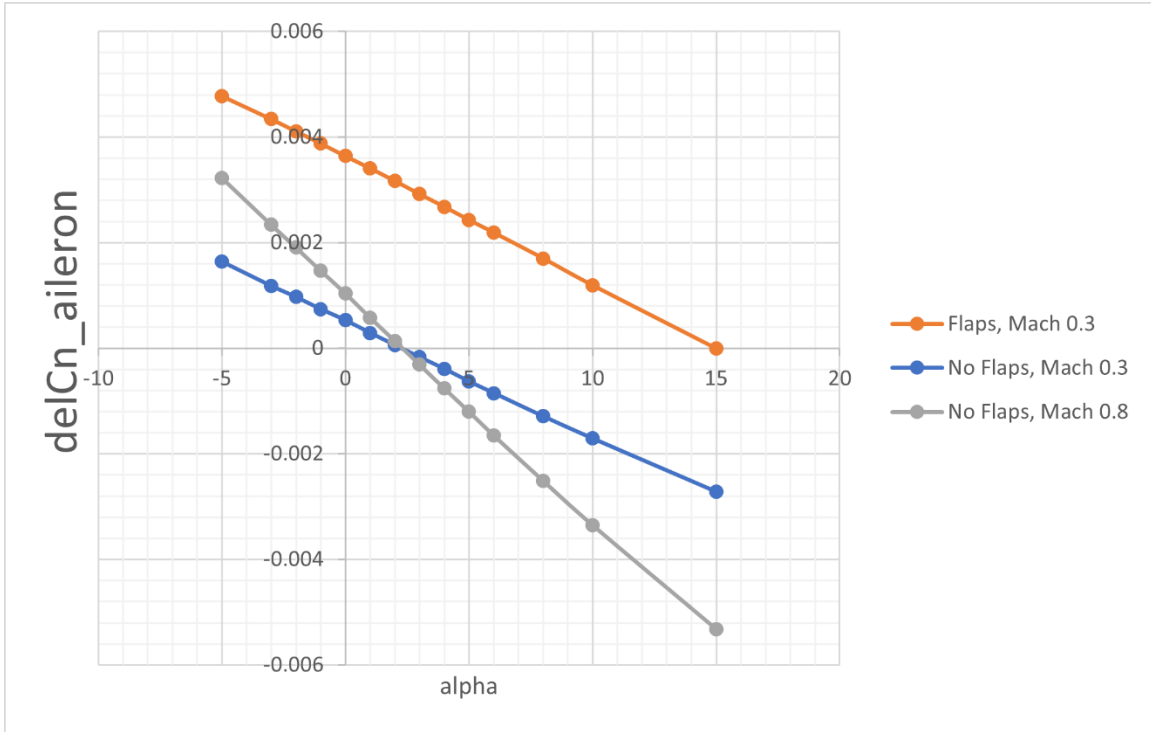


FIGURE F7 -  $C_{n_{\delta_a}}$  vs Alpha

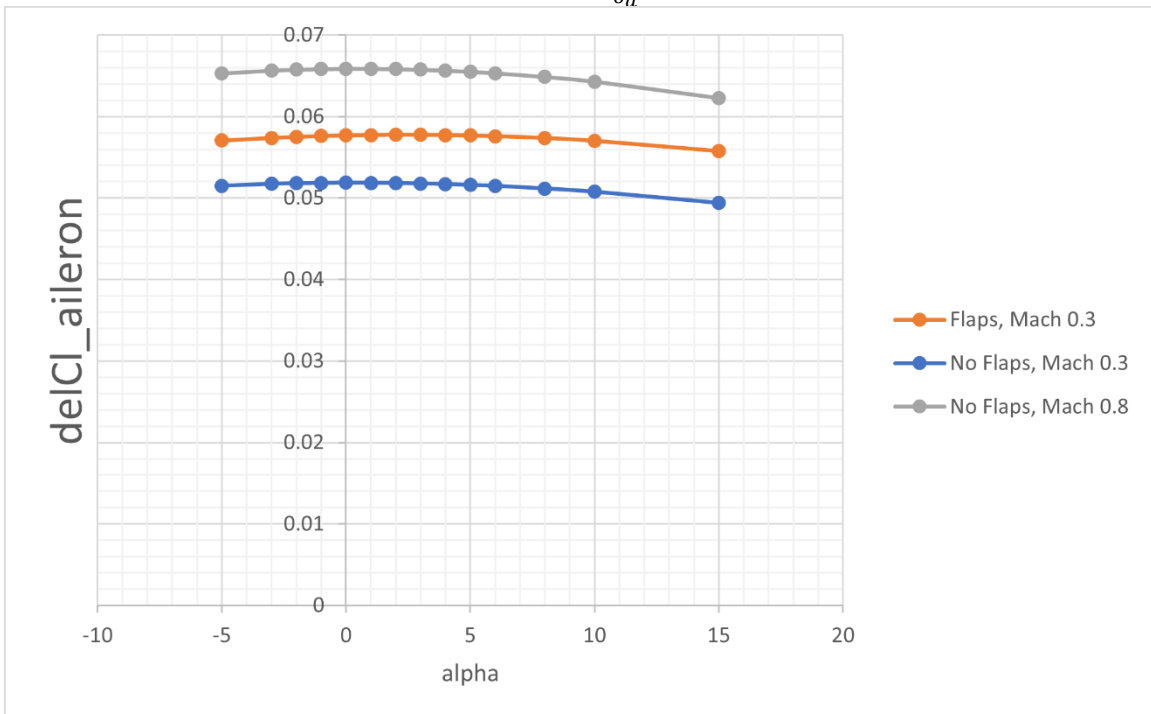


FIGURE F8 -  $C_{l_{\delta_a}}$  vs Alpha

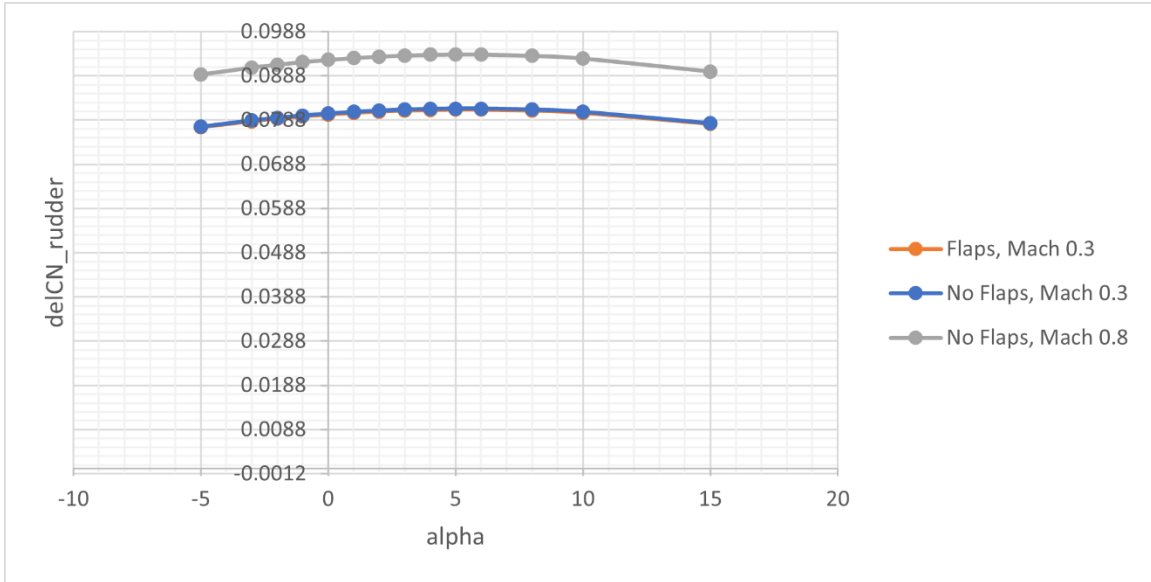


FIGURE F9 -  $C_{n_{\delta r}}$  vs Alpha

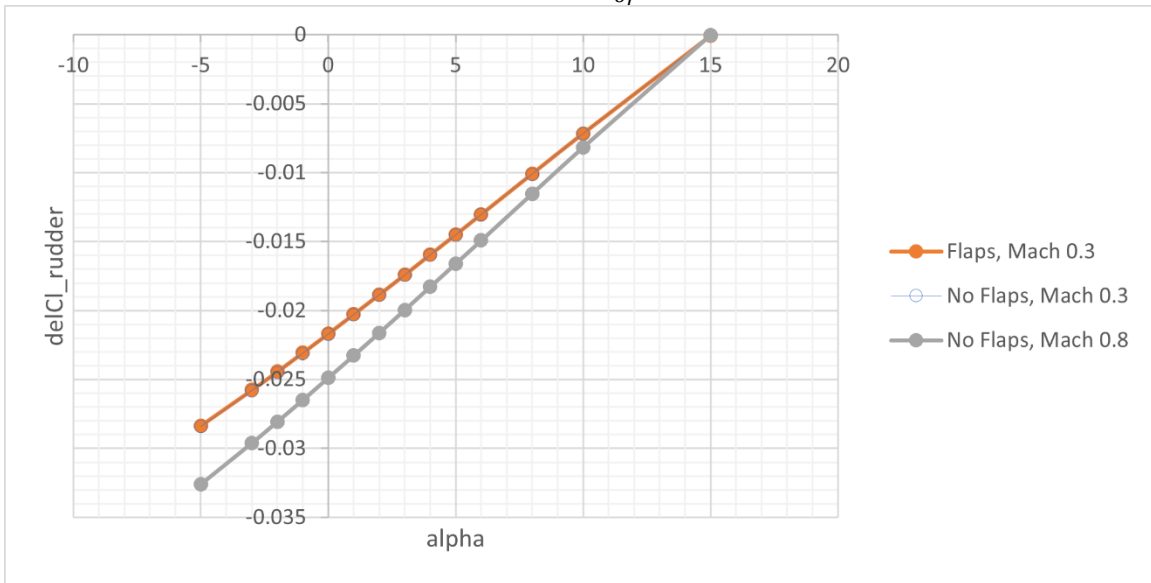


FIGURE F10 -  $C_{l_{\delta r}}$  vs Alpha

## APPENDIX G

### AIRBUS A320 INDEPENDENT SINGLE PANEL MODEL AERODYNAMIC DATA

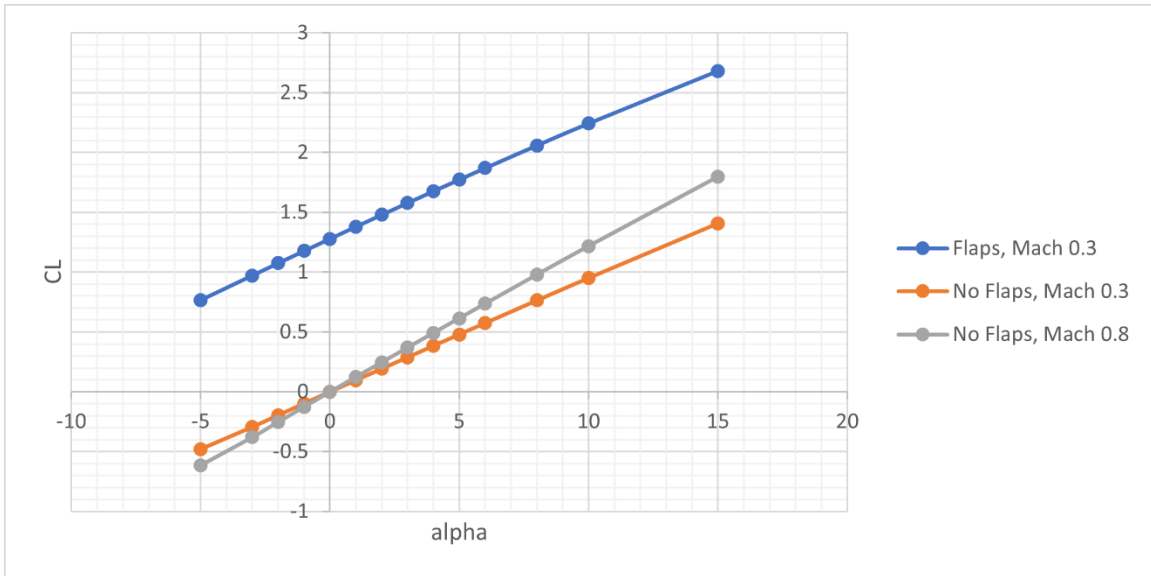


FIGURE G1 - CL vs Alpha

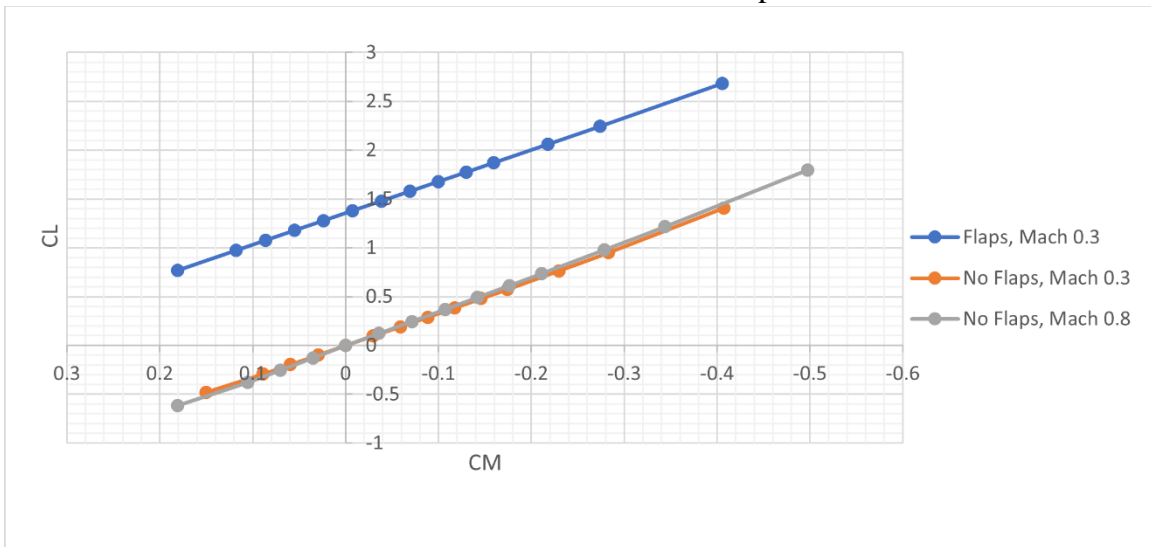


FIGURE G2 - CL vs CM

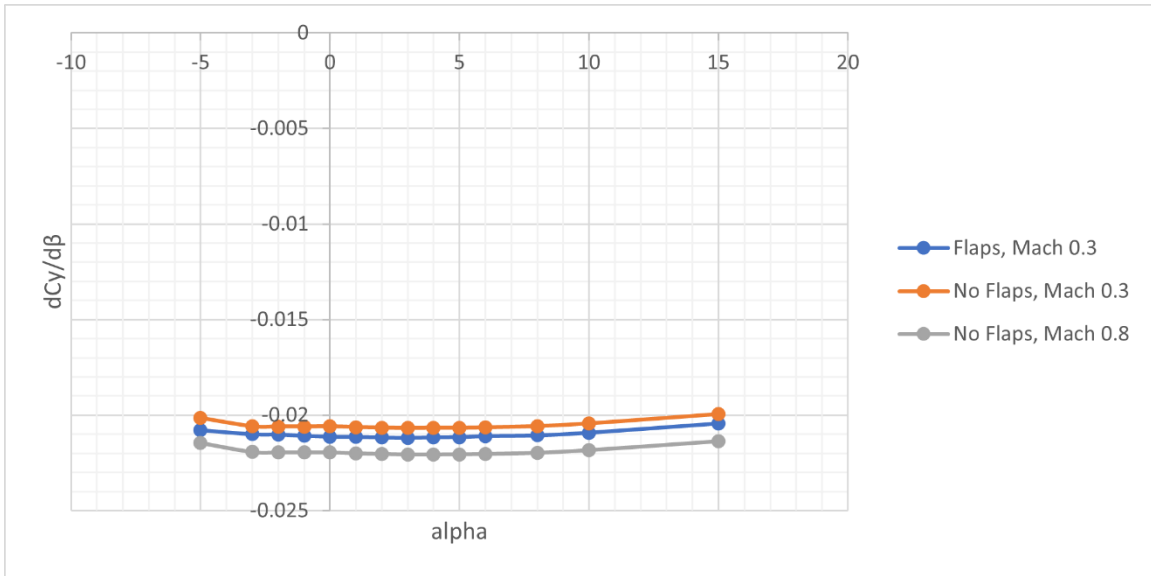


FIGURE G3 -  $C_y\beta$  vs Alpha

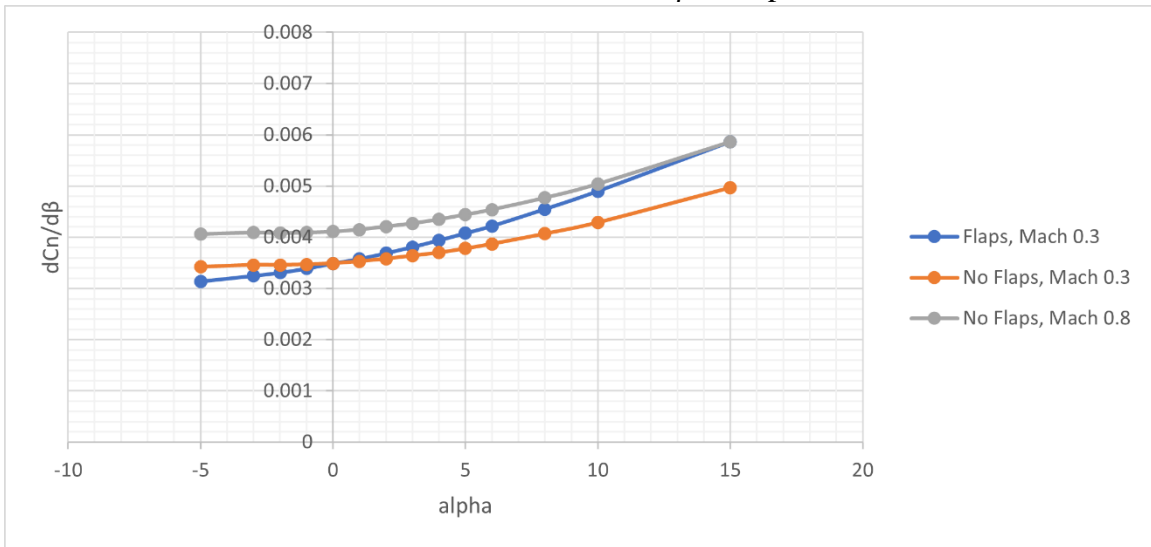


FIGURE G4 -  $C_n\beta$  vs Alpha

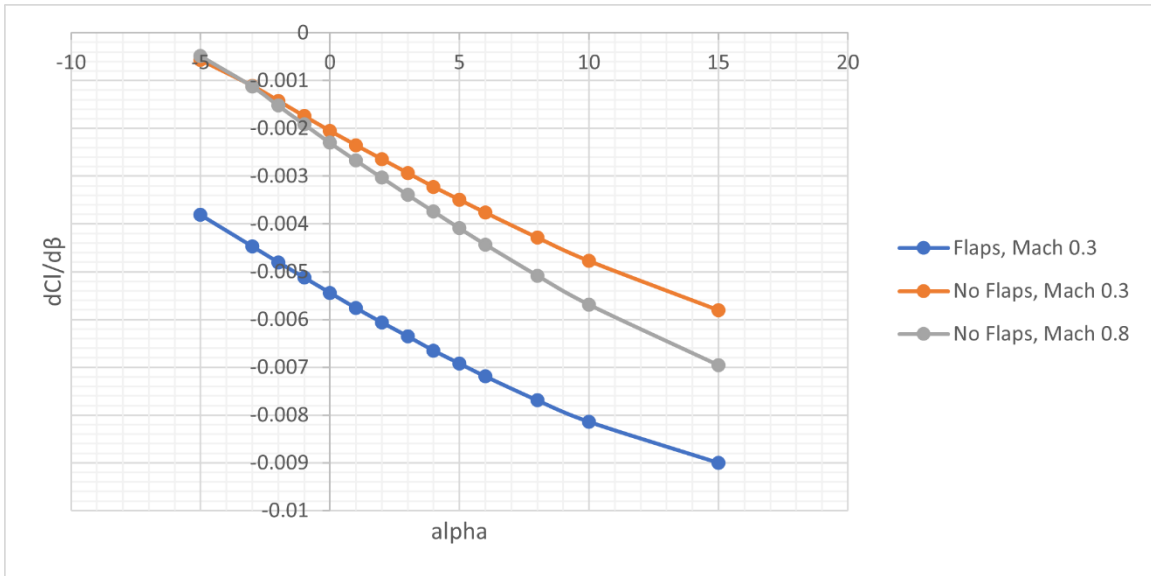


FIGURE G5 -  $C_l\beta$  vs Alpha

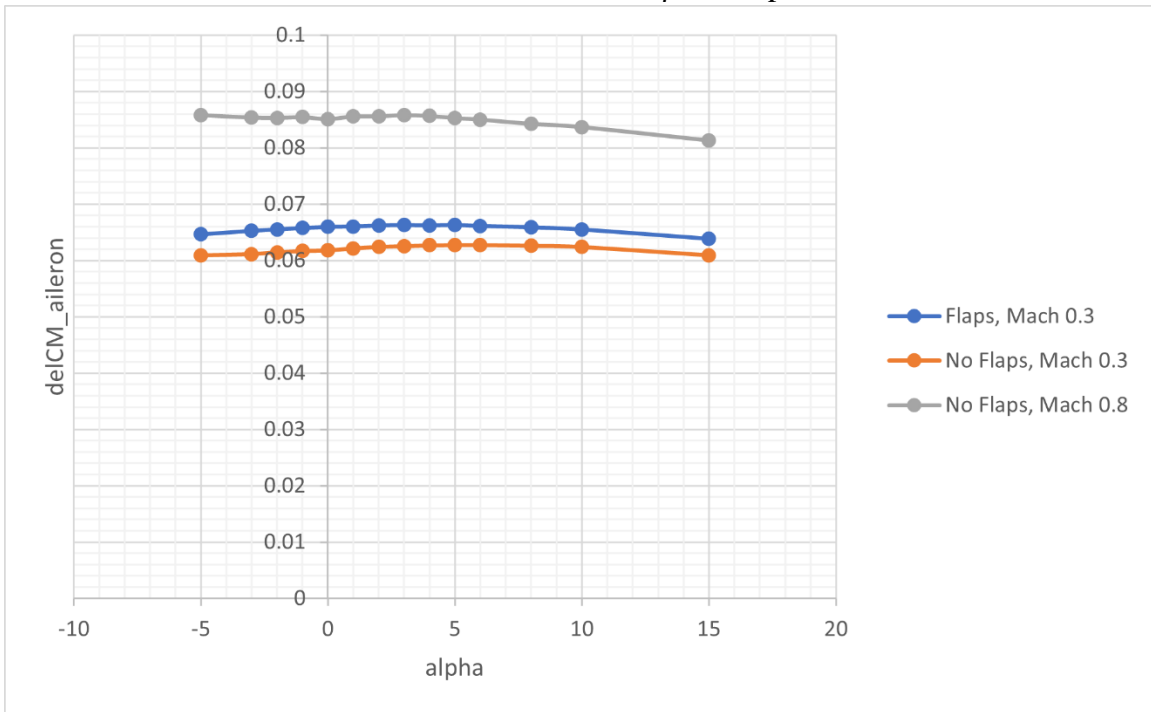


FIGURE G6 -  $C_{m\delta_e}$  vs Alpha, Positive Deflection

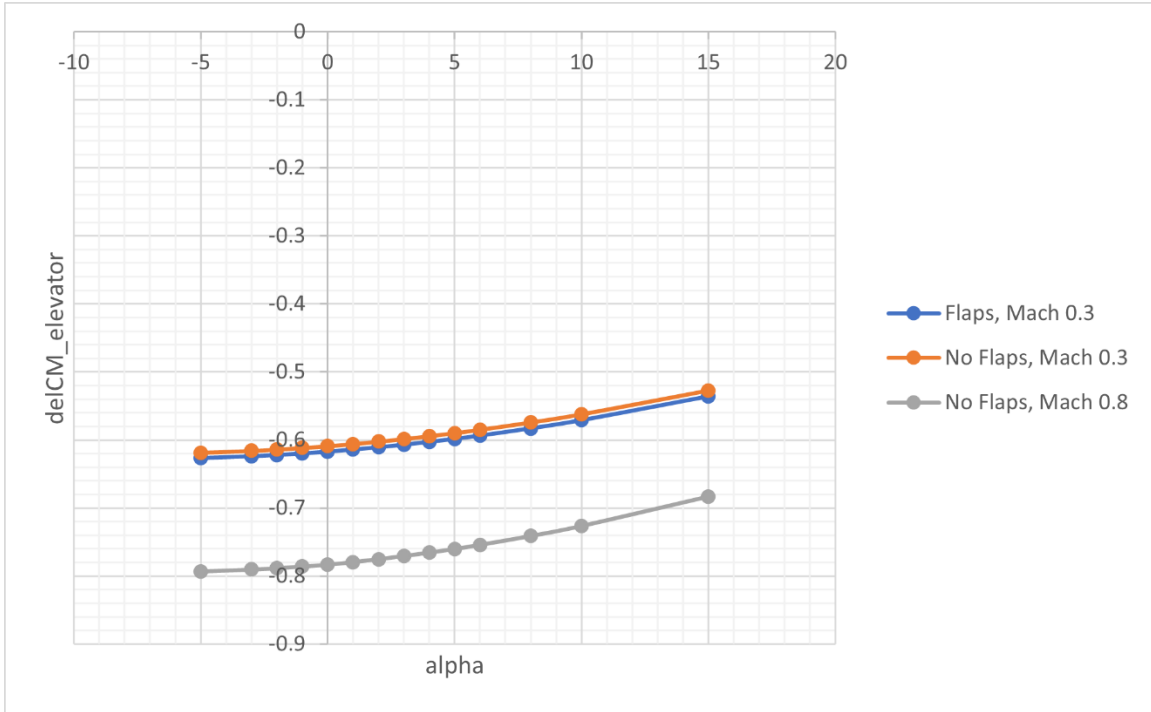


FIGURE G7 -  $C_{m\delta_e}$  vs Alpha, Negative Deflection

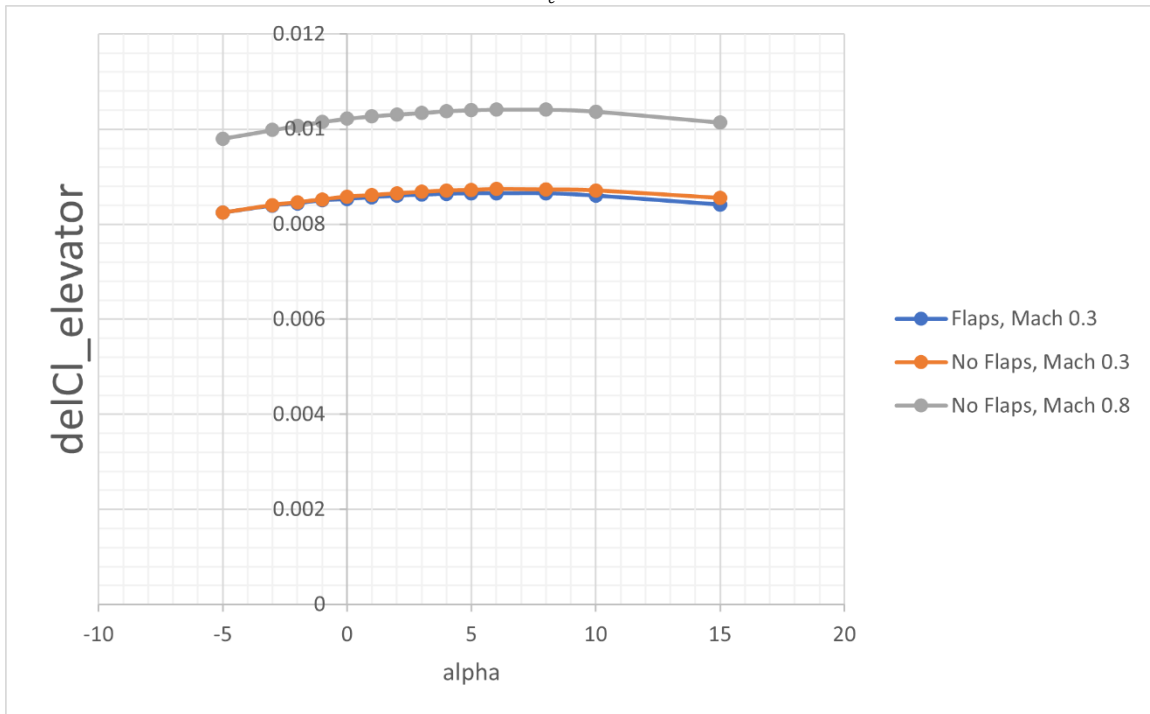


FIGURE G8 -  $C_{l\delta_e}$  vs Alpha, Positive Deflection

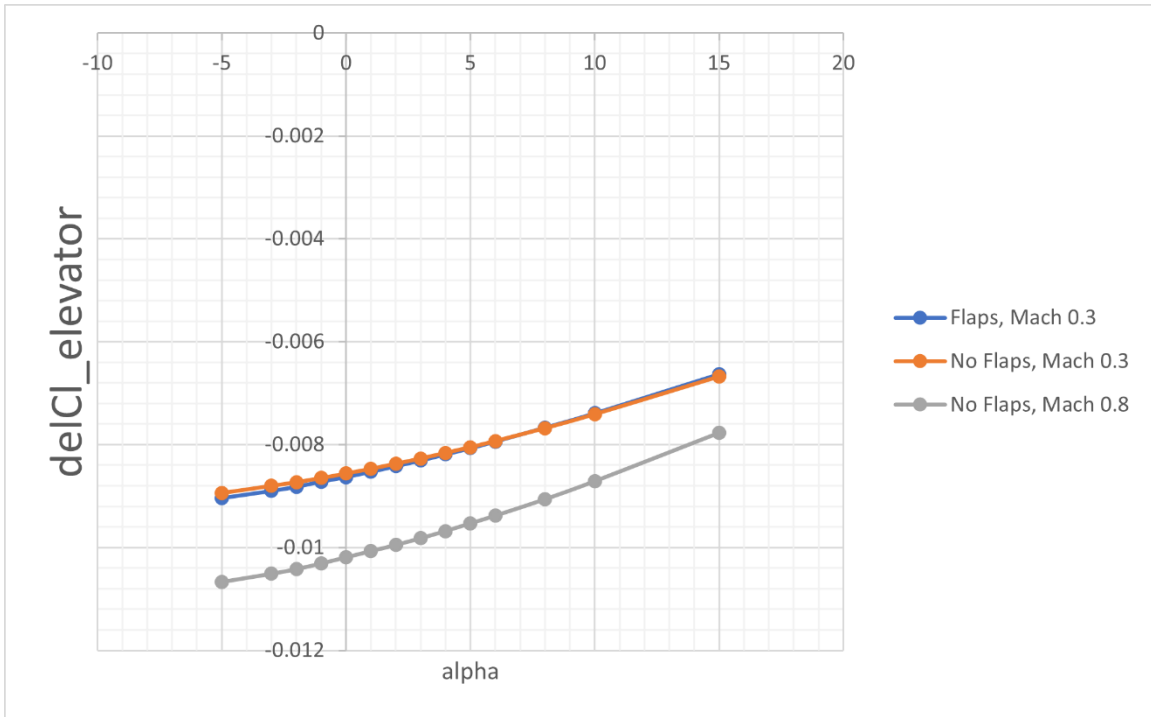


FIGURE G9 -  $C_{l_{\delta_e}}$  vs Alpha, Negative Deflection

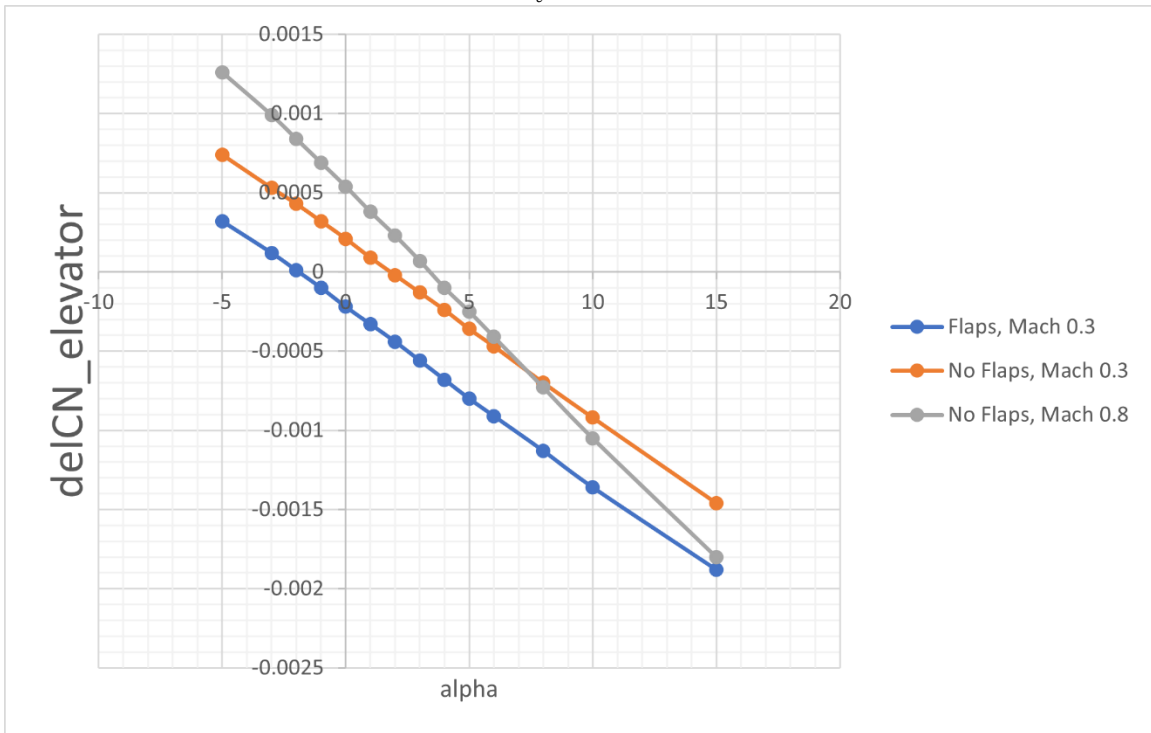


FIGURE G10 -  $C_{n_{\delta_e}}$  vs Alpha, Positive Deflection



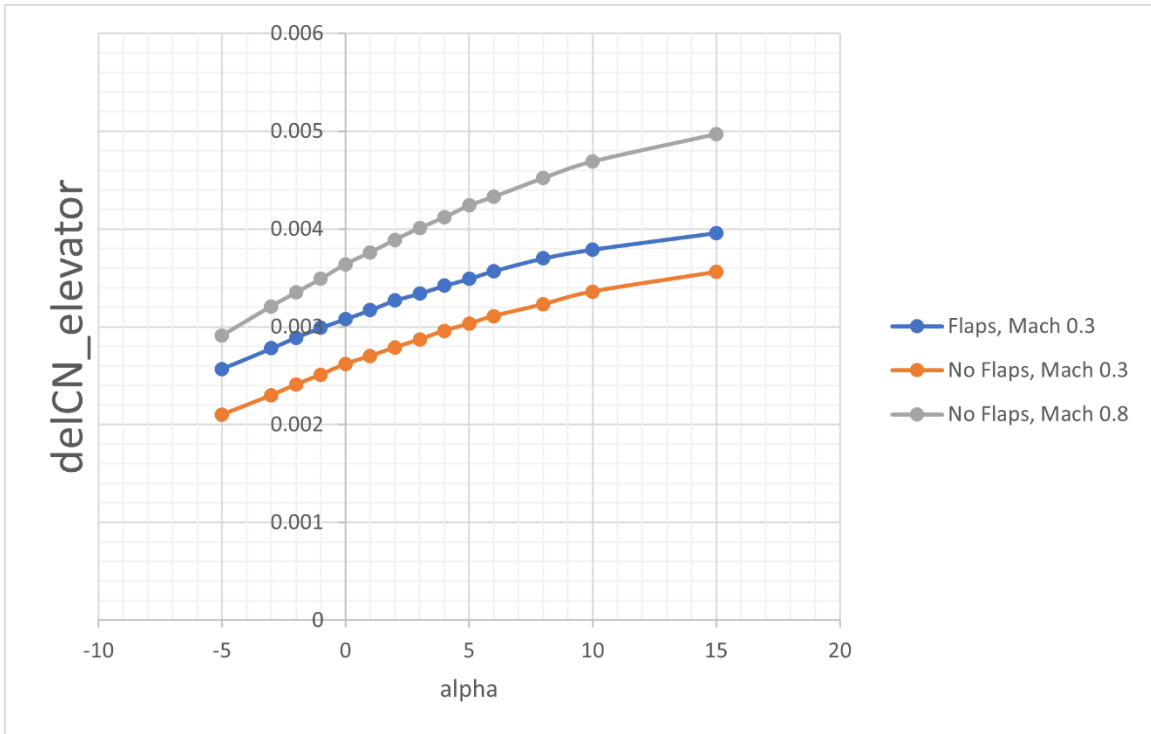


FIGURE G11 -  $C_{n_{\delta_e}}$  vs Alpha, Negative Deflection

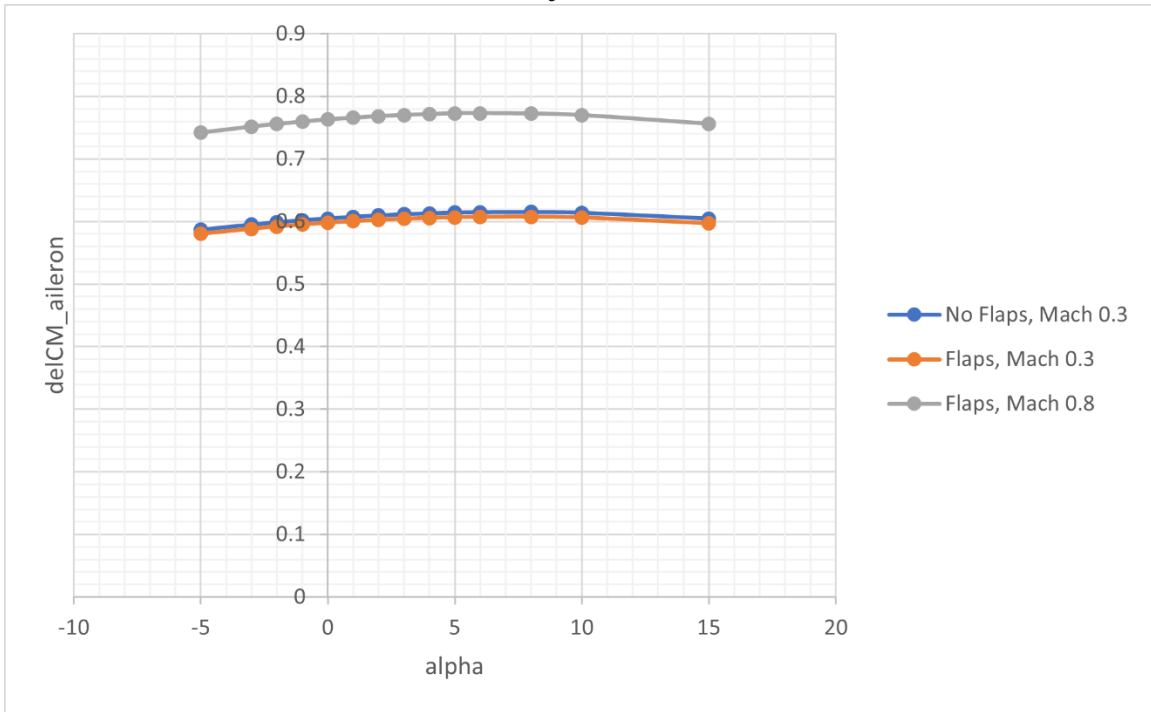


FIGURE G12 -  $C_{m_{\delta_a}}$  vs Alpha, Positive Deflection

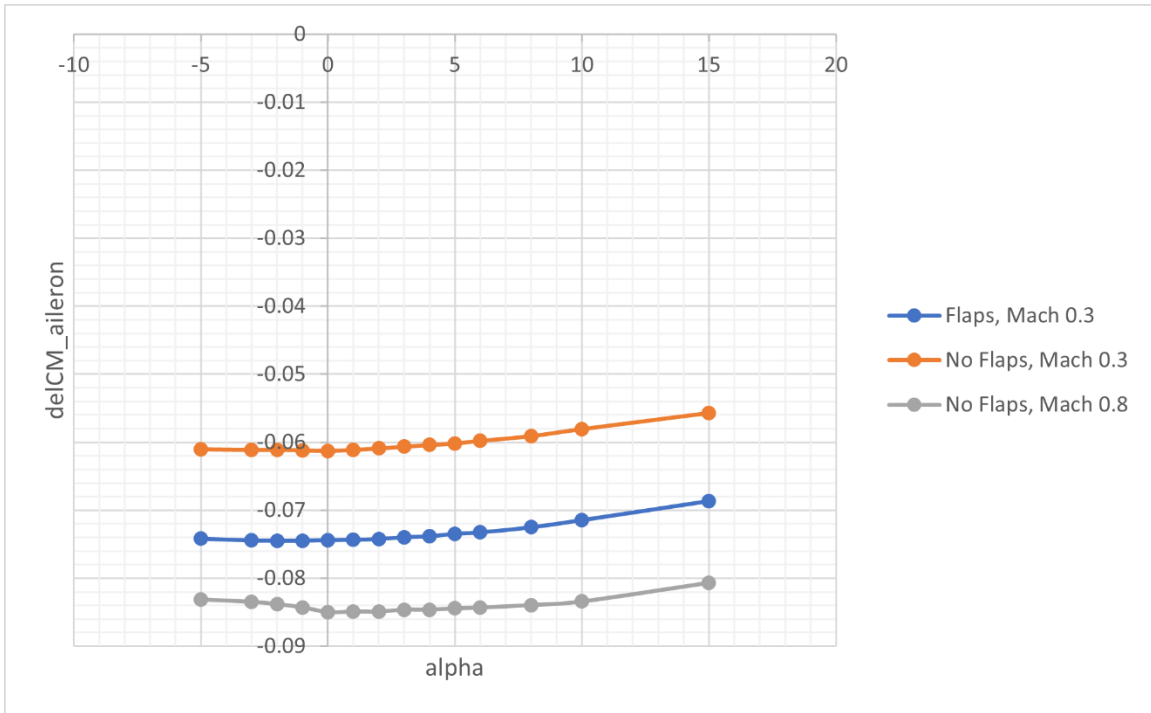


FIGURE G13 -  $C_{m_{\delta a}}$  vs Alpha, Negative Deflection

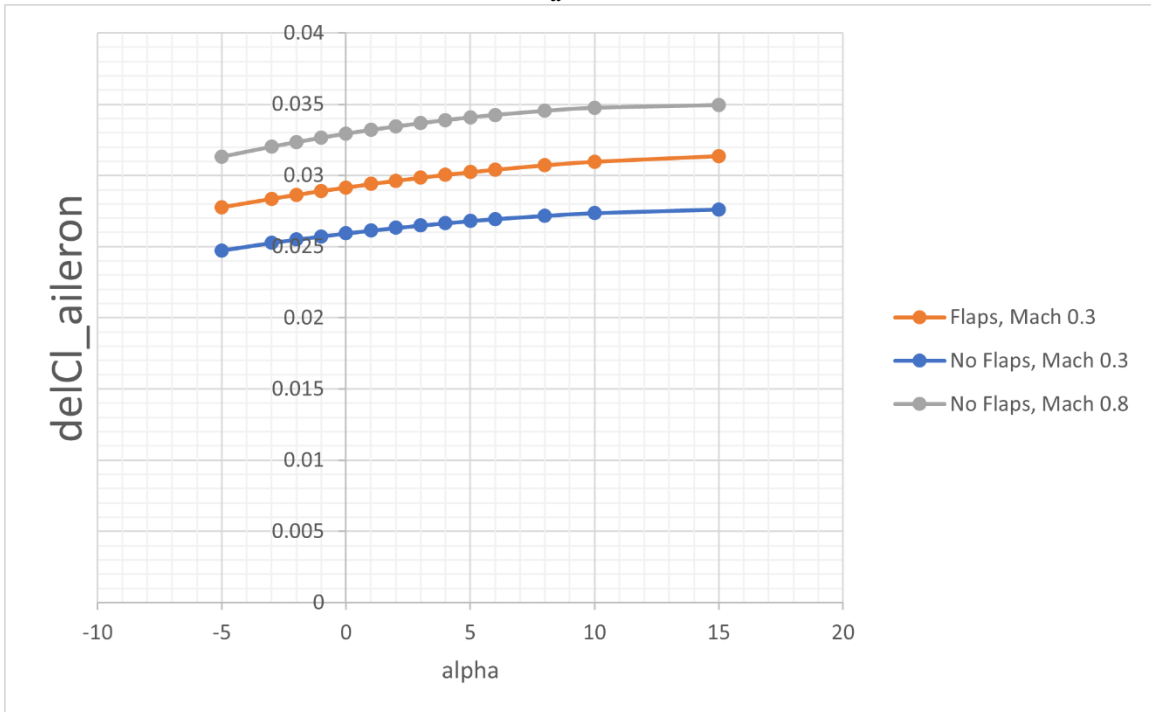


FIGURE G14 -  $C_{l_{\delta a}}$  vs Alpha, Positive Deflection

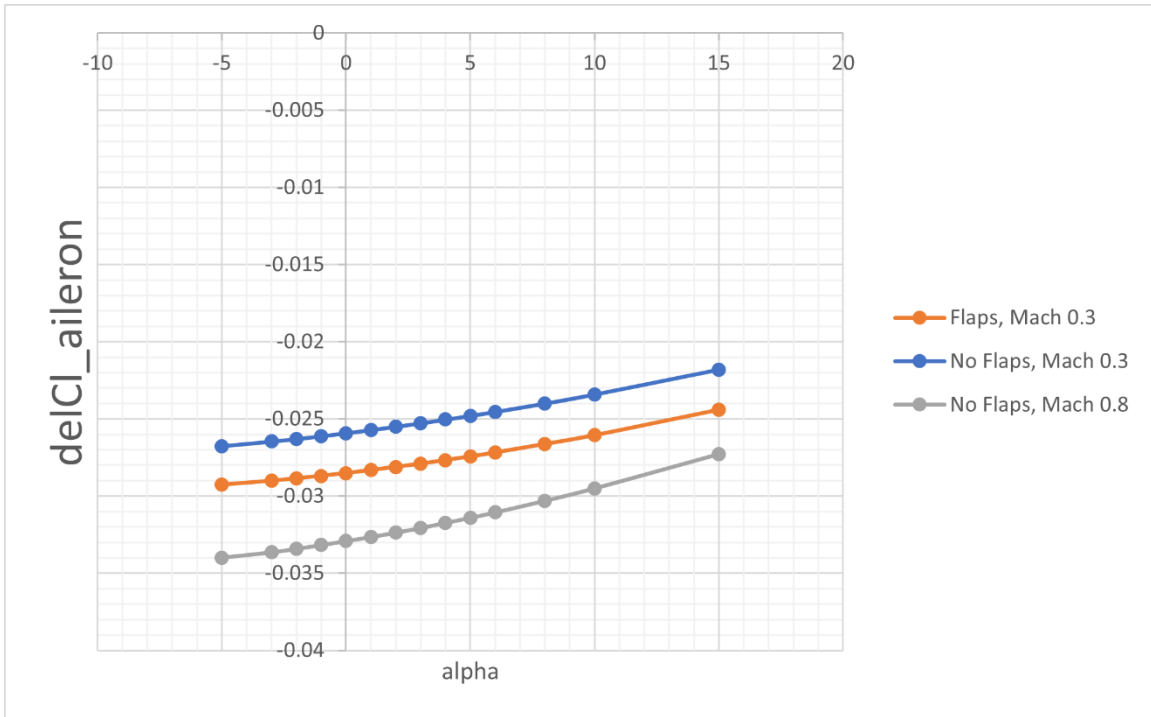


FIGURE G15 -  $C_{l_{\delta\alpha}}$  vs Alpha, Negative Deflection

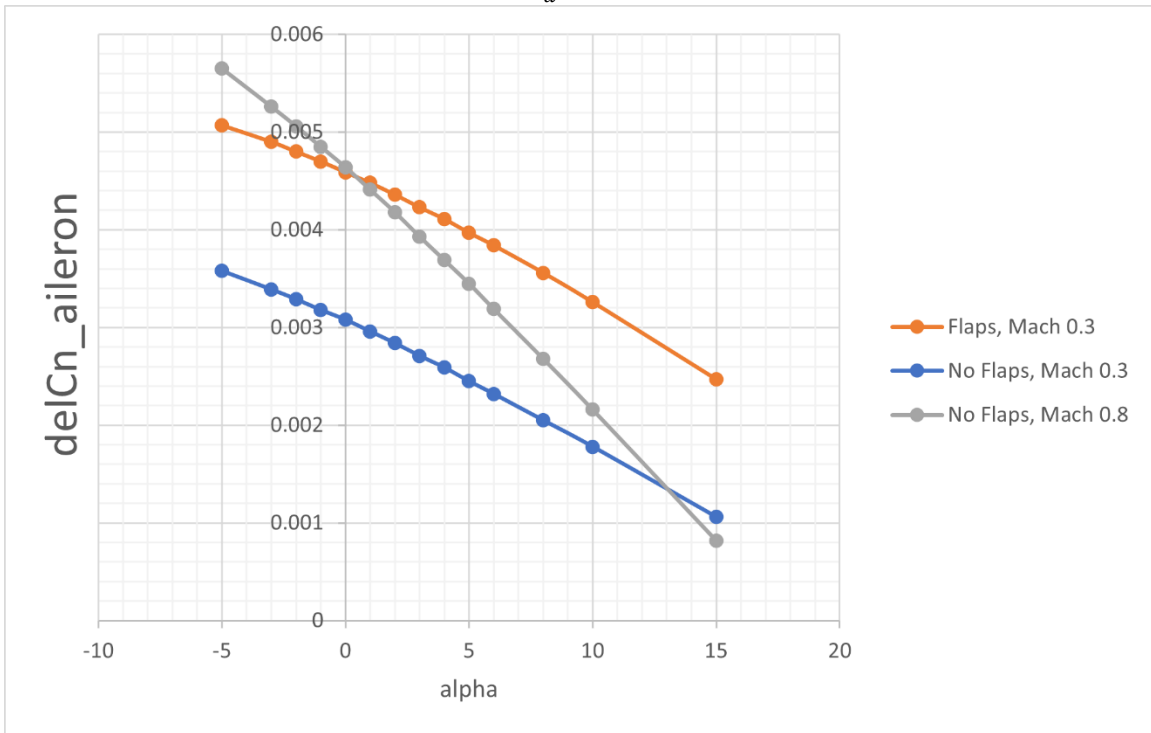


FIGURE G16 -  $C_{n_{\delta\alpha}}$  vs Alpha, Positive Deflection

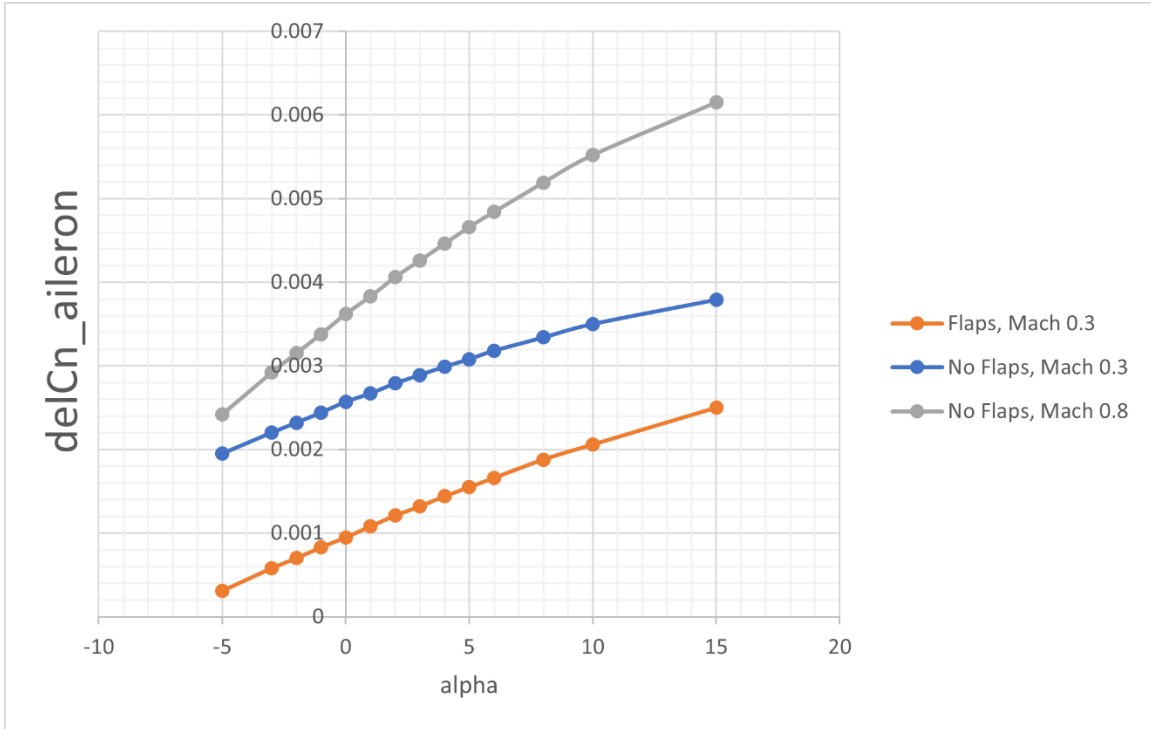


FIGURE G17 -  $C_{n_{\delta a}}$  vs Alpha, Negative Deflection

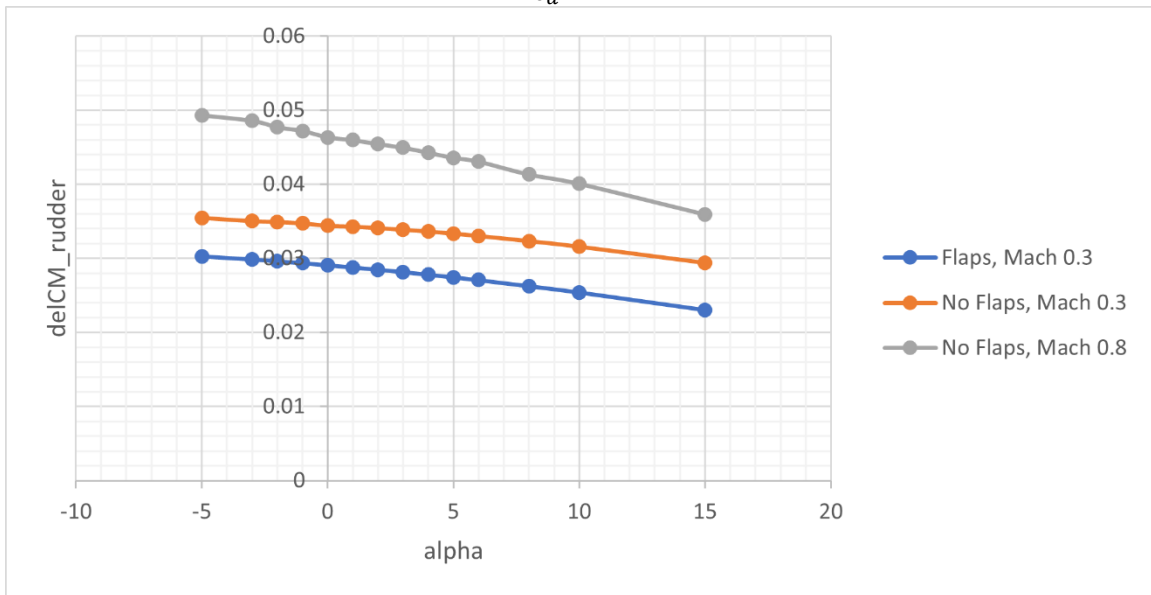


FIGURE G18 -  $C_{m_{\delta r}}$  vs Alpha

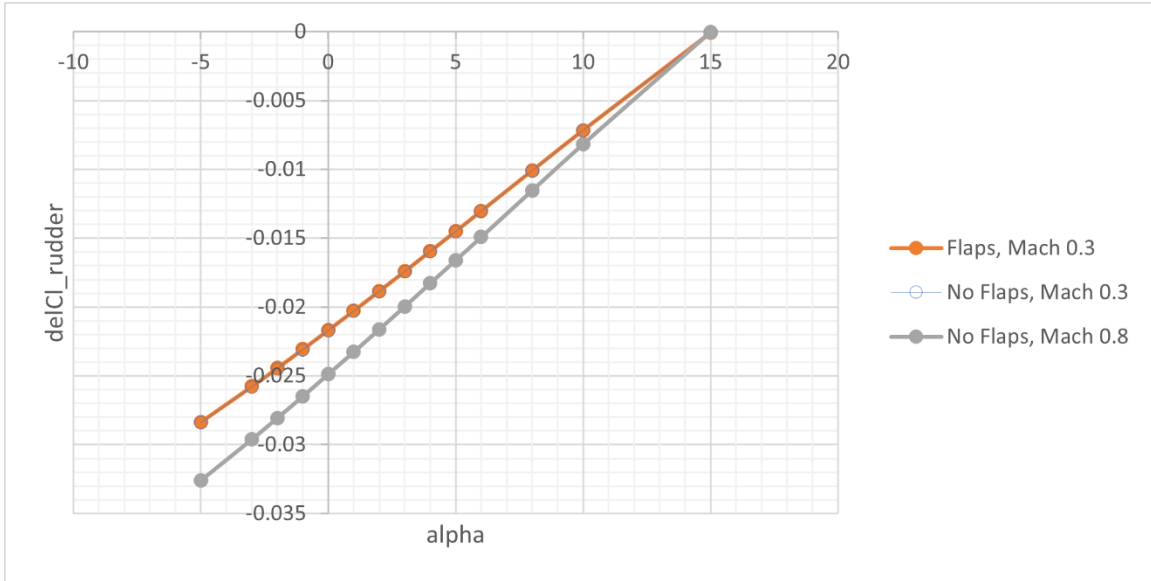


FIGURE G19 -  $C_{l_{\delta r}}$  vs Alpha

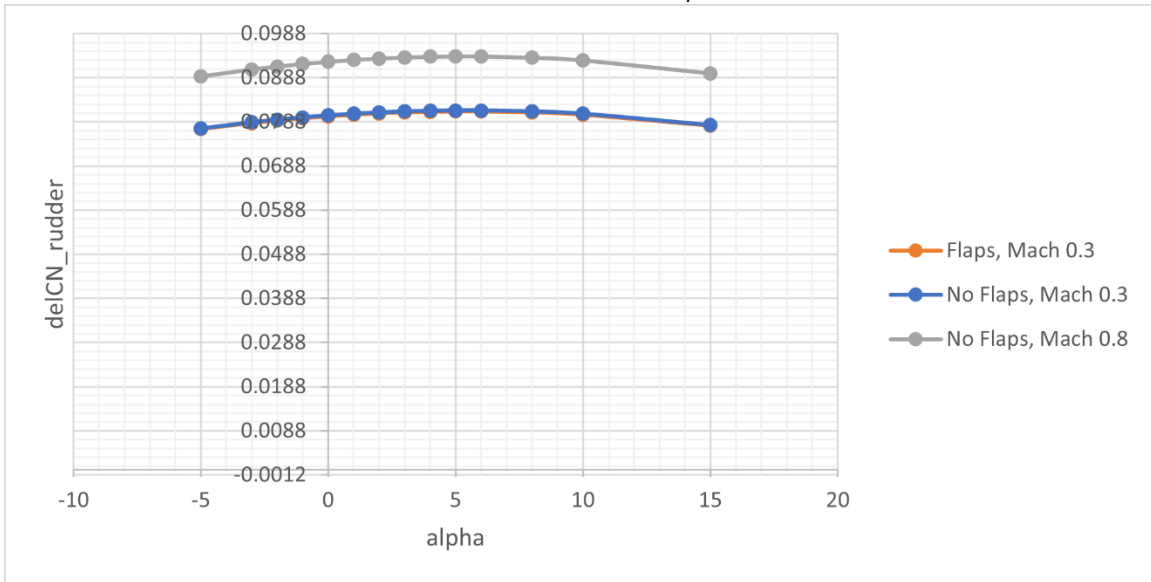


FIGURE G20 -  $C_{n_{\delta r}}$  vs Alpha

APPENDIX H

AIR FORCE GHV AERODYNAMIC DATA

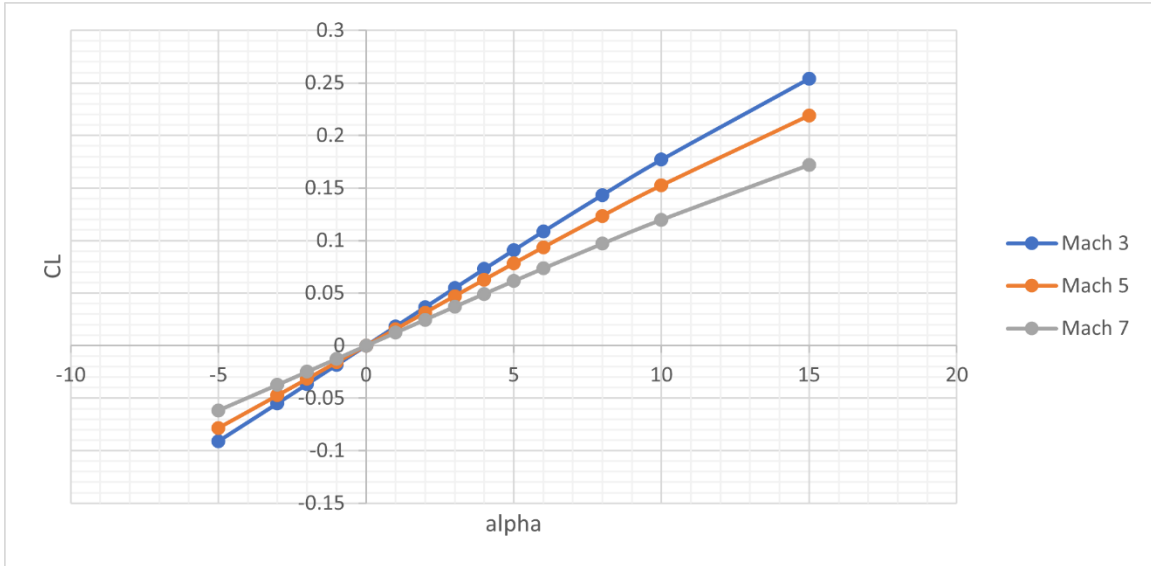


FIGURE H1 – CL vs Alpha

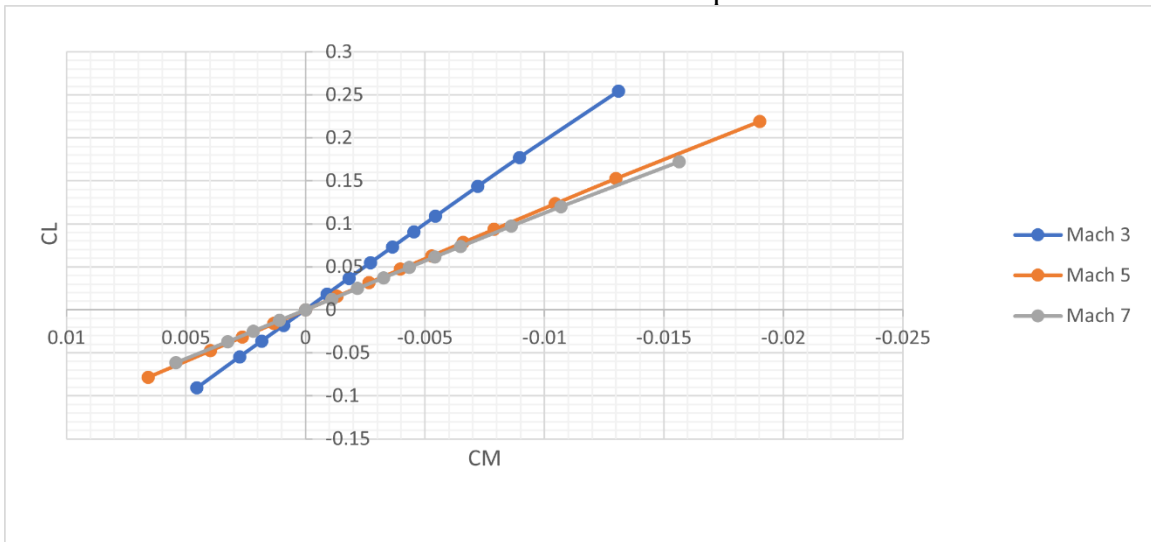


FIGURE H2 – CL vs CM

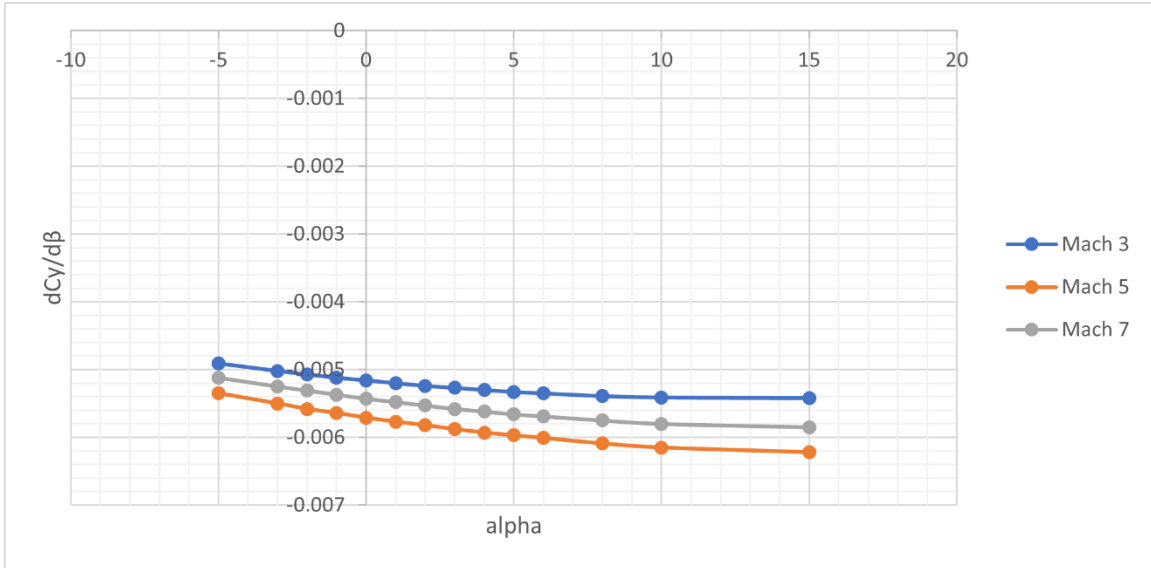


FIGURE H3 –  $C_\gamma\beta$  vs Alpha

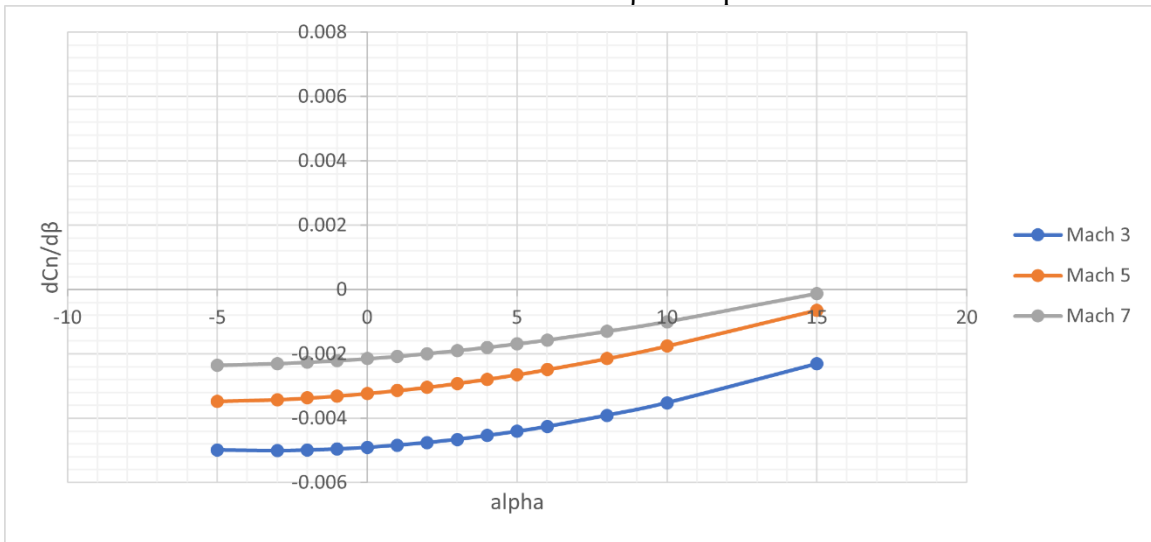


FIGURE H4 –  $C_n\beta$  vs Alpha



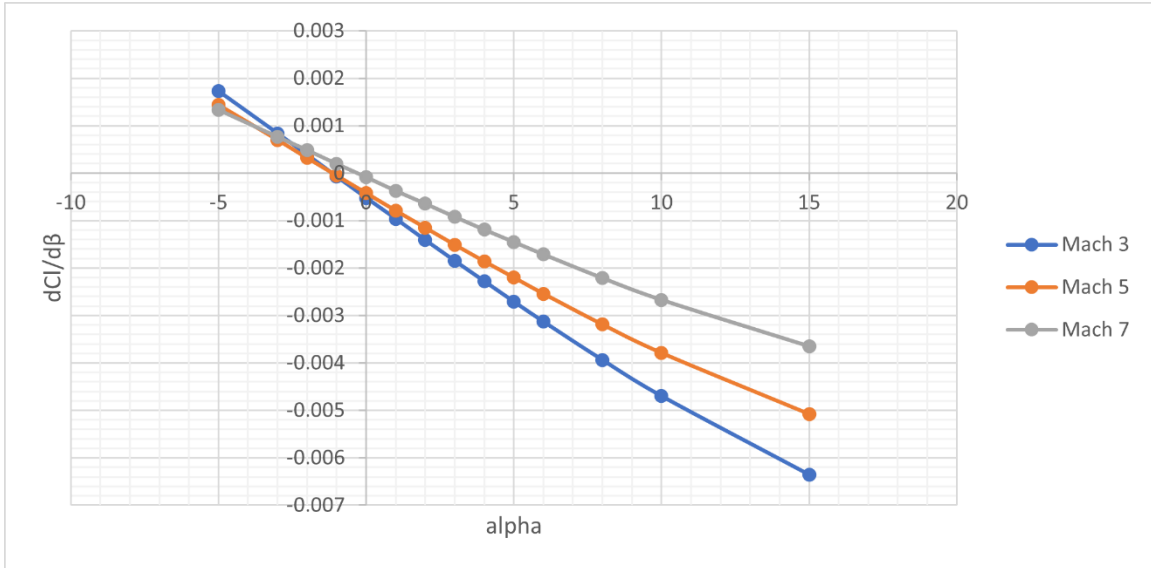


FIGURE H5 –  $C_l\beta$  vs Alpha

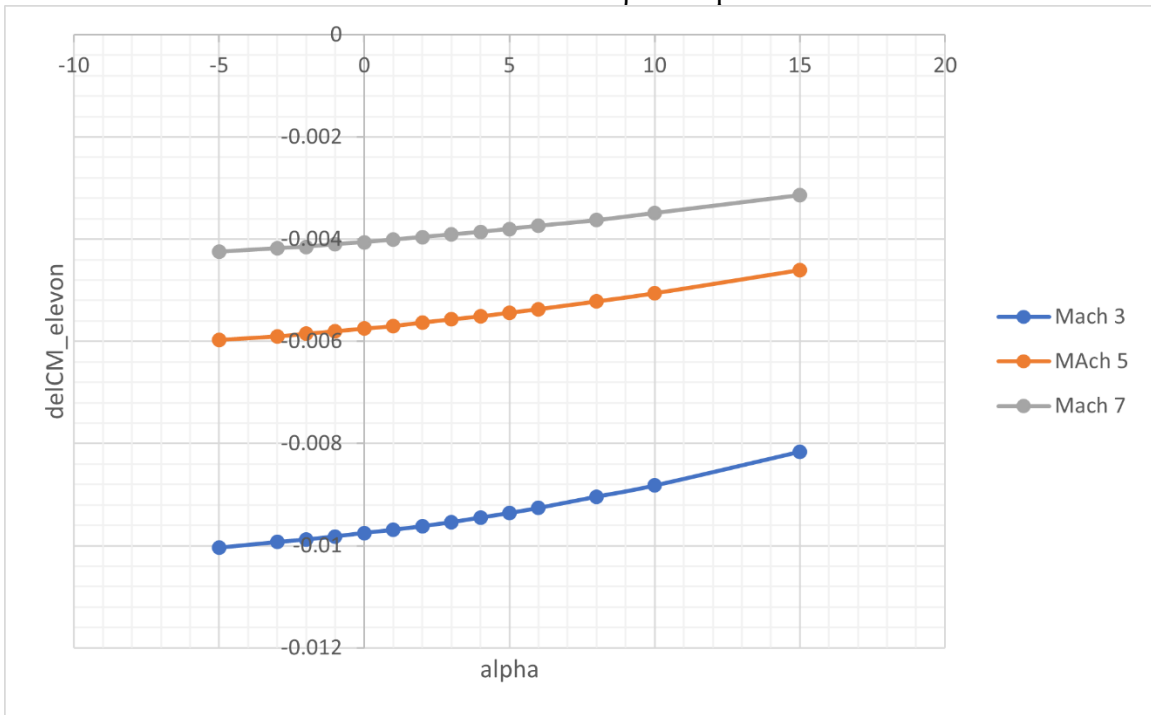


FIGURE H6 –  $C_{m_{\delta_e}}$  vs Alpha, Positive Deflection

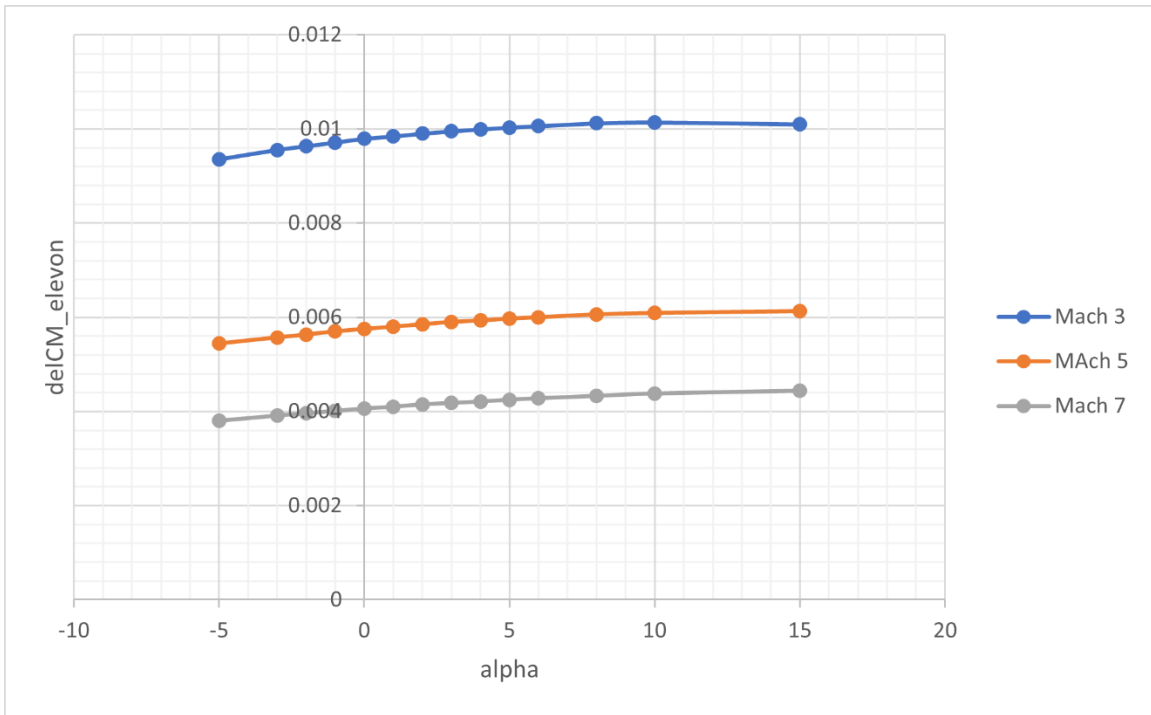


FIGURE H7 –  $C_{m_{\delta_e}}$  vs Alpha, Negative Deflection

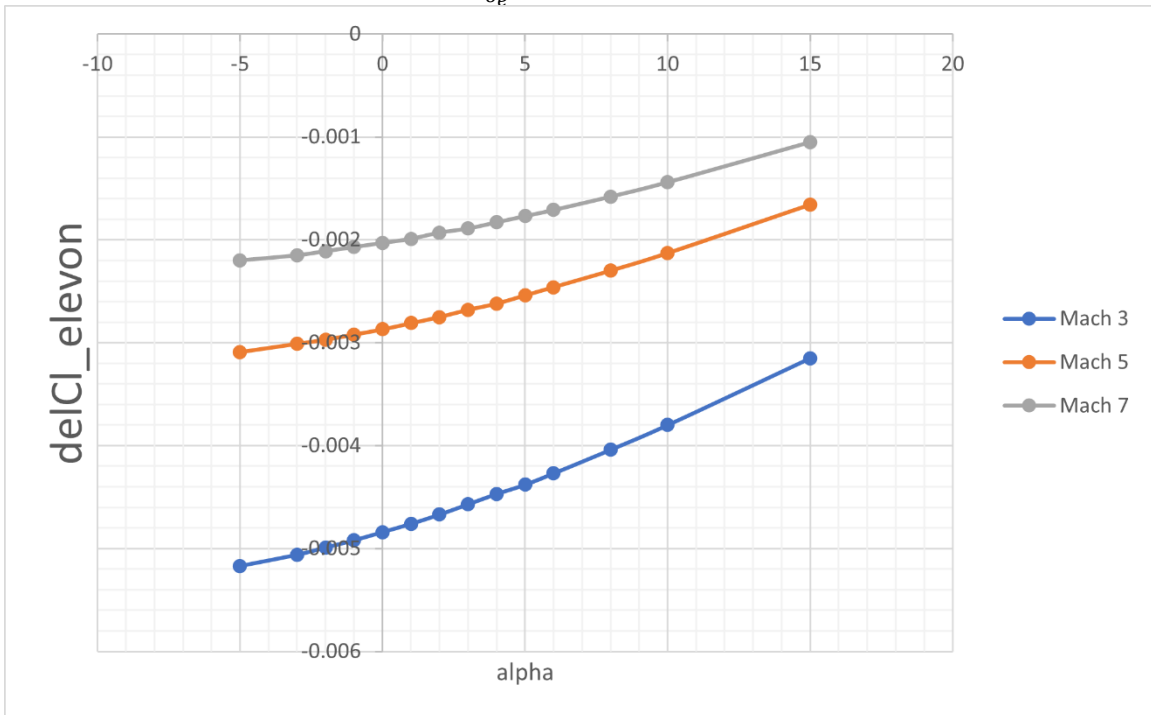


FIGURE H8 –  $C_{l_{\delta_e}}$  vs Alpha, Positive Deflection

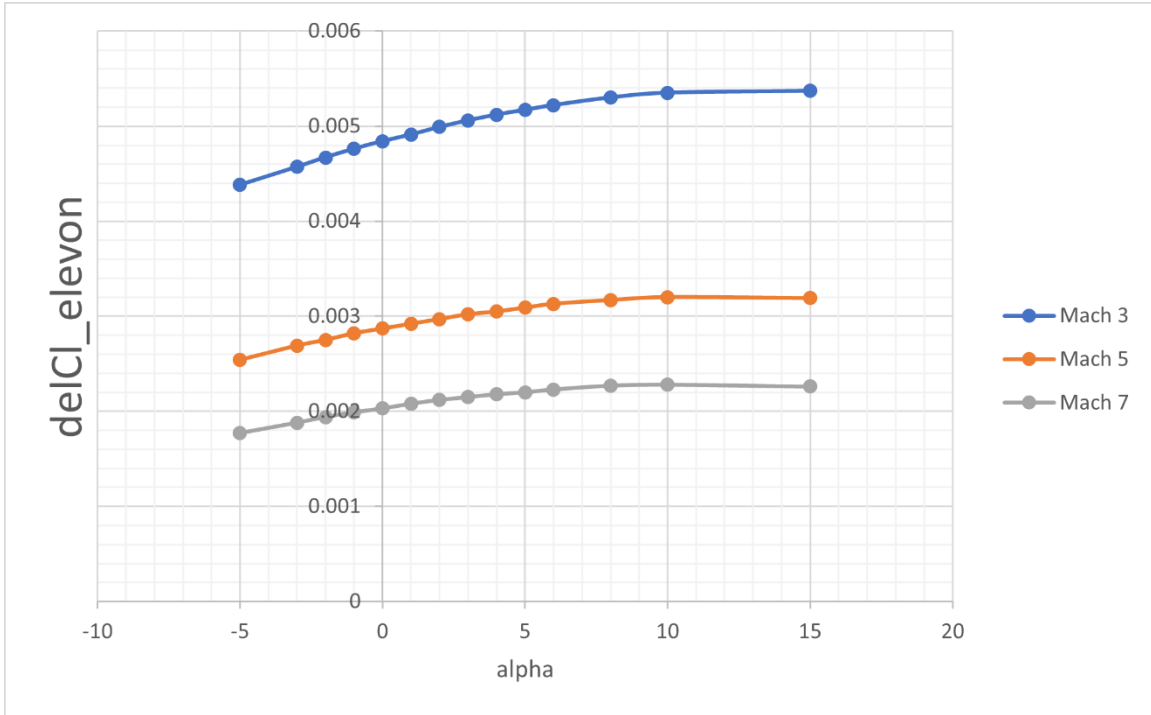


FIGURE H9 –  $C_{l_{\delta_e}}$  vs Alpha, Negative Deflection

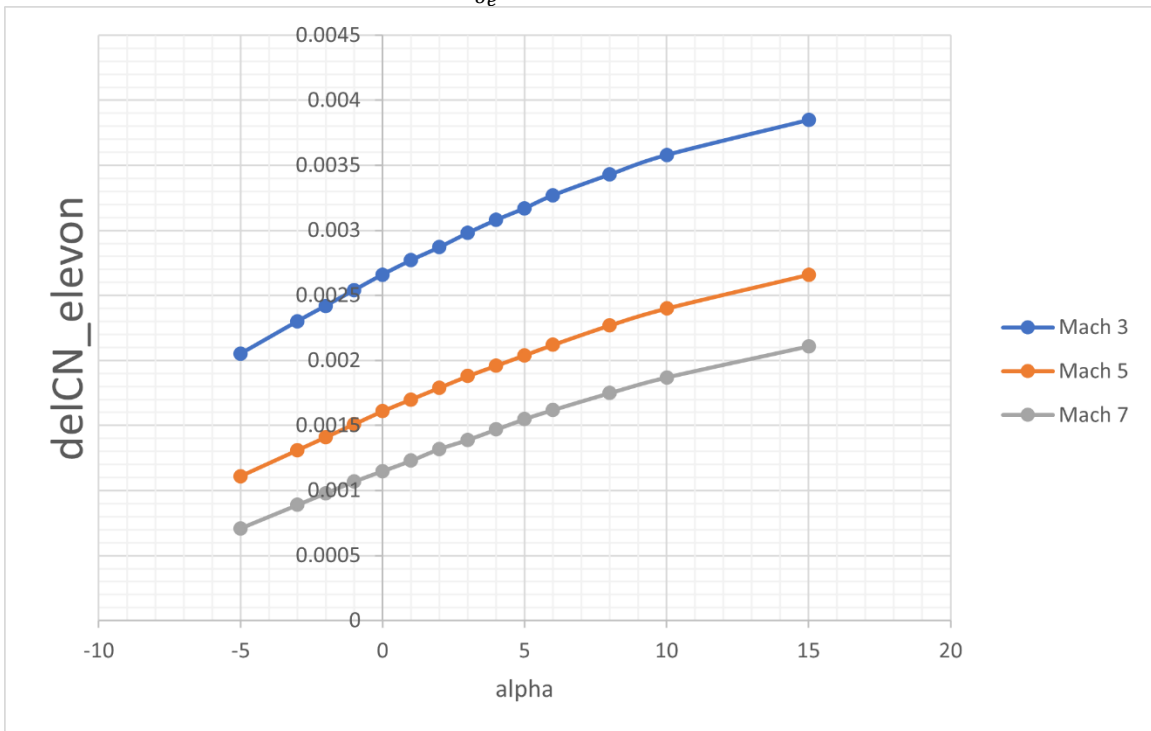


FIGURE H10 –  $C_{n_{\delta_e}}$  vs Alpha, Positive Deflection

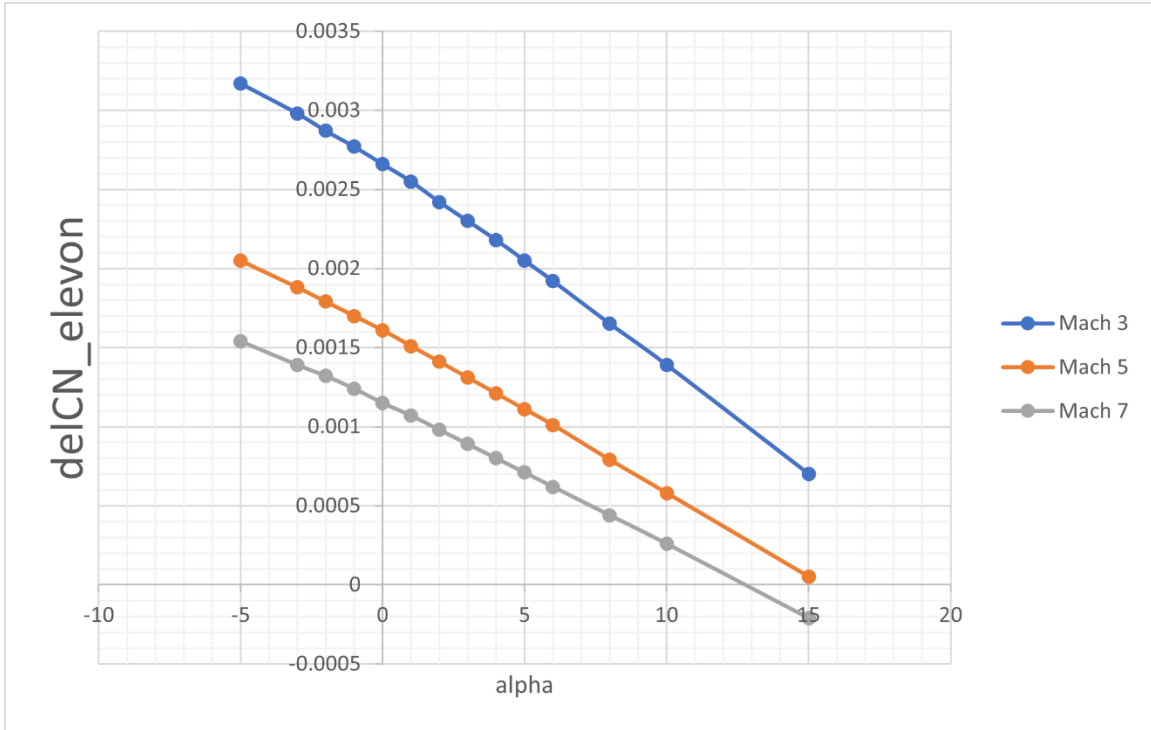


FIGURE H11 –  $C_{n_{\delta_e}}$  vs Alpha, Negative Deflection

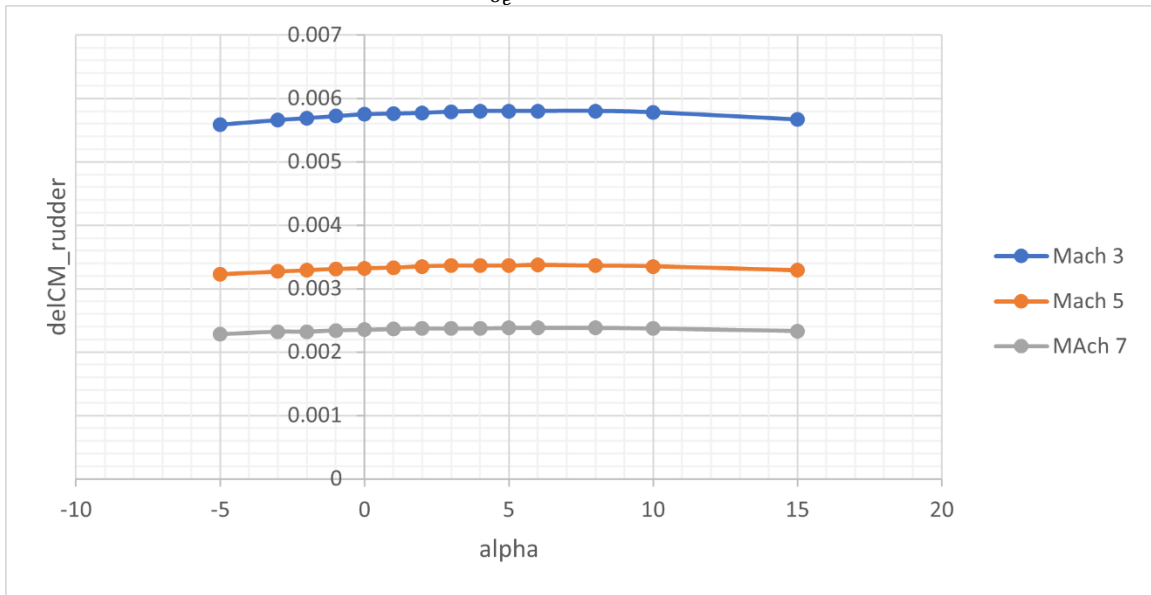


FIGURE H12 –  $C_{m_{\delta_r}}$  vs Alpha, Positive Deflection

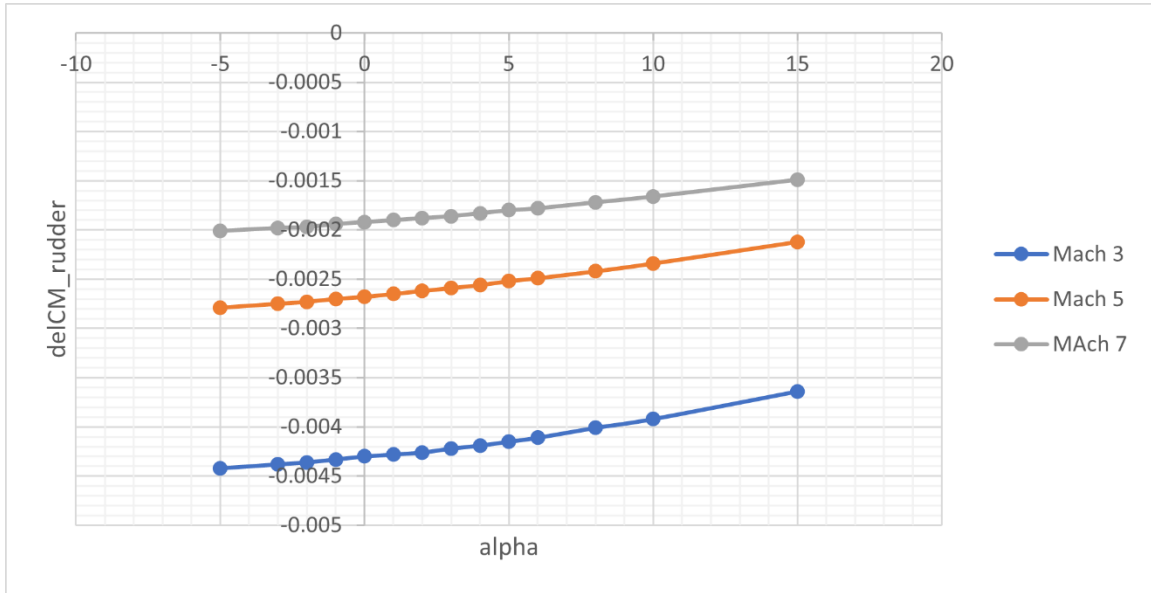


FIGURE H13 –  $C_{m\delta_r}$  vs Alpha, Negative Deflection

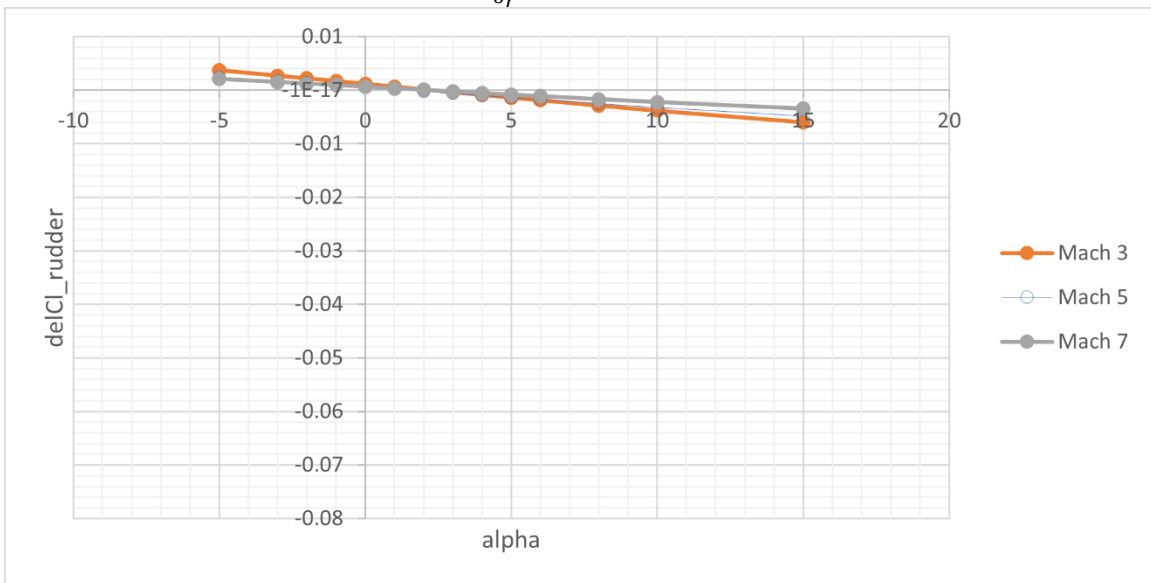


FIGURE H14 –  $C_{l\delta_r}$  vs Alpha, Positive Deflection

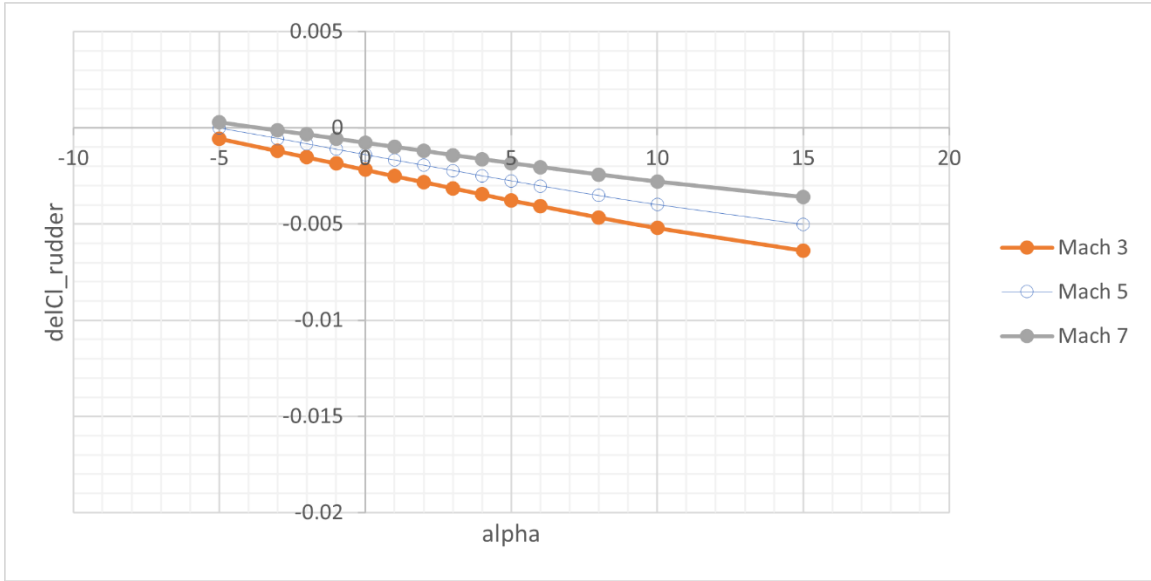


FIGURE H15 –  $C_{l_{\delta r}}$  vs Alpha, Negative Deflection

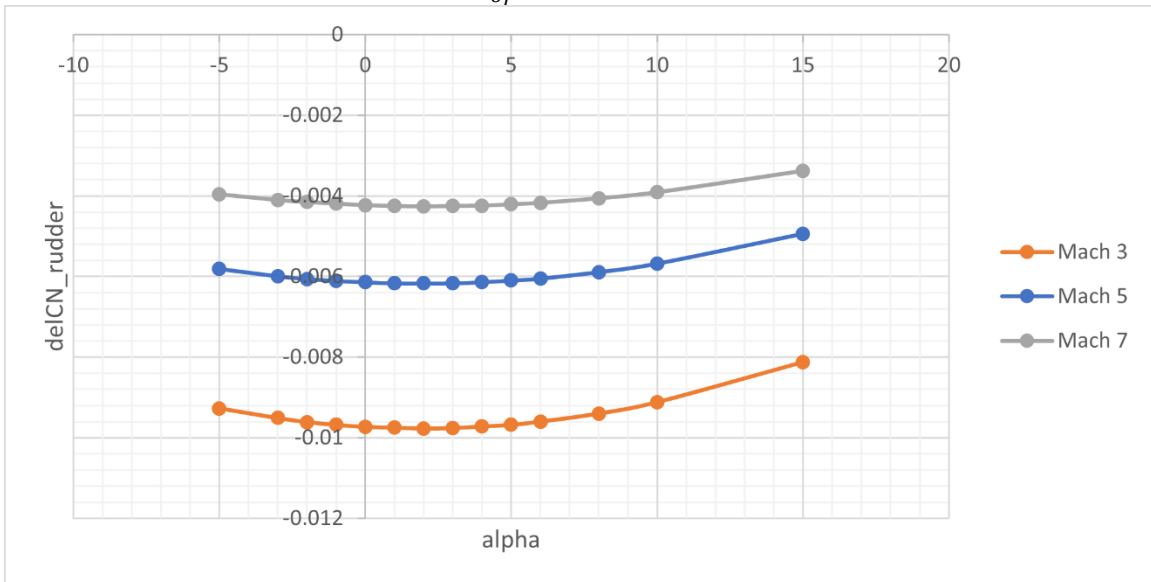


FIGURE H16 –  $C_{n_{\delta r}}$  vs Alpha, Positive Deflection

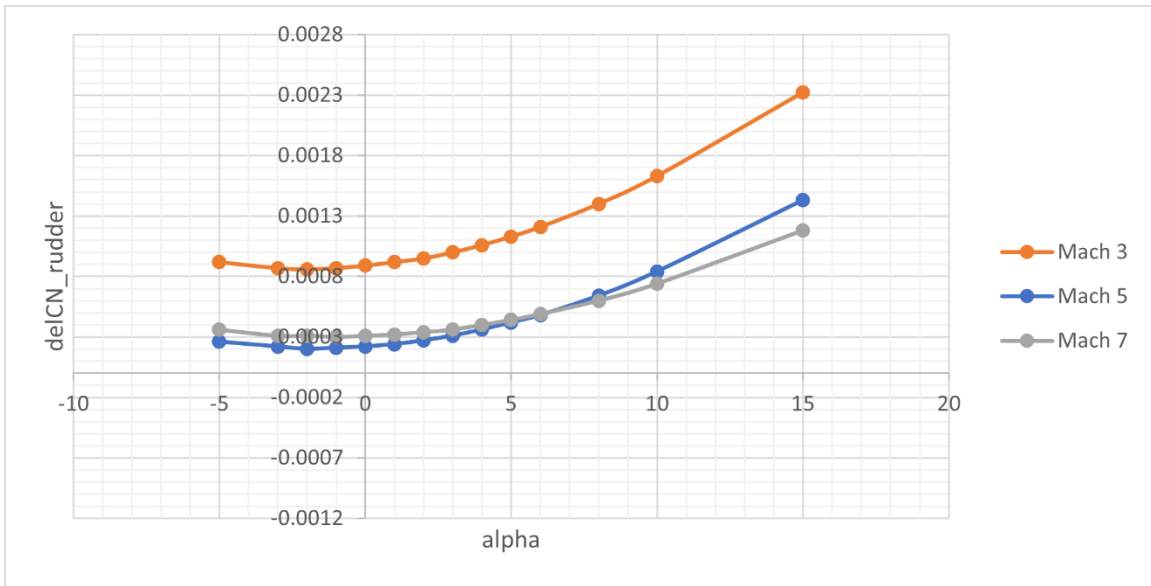


FIGURE H17 –  $C_{n_{\delta_r}}$  vs Alpha, Negative Deflection